ANALYTICA CHIMICA ACTA

International monthly devoted to all branches of analytical chemistry
Revue mensuelle internationale consacrée à tous les domaines de la chimie analytique
Internationale Monatsschrift fur alle Gebiete der analytischen Chemie

ELSEVIER SCIENTIFIC PUBLISHING COMPANY

AMSTERDAM

Anal. Chim. Acta, Vol. 76, No. 2, 237–502, June 1975

Published monthly

Completing Volume 76

ANALYTICA CHIMICA ACTA

Publication Schedule for 1975

Vol. **74,** No. **1**	January 1975	
Vol. **74,** No. **2**	February 1975	**(completing Vol. 74)**
Vol. **75,** No. **1**	March 1975	
Vol. **75,** No. **2**	April 1975	**(completing Vol. 75)**
Vol. **76,** No. **1**	May 1975	
Vol. **76,** No. **2**	June 1975	**(completing Vol. 76)**
Vol. **77,** No. **1**	July 1975	
Vol. **77,** No. **2**	August 1975	**(completing Vol. 77)**
Vol. **78,** No. **1**	September 1975	
Vol. **78,** No. **2**	October 1975	**(completing Vol. 78)**
Vol. **79,** No. **1**	November 1975	
Vol. **79,** No. **2**	December 1975	**(completing Vol. 79)**

Subscription price: Dfl. 570.00 plus Dfl. 54.00 postage; US$ 265.53 inclusive of postage. Subscribers in the U.S.A. and Canada receive their copies by airmail. Additional charges for airmail to other countries are available on request. For advertising rates apply to the publishers.

Subscriptions should be sent to:
Elsevier Scientific Publishing Company, P.O. Box 211, Amsterdam, The Netherlands.

GENERAL INFORMATION

Languages

Papers will be published in English, French or German.

Detailed information

Authors should consult Vol. 73, p. 435 for detailed instructions. Reprints of this information are obtainable from Dr. Macdonald or from: Elsevier Editorial Services Ltd., Mayfield House, 256 Banbury Road, Oxford (Great Britain).

Submission of papers

Papers should be sent to:

PROF. PHILIP W. WEST,
Coates Chemical Laboratories,
College of Chemistry and Physics,
Louisiana State University,
Baton Rouge 3,
La. 70803 (U.S.A.)

or to:

DR. A. M. G. MACDONALD,
Department of Chemistry,
The University,
P.O. Box 363
Birmingham B15 2TT (Great Britain)

Reprints

Fifty reprints will be supplied free of charge. Additional reprints (minimum 100) can be ordered at quoted prices. They must be ordered on order forms which are sent together with the proofs.

PRINTED IN THE NETHERLANDS

Pharmaceutical applications of Thin-Layer and Paper chromatography

edited by **KAREL MACEK**, *Medical Faculty, Charles University, Prague*

1972, xvi + 744 pages, Dfl. 250.00
ISBN 0-444-40939-4

Chromatography is the most widely used modern procedure in analytical chemistry today. With an increasing awareness of the importance of the applications of paper and thin-layer chromatography in the fields of pharmaceutical research, production and control, it has become necessary to survey the possibilities of these methods with their associated literature, and to present this information in a useful form.
With this in mind, the editor provides an introduction to the techniques, the evaluation, and the applications of paper and thin-layer chromatography. Selected procedures such as the preparation of samples, detection methods, choice of solvent systems and sorbents, and the principles of quantitative analysis, are discussed generally and the book is richly tabulated. An appendix outlines the preparation of more than 150 detection reagents. On the basis of these data, readers with an understanding of the principles of the techniques described can solve any analytical problems they may encounter in drug analysis.

CONTENTS: Introduction. Techniques of paper and thin-layer chromatography. Radioactive compounds. Combination of TLC and PC with other chromatographic techniques. Combination of PC and TLC with some spectroscopic methods. Identification of organic compounds by PC and TLC. Documentation of chromatograms. Laboratory for PC and TLC. The tasks of paper and thin-layer chromatography. Synthetic drugs. Steroids. Cardiac glycosides and their genins. Saponins. Peptide and protein hormones. Alkaloids. Vitamins. Antibiotics. Plant extracts. Auxiliary compounds. Investigation of the fate of drugs. Detection reagents. Author index. Subject index. List of substances chromatographed.

CONTRIBUTORS: V. Betina, J. Davídek, I. M. Hais, K. Hiller, J. Janák, G. Katsui, B. P. Lisboa, M. Luckner, K. Macek, L. Nover, V. Rábek, G. Székely, H. D. Woitke.

Elsevier

BOOK DIVISION, P.O. BOX 211
AMSTERDAM - THE NETHERLANDS

f81Ea

The Science of the Total Environment

An international journal for scientific research into the environment and its relationship with man

The journal forms an entirely international medium for the publication of papers dealing with the results of research into all aspects of man's perturbations of the environment, their inter-relationships and implications for life.
The scope is wide, ranging from fundamental aspects to laboratory and field studies and to applied engineering designs, whilst the subject matter embraces all aspects of both air and water pollution, thermal pollution effects and heat re-use, solid waste disposal and re-use, noise, light and electromagnetic interferences. These subjects are considered from any scientific, technological, sociological or legal viewpoint.

Emphasis is also given to establishing the baselines for the chemical composition of living matter in relation to the environment in order that observed abnormalities may be placed in perspective.

The types of contributions include normal length research papers, reviews of specialized topics, shorter communications, preliminary notes, letters to the editors and book reviews. All material is published rapidly, and preliminary notes are normally published within 4-12 weeks of receipt by the publisher. The journal appears quarterly.

Authors should send two copies of their manuscript to one of the editors named. Papers are accepted in English, German or French.

1975: Volume 4 in 4 quarterly issues.

Subscription price for 1975: US$37.95 / Dfl. 95.00 plus US$3.75 / Dfl. 9.00 postage and handling costs.

Sample copies are available.

Orders may be placed with your usual supplier or with Elsevier Publishing Company, Journal Division, P.O. Box 211, Amsterdam - The Netherlands.

Elsevier
P.O. Box 211
Amsterdam - The Netherlands
5069 E

Reagents

MERCK

Test strips for the identification and semi-quantitative determination of ions and compounds.

Particular advantages: **easy to use**
high sensitivity
clearly calibrated
high selectivity

At this time the following Merckoquant Test Strips are available: Fe^{++} Test, Co^{++} Test, Ni^{++} Test, Mn^{++} Test, Cu^{+}/Cu^{++} Test, Fixing Bath Test, Ether peroxide Test, Chromate Test, Nitrite Test, Sulfite Test, Zn^{++} Test.

Please ask for our special brochures.

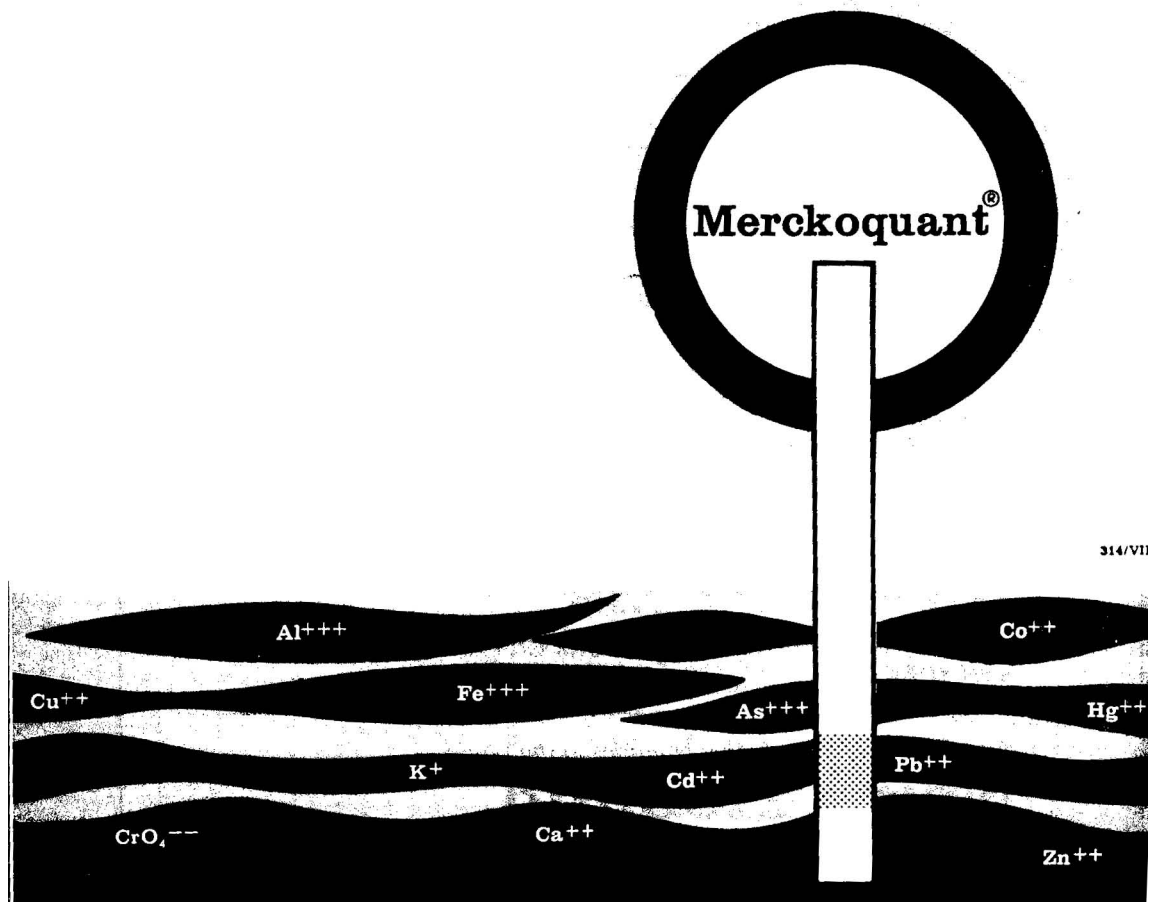

E. Merck, Darmstadt Germany

Analytica Chimica Acta, 76 (1975) 237–244

THE IMMOBILIZED ENZYME STIRRER
PART I. A SPECIFIC ELECTRODE FOR UREA

G. G. GUILBAULT* and W. STOKBRO
Chemistry Department A, Technical University of Denmark, 2800 Lyngby (Denmark)
(Received 25th November 1974)

In the past 5 years, many analytical applications of immobilized enzymes have been proposed[1–5]. One of these has been in the fabrication of enzyme electrodes–electrochemical probes in which the immobilized enzyme is placed over an ion-selective electrode, yielding an electrode highly selective or specific for organic molecules[6]. In all of these past applications, the immobilized enzyme has been stationary, either in a column or in a thin layer, and the solution has been stirred and passed over the enzyme or brought into contact with it. In this paper a new concept is proposed—the enzyme is placed on the surface of a magnetic stirrer forming one unit, that both stirs the solution and catalyzes enzymatic transformations, in one step. The stirrer is stable and economical, being useful for several hundred assays, and permits a very fast assay in a highly accurate and reproducible manner.

Here, the use of such an immobilized urease enzyme stirrer is described for the assay of urea in blood. The ammonia liberated at pH 8.5 is measured with an air-gap electrode, previously used for a specific assay of ammonia and urea[7,8], thereby eliminating all interferences commonly associated with the assay. Direct assays in blood sera are performed in 2 min, with an accuracy and precision of about 2%. The stirrer electrode is stable for over 60 days of use.

Two different forms of immobilized enzyme were used in these experiments; a chemically bound enzyme—Enzygel urease from Boehringer, and a glass bound enzyme from Corning.

EXPERIMENTAL

Apparatus

The air-gap electrode, used to sense the ammonia liberated, was of the same design as previously described[7]. The electrolyte solution was 10^{-3} *M* ammonium chloride (AnalaR) saturated with Victawet 12 (Stauffer Chemical Co).

The enzyme stirring bars were constructed by placing 10 units of immobilized urease (A, Fig. 1) onto a Teflon-coated magnetic 1.5-in. stirring bar (B, Fig. 1). The enzyme layer was covered with a piece of nylon net (C, Fig. 1) (Nytal Nr. 49 (12), 132 μ, Swiss Silk Mfg. Co, CH 9425 Thal St Gall), which was

* Guest Professor of Analytical Chemistry on leave from the University of New Orleans, Louisiana.

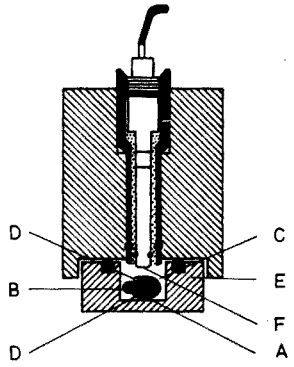

Fig. 1. Air-gap electrode and immobilized enzyme–stirrer. See text for details.

pulled tight so that the enzyme became thinly spread over the stirrer. This process was most easily accomplished by forming the net into a cylinder and pouring the enzyme powder into the cylinder followed by the stirring bar. A thin rubber band, cut from 1-mm rubber tubing, was fitted tightly over the net and stirring bar, being placed 2/3 of the way up the bar (D, Fig. 1). Excess of net was then cut off with scissors. The enzyme stirring bar was then placed into a microchamber (Fig. 1, E) for the assays.

The glass electrode (Radiometer E 5036/0) used in the air gap assembly had a flat pH-sensitive surface (*ca.* 12 mm^2 area) and a combined reference electrode consisting of a silver chloride-covered silver strip. The electrolyte solution (NH_4Cl–Victawet) was used as the reference solution.

A digital pH meter (Radiometer Model 51) and a recorder (Servogor Re 511) were used for measuring and recording all electrode responses.

All pipettes used were Carlsberg micropipettes, 100 and 200 μl ($\pm 1\%$ accuracy; H. E. Pedersen, Denmark).

Reagents

The buffer solution was 0.5 *M* tris(hydroxymethyl)aminomethane adjusted to pH 8.50 with hydrochloric acid.

Urease. Immobilized urease used was from two sources: Boehringer Enzygel, activity 650 units/g, and glass-bound enzyme (Corning, activity about 300 units/g). To make the stirring bars, 15 mg of the Boehringer enzyme or 35 mg of the Corning enzyme were used (activity, *ca.* 10 units).

Urea. The urea used for preparing standard calibration plot was that in freeze-dried blood (Monitrol I and II, Dade-Division, American Hospital Supply Co, Miami, Fla.). Dilution of Monitrol II (urea concentration $1.86 \cdot 10^{-2}$ *M*, as analyzed by the AutoAnalyzer) with doubly distilled water gave the best electrode calibration for use in assaying serum samples.

Serum samples. These were obtained from Rigshospitalet of Copenhagen. The serum samples were obtained fresh and were concurrently analyzed at the hospital (by the AutoAnalyzer method) and by us. The normal background ammonia content of blood ($3–7 \cdot 10^{-5}$ *M*) did not present any interference in urea assays (urea is about 3–30 m*M* in serum), but if the serum samples were over

1 day old, enough hydrolysis of urea to ammonia had occurred (as indicated by high blanks) to make the samples useless.

Procedure

The Monitrol II solution or serum (200 μl) to be assayed and 200 μl of the tris buffer were placed in the microchamber containing the enzyme stirring bar. The solution was stirred and the equilibrium pH (pH_e) recorded. The urea content of blood was read from a calibration plot of pH_e *vs.* log urea concentration, obtained with Monitrol II standards. After each run the microcell containing the immobilized enzyme stirring bar was washed under a distilled water tap for 5–10 s, and the stirring bar was patted dry with a paper towel. The electrode surface was renewed by placing the electrode on the electrode holder thus placing a fresh electrolyte layer on the electrode surface[8].

RESULTS AND DISCUSSION

Principle of Method

Many immobilized enzyme electrodes have been described for the assay of urea based on enzyme-catalyzed ammonium-releasing reactions[9–13]. Problems of selectivity for ammonium ion over Na^+ and K^+ ions commonly present in serum and urine (serum contains *ca.* $5 \cdot 10^{-3}$ *M* urea, $5 \cdot 10^{-3}$ *M* K^+ and 0.14 *M* Na^+) in the use of the ammonium ion glass electrode (Beckman 39137)[9–12] can be partially removed by the use of ion exchangers[11] or an antibiotic nonactin electrode[12,13]. Recently, a specific, simple enzyme electrode has been described for the assay of urea in blood serum[7]; the sensor used was the newly developed air-gap electrode of Růžička and Hansen[8], which has advantages of speed of response and specificity over other previously described ammonia electrodes. In this electrode the ammonia volatilized from solution diffuses to the electrode surface (F, Fig. 1), where it reacts with the ammonium ion present with a resulting decrease in the hydrogen ion concentration. The equilibrium pH indicated, pH_e, is proportional to the log $[NH_4^+]$ of the sample and hence to the concentration of urea:

$$pH_e = \log [\text{urea}]_{\text{sample}} + \text{constant} \qquad (1)$$

Immobilized enzymes (enzymes which are insolubilized and stabilized either by physical entrapment, chemical binding or microencapsulation)[2] have been proposed for many analytical purposes[1–6] including the production of highly selective enzyme electrodes[6]. However, there are even more potential applications of immobilized enzymes in the wide variety of assays performed in clinical laboratories with soluble enzymes[1,14] by spectrophotometric, fluorimetric and electrochemical methods; for example, immobilized enzyme columns and flow systems such as the AutoAnalyzer have been used[15,16].

When enzymes are directly attached to the stirrer used to mix solutions, a significant advantage for enzymatic analysis can be realized. The enzyme stirrer simultaneously mixes the solution and promotes the enzymatic transformation, the products being measured in the same reaction chamber by electrochemical, spectrophotometric or fluorimetric methods. The stirrer can then be moved, manually or automatically, to the next sample chamber, or the chamber can be automatically

flushed and the next sample introduced. Thus a rapid, simple and inexpensive assay can be achieved.

In this paper, the immobilized urease enzyme stirrer is used for the assay of urea in blood, with an air-gap electrode to monitor the ammonium ion produced. In the electrode construction used (Fig. 1), which is based on the air-gap electrode[7], the enzyme stirrer is simply placed in the microchamber which contains sample and buffer, the only reagent required. As constructed, the stirring bar has a fairly even layer of enzyme over 2/3 of its surface, and still turns easily. After a pH_e value has been recorded (about 2–3 min), the stirrer is picked out, washed for 10 s under a distilled water tap and patted dry; the band is pulled back tightly into position and the next assay can then be performed. Less than 1 min is necessary to wash the stirrer and cell and replenish the electrolyte layer on the electrode surface (Fig. 2, C–D).

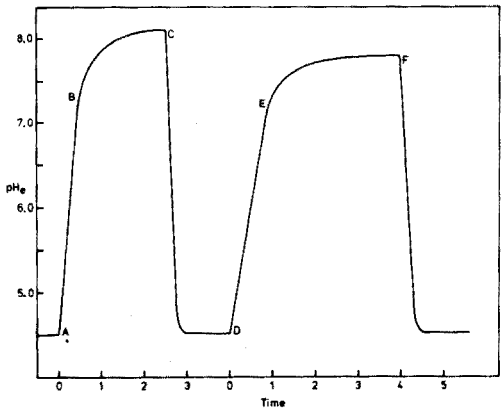

Fig. 2. Response curves for enzyme electrode. A, D, Enzyme stirrer added to cell; B, response to Monitrol II, 17.6 m*M* urea; C,F, electrode placed on electrolyte layer; E, response to Monitrol II, 6.0 m*M* urea.

As in the previous assay[7], a pH of 8.5 is used for the reaction with an ammonium ion concentration at the surface of 10^{-3} *M*. At this pH, the velocity of the enzymatic reaction is still 0.5 V_{max}, and enough free ammonia is liberated to be efficiently measured (ratio of $[NH_3]/[NH_4^+]$ is 0.18 at pH 8.5). With 10^{-3} *M* electrolyte, the response of the enzyme stirrer electrode (Fig. 2, A–C) is quite fast (about 2–3 min from the limit of detection of urea, 10^{-4} *M*, to the maximum measurable concentration, about $5 \cdot 10^{-2}$ *M*. The equilibrium pH is quite stable (Fig. 2).

Figure 3, A shows the resulting plot of pH_e *vs.* log[urea] at pH 8.5, for a newly prepared enzyme stirrer electrode. The line is linear from 10^{-2} *M* to $4 \cdot 10^{-4}$ *M*, as observed with dilutions of freeze-dried blood (Monitrol II), with a slope of 0.95, close to the theoretical value of 1.00.

Effect of enzyme stability of stirrers

Two types of immobilized enzyme were tested for use, the Boehringer Enzygel and the Corning Glass enzyme. Each was fastened to a stirring bar by a

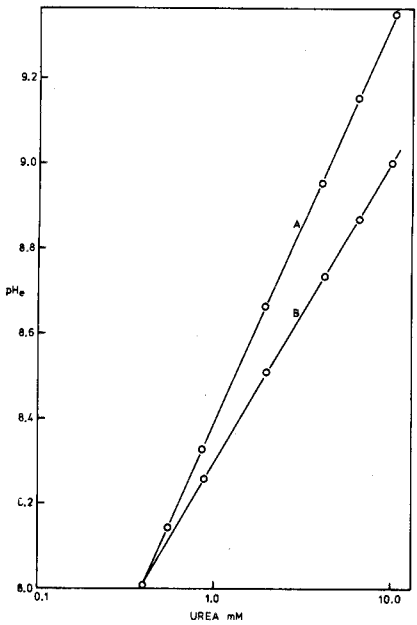

Fig. 3. Calibration curves for Monitrol II obtained with the enzyme stirrer (10 units Enzygel urease, pH 8.5, tris buffer, 0.50 *M*). A, First day after preparation of stirrer; B, sixty days after preparation.

nylon net and a rubber band, and tested as described above with a series of Monitrol standards for a total of 15 weeks. Overnight the stirrers were kept in a tris buffer solution in a refrigerator.

Initially, the responses attained with the two stirrers were quite similar. A steady response was observed within 2 min with the Enzygel and within 4 min with the glass-bound enzyme. The longer response time of the latter is probably due to the larger amount of enzyme used (35 mg *vs.* 15 mg) in order to keep a constant activity level (10 units). The response time difference from the most concentrated solution to the most dilute was very small at the start (1 min).

To see if the stirrers were useful for assay of urea in blood, standard calibration plots were made for each stirrer with a series of dilutions of Monitrol II. Plots like that in Fig. 3, A, were obtained with both stirrers; the glass-bound enzyme stirrer had a slope of 1.05, and the Enzygel a slope of 0.95, both close to the theoretical value of 1.00. A comparison with a plot for ammonium chloride indicated that both electrodes converted about 70% of the urea to ammonia (ΔpH_e between the Monitrol II and NH_4Cl curves was about 0.2 units, compared to the theoretical value of 0.3 ΔpH for two ammonium ions produced from each urea). The results of analyses of 4 urea serum standards with the 2 stirrers are shown in Table I. Samples from 1.80 to 18.0 m*M* (Monitrol II) were analyzed 3–5 times each. Good accuracy and excellent precision ($s_r = 1.5$–2.1%) were obtained.

As time passes and the electrode is subjected to considerable use, two things happen: (a) the slope of the calibration plot decreases from 0.95 to 0.70, as shown for the Enzygel stirrer in Fig. 3, B; this happens because the enzyme can no longer convert all the urea to ammonia, especially at high concentrations; and (b) the

TABLE I

ANALYSIS OF SERUM STANDARDS

Urea (mM)	*Stirrer 1*[a]	*Stirrer 2*[b]
18.0	18.5	18.4
9.00	8.65	9.40
3.60	3.66	3.50
1.80	1.83	1.87
	$s_r = 1.50\%$	$s_r = 2.10\%$

[a] Chemically bound enzyme—3 or more determinations.
[b] Glass bound enzyme—3 or more determinations.

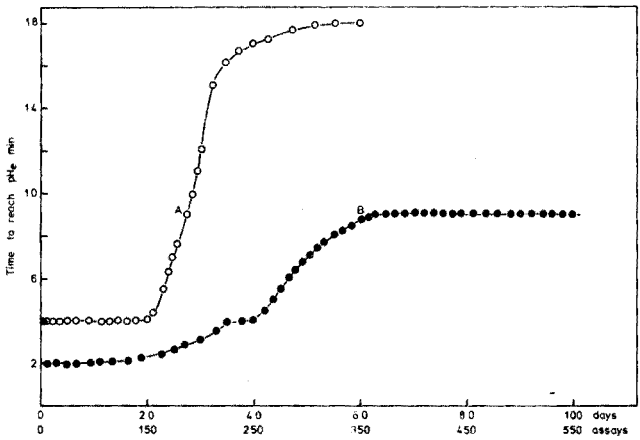

Fig. 4. Stability of enzyme stirrer. Time to reach pH_e response for Monitrol II (9 m*M* urea) as a function of number of days from preparation and number of assays. A, glass-bound enzyme stirrer; B, Enzygel enzyme stirrer.

response time for each stirrer increases as shown in Fig. 4. After 20 days or 150 assays, the response time of the glass-bound enzyme stirrer increased from 4 min to 18 min at 60 days or 350 assays, while the response time of the Enzygel enzyme stirrer for 9 m*M* Monitrol increased from 2 min to 4 min at 40 days (250 assays) and then to 9 min at 60 days. The response time then stayed constant to 100 days or 550 assays. The stirrer, however, was still useful for assays as shown in Fig. 3, B.

To compare the glass-bound enzyme to the chemically bound Enzygel further, a series of experiments was performed in which the enzyme was placed at the bottom of the microcell under the nylon net, in a technique described previously for the Enzygel enzyme[7]; overnight the enzyme was covered with tris buffer. A plot similar to that of Fig. 4, A was obtained for the glass-bound enzyme; the initial response time was about 3.5 min increasing to 12 min after 10 days. A calibration plot similar to that of Fig. 3, A, was initially obtained, with a slope of 0.98; after 15 days, it was no longer possible to obtain a good calibration plot. The Enzygel by comparison[7] was useful for 450 assays or 4 weeks.

These results indicate that a good, workable enzyme stirrer is possible, that can be used for over 500 assays. The chemically bound Enzygel works much better than the glass-bound Corning enzyme in these stirrers (20 days good operational stability compared to about 40 days for the Enzygel), although the glass-bound enzyme has been used for much longer periods in other applications[17,18].

Assay of blood

The results of analyses of 9 blood samples from Rigshospitalet in Copenhagen, performed at the hospital by the colorimetric diacetyl AutoAnalyzer procedure, and by the enzyme stirrer electrode, given in Table II, show excellent agreement, an average difference of only $\pm 1.8\%$ being observed. The assays (3 runs or more on each sample) show a relative standard deviation of only $\pm 2.0\%$. This indicates the enzyme stirrer is indeed an excellent tool for simple and direct assays of urea in blood.

TABLE II

ANALYSIS OF BLOOD SAMPLES

Sample no.	*Urea (mM)*[a]	*Urea (mM)*[b]	*Difference (%)*
1	29.7	29.4	+1.0
2	9.20	9.2	0
3	4.10	4.2	−2.4
4	16.1	15.8	+1.9
5	6.3	6.6	−4.5
6	4.06	4.0	+1.5
7	34.6	35.6	−3.1
8	6.70	6.7	0
9	4.80	4.9	−2.1
		Av. difference	±1.8

[a] Enzygel stirrer method; three or more runs; $s_r = \pm 2.0\%$.
[b] Performed by the AutoAnalyzer.

Conclusions

The utility of an enzyme stirrer containing Enzygel urease for the direct assay of urea has been demonstrated. The method is fast (2–3 min response time), economical (one enzyme sample is useful for several hundred assays), reliable (accuracy and precision about 2%), specific (no interferences from Na^+, K^+, NH_4^+ or other substances in blood), reagentless (only a buffer is needed) and easy to perform.

Such enzyme stirrers can be made for use in spectrophotometric and fluorimetric assays, and results of such studies will soon be published. Although a very useful stirrer results from the use of enzyme placed on a Teflon coated stirring bar, other such enzyme stirrers can be made in many other ways, *e.g.* by direct attachment of the enzyme to a glass stirrer by simple methods[17,18]. Many assays done with soluble enzymes can probably be performed with an immobilized enzyme stirrer with significant advantages.

The financial support of the Danish Natural Science Research Council in the form of a Guest Professorship (G.G.G.) and for this research is gratefully acknowledged. We wish to thank Dr. Jørgen Melchior Rasmussen of Rigshospitalet, Copenhagen, for providing the sera used; Professors Růžička and Hansen for many valuable discussions and assistance with the air-gap electrode; Dr. Dieter Jaworek, Boehringer, Mannheim GmbH, for the sample of high-purity Enzygel urease; and Mr. H. Weetal, Corning Glass Company, for the sample of glass-bound urease.

SUMMARY

A specific simple enzyme stirrer electrode is described for the assay of urea in blood serum. The enzyme is placed directly on a magnetic stirrer and held in place with a nylon net. The enzyme stirrer both stirs the solution and effects an enzymatic transformation, permitting the direct assay of a substrate such as urea. Potassium, Na^+, NH_4^+ and other organic and inorganic species present in blood do not interfere. Linear curves are obtained from $5 \cdot 10^{-2}$ M to $1 \cdot 10^{-4}$ M urea with slopes close to Nernstian, 0.95 pH/decade. Urea in blood was assayed with an accuracy of 1.8% and a precision of 2.0% with immobilized urease in the stirrer. The stirrers were used for 15 weeks and over 500 assays with excellent results.

REFERENCES

1 G. G. Guilbault, *Enzymatic Methods of Analysis*, Pergamon, London, 1969.
2 H. H. Weetall, *Anal. Chem.*, 46 (1974) 602A.
3 O. R. Zaborsky, *Immobilized Enzymes*, CRC Press, Cleveland, Ohio, 1973.
4 G. G. Guilbault, *Biotechnol. Bioeng.*, 3 (1972) 361.
5 G. G. Guilbault, *CRC Critical Reviews in Analytical Chemistry*, 1 (1970) 377.
6 G. G. Guilbault, in H. Weetall (Ed.), *Enzyme Electrode Probes in Immobilized Enzymes*, M. Dekker, New York, 1975.
7 G. G. Guilbault and M. Tarp, *Anal. Chim. Acta*, 73 (1974) 355.
8 J. Růžička and E. Hansen, *Anal. Chim. Acta*, 69 (1974) 129.
9 G. G. Guilbault and J. G. Montalvo, *J. Amer. Chem. Soc.*, 91 (1969) 2164; *Anal. Lett.*, 2 (1969) 283; *J. Amer. Chem. Soc.*, 92 (1970) 2533.
10 G. G. Guilbault, R. K. Smith and J. G. Montalvo, *Anal. Chem.*, 41 (1969) 600.
11 G. G. Guilbault and E. Hrabankova, *Anal. Chim. Acta*, 52 (1970) 287.
12 G. G. Guilbault and G. Nagy, *Anal. Chem.*, 45 (1973) 417.
13 G. G. Guilbault, G. Nagy and S. S. Kuan, *Anal. Chim. Acta*, 67 (1973) 195.
14 H. Bergmeyer, *Methods of Enzymatic Analysis*, Academic Press, New York, 2nd Edn., 1974.
15 M. Weibel, W. Dritschilo, H. Bright and A. Humphrey, *Anal. Biochem.*, 52 (1973) 402.
16 D. J. Inman and W. Hornby, *Biochem. J.*, 129 (1972) 255.
17 H. H. Weetall, *Science*, 166 (1969) 615.
18 H. H. Weetall, N. B. Havewala, W. Pitcher, C. C. Detar, W. P. Van and S. Yaverbaum, *Biotechnol. Bioeng.*, 16 (1974) 295.

Analytica Chimica Acta, 76 (1975) 245–251

A POTENTIOMETRIC ASSAY OF CHOLINESTERASE

K. GIBSON and G. G. GUILBAULT*

Chemistry Department A, Technical University of Denmark, 2800 Lyngby (Denmark)

(Received 10th October 1974)

There has been an accelerated interest in the use of ion-selective electrodes during the past decade, because of their increased availability and reliability[1,2]. Several attempts have been made to apply these sensors to measurements of enzyme activity[3–8]. Enzyme reactions involving cyanide[3,6,8], or organic sulfides[5,7] have been monitored directly, and reactions involving hydrogen peroxide indirectly by coupling with an iodide–iodine indicator reaction and measuring the change in iodide activity[4,6].

Cholinesterase, an enzyme of clinical interest, catalyzes the reaction:

$$R\text{–}COYCH_2CH_2N^+(CH_3)_3 + H_2O \rightleftarrows RCOO^- + H^+ + HYCH_2CH_2N^+(CH_3)_3$$

where Y = O or S. Two cholinesterases of different specificity and origin are present in man[9]. One occurs in erythrocytes, nerve endings and the grey matter of the brain, and the second in liver, pancreas, heart and serum. It is the second enzyme, normally referred to as serum cholinesterase, which is of clinical interest.

The determination of serum cholinesterase activity has significance in the following areas: (1) diagnosis—low values indicate liver disease, high values nephrotic syndrome; (2) toxicology—cholinesterase is inhibited by drugs (alkaloids, prostigmine, neostigmine), and by pesticides (organophosphorus and carbamates); and (3) detection of genetic diseases— individuals with low serum cholinesterease levels have a low tolerance to succinyl dicholine, a drug used as a muscle relaxant in surgery. If undetected, this defect can lead to prolonged post-operative apnea. The atypical enzyme is detected by measuring enzyme activity both with and without addition of an inhibitor, usually dibucaine.

One common accepted method for determination of serum cholinesterase involves the use of acetylthiocholine as substrate[10]. The thiocholine liberated is detected by its reaction with 5,5′-dithio-bis(2-nitrobenzoic acid) to give a colored 5-thio-2-nitrobenzoate. This method has been automated[11] and has an analysis time of about 20 min and a precision of about 5%.

The hydrolysis of choline esters in the physiological pH range results in a release of protons. If the reaction is carried out in a sufficiently weak buffer, this will result in a measurable pH change, and the rate of change of pH can be related to enzyme activity. This has formed the basis of several methods for cholinesterase assay: the methods of Michel[12] (change in pH in 1 h measured wih a glass electrode), of Lavery[13], and Rappaport[14], in which the pH change is monitored

* Guest Professor of Analytical Chemistry on leave from University of New Orleans, Louisiana.

spectrophotometrically with an indicator, and of Chouteau[15]—a pH-stat method.

Guilbault and von Storp[7] have proposed a flow-stream method for cholinesterase using acetylthiocholine as substrate and 2 thiol electrodes as sensors. Although useful, this method is limited by the erratic, sometimes irreproducible, response of the sulfide electrode in the presence of biological fluids. An enzyme-sensing electrode system for cholinesterase formed by coupling a pH sensing electrode to a thin polymer membrane with low-molecular cutoff, and using two thin-layered solutions to form a micro electrochemical cell, was described by Crochet and Montalvo[16].

The method developed herein is more practical in design and is comparable in speed to the spectrophotometric method, being able to analyse 40 samples per hour in the automated form. It is based on the fact that under certain conditions the enzymatic reaction can result in a linear change of pH with time. This follows from: (1) the form of the titration curve of a buffer, since within the range $pH = pK_a \pm 0.2$ this is a very good approximation to a straight line; and (2) the kinetic parameters K_m and V_{max} for cholinesterase, which are insensitive to pH in the range 7.5–8.5. Therefore by choosing tris(hydroxymethyl)aminomethane (tris, $pK_a = 8.1$) as the buffer, and by running the reaction at pH 8.2–7.9, the initial rate of the enzyme reaction could be obtained from the straight line response of pH *vs.* time.

Preliminary experiments were made to test the feasibility of this approach and to optimize the reaction conditions (method I), and then the procedure was put on a continuous flow basis with Auto Analyzer equipment (method II).

EXPERIMENTAL

Reagents

Buffer for method I. Dissolve 0.242 g of tris (2 mmole), 9 g of sodium chloride and 10 ml of 0.10 *M* hydrochloric acid in redistilled water and dilute to 1 l. The pH is 8.10–8.15. The sodium chloride is added to ensure constant ionic strength and to stabilize the electrode response.

Buffer for method II. Use 4 m*M* tris buffer containing 0.9%(w/w) sodium chloride at a pH of 8.15.

Substrate. Prepare a stock 25 m*M* solution of acetylcholine chloride in the appropriate buffer.

Enzyme

Dissolve horse serum cholinesterase (Merck, Darmstadt, W. Germany—4 I.U. mg^{-1}) in redistilled water. Serum samples were obtained frozen from Rigs-hospital, Copenhagen, and Monitrol (freeze-dried preanalyzed serum, Dade, Miami, Florida), was reconstituted with redistilled water. In method II, the serum samples were diluted 1 + 14 with water.

Apparatus

Method I. The reaction cell (Fig. 1) was constructed from a polythene beaker of diameter 2 cm and height 3 cm fitted with a tight-fitting lid. Holes in the lid were made to place a flat-tipped glass electrode and a calomel electrode (Radio-

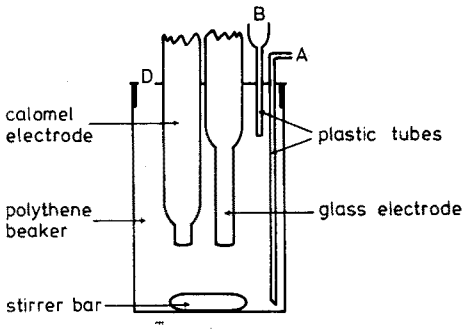

Fig. 1. Reaction cell for method I.

meter, Copenhagen, models G 267C and K 401, respectively) and thin plastic tubes A and B. An additional hole D was used for addition of sample with a micropipette. The vessel was immersed in a water bath placed over a magnetic stirrer which actuated a 1-cm stirring bar. The electrode response was recorded on a Radiometer Servograph REC 51 equipped with a high-sensitivity unit REA 112 adjusted so that 0.1 pH unit corresponded to 5 cm on the paper, and on a Radiometer pH meter, model 51.

Method II: continuous flow approach. The flow-cell constructed for use with a Radiometer GK2320C combined glass–calomel electrode is shown in Fig. 2. It was used in conjunction with an Auto Analyzer Sampler II and Proportioning Pump II as shown in Fig. 3. The electrode response was recorded as in Method I above.

Assay procedures

Method I. Equilibrate the water bath and stock substrate solution at 25°C. Using a calibrated syringe, add 3.0 ml of substrate–buffer (10 m*M* acetylcholine chloride for the assay of cholinesterase) to the cell via tube B which is then connected to a supply of nitrogen. The gas flow ensures that no drops remain in the tube and is continued throughout the experiment to prevent entry of CO_2. When a steady pH

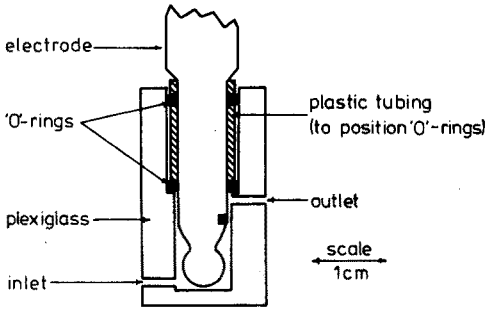

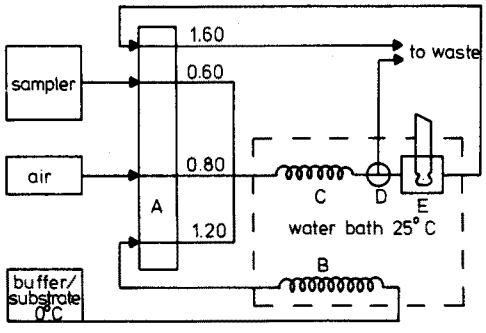

Fig. 2. Construction of flow-cell for glass–calomel electrode type GK 2320 C.

Fig. 3. Flow diagram for AutoAnalyzer. Numbers are flow rates in ml min^{-1}. (A) proportionating pump, (B) delay coil (5 min), (C) mixing coil, (D) debubbler, (E) flow cell. Reaction time 3.6 min.

reading is observed, add 100 μl of the enzyme sample and record the pH change for *ca.* 2 min. Then suck the contents of the beaker to waste via tube A and wash the system with 4 ml of distilled water (added through B and removed through A). Measurements can be made at the rate of 12 per hour.

For calibration of the system, add 100-μl aliquots of standard acetic acid instead of the enzyme samples. The resulting pH jumps are used to: (1) check the strength of the buffer; and (2) facilitate a conversion of the observed reaction rate units from ΔpH min^{-1} to μmoles H^+ released min^{-1}.

Method II. Place the substrate solution (25 m*M* in buffer) in an ice bath. Operate the samples at a sample-to-wash ratio of 2:1 (*i.e.* t s sample, $\frac{1}{2}t$ s distilled water, t s next sample, etc.) and at sampling speeds between 10 and 40 per h. The reaction time is *ca.* 3.6 min, and the water bath temperature is 25°C. The various flow rates are given in Fig. 3.

RESULTS

Method I

The effect on the initial reaction rate of varying the acetylcholine chloride concentration from 0.4 to 20 m*M* was investigated for a constant concentration of horse serum cholinesterase. From the results shown in Figs. 4 and 5, the values $K_m = 1.65$ m*M* and $V_{max} = 0.465$ per mole H^+ min^{-1} were obtained, which are in excellent agreement with previously found values[10–15].

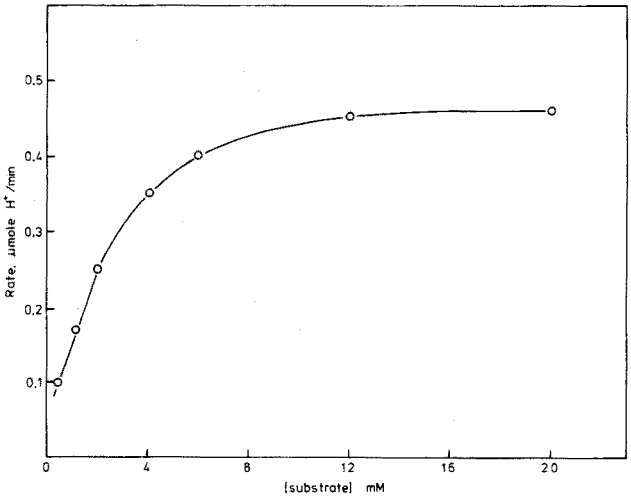

Fig. 4. Reaction rate as a function of substrate concentration. 100 μl of enzyme solution (1 mg ml^{-1}) added to 3.0 ml of substrate in 2.0 mM tris, pH 8.1, 25°C.

Figure 6 shows some typical rate curves obtained in these experiments. From such curves, a plot of the observed rate, in μmole H^+ min^{-1} *vs.* enzyme concentration, in I.U./100 μl of sample added, can be constructed. In a typical run a rectilinear plot was found over the range 0.1–0.9 I.U. cholinesterase per 100 μl of sample, the rate increasing from about 0.06 to almost 1 μmole H^+ min^{-1}. The

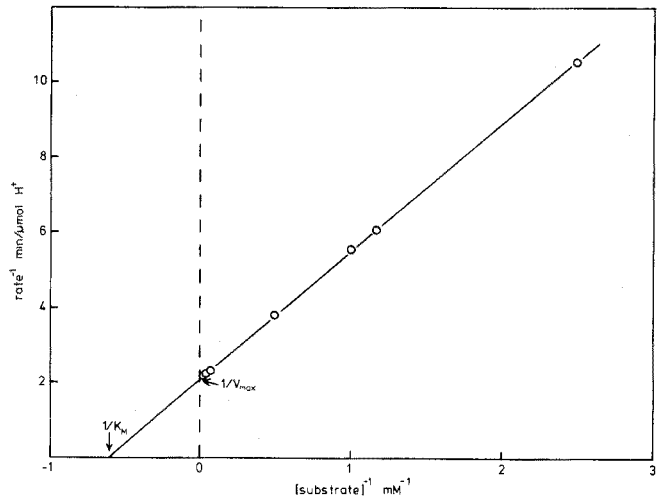

Fig. 5. Double reciprocal plot of data in Fig. 4. $K_m = 1.65$ mM, $V_{max} = 0.465$ μmole min^{-1}.

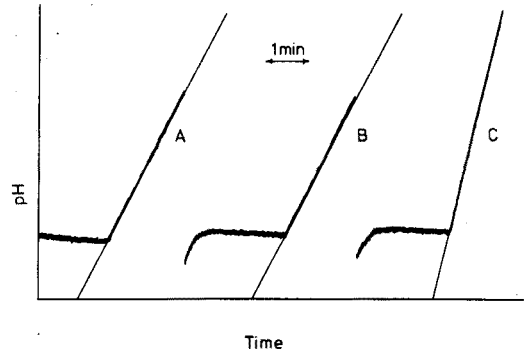

Fig. 6. Example of recorder output for method I. Substrate 10 mM acetylcholine chloride; buffer 3.0 ml 2 mM tris, pH 8.12; 25°C. (A, B) 0.70 units cholinesterase, slope 0.075 pH min^{-1} (C) 1.4 units cholinesterase, slope 0.512 pH min^{-1}.

range of enzyme activities used here corresponds to the limits normally found in human serum[9].

Measurements on serum samples were used to test the reproducibility of the method. The mean and standard deviations (in parenthesis) from five assays on human serum pool and five assays on Monitrol II were 0.688 (0.025) and 0.346 (0.021) μmole H$^+$ min^{-1}, respectively.

Method II

The response time of the system (95% of final response) was 25–30 s for pH changes of 0.2 units, stable readings being first reached after 90 s. Analyses could therefore be run at up to 40/h without appreciable loss of accuracy. An example of the recorder output is reproduced in Fig. 7. In one experiment enzyme samples containing 0.317, 0.238, 0.158 and 0.0776 I.U. enzyme ml^{-1} were each run 10 times over

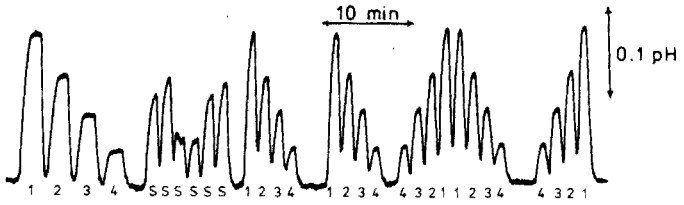

Fig. 7. Example of recorder output for continuous flow determination of cholinesterase. 1, 2, 3 and 4 indicate standards, S indicates serum samples.

a period of 1.5 h. The mean peak height in cm and standard deviations (in parentheses) were 7.78 (0.16), 5.77 (0.07), 3.93 (0.08) and 1.90 (0.10), or an average relative standard deviation of 2.6%. The calibration graph plotted from these data was a straight line through the origin. Again this calibration covers the limits of cholinesterase activity expected in the diluted serum samples. In all experiments the base line drifted slowly (*ca.* 0.02 pH units h^{-1}) owing to spontaneous decomposition of the substrate.

DISCUSSION

The above results show that cholinesterase can be assayed rapidly and accurately by monitoring the pH change with a glass electrode. However, the method has limitations since factors other than the hydrolysis of acetylcholine may result in a change of pH of the very weak buffer used.

The horse serum enzyme was dissolved in distilled water and these solutions had negligible buffer capacity and did not interfere. However, normal serum has an appreciable buffer capacity, mainly because of H_2CO_3/HCO_3^- equilibria[9], and with the dilution of 1+30 described in method I jumps in pH of up to ± 0.02 pH units were observed on addition of sample. Moreover, these jumps depended on the age of the serum samples, since on standing carbon dioxide is lost from serum to the air, and ammonia is produced by decomposition[9], both factors causing a pH drop. As method I leads to a continuous rate recording, a small initial jump is unimportant. However the continuous flow approach affects a single measurement after a fixed time and thus requires a constant starting pH in order to determine a reaction rate. Therefore a stronger buffer and a greater dilution of serum were used on the AutoAnalyzer, together with a longer reaction time. While no significant pH jumps were observed when fresh samples of Monitrol were used under these conditions, before the method can be used with confidence on routine serum samples, it must be demonstrated that such interference never occurs. A possible way round this problem would be to use two electrodes in series to measure the pH after mixing and again after a suitable interval.

The absorbance of atmospheric carbon dioxide by the buffer was a second problem source. In method I the system was protected by nitrogen. In the continuous flow method the system is closed, apart from the samples which stand open on the sampler rack. One of the cholinesterase assay procedures performed in the clinical laboratory is that of dibucaine inhibition studies. This involves preincubation of the sample with the inhibitor at known pH and temperature. This cannot be conveniently carried out with the present apparatus owing to the risk of significant absorbance of carbon dioxide during incubation.

Conclusion

In conclusion, cholinesterase activity can readily be obtained from the linear rate of change of pH of a weak tris buffer at a pH around its pK_a value, measured with a glass electrode. However, possible interference from other acid–base equilibria might pose some problems in routine clinical analysis.

The financial support of the Danish Natural Science Research Council in the form of a Guest Professorship for one of us (G.G.G.) and a post-doctoral fellowship for the second (K.G.) is gratefully acknowledged. Thanks are also extended to Rigshospitalet of Copenhagen for providing the serum samples used.

SUMMARY

Methods are described for the assay of cholinesterase activity, based on the linear rate of change of pH of a weak tris buffer at a pH around its pK_a value, measured with a glass electrode. Two methods are proposed: one a static semi-automatic method capable of doing up to 12 assays per hour, the second an automated continuous flow approach which does 40 assays per hour. The methods developed are practical in design and are comparable in speed to automated spectrophotometric methods. The precision obtained (2.6%) is better than that obtained with the spectrophotometric method (5.0%).

REFERENCES

1 R. P. Buck, *Anal. Chem.*, 46 (1974) 28R.
2 G. J. Moody and J. D. R. Thomas, *Talanta*, 19 (1972) 623.
3 M. Mascini and A. Liberti, *Anal. Chim. Acta*, 64 (1974) 177.
4 T. T. Ngo and P. D. Shargool, *Anal. Biochem.*, 54 (1973) 247.
5 G. Baum and F. B. Ward, *Clin. Chim. Acta*, 36 (1972) 405.
6 R. A. Llenado and G. A. Rechnitz, *Anal. Chem.*, 44 (1972) 1366; 44 (1972) 468; 45 (1973) 826.
7 G. G. Guilbault and H. von Storp, *Anal. Chim. Acta*, 62 (1972) 425.
8 G. G. Guilbault, W. F. Gutknecht, S. S. Kuan and R. Cochran, *Anal. Biochem.*, 46 (1972) 206.
9 N. W. Tietz, *Fundamentals of Clinical Chemistry*, Saunders, 1970.
10 A. A. Dietz, H. M. Rubinstein and T. Lubrano, *Clin. Chem.*, 19 (1973) 1309.
11 W. Gerhardt, *Rigshospitalets Centrallaboratorium A, Analyseforskrift no. 730-15*, 1971.
12 H. O. Michel, *J. Lab. Clin. Med.*, 34 (1949) 1566.
13 T. D. Lavery, *Clin. Chim. Acta*, 43 (1973) 143.
14 F. Rappaport, J. Fischl. and N. Pintio, *Clin. Chim. Acta*, 4 (1959) 227.
15 J. Chouteau, P. Rancien and A. Karamanicin, *Bull. Soc. Chim. Biol., (Paris)*, 38 (1956) 139.
16 K. L. Crochet and J. G. Montalvo, *Anal. Chim. Acta*, 66 (1973) 259.
17 K. J. Laidler, *Trans. Faraday Soc.*, 51 (1955) 550.

Analytica Chimica Acta, 76 (1975) 253–259

POTENTIOMETRIC GAS SENSORS FOR AMMONIA BASED ON ION-SELECTIVE ELECTRODES FOR SILVER(I), COPPER(II) AND MERCURY-(II)

TORBJÖRN ANFÄLT, ANDERS GRANELI and DANIEL JAGNER

Department of Analytical Chemistry, University of Göteborg, Fack, S-402 20 Göteborg 5 (Sweden)

(Received 18th November 1974)

Since the introduction of the carbon dioxide sensor[1–3], various sensors of the same type have become commercially available. It was, however, not until recently that potentiometric sensors for gases other than carbon dioxide were developed. Thus, sensors for ammonia, sulfur dioxide, nitrogen dioxide, hydrogen sulfide and hydrogen cyanide are today commercially available. A thorough treatment of the theory of operation of these sensors has been given by Ross *et al.*[4]. The ammonia sensor is based on the same principle as the carbon dioxide sensor, *i.e.* the pH of the internal electrolyte, separated from the sample solution by a gas-permeable membrane, is measured with a glass electrode[5]. Another type of potentiometric gas sensor, where the gas-permeable membrane is replaced by an air gap, has been developed by Růžička and Hansen[6]. With this type of potentiometric gas sensor, Růžička and Hansen measured the content of urea in blood by enzymatic conversion of urea to ammonia. The ammonia content in waste water has also been determined with this sensor[7]. In this Department, an urea electrode[8] was developed with the enzyme directly fixed on to the gas diffusion membrane of an Orion ammonia probe. In the search for a better indicator electrode than the high-impedance glass electrode used by Orion, attention was turned to the complexation reactions between ammonia and silver(I), copper(II) or mercury(II). Instead of measuring the change in pH of the internal electrolyte, the change in pM, where M is Ag^+, Cu^{2+} or Hg^{2+}, could be measured by means of the ion-selective electrode for the metal ions involved. The systems involving silver and copper have also been proposed by Ross *et al.*[4].

THEORY

A potentiometric gas sensor contains an internal electrolyte separated from the sample solution by a hydrophobic gas-permeable membrane. An indicator and a reference electrode are immersed in the internal electrolyte and made to fit almost exactly in the outer electrode body in order to minimize the total volume of electrolyte. For example, as reference electrode, a fluoride-sensitive electrode may be used if the internal electrolyte contains fixed levels of fluoride ions. The indicator electrodes used here are precipitate-based electrodes sensitive to Ag^+, Cu^{2+} or Hg^{2+}. When the gas sensor is immersed into a sample solution containing ammonia, the partial pressure of the gas will cause it to diffuse across the

gas-permeable membrane until a steady concentration of ammonia is reached in the internal electrolyte. If this contains silver(I), copper(II) or mercury(II), complex formation will occur between these and ammonia according to

$$M^{n+} + iNH_3 \rightleftharpoons M(NH_3)_i^{n+}$$

where the metal ion is denoted by M^{n+} and the complex formation number by i. The cumulative complex formation constant for the equilibrium is defined as

$$\beta_i = [M(NH_3)_i^{n+}]/[M^{n+}][NH_3]^i \qquad (i=1,2,3\ldots N)$$

The total metal concentration can be expressed as

$$[M]_{tot} = [M^{n+}]\left(1 + \sum_{i=1}^{N} \beta_i [NH_3]^i\right)$$

Thus, the free metal concentration is

$$[M^{n+}] = [M]_{tot}/\left(1 + \sum_{i=1}^{N} [NH_3]^i\right) \qquad (1)$$

The indicator electrode measures the activity of M^{n+} in the small volume region between the gas-permeable membrane and the tip of the electrode according to

$$E = E^0 + RT(\ln 10)\log[M^{n+}]/nF \qquad (2)$$

Equation (1) substituted into eqn. (2) gives

$$E = E^{0\prime} - RT(\ln 10)\log\left(1 + \sum_{i=1}^{N} \beta_i [NH_3]^i\right)/nF \qquad (3)$$

where

$$E^{0\prime} = E^0 + RT(\ln 10)\log[M]_{tot}/nF$$

If $\sum_{i=1}^{N} \beta_i [NH_3]^i \gg 1$, eqn. (3) is reduced to

$$E = E^{0\prime} - RT(\ln 10)\log\left(\sum_{i=1}^{N} \beta_i [NH_3]^i\right)/nF \qquad (4)$$

and thus the electrode responds to changes in ammonia concentrations. Since the potentiometric gas sensor primarily measures $[M^{n+}]$, a theoretical response of the electrode could be obtained by varying $[NH_3]$ and calculating $[M^{n+}]$. In an internal electrolyte solution consisting of ammonium nitrate, metal nitrate and sodium fluoride, the metal ion may, however, be involved in other equilibria than that with ammonia.

Hydroxide and fluoride complexes may, for instance, be formed. Calculating $[M^{n+}]$ as a function of ammonia concentration could thus be rather complicated, but with the aid of the computer program HALTAFALL[9,10] it is easily accomplished. In the calculations it has been assumed that the ammonia concentration is equal on both sides of the membrane. The set of equilibria considered for each case i.e. Ag^+, Cu^{2+} or Hg^{2+}, together with the stability constants chosen[11] are listed in Table I.

If there is no initial ammonium concentration in the internal electrolyte,

TABLE I

CONSTANTS CHOSEN FOR THE CALCULATION OF M^{n+} AS A FUNCTION OF NH_3 IN AN INTERNAL ELECTROLYTE OF NH_4NO_3, $M(NO_3)_n$ AND NaF

Equilibria	*log (stab. const.)*	*Equilibria*	*log (stab. const.)*
$H^+ + NH_3 = NH_4^+$	9.24	$Cu^{2+} + OH^- = CuOH^+$	6.0
$H^+ + OH^- = H_2O$	14.00	$Cu^{2+} + 2\ OH^- = Cu(OH)_2$	13.18
$H^+ + F^- = HF$	3.18	$Cu^{2+} + 3\ OH^- = Cu(OH)_3^-$	14.42
$Ag^+ + NH_3 = AgNH_3^+$	3.31	$Cu^{2+} + 4\ OH^- = Cu(OH)_4^{2-}$	14.56
$Ag^+ + 2\ NH_3 = Ag(NH_3)_2^+$	7.21	$Cu^{2+} + F^- = CuF^+$	1.23
$0.5\ Ag_2O + 0.5\ H_2O = Ag^+ + OH^-$	− 8.17	$Hg^{2+} + NH_3 = HgNH_3^{2+}$	8.8
$Ag^+ + OH^- = AgOH$	3.02	$Hg^{2+} + 2\ NH_3 = Hg(NH_3)_2^{2+}$	17.5
$Ag^+ + 2\ OH^- = Ag(OH)_2^-$	4.69	$Hg^{2+} + 3\ NH_3 = Hg(NH_3)_3^{2+}$	18.5
$Ag^+ + F^- = AgF$	0.38	$Hg^{2+} + 4\ NH_3 = Hg(NH_3)_4^{2+}$	19.3
$Cu^{2+} + NH_3 = CuNH_3^{2+}$	4.15	$Hg^{2+} + OH^- = HgOH^+$	10.3
$Cu^{2+} + 2\ NH_3 = Cu(NH_3)_2^{2+}$	7.65	$Hg^{2+} + 2\ OH^- = Hg(OH)_2$	21.7
$Cu^{2+} + 3\ NH_3 = Cu(NH_3)_3^{2+}$	10.54	$Hg^{2+} + F^- = HgF^+$	1.03
$Cu^{2+} + 4\ NH_3 = Cu(NH_3)_4^{2+}$	12.67	$Hg(OH)_2(s) = Hg^{2+} + 2\ OH^-$	−25.4
$CuO(s) + H_2O = Cu^{2+} + 2OH^-$	−18.3		

ammonia will be readily consumed by the metal ions forming metal–ammonia complexes. In order to minimize this mass transport, which considerably increases the response time of the electrode, ammonium nitrate is used to buffer the internal solution. For example, in the case of silver(I) the following equilibrium is set up

$$2\ NH_4^+ + Ag^+ \rightleftharpoons Ag(NH_3)_2^+ + 2\ H^+$$

The equilibrium constant is $10^{-11.27}$, compared with $10^{7.21}$ in the case of an ammonium nitrate-free internal solution.

EXPERIMENTAL

Apparatus

The indicator electrode used in the experiments was a Radiometer Selectrode[12]. This electrode consists of a hydrophobized graphite rod which can be made sensitive to the metal ion by rubbing the electroactive material, *i.e.* HgS, Ag_2S or a mixture of Ag_2S and CuS, into its tip. The reference electrode used was an Orion fluoride electrode. The gas-permeable membranes (Fluoropore, 1-μm pore size), made of teflon with a polyethylene backing[13] were obtained from Millipore. E.m.f. readings were made on a Fluke 8200 digital voltmeter incorporated in a data acquisition and processing computer system developed in this department[14].

Reagents

The potentiometric gas sensor was calibrated in 0.1 *M* sodium hydroxide by additions of ammonium chloride. The internal electrolyte solutions were all 0.01 *M* in sodium fluoride and 0.1 *M* in ammonium nitrate in addition to the various concentrations of silver, copper or mercury nitrates.

RESULTS AND DISCUSSION

The calculated calibration curves for the three potentiometric ammonia sensors based on the Ag_2S, Ag_2S/CuS and HgS electrodes respectively are shown in Figs. 1–3. The calculations were performed for a total concentration of 10 m*M* silver nitrate, 1 m*M* copper(II) nitrate and 1 m*M* mercury(II) nitrate, respectively, in addition to the 0.1 *M* ammonium nitrate and 10 m*M* sodium fluoride used in all three cases. The logarithmic values of the free metal ion concentration obtained from the HALTAFALL program calculation were converted to *E* mV by the Nernst equation for an arbitrary E^0 value. This was done to put the theoretical calibration curves on scale with those obtained experimentally for convenient comparison.

Theoretical and experimental calibration curves agree well in the silver system (Fig. 1). The slope of the linear part of the experimental curve is 107.5 mV/log[NH_3] compared with 118 mV/log[NH_3] for the theoretical curve. The calculation shows that the $Ag(NH_3)_2^+$-complex is dominant in the high concentration region. Equation 4 will thus be simplified to

$$E = E_0 - 2RT \ln 10 \log[NH_3]/F$$

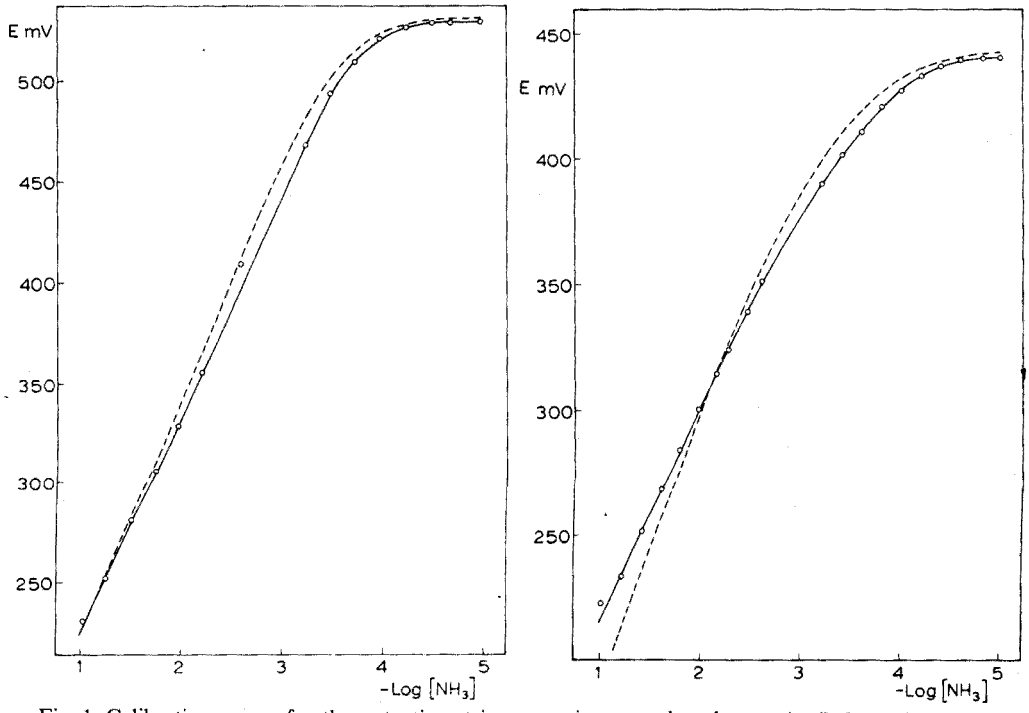

Fig. 1. Calibration curves for the potentiometric ammonia sensor based on a Ag_2S-electrode and an internal electrolyte of 10 mM $AgNO_3$, 0.1 M NH_4NO_3 and 10 mM NaF. Theoretical curve (---). experimental curve (—).

Fig. 2. Calibration curves for the potentiometric ammonia sensor based on a CuS/Ag_2S-electrode and an internal electrolyte of 1 mM $Cu(NO_3)_2$, 0.1 M NH_4NO_3 and 10 mM NaF. Theoretical curve (---), experimental curve (—).

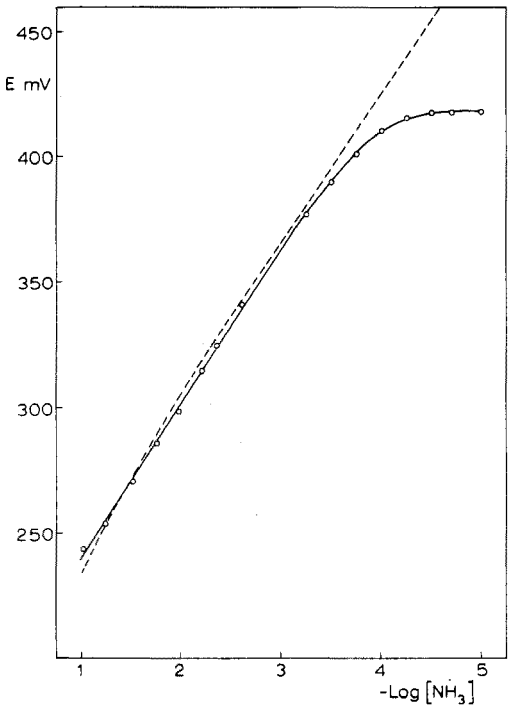

Fig. 3. Calibration curves for the potentiometric ammonia sensor based on a HgS-electrode and an internal electrolyte of 1 mM $Hg(NO_3)_2$, 0.1 M NH_4NO_3 and 10 mM NaF. Theoretical curve (---), experimental curve (—).

As can be seen from eqn. (3) the electrode responds to ammonia only if $[NH_3] > \beta_2^{-0.5} \approx 10^{-3.6}$ M, which is in excellent agreement with the experimental value.

The response time of this electrode system was measured by rapidly changing the ammonia concentration in the sample from 10^{-3} M to 10^{-2} M. The result is shown in Fig. 4. A 90% response was obtained within 5 s, and a 99% response within 17 s. However, in case of a sudden decrease of the ammonia concentration, the response time is somewhat greater.

The copper-sulfide based electrode system shows no completely linear region in the calibration curve (Fig. 2). This is because none of the four copper–ammonia complexes listed in Table I is completely dominant in the concentration region investigated. However, the shape of the experimental curve corresponds well with the theoretical curve. The shape of the latter depends very much on the choice of K_{so} for CuO (Table I), since for slightly smaller values of this constant, a precipitate is formed. No precipitate, however, was observed during the calibration. The response time of this electrode is approximately the same as for the silver sulfide-based electrode. The copper sulfide-based electrode can be used for ammonia concentrations greater than 10^{-4} M.

The mercury-sulfide based electrode system shows a deviation from the theoretical behaviour in the region of low ammonia concentration (*cf.* Fig. 3).

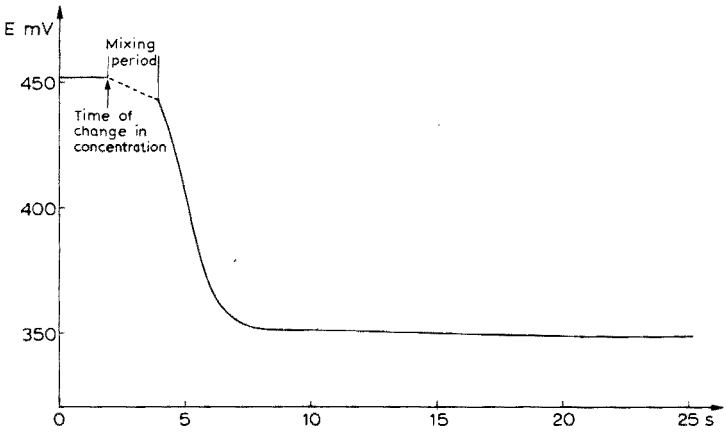

Fig. 4. Response of the potentiometric ammonia sensor, based on a Ag_2S-electrode, to a sudden change in ammonia concentration from 10^{-3} *M* to 10^{-2} *M*.

This is probably due to the difficulty in preparing a homogeneous membrane of mercury(II) sulfide. Cracks are formed in the electroactive membrane where mercury(II) ions may then be absorbed. This absorption will be more pronounced the greater the free mercury(II) concentration. In low ammonia concentrations, *i.e.* high mercury(II) concentrations, a deviation from the theoretical curve may be expected. This can be seen in Fig. 3. The mercury sulfide electrode was separately calibrated against mercury(II) concentrations by the "metal buffer procedure"[15]. The electrode showed a Nernstian behaviour in the low concentration region ($<10^{-8}$ *M*). However, major difficulties arose when the electrode was calibrated in the concentration region 10^{-6}–10^{-3} *M*, owing to a sluggish response of the electrode. This can probably be attributed to absorption on the electrode surface.

In ammonia concentrations greater than $10^{-3.5}$ *M*, the electrode behaves as predicted from theory, and from the calculations it is shown that $Hg(NH_3)_2^{2+}$ dominates. Thus eqn. (4) is reduced to:

$$E = E_0 - RT \ln 10 \log[NH_3]/F$$

The theoretical response, 59.2 mV/log[NH_3] is in good agreement with the experimental value 60.8 mV/log[NH_3]. However, the response time of this electrode is greater than that of the two previous ones.

Conclusions

The potentiometric gas sensor based on the selective silver or copper electrode is well suited to measurements of ammonia concentrations greater than $10^{-3.5}$ *M*. The response of the sensors is approximately 100 mV/log[NH_3] which enhances the accuracy of the measurement. Moreover, the response time is shorter than for sensors based on a glass electrode, and, owing to their lower impedance, the sensors are less susceptible to electrostatic noise. The potentiometric gas sensor based on mercury(II) sulfide can also be used as a sensor for ammonia concentrations higher than $10^{-3.5}$ *M*. However, if a completely homogenous HgS membrane could be prepared, it would be possible to use the sensor in concentrations of ammonia considerably less than $10^{-3.5}$ *M*.

The authors express their gratitude to Professor David Dyrssen for valuable discussions. Grants from the Swedish Natural Science Council and Knut och Alice Wallenbergstiftelsen are gratefully acknowledged. We are also indebted to Mrs. Enrica Ratti-Moberg for revising the English text.

SUMMARY

Potentiometric gas sensors sensitive to ammonia were prepared with ion-selective electrodes for silver(I), copper(II) or mercury(II). These electrodes measure the degree of the complexation between the metal ions and ammonia. Ammonia concentrations above $10^{-3.5}$ *M* can be measured by these sensors. The response to changes in ammonia concentrations is rapid. The Ag^+- and Cu^{2+}-based sensors gave a response of approximately 100 mV/log[NH_3] while the Hg^{2+}-based sensor gave a 60 mV/log[NH_3] response.

REFERENCES

1 R. Stow, R. Baer and B. Rondall, *Arch. Phys. Med. Rehabil.*, 38 (1957) 646.
2 W. Sveringhaus and A. Bradley, *J. App. Physiol.*, 13 (1958) 515.
3 C. Hertz and B. Siesjö, *Acta Physiol. Scand.*, 47 (1959) 115.
4 J. Ross, J. Riseman and J. Kreuger, *Plenary Lecture, International Symposium on Selective Ion-Sensitive Electrodes, Cardiff, 1973.*
5 *Instruction Manual for Ammonia Electrode Model 95-10*, Orion Research Inc., Cambridge, U.S.A.
6 J. Růžička and E. Hansen, *Anal. Chim. Acta*, 69 (1974) 129.
7 J. Růžička and E. Hansen, *Anal. Chim. Acta*, 72 (1974) 215.
8 T. Anfält, A. Graneli and D. Jagner, *Anal. Lett.*, 6 (1973) 969.
9 N. Ingri, W. Kakolowicz, L. Sillén and B. Warnqvist, *Talanta*, 14 (1967) 1261; 15 (1968) p. xi.
10 D. Dyrssen, D. Jagner and F. Wengelin: *Computer calculation of Ionic Equilibria and Titration Procedures*, Almqvist and Wiksell, Stockholm, 1968, pp. 66–80.
11 L. Sillén and A. Martell, *Stability Constants*, The Chemical Society, London.
12 J. Růžička, C. Lamm and J. Tjell, *Anal. Chim. Acta*, 62 (1972) 15.
13 *Millipore Specification List on Fluorocarbon Filtration Elements, Bulletin MB 411.*
14 T. Anfält and D. Jagner, *Anal. Chem.*, in press.
15 E. Hansen, G. Lamm and J. Růžička, *Anal. Chim. Acta*, 59 (1972) 403.

Analytica Chimica Acta, 76 (1975) 261–268

SOLID-STATE ION-SELECTIVE ELECTRODES AS END-POINT DETECTORS IN COMPLEXIMETRIC TITRATIONS

PART I. THE TITRATION OF MIXTURES OF TWO METALS

J. M. VAN DER MEER, G. DEN BOEF and W. E. VAN DER LINDEN

Laboratory for Analytical Chemistry, University of Amsterdam, Nieuwe Achtergracht 166, Amsterdam (The Netherlands)

(Received 30th December 1974)

Potentiometric titrations have several advantages over direct potentiometric measurements in the determination of electroactive materials. For several reasons, this is especially true when ion-selective electrodes are used for the determination of metal ions. First, most of the currently available ion-selective electrodes do not exhibit long-term stable sensitivity. Furthermore, the sensitivity is often not constant over the entire concentration range. Perhaps the greatest inconvenience of ion-selective electrodes, however, is that although they are selective they are rarely specific, which results in interferences by other substances in direct measurements. Direct potentiometric determinations are therefore restricted to well defined samples in which there is no influence of other compounds or for which the influence of other substances is accurately known.

When interfering substances are present, titrimetric procedures are often possible, because only changes of concentration are used for the end-point determinations. The error in the end-point caused by the presence of interfering ions has been discussed by Schultz[1].

In the present paper the complexiметric titration of mixtures of metal ions by means of an ion-selective electrode is discussed. A copper(II)-sensitive CuS/Ag_2S precipitate-based electrode, developed by Růžička *et al.* and already successfully applied to the determination of copper(II)[2], was used. A theoretical treatment[3] of titration curves for complexiметric titrations by means of potentiometric indication with a mercury electrode could be used in this case.

The problems associated with the use of this type of solid-state electrode are discussed, as well as the possibilities for logarithmic and linear end-point indication.

THEORETICAL TITRATION CURVES

The relationship between the titration parameter f and the metal ion concentrations [M] and [N] for the complexiметric titration of a mixture of two metal ions M and N with a ligand L, with the simplification that the volume does not change during the titration, is given by:

$$f = 1 - \frac{[M]}{c} + \frac{c_M}{c}\frac{1}{[M]K_{ML}} - \frac{c_N}{c}\frac{1}{(c_M/[M]-1)K_{NL}/K_{ML}+1} - \frac{1}{cK_{ML}} \qquad (1)$$

and

$$[N] = \frac{c_N}{(c_M/[M]-1)K_{NL}/K_{ML}+1} \tag{2}$$

in which c_M, c_N and c_L are the concentrations of M, N and L in any form; $c = c_M + c_N$; [M] and [N] are the concentrations of the metal ions M and N in any form, the chelates ML and NL excepted; $f = c_L/c$ is the titration parameter; and K_{ML} and K_{NL} are the conditional stability constants of the complexes ML and NL.

In order to obtain a theoretical titration curve (f *vs.* E), an equation for the cell potential is needed. The cell consists of a solid-state electrode sensitive for the metal ion M in a solution containing the metal ions M and N, and a reference electrode.

The slightly modified Nikolsky equation, used by Rechnitz and Lin[4] in their study on complexiметric titrations with potentiometric end-point indication, was used:

$$E = E'' + S \log\left\{\frac{\gamma_M[M]}{\alpha_M} + K_{M,N}\frac{\gamma_N[N]^{Z_M/Z_N}}{\alpha_N}\right\} \tag{3}$$

in which E is the cell potential; E'' is a potential value depending on the standard potential of the ion-selective electrode, the type of reference electrode and the liquid-junction potentials; $K_{M,N}$ is the selectivity coefficient of the electrode for the metal ion N; Z_M and Z_N are the charges of the metal ions M and N, respectively; γ_M and γ_N are the activity coefficients for M and N; S is the slope factor of the electrode response; and α_M and α_N are the overall side-reaction coefficients for M and N.

In the present work, a copper(II)-selective electrode was used. In most cases, the metal ion N was a divalent ion so that $Z_M/Z_N = 1$ and $\gamma_M = \gamma_N$. For these conditions, eqn. (3) can be converted to the more practicable form:

$$E = E' + S \log\{[Cu] + K'_{Cu,N}[N]\} \tag{4}$$

in which

$$E' = E'' + S \log\frac{\gamma_{Cu}}{\alpha_{Cu}}$$

and

$$K'_{Cu,N} = K_{Cu,N}\frac{\alpha_{Cu}}{\alpha_N}$$

which could be called a conditional selectivity coefficient. This has to be modified in the case of non-divalent metal ions.

When [M] and [N] reach very low values, the cell potential is finally determined by the limit of detection of the electrode, which is mainly set by the solubility of the electrode material. This limit D_{Cu} is not a constant but depends on the conditions in the solutions. Thus, finally, the equation which allows calculation of the theoretical titration curves is:

$$E = E' + S \log\{[Cu] + K'_{Cu,N}[N] + D_{Cu}\} \tag{5}$$

EXPERIMENTAL

Reagents

All solutions were prepared from analytical reagent-grade chemicals and redistilled water. Metal ions were added as sulphates or nitrates.

The Ag_2S/CuS (1 : 1) precipitate was prepared by homogeneous precipitation from a solution containing the metal ions and thioacetamide as described by Růžička *et al.*[2].

Apparatus

All measurements were carried out with a Beckman-Electroscan in its pH mode; the recorder span was 150 mV/250 mm.

The reference electrode was a Beckman satuated calomel electrode with an asbestos fibre junction.

The ion-selective electrode body was simply a piece of Teflon tube (length 50 mm; diameter 5 mm) in which a piece of "Eriflon" Teflon–graphite (75%/25% w/w; length 12 mm; diameter 6 mm; Eriks, Alkmaar, The Netherlands) had been pressed. Electrical contact was made by a brass screw and a rust-proof steel wire hot-soldered to the screw. The Teflon–graphite surface was polished on polishing paper grade 4/0. Then some of the sulphide was rubbed on the surface until a thin shining layer covered the surface. In order to remove any free copper(II) from the electroactive surface the electrodes were conditioned in 10^{-3} *M* EDTA for 24 h. To avoid electrical noise, the rotor of the magnetic stirrer was driven by air.

Calibration of the electrodes

The electrodes were calibrated for several pH values with solutions of copper(II) for concentrations down to 10^{-5} *M* and with metal buffer solutions[2] for concentrations lower than 10^{-5} *M*. Selectivity coefficients were determined by the method suitable for low $K_{M,N}$ values, described by Srinavasan and Rechnitz[5].

The limit of detection of the electrode was determined as a function of the free ligand concentration.

Procedure for potentiometric titrations

The solution (10 ml) containing the metal ions and buffered at pH 4.75 with $5 \cdot 10^{-2}$ *M* acetate buffer, was placed in the titration vessel; 5- or 10-μl increments of titrant were added each 2 min from a Metrohm microburette E 457. The concentration of the titrant was such that between 100 and 200 μl were needed to reach the equivalence point.

RESULTS

The theoretical titration curves were calculated by means of eqn. (5). In the presence of iron, the equation has to be adapted by taking $K'_{Cu,Fe(III)}[Fe(III)]^{\frac{2}{3}}$. The numerical values in this equation were determined for the experimental conditions of the titrations, *i.e.* $5 \cdot 10^{-2}$ *M* acetate buffer pH 4.75. The following values were obtained: $E' = 361.2$ mV; $S = 32.4$ mV; $K'_{Cu,Fe(III)} = 2 \cdot 10^{-2}$; $K'_{Cu,Ni} = 5 \cdot 10^{-4}$; $K'_{Cu,Mn} = 3 \cdot 10^{-4}$; $K'_{Cu,Zn} = K'_{Cu,Cd} = 10^{-3}$.

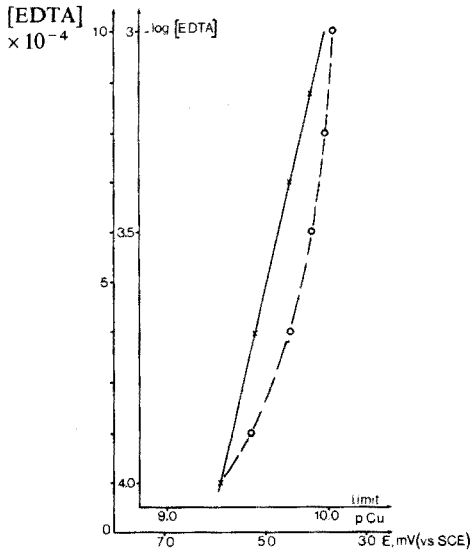

Fig. 1. Experimental electrode limit D_{Cu} as a function of the ligand concentration. (—○—) Plot of [EDTA] *vs.* the potential, (—×—) plot of log [EDTA] *vs.* the potential or the corresponding pCu value.

The limit of detection, D_{Cu}, appears to be a function of [L]. Figure 1 presents this limit as a function of the concentration of the free ligand. The plot log [L] *vs.* pD_{Cu} appears to produce a straight line in this concentration range.

Conditional stability constants of all complexes involved were taken from Ringbom[6].

f–E Curves

Figure 2 gives the theoretical curve of a mixture of 10^{-3} *M* copper(II) with 10^{-3} *M* iron(III), nickel(II), cadmium(II) and manganese(II). Figure 3 gives the corresponding experimental curves, which agree very well with the theoretical ones. Correct end-points can be obtained only for the sum of both metals, except in the case of the mixture of copper(II) and manganese(II) where the amount of copper(II) can be found individually from the titration curve.

Figures 4 and 5 give the theoretical and experimental curves for equimolar mixtures of copper(II) and zinc(II) at different concentrations. There is a good agreement between theory and experiment for 10^{-3} *M* and 10^{-4} *M* solutions and the sum of the concentrations of the two metal ions can be found from the titration. Curve C, which is the curve for the mixture of 10^{-5} *M* copper(II) and 10^{-5} *M* zinc(II) needs some comment; the line in Fig. 4 before the equivalence point does not take into account the limit of detection, whereas the line after the equivalence point is the curve of the detection limit D_{Cu} as a function of the free EDTA concentration, partly taken from Fig. 1, but extrapolated to lower values of the free EDTA concentration. From the experimental curve C in Fig. 5, it can be seen that the limit of detection begins to affect the titration curve already at about $f=0.5$. The result is that no correct end-point can be obtained in this case. Figures

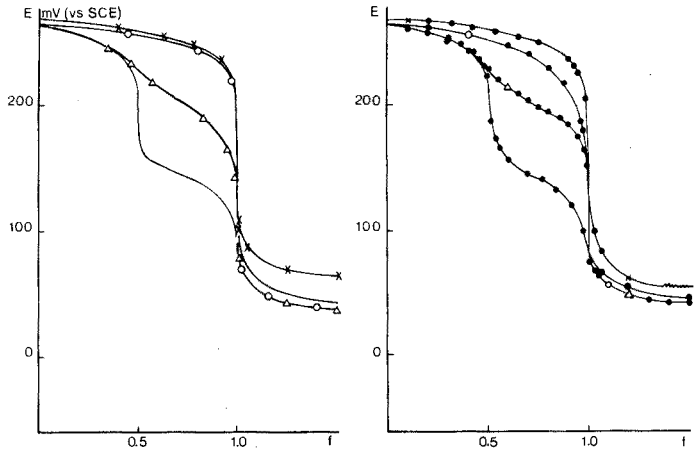

Fig. 2. Theoretical titration curves for a mixture of 10^{-3} *M* copper(II) with 10^{-3} *M* iron(III) (—×—), nickel(II) (—○—), cadmium(II) or zinc(II) (—△—), and manganese(II) (——), with EDTA as the ligand.

Fig. 3. Experimental curves, corresponding to Fig. 2.

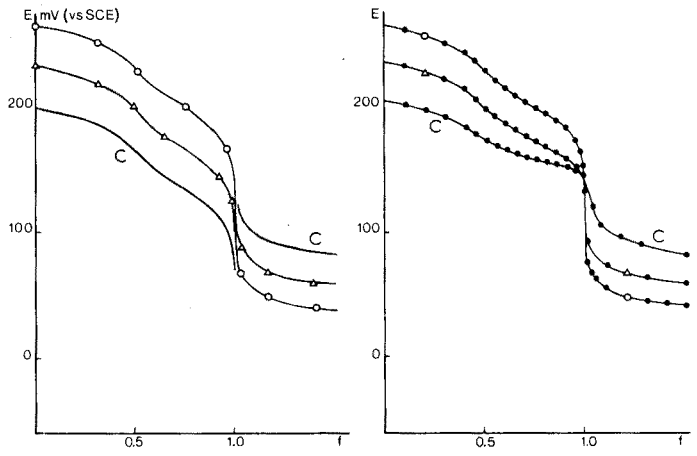

Fig. 4. Theoretical titration curves for equimolar mixtures of copper(II) and zinc(II) of different concentrations with EDTA as the ligand. (—○—) 10^{-3} *M*, (—△—) 10^{-4} *M*, (——) 10^{-5} *M*.

Fig. 5. Experimental curves, corresponding to Fig. 4.

6–9 show the theoretical and experimental titration curves for 10^{-3} *M* and 10^{-4} *M* cadmium(II) in the presence of decreasing concentrations of copper(II). The curves with the lowest concentrations of copper(II) represent the use of copper(II) as an indicator ion for the determination of cadmium(II). All experimental curves show a behaviour similar to that in previous cases. The agreement between theory and experiments is good and the determination of 10^{-3} *M* and 10^{-4} *M* cadmium(II) appears to be possible.

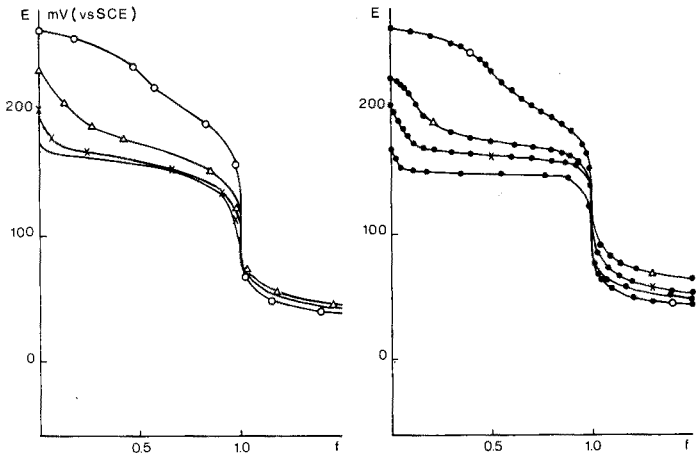

Fig. 6. Theoretical titration curves for 10^{-3} *M* cadmium(II) in the presence of decreasing concentrations of copper(II) with EDTA as the ligand. (—○—) 10^{-3} *M*, (—△—) 10^{-4} *M*, (—×—) 10^{-5} *M*, (——) 10^{-6} *M*.

Fig. 7. Experimental curves, corresponding to Fig. 6.

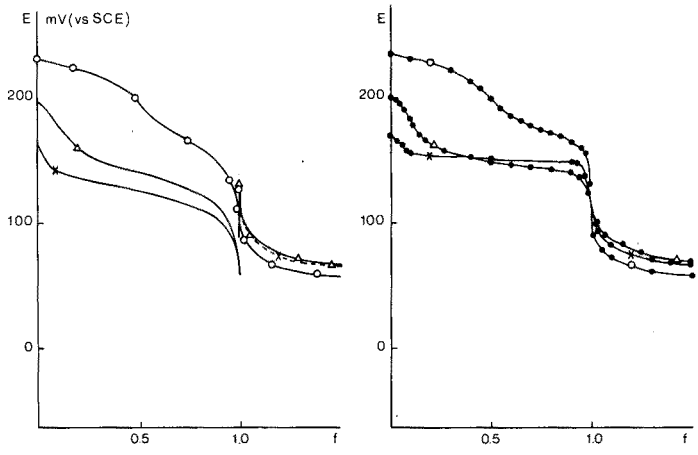

Fig. 8. Theoretical titration curves for 10^{-4} *M* cadmium(II) in the presence of decreasing concentrations of copper(II) with EDTA as the ligand. (—○—) 10^{-4} *M*, (—△—) 10^{-5} *M*, (—×—) 10^{-6} *M*.

Fig. 9. Experimental curves, corresponding to Fig. 8.

f–[M] Curves

As the *f–E* curves do not always produce satisfactory end-points, an attempt was made to calculate the concentration of [M] from the potential measurements in order to draw *f*–[M] curves. These linear titration curves are often helpful when *f–E* curves fail. Equation 5 can be written as

$$10^{(E-E')/S} = [\mathrm{Cu}] + K'_{\mathrm{Cu,N}}[\mathrm{N}] + D_{\mathrm{Cu}} \qquad (6)$$

where N is a divalent ion.

In all cases mentioned above the following condition holds for the conditional stability constants: $K'_{CuEDTA} \gg K'_{NEDTA}$, when N is a divalent ion. Therefore copper(II) is complexed first. A plot of f *vs.* $10^{(E-E')/S}$ will then produce an end-point from which the concentration of copper(II) can be found. When the electrode is not sensitive for N, a second end-point in the plot f *vs.* $10^{(E-E')/S}$ corresponding to the concentration of N may occur, caused by a change in the copper(II) concentration during the complexation of N. When, however, the electrode is selective for N as well, though to a slighter extent, the plot of f *vs.* $10^{(E-E')/S}$ after the first end-point will be mainly determined by the second term at the right-hand side of eqn. (6). This is the case in the examples presented in this paper and this obviously also results in a second end-point in the f *vs.* $10^{(E-E')/S}$ plot.

Figure 10 shows some results of these plots for the titration of solutions which are equimolar in copper(II) and zinc(II) (10^{-3}, 10^{-4} and 10^{-5} M). At all three concentration levels, the first end-point, corresponding to the determination of copper is sharp, even for 10^{-5} M. The second end-point is good for 10^{-3} M and 10^{-4} M but not for 10^{-5} M, obviously because of the influence of the detection limit of the electrode in the latter case. Similar results were obtained for solutions equimolar in copper(II) and cadmium(II).

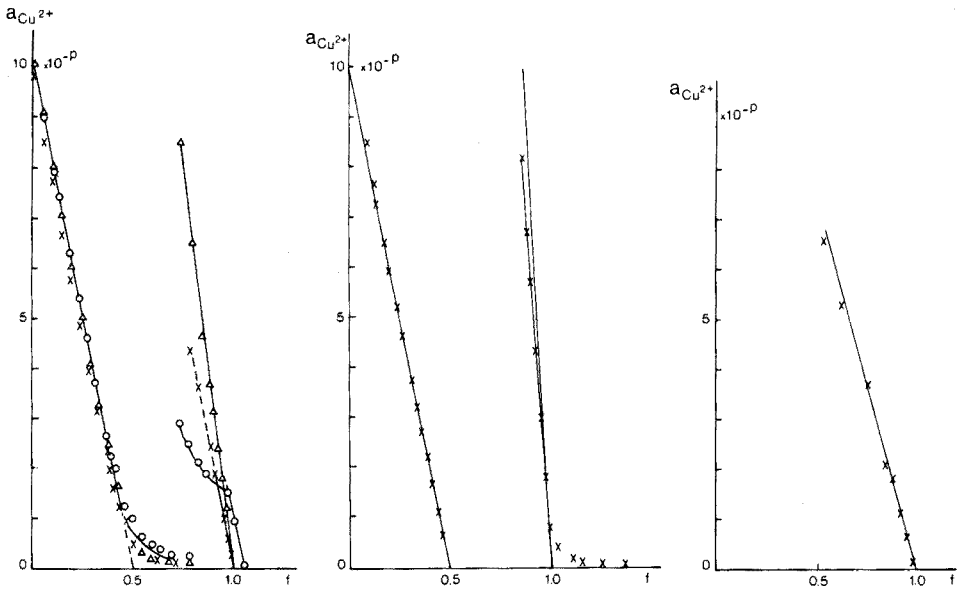

Fig. 10. Theoretical and experimental plots of the copper(II) activity *vs.* the titration parameter for equimolar mixtures of copper(II) and zinc(II). (——) Theoretical, (×) 10^{-3} M, (△) 10^{-4} M, (○) 10^{-5} M. For $f<0.5$: $p_{\times}=4$, $p_{\triangle}=5$, $p_{\bigcirc}=6$. For $f>0.5$: $p_{\times}=6$, $p_{\triangle}=7$, $p_{\bigcirc}=7$.

Fig. 11. Theoretical and experimental plots of the copper(II) activity *vs.* the titration parameter for a mixture of 10^{-3} M copper(II) with 10^{-3} M manganese(II). (——) Theoretical, (×) experimental. For $f<0.5$, $p=4$; for $f>0.5$, $p=8$.

Fig. 12. Theoretical and experimental plots of the copper(II) activity *vs.* the titration parameter for a mixture of 10^{-3} M copper(II) with 10^{-3} M iron(III). (——) Theoretical, (×) experimental. $p=4$.

Figure 11 shows that both end-points are also sharp for a mixture of 10^{-3} M copper(II) and 10^{-3} M manganese(II). In the case of 10^{-3} M copper(II) and 10^{-3} M iron(III) (Fig. 12), only the sum of the two metal ion concentrations can be found, which is also to be expected theoretically. In all cases, the experimental curves closely agree with the theoretical curves.

When, within the concentration range 10^{-3}–10^{-5} M, the concentration of copper(II) is much smaller than that of the other metal ion ($c_{Cu} < 0.5\ c_N$), sharp linear end-points no longer occur. When, within the same concentration range, the concentration of copper(II) is much larger than that of the other metal ion, the first end-point will be correct (determination of copper(II)), but the second end-point cannot be determined, because of the influence of the detection limit.

DISCUSSION

The solid-state copper(II)-sensitive CuS/Ag_2S precipitate-based electrode ("Selectrode") appears to be very suitable for the complexiметric determination of mixtures of copper(II) and another metal ion.

Potentiometric titration curves as well as linearized curves produce very well defined end-points even for 10^{-5} M solutions. The copper concentration preferably should be determined by means of a linearized curve, and the sum of both metal ions by an ordinary potentiometric curve.

SUMMARY

The complexiметric titration of mixtures of copper(II) and other metal ions by means of potentiometric indication with a copper(II)-selective electrode has been investigated. The theoretical titration curves have been calculated, the effects of the selectivity of the electrode and the limit of detection of the electrode being taken into account. The experimental curves generally agree very well with the theoretical curves. Determinations in the range 10^{-3}–10^{-5} M are possible.

REFERENCES

1 F. A. Schultz, *Anal. Chem.*, 43 (1971) 1523.
2 J. Růžička, C. G. Lamm and J. Chr. Tjell, *Anal. Chim. Acta*, 62 (1972) 15.
3 U. Hannema and G. den Boef, *Anal. Chim. Acta*, 39 (1967) 167.
4 G. A. Rechnitz and Z. F. Lin, *Anal. Chem.*, 40 (1968) 696.
5 K. Srinavasan and G. A. Rechnitz, *Anal. Chem.*, 41 (1969) 1203.
6 A. Ringbom, *Complexation in Analytical Chemistry*, Interscience, New York, 1963.

Analytica Chimica Acta, 76 (1975) 269–277

SOME ALKYLPHOSPHORIC ACID ESTERS FOR USE IN COATED-WIRE CALCIUM-SELECTIVE ELECTRODES

PART I. RESPONSE CHARACTERISTICS

R. W. CATTRALL and D. M. DREW*

Department of Inorganic and Analytical Chemistry, La Trobe University, Bundoora 3083, Victoria (Australia)

I. C. HAMILTON

Department of Chemistry, Footscray Institute of Technology, Footscray 3011, Victoria (Australia)

(Received 24th October 1974)

The development of the calcium-selective electrode from the very early work of Luther[1] to the more recent report by Ross[2] of the liquid membrane electrode has recently been described[3]. The various commercially available electrodes are normally based on a liquid membrane consisting of the calcium salt of a di-alkylphosphoric acid dissolved in a water-immiscible diluent such as dioctylphenyl-phosphonate. As pointed out by Růžička *et al.*[3], the most successful attempt to convert the liquid membrane in these electrodes to a solid-state type has been made by Moody *et al.*[4,5] who combined the organic liquid with polyvinyl chloride.

Several attempts have been made to eliminate the internal aqueous reference system in these electrodes. The first was reported by Cattrall and Freiser[6] who coated a platinum wire with a polyvinyl chloride film containing the Orion liquid cation exchanger 92-20-01. This produced a functional electrode with characteristics quite similar to the commercial liquid membrane electrode. This technique has received some criticism[3,7,8], because of the apparent lack of a well defined internal reference system in the electrode; the point is discussed in more detail below. Another technique was reported by Ansaldi and Epstein[9], who applied a poly-vinyl chloride membrane similar to that of Moody *et al.*[4,5] direct to a graphite rod substrate. A third technique was proposed by Růžička *et al.*[3], who constructed a polyvinyl chloride membrane electrode containing an internal reference system composed of a calomel paste on the teflon–graphite surface of a Selectrode[10]; Růžička *et al.* recommended di-(n-octylphenyl)phosphoric acid as the liquid ion-exchanger.

It should be noted that in all of these polyvinyl chloride membrane electrodes the composition of the membranes is quite similar. They contain the calcium salt of an alkylphosphoric acid as the electroactive material.

In this paper, the use of a number of commercially available alkylphosphoric acids in the construction of coated-wire calcium-sensitive electrodes is reported.

---

* Present address: Research Laboratory, Kodak (Australasia) Pty. Ltd., Coburg, Victoria 3058, Australia.

EXPERIMENTAL

Materials

The following phosphoric acid esters were investigated: di-(2-ethylhexyl)phosphoric acid (HDEHP; B.D.H. Laboratory reagent grade), di-n-octylphosphoric acid (HDOP; City Chemical Corporation, New York, code D2896), di-n-octadecylphosphoric acid (HDODP; Aldrich Chemical Co.), iso-octylphosphoric acid (IOPA, 70/30 mixture of di/mono-esters, Mobil Chemical Co., Richmond, Virginia), and octylphenylphosphoric acid (OPPA, 70/30 mixture of di/mono-esters, Mobil Chemical Co., Richmond, Virginia). All these esters were used without purification. In addition, the di- and mono-esters were separated from octylphenylphosphoric acid by the procedure given below.

Where possible formula weights were determined by titration with sodium hydroxide in an aqueous ethanolic medium. HDEHP (found: 321, calculated: 322); HDOP (found: 318, calculated: 322); di-n-octadecylphosphoric acid was not soluble enough for titration and hence was subjected to elemental analysis (found: 70.5% C, 12.2% H, 5.8% P; calculated for $C_{36}H_{75}O_4P$: 71.6% C, 12.4% H, 5.1% P).

Polyvinyl chloride (PVC; Monsanto Co.) and tetrahydrofuran (May and Baker reagent grade) were used as received. Platinum wire (0.028-in. diam.) was normally used without surface preparation. Di-(2-ethylhexyl)-2-ethylhexylphosphonate (DEHEHP; Mobil Chemical Co., Richmond, Virginia) was used as received; (found: 68.6% C, 12.0% H, 7.6% P; calculated for $C_{24}H_{51}O_3P$: 68.9% C, 12.2% H, 7.4% P). All other chemicals were of laboratory reagent grade.

Separation of octylphenylphosphoric acid. The commercially available octylphenylphosphoric acid consists of a 70/30 mixture of the di/mono-esters ($(RO)_2POOH$ and $(RO)PO(OH)_2$ respectively, where R is $C_8H_{17}C_6H_4$). The esters were separated by a procedure similar to that of Stewart and Crandall[11] as modified by Griffiths *et al.*[12].

Dissolve *ca.* 10 g of the light amber, waxy solid in 50 cm^3 of benzene and extract with ten 50-cm^3 portions of ethylene glycol. Wash the benzene solution twice with 200 cm^3 of water to remove traces of ethylene glycol, dry over anhydrous sodium sulphate and evaporate the solvent. Di-(n-octylphenyl)phosphoric acid (HDOPP) was obtained as a white, waxy solid (m.p. 94–95°C). (Found: 70.8% C, 9.3% H, 6.5% P; calculated for $C_{28}H_{43}O_4P$: 71.0% C, 9.1% H, 6.6% P.) Titration with sodium hydroxide in a 50% (v/v) aqueous ethanolic medium yielded a formula weight of 470 (theoretical 474).

Wash the combined ethylene glycol extracts twice with 200 cm^3 of benzene and add 500 cm^3 of water. The solution turns milky-white. Adjust the pH to about 1 with 6 *M* hydrochloric acid and extract the mono-ester into 200 cm^3 of diethyl ether. Wash the ether layer twice with 250 cm^3 of water, dry over anhydrous sodium sulphate and evaporate the solvent. The mono-octylphenylphosphoric acid (H_2MOPP) was obtained as a white amorphous solid (m.p. 92–93°C). (Found: 58.7% C, 8.0% H, 11.6% P; calculated for $C_{14}H_{23}O_4P$: 58.8% C, 8.1% H, 11.9% P.) Titration with sodium hydroxide gave a formula weight of 286 (theoretical 286).

Preparation of calcium salts

Bis(di-(2-ethylhexyl)phosphato)calcium(II). Dissolve 10 g (0.03 mole) of di-(2-ethylhexyl)phosphoric acid in 100 cm^3 of a 90% (v/v) ethanol–water mixture

and add excess of solid calcium carbonate. Shake in a separating funnel until evolution of CO_2 ceases. Filter off the excess of solid calcium carbonate and wash with boiling ethanol to remove any occluded calcium complex. Remove the solvent, leaving a white waxy solid which is recrystallized twice from ethanol. (Found: 55.0% C, 10.2% H, 9.4% P; calculated for $C_{32}H_{68}O_8P_2Ca$: 56.2% C, 10.0% H, 9.1% P.)

Bis(di-n-octylphosphato)calcium(II). Prepare as above and recrystallize twice from ethanol, to yield a white waxy solid. (Found: 55.5% C, 10.1% H, 10.1% P; calculated for $C_{32}H_{68}O_8P_2Ca$: 56.2% C, 10.0% H, 9.1% P.)

Bis(di-(octylphenyl)phosphato)calcium(II). Dissolve 5.0 g (0.01 mole) of di-(octylphenyl)phosphoric acid in 400 cm^3 of ethanol and 100 cm^3 of water and add 7.5 g (0.1 mole) of solid calcium hydroxide with stirring. Stir for a further 4 h, and then add 200 cm^3 of water to precipitate the calcium complex. Collect the complex, wash with water and recrystallize twice from ethanol to yield a white solid. (Found: 67.8% C, 8.6% H, 6.6% P; calculated for $C_{56}H_{84}O_8P_2Ca$: 68.1% C, 8.5% H, 6.3% P.)

Calcium complexes of the commercial mixtures. Prepare the calcium complexes of the di/mono-isooctylphosphoric acid and di/mono-octylphenylphosphoric acid as described for the di-(octylphenyl) complex. No attempt was made to separate the mixture of calcium salts for each acid, and these mixtures were used as prepared for certain electrodes.

Bis(di-n-octadecylphosphato)calcium(II). Dissolve 5.0 g (0.008 mole) of di-n-octadecylphosphoric acid in 100 cm^3 of a 75% mixture of ethanol–water. Add 50 cm^3 of the filtered supernate from a saturated calcium hydroxide solution and wash the precipitated white solid with 200 cm^3 of ethanol and 500 cm^3 of water. This method of preparation was used because the extreme insolubility of the resultant white complex prevented recrystallization. (Found: 66.6% C, 11.4% H, 5.6% P; calculated for $C_{72}H_{148}O_8P_2Ca$: 69.5% C, 12.0% H, 5.0% P.)

Monooctylphenylphosphatocalcium(II). Prepare in the same way as the di-n-octadecyl complex, because of the extreme insolubility of the complex. (Found: 47.8% C, 7.3% H, 8.9% P; calculated for $C_{14}H_{21}O_4PCa2H_2O$: 46.7% C, 7.0% H, 8.6% P.)

Preparation of electrodes[6,13]

Dissolve weighed amounts of the reagents and PVC in a minimum (3 cm^3) of tetrahydrofuran and coat a metallic bead formed on the end of a platinum wire by repeatedly dipping it into the mixture until a uniform plastic coating is obtained. Air-dry the electrode at room temperature for about one week. Wrap the exposed part of the platinum wire tightly with paraffin film and examine the bead under the microscope to check for entrapped air bubbles and membrane defects.

Many membrane compositions were investigated for each reagent to establish the optimal composition and these have been reported in detail by Drew[14]. These compositions are listed in Table I as the approximate percentage by weight of PVC and the ratio (by weight) of plasticizer (di-(2-ethylhexyl)-2-ethylhexylphosphonate) to electroactive reagent. In some cases no phosphonate plasticizer was used. Compositions A–F were used for each reagent whereas compositions G–K were used only for some reagents.

TABLE I

COMPOSITIONS (BY MASS) OF THE MEMBRANES INVESTIGATED

Mixture type	*Composition*
A	30% PVC + 10:1 DEHEHP–CaH_2X_4 (CaY, HY)[a]
B	40% PVC + 10:1 DEHEHP–CaH_2X_4 (CaH_2X_4 (CaY, HY)
C	30% PVC + 10:1 DEHEHP–CaX_2
D	30% PVC + 10:1 DEHEHP–HX
E	30% PVC + CaX_2
F	30% PVC + HX
G	50% PVC + 10:1 DEHEHP–CaH_2X_4
H	30% PVC + 1:1 DEHEHP–CaX_2
I	45% PVC + 10:1 DEHEHP–CaY
J	35% PVC + 3:1 DEHEHP–CaY
K	30% PVC + (CaY, HY)

[a] The calcium acid salts of the di-esters[5] (CaH_2X_4) were prepared by mixing a 1:2 mole ratio of the calcium salt (CaX_2) with the phosphoric acid ester (HX). In the case of the mono-ester, monooctylphenylphosphoric acid, the acid salt (CaY, HY) was prepared by mixing a 1:1 mole ratio of monooctylphenylphosphatocalcium(II) (CaY) with the free acid (HY).

TABLE II

MEMBRANE COMPOSITIONS FOR Di-n-OCTYLPHOSPHORIC ACID

Mixture type	*PVC (g)*	*DEHEHP (g)*	*CaX_2 (g)*	*HX (g)*	*% PVC*
A	0.160	0.358	0.018	0.017	28.8
B	0.247	0.364	0.018	0.018	38.2
C	0.161	0.365	0.036		28.7
D	0.190	0.382		0.036	31.3
E	0.087		0.204		30.4
F	0.085			0.200	29.8

A typical set of membrane compositions is shown in Table II.

In addition to the coated wire electrodes, some membrane electrodes were constructed by the technique of Moody *et al.*[4,5] to produce electrodes which contained an internal aqueous reference system.

Standard calcium solutions

These were prepared from a standard stock solution (0.1 *M*) of calcium chloride by dilution.

Potential measurements

An Orion Model 801 digital pH meter was used with a double-junction calomel electrode containing 1.25 *M* ammonium nitrate in the outer compartment. Generally, the most dilute solutions were measured first; if the electrode was to be transferred from a concentrated solution to a dilute one (*e.g.* 10^{-1} *M* to 10^{-5} *M*) it was washed, soaked in distilled water for 2–3 min and wiped before transfer.

Activities were calculated from the extended Debye–Hückel equation[15].

RESULTS AND DISCUSSION

Electrode conditioning

Coated wire electrodes were stored in air at room temperature. For conditioning, they were soaked in 10^{-5} *M* calcium chloride or distilled water for 1 h. The amount of water absorbed depended on the membrane composition; water was rapidly absorbed until an equilibrium hydration state was achieved, and absorption was then much slower. This was concluded from the fact that an unconditioned electrode placed in a 10^{-5} *M* calcium(II) solution exhibited an initial potential which increased by about 20 mV over 30–60 min, after which the potential remained substantially constant for 3–4 h. During the conditioning process, the membranes changed from a clear yellow colour to pale yellow with slight opaqueness. The opaqueness disappeared on storing the electrode in air for 1–2 h.

Potential responses

All the electrodes prepared (78 in number) were studied by determining their potential responses in pure aqueous calcium chloride solutions in the concentration range 10^{-5}–10^{-1} *M*. Complete sets of data for each electrode have been reported elsewhere[14]. Particular regard was given to the following characteristics: (a) region of linear response (close to Nernstian behaviour), (b) response time and stability, (c) reproducibility of gradient, and (d) short and long term reproducibility of readings.

The results for 29 electrodes are summarized in Table III; the Orion commercial liquid membrane electrode (No. 11) is included for comparison. It can be seen that electrodes 1–10 exhibit a linear response over a fairly large activity range, and that the response gradients are very close to the theoretical value. Electrodes 12–30 do not exhibit the same degree of reproducibility, but with careful standardization could be used for direct potentiometry.

Functioning electrodes could not be produced from the calcium salt of di-n-octadecylphosphoric acid, which is probably due to the extreme insolubility of the salt in organic solvents, and the consequent difficulty of obtaining homogeneous membranes. This solubility effect was reported by Ross[16] who stated that increasing the carbon chain length of the phosphoric acid ester beyond C_{16} causes precipitation or gelling in the membrane phase resulting in a lack of response because of reduced ionic mobility. Fiedler and Růžička[17] have reported some observations regarding the properties of polymer membranes which appear necessary to produce functional electrodes; one of these is that the components of the membrane should form a one-phase system. This agrees with the present observations.

The results in Table III demonstrate that superior electrodes (1, 3, 5–9) are obtained by using the calcium acid salt of the appropriate phosphoric acid ester (CaH_2X_4). This was previously observed by Griffiths *et al.*[5]. The acid salt, which according to Baes[18] has a structure which is distinct from the structures of the free acid (HX) and the neutral calcium salt (CaX_2), is prepared by mixing a 1:2 mole ratio of the neutral calcium salt with the free acid ester.

Of course, one other important requirement of an ion-selective electrode for analytical work is that it must be selective; the selectivities of the electrodes studied are reported in the following paper.

TABLE III

RESPONSE CHARACTERISTICS

No.	*Reagent*	*Composition*	*Region of linear response*		*Response gradient (mV/activity decade)*	*Response time (min)*
			Upper activity limit (M)	*Lower activity limit (M)*		
1	HDEHP	B	$1 \cdot 10^{-2}$	$2 \cdot 10^{-4}$	29.5[a,b]	5–10
2	HDEHP	E	$1 \cdot 10^{-2}$	$4 \cdot 10^{-4}$	28[a,b]	5–10
3[c]	HDEHP	A	$3 \cdot 10^{-2}$	$4 \cdot 10^{-4}$	28[a,b]	5–10
4	HDOP	E	$3 \cdot 10^{-2}$	$2.5 \cdot 10^{-3}$	30[a,b]	5–10
5[c]	HDOP	A	$3 \cdot 10^{-2}$	$5 \cdot 10^{-4}$	29[a,b]	5–10
6	IOPA	B	$3 \cdot 10^{-2}$	$2.5 \cdot 10^{-4}$	34[a,b]	10
7	OPPA	B	$3 \cdot 10^{-2}$	$1.4 \cdot 10^{-5}$	30[a,b]	10
8[c]	OPPA	A	$3 \cdot 10^{-2}$	$4 \cdot 10^{-4}$	29[a,b]	10
9	HDOPP	A	$2.5 \cdot 10^{-2}$	$6 \cdot 10^{-5}$	29[a,b]	5
10	H_2MOPP	I	$3 \cdot 10^{-2}$	$2 \cdot 10^{-4}$	27.5[a,b]	10–15
11	92-20-01	Orion liquid	$2.5 \cdot 10^{-2}$	$4 \cdot 10^{-4}$	30[a,b]	10–15
12	HDEHP	D	$3 \cdot 10^{-2}$	$1 \cdot 10^{-4}$	29[d,e]	10
13	HDEHP	F	$3 \cdot 10^{-2}$	$4 \cdot 10^{-4}$	29.5[d,e]	5–10
14	HDOP	A	$1 \cdot 10^{-2}$	$2 \cdot 10^{-4}$	30[a,e]	5
15	HDOP	B	$1 \cdot 10^{-2}$	$3 \cdot 10^{-4}$	38[a,e]	5–10
16	HDOP	C	$2 \cdot 10^{-2}$	$5 \cdot 10^{-4}$	35[a,e]	20
17	HDOP	D	$3 \cdot 10^{-2}$	$1 \cdot 10^{-4}$	28[a,e]	10
18	IOPA	A	$3 \cdot 10^{-2}$	$2.5 \cdot 10^{-4}$	35[a,e]	5
19	IOPA	G	$3 \cdot 10^{-2}$	$2.5 \cdot 10^{-4}$	38[a,e]	30
20	IOPA	C	$3 \cdot 10^{-2}$	$2.5 \cdot 10^{-4}$	39[a,e]	12
21	IOPA	F	$4 \cdot 10^{-3}$	$1 \cdot 10^{-4}$	29.5[d,e]	20
22[c]	IOPA	A	$3 \cdot 10^{-2}$	$2.5 \cdot 10^{-4}$	29[a,e]	10
23	OPPA	C	$3 \cdot 10^{-2}$	$1.6 \cdot 10^{-4}$	31[a,e]	20
24	OPPA	F	$3 \cdot 10^{-2}$	$1 \cdot 10^{-4}$	27[d,e]	10
25	HDOPP	D	$3 \cdot 10^{-2}$	$1.6 \cdot 10^{-5}$	30[a,e]	5–10
26	HDOPP	H	$3 \cdot 10^{-2}$	$1 \cdot 10^{-5}$	25[a,e]	5–10
27	H_2MOPP	A	$3 \cdot 10^{-2}$	$6 \cdot 10^{-4}$	22[a,e]	10
28	H_2MOPP	B	$3 \cdot 10^{-2}$	$4 \cdot 10^{-4}$	32[a,e]	5–10
29	H_2MOPP	J	$3 \cdot 10^{-2}$	$4 \cdot 10^{-4}$	26.5[d,e]	10
30	H_2MOPP	K	$3 \cdot 10^{-2}$	$6 \cdot 10^{-4}$	27[a,e]	10

[a] Reproducible slope.
[b] Short-term reproducibility to within ±1 mV.
[c] Moody configuration.
[d] Non-reproducible slope.
[e] Short-term reproducibility to within ±2 mV.

Region of linear response

Table III lists the regions of linear response. In most cases, the upper limit corresponds to the highest activity solution studied ($3 \cdot 10^{-2}$ *M*). The lower limit of linearity is in part determined by the partition coefficient of the electroactive complex between the membrane phase and the aqueous solution, and there is a correlation between the lower limit of linearity and the water solubility of the calcium complex. This is qualitatively seen in Table III for the calcium salts of

the octylphenylphosphoric acids (electrodes 7, 9, 25, 26) which have a marginally smaller lower activity limit than most of the others. The calcium salts of the octylphenylphosphoric acids seem to be less soluble in water than the others tested.

Response time

The response times listed in Table III are the mean times required for the readings in five standard solutions (10^{-5}–10^{-1} *M*) to reach a steady potential (± 0.2 mV). For many electrodes the response time in the more concentrated solutions was less than 30 s, but in the most dilute solutions, response times of 15–30 min were not uncommon.

The response times for the coated wire electrodes depended on the amount of plasticizer in the membrane (compare electrodes 18 and 19 which contained 30 and 50% PVC, respectively). The response time increased with a decrease in the amount of plasticizer, which is consistent with reduced charge mobility in the membrane. It was also observed that the absolute potential values became more positive with decrease in the plasticizer content.

Reproducibility of response gradient

Most of the electrodes gave plots of potential against the logarithm of the calcium ion activity which had reproducible (± 2 mV) gradients for consecutive measurements of calcium standards. This is essential for satisfactory analytical application; electrodes 1–11 gave particularly good results. Some electrodes (*e.g.* 15, 16, 18, 19, 20) showed a hyper-Nernstian effect with gradients greater than the theoretical value; the reason for this is unclear. It should be noted that similar unexplained effects have been reported by Griffiths *et al.*[5], and Cattrall and Freiser[6].

Reproducibility of potential readings

The short-term reproducibility of the electrodes is indicated in Table III. For the most satisfactory electrodes (1–10), the potential of an individual standard calcium solution could be reproduced, for consecutive measurements, to within ± 1 mV. For the other electrodes, the reproducibility was somewhat worse (± 2 mV). The short-term reproducibility depended on the membrane composition; decreasing the plasticizer content of the membrane tended to improve the reproducibility, but this had the disadvantage of increasing the response time. A compromise must be reached between reproducibility and response time. This problem is manageable in an analytical situation with frequent standardization.

All the electrodes (including the Orion electrode) showed a long-term drift which could be as much as 5–10 mV during one day. This phenomenon has been reported previously for liquid membrane electrodes[19–22], and necessitates careful and frequent standardization.

Effect of plasticizer

Fiedler and Růžička[17] have reported that a PVC membrane, to produce a satisfactory ion-selective electrode, should have a glass transition temperature which is below room temperature. Presumably this is necessary to provide charge

conduction in the membrane phase, and is normally achieved in plastic membranes by the addition of a plasticizer. In the present work, di-(2-ethylhexyl)-2-ethylhexylphosphonate acted in most cases as the plasticizer. Certain membranes, however, produced electrodes (2 and 4) with excellent functional characteristics without the addition of DEHEHP. In these cases, the reagents themselves [bis(di-(2-ethylhexyl)-phosphato)calcium(II), bis(di-n-octylphosphato)calcium(II), or the free acids] possessed characteristics which enabled them to serve as plasticizers in their own right.

When DEHEHP was used as the plasticizer, the most satisfactory electrodes contained 40–55% (w/w) plasticizer (*e.g.* electrodes 1, 6, 7, 10). Electrodes containing 80–90% DEHEHP (not included in Table III) had exceedingly short response times, but the excessive water transport through the membranes caused these electrodes to become opaque after only 10 min in water and led to severe potential drifts.

The internal reference system

There is some apprehension in the literature[3,7,8] concerning the reliability of the coated wire electrodes, because of the apparent absence of a thermodynamically reversible process at the PVC–platinum wire interface to facilitate charge transport. However, these electrodes do, in fact, appear to have an internal reference system built into them, albeit fortuitously. Since PVC is permeable to both oxygen and water[23], an oxygen electrode will be set up at the platinum–PVC interface, and may function as an internal reference. Work is being carried out at present to test this hypothesis. According to this approach, coated wire electrodes consist of an oxygen, water/platinum internal reference connected to a PVC/ion-exchanger membrane and function in an analogous way to the Moody-type[4,5] electrodes.

We are grateful to the Mobil Chemical Co. for gifts of IOPA, OPPA, and DEHEHP, and to the Australian Research Grants Committee for financial support; one of us (DMD) wishes to thank Kodak (Australasia) Pty. Ltd. for generous leave of absence.

SUMMARY

The use of several alkylphosphoric acid esters in the production of PVC membranes for use as calcium-sensitive, coated-wire electrodes is reported. The response characteristics, reproducibility, region of linear response for, and effect of plasticizer on, the electrodes are discussed.

REFERENCES

1 R. Z. Luther, *Phys. Chem.*, 27 (1898) 364.
2 J. W. Ross, *Science*, 156 (1967) 1378.
3 J. Růžička, E. H. Hansen and J. Chr. Tjell, *Anal. Chim. Acta*, 67 (1973) 155.
4 G. J. Moody, R. B. Oke and J. D. R. Thomas, *Analyst (London)*, 95 (1970) 910.
5 G. H. Griffiths, G. J. Moody and J. D. R. Thomas, *Analyst (London)*, 97 (1972) 420.

6 R. W. Cattrall and H. Freiser, *Anal. Chem.*, 43 (1971) 1905.
7 M. D. Smith, M. A. Genshaw and J. Greyson, *Anal. Chem.*, 45 (1973) 1782.
8 A. K. Covington, *CRC Crit. Revs. Anal. Chem.*, 3 (1974) 355.
9 A. Ansaldi and S. I. Epstein, *Anal. Chem.*, 45 (1973) 595.
10 J. Růžička, C. G. Lamm and J. Chr. Tjell, *Anal. Chim. Acta*, 62 (1972) 15.
11 D. C. Stewart and H. W. Crandall, *J. Amer. Chem. Soc.*, 73 (1951) 1377.
12 G. H. Griffiths, G. J. Moody and J. D. R. Thomas, *J. Inorg. Nucl. Chem.*, 34 (1972) 3043.
13 H. James, G. Carmack and H. Freiser, *Anal. Chem.*, 44 (1972) 856.
14 D. M. Drew, M.Sc. Thesis, La Trobe University, 1974.
15 R. G. Bates, B. R. Staples and R. A. Robinson, *Anal. Chem.*, 42 (1970) 867.
16 J. W. Ross in R. A. Durst (Ed.), *Ion-Selective Electrodes*, National Bureau of Standards special publication No. 314, U.S. Government Printing Office, Washington, D.C., 1969, p. 66.
17 U. Fiedler and J. Růžička, *Anal. Chim. Acta*, 67 (1973) 179.
18 C. F. Baes, *J. Inorg. Nucl. Chem.*, 24 (1962) 707.
19 A. Hulanicki and M. Trojanowicz, *Talanta*, 20 (1973) 599.
20 M. Mascini, *Anal. Chim. Acta*, 56 (1971) 316.
21 G. A. Rechnitz and Z. F. Lin, *Anal. Chem.*, 40 (1968) 696.
22 E. W. Moore in ref. 16, p. 224.
23 *Modern Plastics Encyclopaedia*, Modern Plastics, New York, 2nd edn., 1964, p. 828.

Analytica Chimica Acta, 76 (1975) 279–287

A SELF-GENERATING THIRD-ORDER ELECTRODE

PART I. TITRATIONS OF TRANSITION METAL, SULPHIDE, AND CHLORIDE IONS WITH A SILVER–SILVER SULPHIDE ELECTRODE

JØRGEN BIRGER JENSEN

Fysisk-Kemisk Institut, Danmarks Tekniske Højskole, DK 2800 Lyngby (Denmark)

(Received 21st January 1974)

Many analytical applications of solid-state silver sulphide membrane electrodes have been reported in the recent literature[1–14]; very little attention has been paid to the silver–silver sulphide electrode. Since the work of Hiltner and Grundmann[15], very few studies of the silver–silver sulphide electrode have been reported[16,17]. In the present paper, some theoretical explanations are given for the behaviour of the silver–silver sulphide electrode, which is proposed as a simple, inexpensive, rapid, stable and reproducible alternative to many more complicated commercial solid-state membrane electrodes; for a number of metal ions, *i.e.* those forming sparingly soluble sulphide precipitates, the silver–silver sulphide electrode simply acts as a self-generating third-order electrode.

EXPERIMENTAL

Apparatus

All the instrumentation used was obtained from Radiometer A/S, Copenhagen. An expanded-scale precision pH meter (PHM 26) was used with automatic titration equipment (ABU 1, SBR 2) and a Servograph Recorder (REC 1). The indicator electrode was a silver metal electrode (P 4011) on which silver sulphide was electrolyzed. The reference electrode was a $Hg/HgSO_4$ (saturated sodium sulphate) electrode (K 601). The pH was measured with a glass electrode G 202 C in connection with the above reference electrode. Measurements were made in a thermostated cell at 25 ± 0.1°C.

Reagents

All the chemicals used were of analytical grade and were used without further purification. Stock solutions of sodium sulphide was freshly prepared every week[8]. Generally, the ionic strength was kept constant at 1.0 by means of sodium nitrate or sodium perchlorate.

Preparation of sulphide electrode

Before electrolysis, the silver metal electrode was cleaned in cold concentrated nitric acid, and washed with distilled water and ethanol; it was then dried in a nitrogen atmosphere to avoid oxidation. To deposit the silver sulphide, the silver

electrode was anodically oxidized in a pure solution of 0.1 *M* sodium sulphide with a current of 5 mA cm^{-2} for 5 min; as counter electrode a platinum wire was used. The entire preparation required about 30 min. After storing for about 30 min in 0.1 *M* sodium sulphide, the electrode was ready for use.

The electrode was found to be sensitive to sulphide ions and to silver(I), copper(II), cadmium(II), lead(II) and zinc(II). Electrode potentials were obtained rapidly and in every case the equilibrium potential was reached within 30 s of immersion of the electrodes. The reproducibility of the electrodes was within ± 2 mV, and no potential drift was observed.

THEORY

According to Rickert[18] and Wagner[19], silver sulphide is an ionic conductor which allows silver ions to pass freely between the test solution and the metallic silver phase. Thus equilibrium conditions are established when

$$\bar{\mu}_{Ag^+}(\text{metallic silver}) = \bar{\mu}_{Ag^+}(\text{test solution}) \tag{1}$$

and the potential of the electrode is given by the Nernst equation:

$$E = E^0_{Ag/Ag^+} + \frac{RT}{F} \ln a_{Ag^+} \tag{2}$$

If the test solution originally contains no silver ions, a small number of ions is produced by the very low, but finite, solubility of the silver sulphide, and the electrode then acts as a second-order electrode, responding to sulphide ion activity in the solution:

$$E = E^0_{Ag/Ag^+} + \frac{RT}{2F} \ln S_{Ag_2S} - \frac{RT}{2F} \ln a_S^{2-} \tag{3}$$

where S_{Ag_2S} is the solubility product of silver sulphide. When divalent metal ions are added to the solution, the metal sulphide will precipitate provided that

$$a_{Me^{2+}} > \frac{S_{MeS}}{(\frac{1}{4} \cdot S_{Ag_2S})^{\frac{1}{2}}} \tag{4}$$

where S_{MeS} is the solubility product of the metal sulphide. Consequently, at the silver sulphide surface:

$$Me^{2+} + Ag_2S(s) \rightleftarrows MeS(s) + 2\,Ag^+ \tag{5}$$

The electrode can be considered to consist of a layer of metal sulphide on silver sulphide, and can be regarded as a self-generating third-order electrode schematically shown as $Ag/Ag_2S/MeS$. As long as a precipitate of MeS is present, the activity of silver ions is determined by the activity of metal ions, and the potential of the electrode will be:

$$E = E^0_{Ag/Ag^+} + \frac{RT}{2F} \ln \frac{S_{Ag_2S}}{S_{MeS}} + \frac{RT}{2F} \ln a_{Me^{2+}} \tag{6}$$

RESULTS

The performance of the silver–silver sulphide electrode as a third-order cadmium electrode is shown in Fig. 1. For these measurements, a series of cadmium(II) buffers were prepared by mixing cadmium nitrate and imidazole in given ratios; the free cadmium(II) concentration was calculated with the stability constants for the cadmium–imidazole complexes[20]. The pCd range covered is 2.0–12.4; a least-squares curve-fitting procedure on the points down to pCd 10.6 gave:

$$E = -45 - 29.2\,\text{pCd} \quad (\text{mV at } 25°\text{C}) \tag{7}$$

The uncertainties on the intercept and the slope are ± 3.1 mV and ± 0.7 mV/pCd, respectively. The value obtained on the intercept is in good agreement with literature data[21] taking into account the difficulties in determining the activity coefficients. The slope is very close to the theoretical Nernstian value.

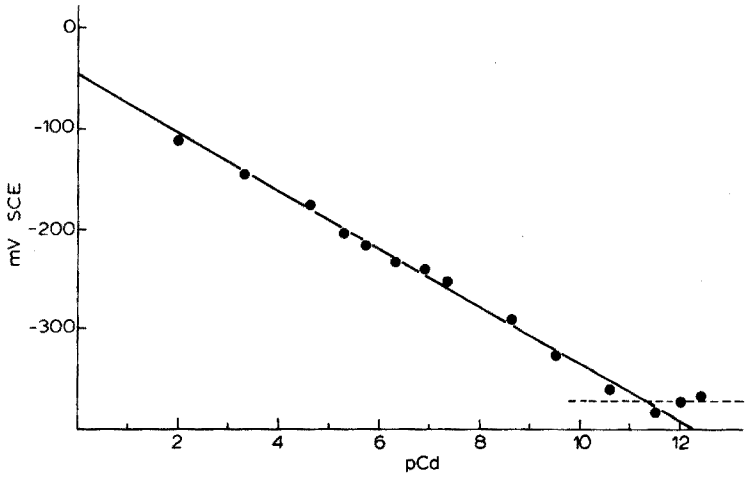

Fig. 1. The Ag/Ag_2S electrode used as a cadmium(II) electrode. pH = 9.5 except in solution pCd = 2, where pH = 8. Limit of detection is indicated with the horizontal dotted line. Ionic strength 1.0 ($NaClO_4$). Reference electrode: Hg/Hg_2SO_4, Na_2SO_4 (sat.). Potentials calculated relative to SCE.

In order to evaluate the limit of sensitivity, it must be noted that eqn. (6) is valid only if the solubility product of CdS is exceeded in the solution. Consequently, the condition for measuring cadmium(II) with this electrode is, from eqn. (4):

$$a_{Cd^{2+}} \cong 10^{-13}\,M \tag{8}$$

This is in reasonably good agreement with the result from Fig. 1. Generally the limiting value for a metal ion forming an insoluble sulphide can be calculated from an equation similar to eqn. (4). Thus zinc(II) should theoretically be measurable with a silver–silver sulphide electrode with a Nernstian slope down to a concentration of about 10^{-7} M.

For many electrodes, selectivity constants provide a difficult problem. For the silver–silver sulphide electrode, the behaviour is easily explained on the basis of the law of mass action and the idea of the electrode as a third-order electrode. For

instance, if the solution contains two metal ions—$Me(1)^{2+}$ and $Me(2)^{2+}$—both forming insoluble metal sulphides, then the electrode behaves as a third-order electrode for $Me(1)^{2+}$ ions if (neglecting the contribution from activity coefficients):

$$[Me(1)^{2+}] > \frac{S_{Me(1)S}}{S_{Me(2)S}}[Me(2)^{2+}]$$

If the inequality is reversed, then the electrode is sensitive only to $Me(2)^{2+}$ ions. The selectivity constant, K, of the silver–silver sulphide electrode for $Me(1)^{2+}$ ions with respect to $Me(2)^{2+}$ ions is simply defined as $S_{Me(1)S}/S_{Me(2)S}$ and the electrode potential can be expressed by the following equation[14]:

$$E = \text{const} + \frac{RT}{zF} \ln (a_{Me(1)^{2+}} + K a_{Me(2)^{2+}}) \tag{9}$$

Potentiometric titrations with sodium sulphide

As a test of the function of the electrode, some titrations with sodium sulphide were carried out. These titrations will, of course, be largely of academic interest, since sodium sulphide is not usually recommended as a titrant.

Titrations of silver(I). In titration of silver nitrate with sodium sulphide, the electrode potentials can be calculated from eqn. (2) or eqn. (3). Figure 2 shows the titration curves for three different concentrations of silver(I), together with pH variations during titrations. In contrast to the report by Hseu and Rechnitz[8], no significant loss of sulphide (as H_2S) was observed; moreover, a decrease in pH was observed before the equivalence point was reached. Both observations can be explained by formation of the Ag(HS) complex with release of a hydrogen ion, and by the very high stability constant[22]:

$$K = \frac{a_{Ag(HS)} \cdot a_{H^+}}{a_{Ag^+} \cdot a_{H_2S}} = 1.76 \cdot 10^9$$

For these titrations, the accuracy is estimated as within 0.5%, most of the error arising from the standardization process.

Titration of copper(II), cadmium(II) and zinc(II). The results in Fig. 2 indicate that the silver–silver sulphide electrode responds faithfully to sulphide activity, and according to eqn. (6) the electrode should be suitable as an indicator electrode in potentiometric titrations of metals forming sparingly soluble metal sulphides. Of course, the concentration of the silver ions determined from eqn. (5) must be much smaller than that of the metal ions to be titrated, otherwise misleading results would be obtained. This is visualized in Fig. 3 where pS ($pS = -\log a_{S^{2-}}$) is plotted against pMe in saturated solutions of metal sulphides. With divalent metal ions—Hg^{2+}, Cu^{2+}, Cd^{2+}, Zn^{2+}, Fe^{2+}—the plot gives a straight line with a slope of -1 and with intercepts on both axes at the values of the corresponding solubility products. With monovalent ions—Cu^+ and Ag^+—a straight line is obtained with a slope -2, and only the intercepts on the ordinate axis give the value of the solubility products. At the equivalence point $pMe = pS$ for divalent ions and $pS = pMe + \log 2$ for monovalent ions. These two straight lines obtained by the equation for equivalent conditions practically coincide when plotted on the scale used in Fig. 3. The points of intercepts with this line and the lines representing

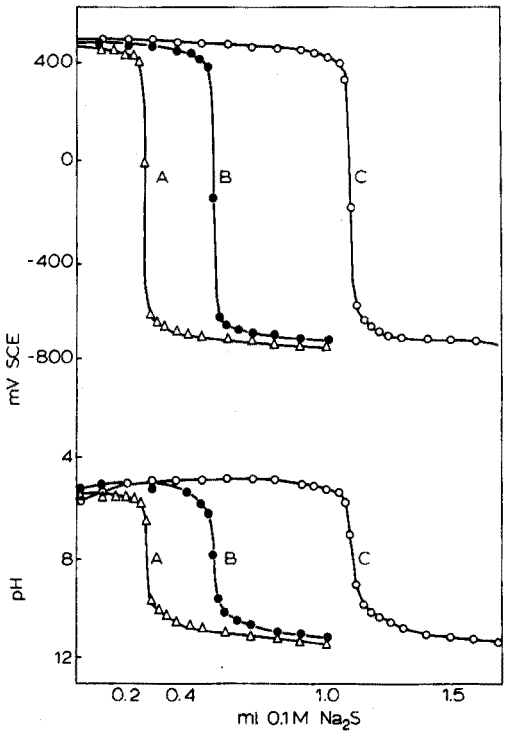

Fig. 2. The Ag/Ag_2S electrode used as a silver(I) electrode. Upper part, titration of $AgNO_3$ with Na_2S. Concentrations of $AgNO_3$: (A) $2.5 \cdot 10^{-3}$ *M*; (B) $5.0 \cdot 10^{-3}$ *M*; (C) 10^{-2} *M*. Lower part, pH variation during the titration. Reference electrode: Hg/Hg_2SO_4, Na_2SO_4 (sat.). Potentials calculated relative to SCE.

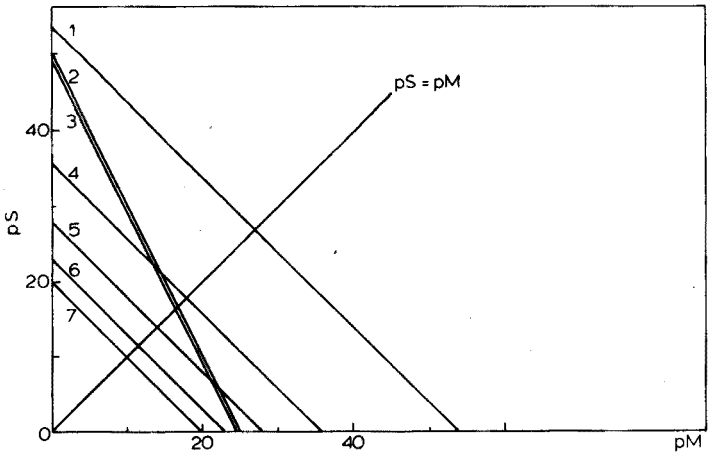

Fig. 3. The plot of pS *vs.* pM in saturated solutions of metal sulphides at ionic strength $\cong 0$. Curve (1) HgS, (2) Ag_2S, (3) Cu_2S, (4) CuS, (5) CdS, (6) ZnS, (7) FeS. Solubility products were obtained from Latimer[21]. (For further details see text.)

the solubility products indicate the equivalence points in each individual case. If it is assumed that a solution of copper(II) is to be titrated with sodium sulphide to a silver–silver sulphide indicator electrode, and that no side-reactions occur, then the relation between the activities of silver(I) and copper(II) is governed by:

$$a_{Ag^+} = \left(\frac{S_{Ag_2S}}{S_{CuS}} \cdot a_{Cu^{2+}}\right)^{\frac{1}{2}}$$

This relation is, of course, valid at any point of the titration curve. At the beginning of the titration, $a_{Cu^{2+}} \gg a_{Ag^+}$ but as the titration proceeds, the copper(II) activity decreases much more rapidly than the silver(I) activity. It can be calculated, from the data of Latimer[21] and by neglecting the contribution from activity coefficients, that $a_{Cu^{2+}} = a_{Ag^+} \approx 10^{-14}$, *i.e.* before the equivalence point for both copper(II) and silver(I). From this point $a_{Ag^+} > a_{Cu^{2+}}$, and the titration finishes as a titration of silver ions. The point on the titration curve with the greatest slope corresponds to the equivalence point on the titration curve of silver ions.

If, however, the solution contains only copper(I) it can be calculated analogously that $a_{Ag^+} \cong 0.2\ a_{Cu^+}$. If no corrections are made for silver ions, the titration error will be about 20%. Likewise Fig. 3 shows why mercury(II) must be absent when a silver–silver sulphide is used; mercury(II) sulphide will form by dissolution of silver sulphide and the electrode will become unusable. However, solutions containing cadmium ions and zinc ions can be measured by titrations or by direct potentiometric measurements. Figure 4 shows a titration curve of zinc(II) together with the pH variation during titration. Titrations of cadmium(II) with sulphide have been reported earlier[23].

Special problems arise when copper(II) is titrated with sodium sulphide solution. Besides the problem mentioned above, very careful exclusion of oxygen

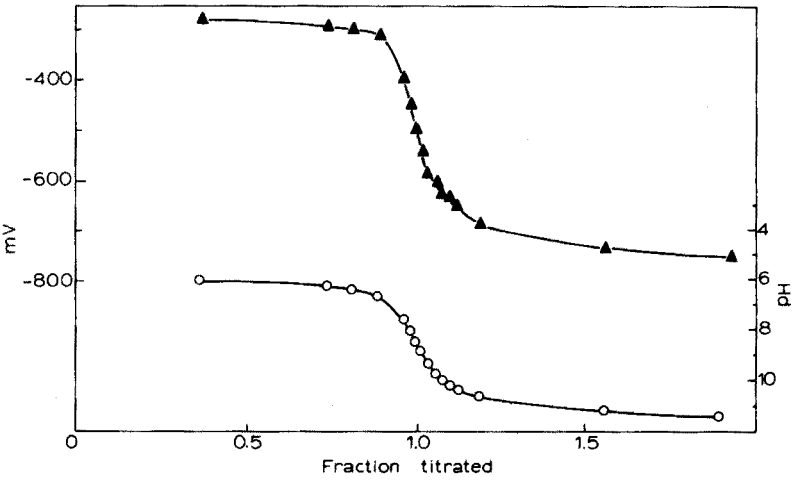

Fig. 4. The Ag/Ag_2S electrode used as a zinc(II) electrode. Upper part, titration of 10^{-2} *M* $ZnCl_2$ with Na_2S. Lower part, pH variation during the titration. Reference electrode: Hg/Hg_2SO_4, Na_2SO_4 (sat.). Potentials calculated relative to SCE.

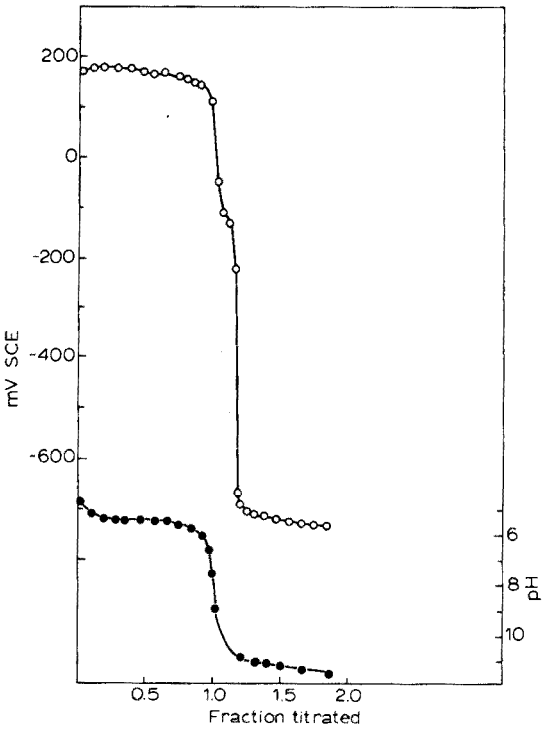

Fig. 5. The Ag/Ag_2S electrode used as a copper(II) electrode. Upper part, titration of 10^{-2} *M* $CuSO_4$ with Na_2S. Nitrogen was bubbled through the solution before titration. The small shoulder at *ca.* −150 mV is explained by the presence of some oxygen. Lower part, pH variation during the titration. Reference electrode: Hg/Hg_2SO_4, Na_2SO_4 (sat.). Potentials calculated relative to SCE.

was necessary; Fig. 5 shows a titration curve carried out in a nitrogen atmosphere. The effect of oxygen is under further investigation.

Complexometric titrations

In order to illustrate the practical application of the electrode, some potentiometric titrations of copper(II) and cadmium(II) with EDTA were followed. The potential jumps (Figs. 6 and 7) in both titrations were satisfactory, and coincided with the theoretical equivalence points. The reproducibility of the results was found to be $\pm 1\%$.

Chloride titrations

Further practical application of the Ag/Ag_2S electrode is shown in Fig. 8. In these experiments, both an Ag/Ag_2S and an Ag/AgCl electrode were immersed in the same solution and measured simultaneously against the same reference electrode. Essentially the same titration curves were found for both indicator electrodes. The very small differences found between the electrode potential of the Ag/Ag_2S and Ag/AgCl electrodes—*i.e.* $E_{Ag/Ag_2S} - E_{Ag/AgCl}$—are plotted at the bottom of Fig. 8; clearly, during the titration, the potentials of the two indicator electrodes were almost identical. The slight deviation at the equivalence point can be explained

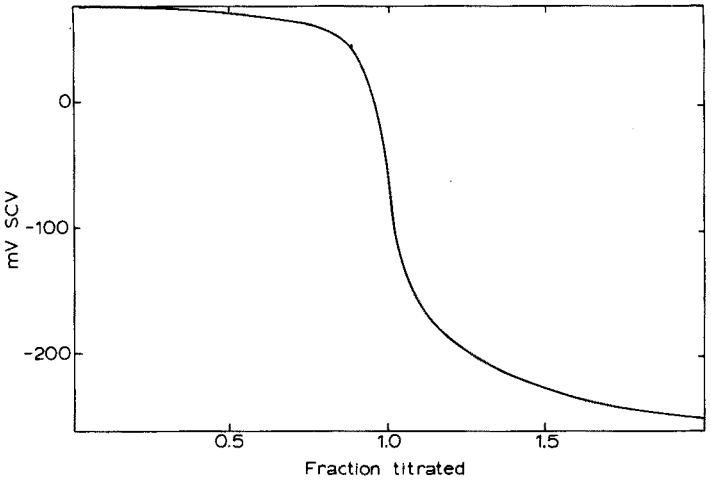

Fig. 6. The Ag/Ag_2S electrode used as a copper(II) electrode. Titration of 10^{-2} *M* $CuSO_4$ with EDTA at pH 7.5. The titration was carried out in 1.0 *M* sodium acetate solution at constant pH. Reference electrode: Hg/Hg_2SO_4, Na_2SO_4 (sat.). Potentials calculated relative to SCE.

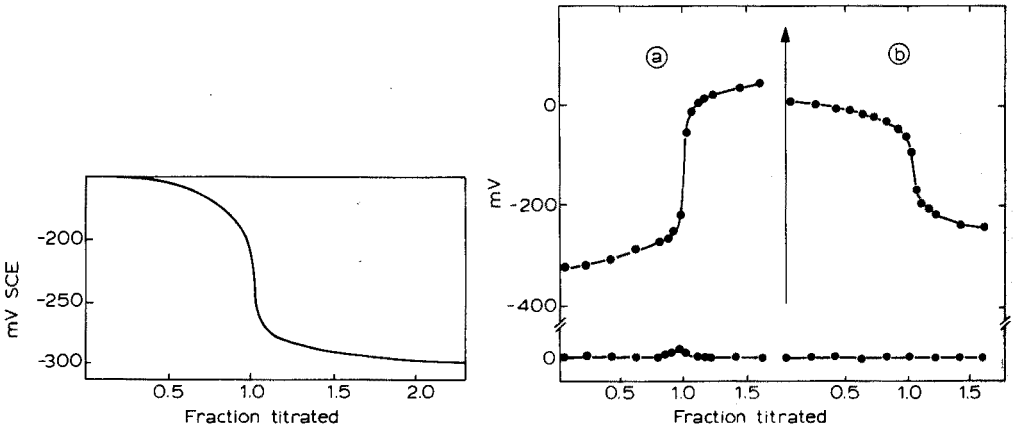

Fig. 7. The Ag/Ag_2S electrode used as a cadmium(II) electrode. Titration of 10^{-2} *M* $CdSO_4$ with EDTA at pH 8.1. Other conditions as for Fig. 6.

Fig. 8. The Ag/Ag_2S electrode used as a chloride electrode. (a) Titration of $5 \cdot 10^{-2}$ *M* NaCl with $AgNO_3$. (b) Titration of $5 \cdot 10^{-3}$ *M* $AgNO_3$ with NaCl. Reference electrode: Hg_2SO_4, Na_2SO_4 (sat.). The two lines at the bottom of the figure represent the differences in silver–silver sulphide and silver–silver chloride electrode potentials, *i.e.* $E_{Ag/Ag_2S} - E_{Ag/AgCl}$, during the titration. Ionic strength = 1.0 ($NaNO_3$).

by a slight difference in response time for the two electrodes, the response time of the Ag/Ag_2S electrode being equal to or better than that of an Ag/AgCl electrode.

Storage of electrodes

When not in use the Ag/Ag_2S electrodes were stored either in distilled water or, preferably, in 0.1 *M* sodium sulphide solution. Stored in this way, they performed for more than 6 months without ageing—*i.e.* erroneous results, decrease in response

time or unstable potentials. The electrodes were always ready for use and no memory effects were observed. The electrodes were left unprotected against illumination under normal laboratory conditions; in this respect, the Ag/Ag_2S electrodes are superior to the Ag/AgCl electrodes.

The author expresses his thanks to Professor Jørgen Koefoed for advice, encouraging discussions, and valuable linguistic criticism and to Mrs. Jette Klausen for skilled technical assistance.

SUMMARY

Ag/Ag_2S electrodes were prepared by electrolytic deposition of silver sulphide on a silver rod. These electrodes responded in a Nernstian fashion to cadmium(II) in the pCd range 2.0–10.6; they gave satisfactory results in titrations of silver(I), copper(II), cadmium(II) and zinc(II) with sodium sulphide solution, in titrations of copper(II) and cadmium(II) with EDTA solution, and in titrations of chloride with silver(I) solution. The electrode appears to behave as a third-order self-generating electrode. The Ag/Ag_2S electrode was found to be reliable, stable over long periods, unaffected by light under normal laboratory conditions and convenient in use.

REFERENCES

1 J. Růžička and C. G. Lamm, *Anal. Chim. Acta*, 54 (1971) 1.
2 E. H. Hansen, C. G. Lamm and J. Růžička, *Anal. Chim. Acta*, 59 (1972) 403.
3 J. Růžička, C. G. Lamm and J. Chr. Tjell, *Anal. Chim. Acta*, 62 (1972) 15.
4 J. Růžička and E. H. Hansen, *Anal. Chim. Acta*, 63 (1973) 115.
5 M. J. D. Brand, J. J. Militello and G. A. Rechnitz, *Anal. Lett.*, 2 (1969) 523.
6 M. Mascini and A. Liberti, *Anal. Chim. Acta*, 64 (1973) 63.
7 M. Mascini and A. Liberti, *Anal. Chim. Acta*, 60 (1970) 405.
8 T. M. Hseu and G. A. Rechnitz, *Anal. Chem.*, 40 (1968) 1054.
9 J. Pick, K. Toth and E. Pungor, *Anal. Chim. Acta*, 61 (1972) 169.
10 T. S. Light and J. L. Swartz, *Anal. Lett.*, 1 (1968) 825.
11 J. Vesely, O. J. Jensen and B. Nicolaisen, *Anal. Chim. Acta*, 62 (1972) 1.
12 I. C. Popescu and C. Liteanu, *Rev. Roum. Chim.*, 17 (1972) 1629.
13 R. Bock and H. J. Puff, *Z. Anal. Chem.*, 240 (1968) 381.
14 J. Koryta, *Anal. Chim. Acta*, 61 (1972) 329.
15 W. Hiltner and W. Grundmann, *Z. Phys. Chém., Abt. A, Leipzig*, 168 (1933) 291.
16 T. Anfält and D. Jagner, *Anal. Chim. Acta*, 56 (1971) 477.
17 A. Mirna, *Z. Anal. Chem.*, 254 (1971) 114.
18 H. Rickert, *Festkörperprobleme VI*, Friedr. Vieweg und Sohn, Braunschweig, 1966, p. 85.
19 C. Wagner, *Z. Phys. Chem., Abt. B*, 21 (1933) 42; 23 (1933) 469; *J. Chem. Phys.*, 21 (1953) 1819.
20 J. B. Jensen, *Acta Chem. Scand.*, 26 (1972) 4031.
21 W. M. Latimer, *The Oxidation States of the Elements and their Potentials in Aqueous Solutions*, Prentice-Hall, Englewood Cliffs, New York, 2nd edn., 1952.
22 W. L. Freyberger and P. L. Bruyn, *J. Phys. Chem.*, 61 (1957) 586.
23 J. B. Jensen, *Acta Chem. Scand.*, 27 (1973) 3563.

Analytica Chimica Acta, 76 (1975) 289–297

A SPECTRAL AND POLAROGRAPHIC STUDY OF POTASSIUM CHLORAZEPATE

W. FRANKLIN SMYTH and B. LEO

Chemistry Department, Chelsea College, Manresa Road, London SW3 6LX (England)

(Received 4th November 1974)

Potassium chlorazepate (I; Tranxene) is a minor tranquillizer belonging to the 1,4-benzodiazepine group. Papers on this drug have only recently appeared and these are of a pharmacological and physiological nature[1–4]. The chemistry of this structurally unique 1,4-benzodiazepine, in particular its acid–base equilibria in aqueous solutions and polarographic methods of analysis, does not seem to have been described. Such material has been collected for other 1,4-benzodiazepines in a recent review by Clifford and Smyth[5].

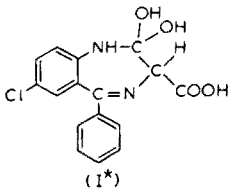

(I*)

In this paper, a detailed study of the spectral and polarographic behaviour and extraction profile of potassium chlorazepate over a wide pH range is described. This provides information on the acid–base equilibria existing in aqueous solutions of the drug and, in addition, suggests an analytical method for the separation and polarographic determination of potassium chlorazepate in body fluids in the presence of other 1,4-benzodiazepines when its acid–base equilibria are compared with chlordiazepoxide (Librium) and nitrazepam (Mogadon), used as marker compounds.

EXPERIMENTAL

Apparatus

Spectra over the ultraviolet range were recorded in solutions maintained at 20°C, with a Perkin-Elmer double-beam 137 ultraviolet–visible spectrophotometer. Matched 1-cm silica cells were used and the instrument was flushed with dry nitrogen to eliminate stray radiation effects.

Polarographic curves were recorded with a P.A.R. Model 174 Polarographic Analyser operated in the sampled d.c. mode with a scan speed of 10 mV s^{-1} and a drop time of 1 s, and a cathode-ray polarograph (Davis A 1660) operated in the

* The structure of the free acid rather than the dipotassium salt is given.

single-cell mode and connected to a fast recorder utilizing light-sensitive paper. A micro Kalousek vessel with a saturated calomel electrode was used as polarographic cell in both cases. The dropping mercury electrode used had the following characteristics: outflow velocity $m = 1.73$ mg s^{-1}, drop time = 4 s at the potential of the saturated calomel electrode and at a mercury height of 80 cm in 1 *M* KCl.

Chemicals and reagents

Samples of potassium chlorazepate were obtained from A. Clatworthy, Police Forensic Science Laboratories, London and Dr. P. F. Cooper, Boehringer–Ingelheim Ltd, Brackwell, Berks.

Acid–base equilibria were studied in Britton–Robinson buffers in the pH range 2–12 and with hydrochloric acid and sodium hydroxide at the extremes of this range. These solutions were also used in the analytical studies.

Experimental techniques

Solutions were prepared for spectrophotometry by diluting the appropriate amount of stock benzodiazepine solution with the appropriate buffer to give a drug concentration of $5 \cdot 10^{-5}$ *M*. To extend the pH range studied at either end of the scale, *M* HCl, 0.1 *M* HCl, 0.1 *M* NaOH and *M* NaOH were used. The range from pH 0–14 was scanned for the drug in increments of 1 pH unit to determine the approximate position of each pK_a value by observation of the spectral changes over the whole range. The region around each pK_a value was then studied in more detail with buffers differing by increments of *ca.* 0.3 pH units. From the spectra obtained, pK_a values were evaluated from the Henderson equation[6]. The wavelength range scanned was 200–390 nm. A slow scan speed (8 min for the range) was used, and the instrument reference beam contained a blank of buffer solution with the same amount of methanol as the samples.

In studying the variation of $E_{\frac{1}{2}}$ and i_d with pH, 2 ml of $5 \cdot 10^{-5}$ *M* benzodiazepine in the appropriate supporting electrolyte was deaerated by a stream of nitrogen for 3 min, and the *i–E* curve was recorded at a rate of 10 mV s^{-1} and a modulation amplitude of 100 mV.

Polarography was used to monitor the benzodiazepine content of the aqueous phase (5 ml of $5 \cdot 10^{-5}$ *M* benzodiazepine buffered at a particular pH or in hydrochloric acid or sodium hydroxide) in the extraction studies. Ethyl acetate was used as solvent. The *i–E* curves of the aqueous phase were recorded before and after 10 min shaking with 5 ml of the solvent and the extraction profiles were constructed from these results.

In the extraction of benzodiazepines 'spiked' into urine, the pH of the body fluid was adjusted with *M* hydrochloric acid or *M* sodium hydroxide to the desired pH and then this solution was buffered with the appropriate Britton–Robinson buffer till the volume of the original solution was doubled. This solution was then extracted for 10 min with a 4-fold excess of ethyl acetate, followed by centrifugation for 15 min. The organic layer was taken off and evaporated to dryness on a water bath. The residue was made up and dissolved in Britton–Robinson buffer, pH 4, before cathode ray polarographic analysis. This was referred to a calibration plot of peak height *vs.* concentration, constructed by a continuous addition method, or to a standard solution of the drug before extraction so that the recovery of the drug from urine could be estimated.

RESULTS AND DISCUSSION

U.v. spectra, pK_a values and their interpretation

Potassium chlorazepate at a concentration of $5 \cdot 10^{-5}$ *M* shows three u.v.-absorbing forms in the pH range 0–14. In acidic media, below pH 1, there exist two major bands at 243 nm (band 1), and 280 nm (band 2) with molar absorptivities of $3.4 \cdot 10^4$ and $2.2 \cdot 10^4$ l mole^{-1} cm^{-1}, respectively. These bands undergo a blue shift with increase in pH, giving rise to 2 major bands at 230 nm (band 1) and 250 nm (band 2) with molar absorptivities of $3.8 \cdot 10^4$ and $2.8 \cdot 10^4$ l mole^{-1} cm^{-1}, respectively, in the pH range 5–11. A shift to the red occurs in more alkaline media; band 1 appearing at 235 nm ($\varepsilon = 3.6 \cdot 10^4$) and band 2 at 260 nm ($\varepsilon = 2.2 \cdot 10^4$). The shift in acidic media corresponds to a pK_1 value of 3.5, measured at 220 nm and calculated from the Henderson equation (Fig. 1) whereas the shift in alkaline media corresponds to a pK_3 value of 12.5.

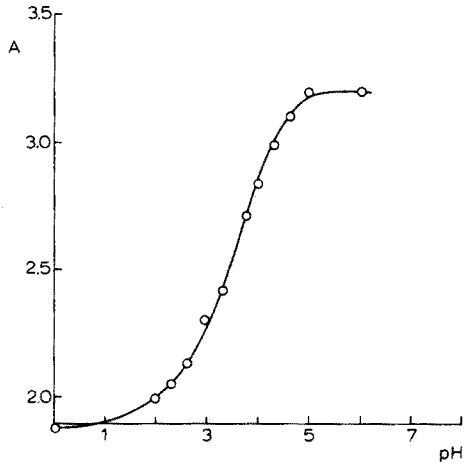

Fig. 1. The variation of absorbance with pH for potassium chlorazepate measured at 200 nm.

The results are consistent with the explanation that the spectra of the 1,4-benzodiazepines are the superimposed spectra of two substituted benzene rings within the complete molecule, one monosubstituted (band 1) and one trisubstituted (band 2). The shift in acidic media corresponds to protonation on the nitrogen atom in the 4-position since both bands are shifted. Band 2 undergoes a larger red shift than band 1 (30 nm as compared with 13 nm), which suggests that protonation of =C=N– aligns this group more to the trisubstituted ring than the monosubstituted one. The shift in alkaline media corresponds to removal of a proton from the nitrogen atom in the 1-position, the resulting anion having its =C=N– group slightly better aligned with the two phenyl rings compared with the neutral molecule.

The spectrum of the neutral molecule, HA, for potassium chlorazepate, is the same as that of N-desmethyldiazepam (II) (230, 250 nm) which has an identical chromophoric constitution, and is similar to that of medazepam (III) (233, 252 nm), in which the 2-C atom is sp^3-hybridized. Protonation of N-des-

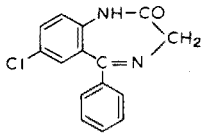
(II)

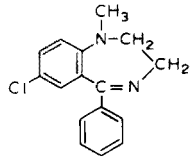
(III)

methyldiazepam gives two major bands at 235 and 283 nm with a pK_1 value of 3.5; protonation of medazepam also gives two major bands at longer wavelengths (255 and 290 nm) with a pK_1 value of 4.4. This is consistent with the protonated potassium chlorazepate (*i.e.* protonated on the 4-N atom) having a similar conformation to mono-protonated N-desmethyldiazepam rather than monoprotonated medazepam, possibly because of hydrogen bonding between the 3-carboxylic acid group and the protonated azomethine group, a bonding that is absent in the neutral molecule (see IV).

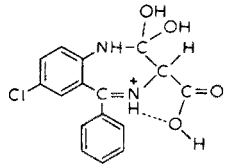
(IV)

The pK_1 value of 3.5 for potassium chlorazepate is much higher than the values for other 3-substituted 1,4-benzodiazepines (*e.g.* oxazepam, 1.7; lorazepam, 1.3), and is presumably further evidence for the existence of the depicted cation (IV).

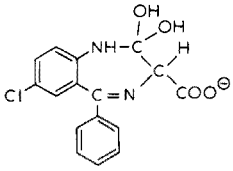
(V)

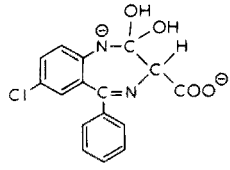
(VI)

Deprotonation of potassium chlorazepate yields successively the monoanion (V) and the dianion (VI). The loss of a proton from the carboxylic acid group is not seen spectrally but polarographic evidence discussed later, suggests a pK_2 value of approximately 5. Deprotonation on the 1-N atom causes both major bands to move slightly to the red, which suggests some measure of delocalization of the resulting negative charge in the conjugated system. The pK_3 value of 12.5 illustrates the difficulty of formation of anions of this type, which is consistent with the behaviour of other 7-chloro-1,4-benzodiazepines[7].

Polarographic behaviour

Potassium chlorazepate in the concentration range $5 \cdot 10^{-5}$–10^{-4} M is reduced in a well defined 2-electron step over the pH range 0–14 (Fig. 2). The wave has a similar height to those of other 1,4-benzodiazepines such as medaze-

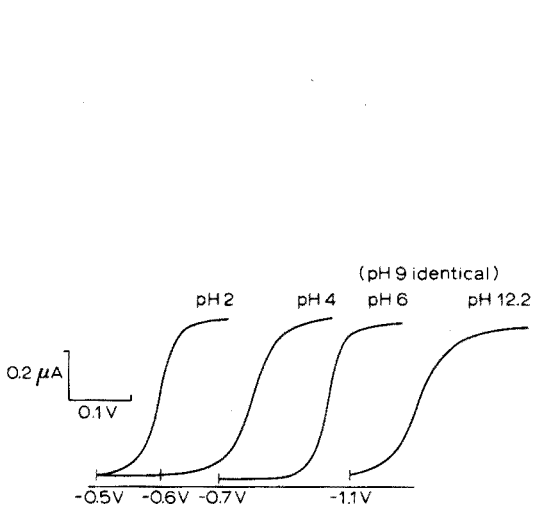

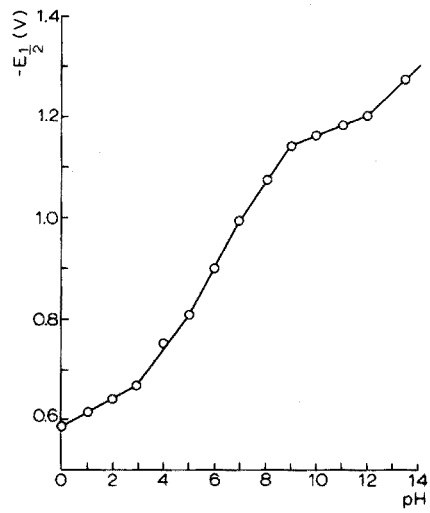

Fig. 2. Polarographic waves of potassium chlorazepate (10^{-4} *M*) at various pH values.

Fig. 3. The variation of half-wave potential *vs.* pH for 10^{-4} *M* potassium chlorazepate.

pam and diazepam under the same conditions, and involves the reduction of the 4,5-azomethine group. In contrast to 3-hydroxybenzodiazepines[8], the 2-hydroxy groups in this drug do not undergo surface protonation and are not reducible. The variation of $E_{\frac{1}{2}}$ with pH (Fig. 3) shows six linear portions with slopes of 27 mV/pH (pH 0–3), 75 mV/pH (pH 3–5), 90 mV/pH (pH 5–7), 75 mV/pH (pH 7–9), 20 mV/pH (pH 9–12), 47 mV/pH (above pH 12). The breaks at pH 3, 5 and 12 can be attributed to pK_1, pK_2 and pK_3, and those at 7 and 9 to pK'_1 and pK'_2. Logarithmic analysis (*i.e.* $\log[i/(i_d - i)]$ *vs.* E) of the waves at pH 2, 4, 6, 9 and 12.2 was carried out. At pH 2, two linear portions were obtained in the logarithmic plot with values of $\alpha n_\alpha = 1.7$ and $p = 0.85$ resulting from analysis of the first portion. A linear plot was found at pH 4 with $\alpha n_\alpha = 1.5$ and $p = 1.7$. Similar linearity was found at pH 6 or 9, with $\alpha n_\alpha = 1.9$ and $p = 2.5$. At pH 12.2, the plot was again linear with $\alpha n_\alpha = 1.07$ and $p = 0.80$. All these results suggest comparatively large α values for the azomethine reduction in potassium chlorazepate. This has already been observed for other 1,4-benzodiazepines[9–11] and oximes[12]. The fact that the plot at pH 2 gives two linear parts indicates two slow steps and is perhaps further evidence for the existence of the cation (IV); alternatively, the wave shape may be complicated by the presence of the decomposition product, nordesmethyl diazepam, which is formed rather rapidly at this pH and is reduced at a similar potential. The p value of 0.85 is in keeping with protonation of the azomethine group in the bulk of the solution followed by the addition of two electrons and one proton in the electrode process. At pH 4, 6 and 9, the linearity of the log plot suggests one rate-determining step with simultaneous addition of two electrons and two protons in each of the three cases. The behaviour above pH 12 is somewhat different; the values of αn_α and p suggest that the rate-determining step is the addition of one electron and one

proton, followed by rapid addition of the remaining electron and proton. The results of these spectral and polarographic studies are collected together in the following scheme, where *s* indicates a spectral result and *p* a polarographic result.

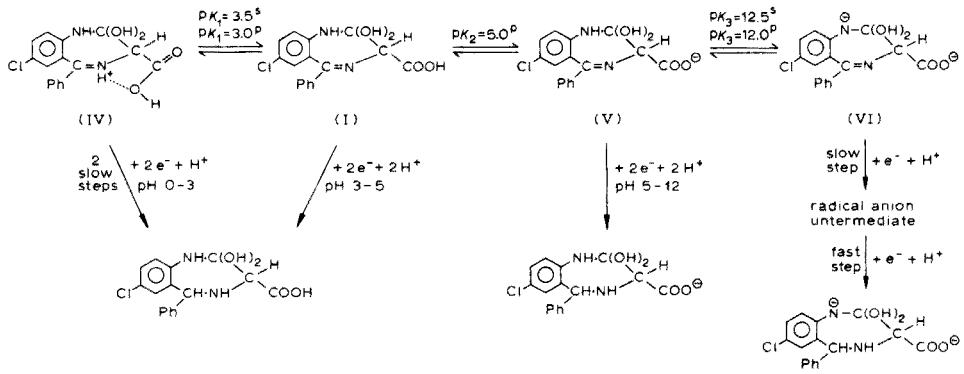

The variation of peak height with concentration was studied in pH 4 buffer by cathode ray polarography in the normal mode. The resulting graph (Fig. 4) shows linearity of response over the range 10^{-7} *M*–$3 \cdot 10^{-5}$ *M*. The graph begins to curve at concentrations above $3 \cdot 10^{-5}$ *M*, because of adsorption processes which have also been noted for other 1,4-benzodiazepines[8,13].

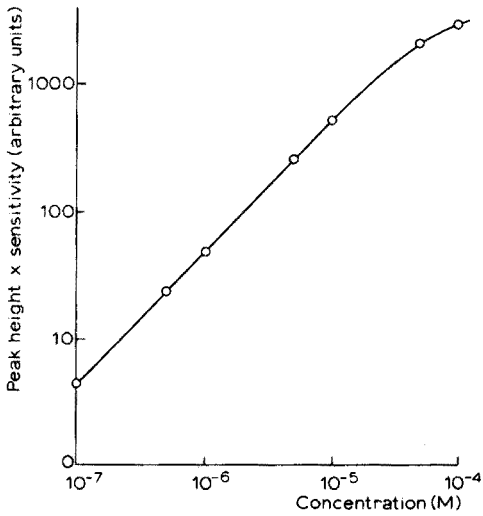

Fig. 4. The variation of peak height with concentration for potassium chlorazepate in cathode ray polarography.

Solvent extraction

Polarography was used to monitor the degree to which 10^{-5} *M* potassium chlorazepate was extracted by ethyl acetate from aqueous solutions of pH 0–14; extractions were performed at intervals of 1 pH units. This was repeated with two other benzodiazepines, chlordiazepoxide and nitrazepam, to see if there were any

inherent differences in the extraction profiles that would enable potassium chlorazepate to be determined in the presence of other benzodiazepines. These two compounds were also used as 'marker'compounds, since their different polarographic behaviour could be used to check whether in a given separation scheme they were actually being separated from potassium chlorazepate. Figure 5 shows the extraction profiles of these three benzodiazepines from aqueous solutions into equal volumes of ethyl acetate. All three were extracted at pH 4 (97–100%) but below pH 4, the percentage extraction decreased owing to the formation of the inextractible monoprotonated benzodiazepines of potassium chlorazepate (IV), chlordiazepoxide (VII)[14] and nitrazepam (VIII)[14]. This decrease occurred in the order of the pK_1

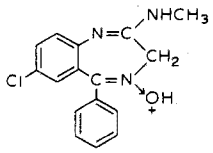

(VII)

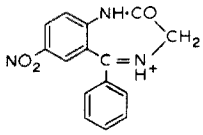

(VIII)

values, *i.e.* chlordiazepoxide $pK_1 = 4.6$, potassium chlorazepate $pK_1 = 3.5$ and nitrazepam $pK_1 = 3.2$.

Significant differences occurred in the extraction profiles above pH 4. Chlordiazepoxide and nitrazepam were both extracted in the pH range 4–12, the latter exhibiting a minor decrease above pH 12 because of the formation of the anion (IX)[14]. Chlordiazepoxide cannot undergo any such deprotonation[14]. Above

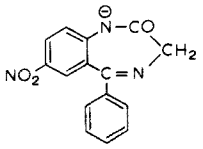

(IX)

pH 5 the percentage extraction of potassium chlorazepate decreased markedly owing to the formation of the inextractible monoanion (V). The percentage extraction reached zero by pH 9. The same phenomenon has been observed for the acetic acid metabolite of flurazepam[11].

This phenomenon provides the basis of an analytical method in that potassium chlorazepate is the only benzodiazepine which is not extracted at pH 9 whereas they are all extracted at pH 4. This was checked for the following benzodiazepines: prazepam, lorazepam, diazepam, oxazepam, chlorazepam and medazepam, all of which were extracted into ethyl acetate (95–100%) in the pH range 4–9 under the above conditions.

Analytical applications

After these encouraging results had been obtained in aqueous solutions, a urine sample (2.5 ml) was spiked with potassium chlorazepate, chlordiazepoxide and nitrazepam to give a concentration of $2 \cdot 10^{-5}$ *M* in each. The pH was adjusted with *M* sodium hydroxide to give a pH of 9; 2.5 ml of pH 9 Britton–Robinson buffer was added and the resulting solution was extracted with 20 ml of

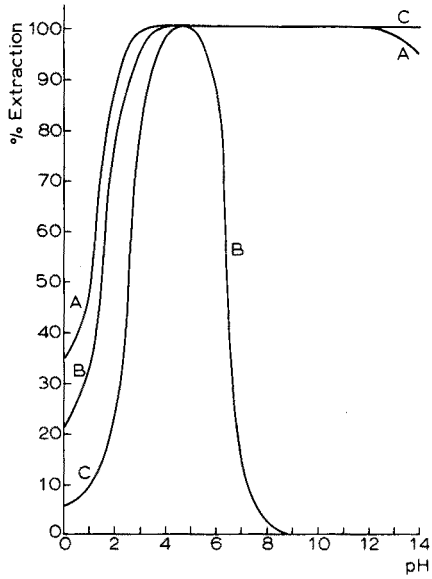

Fig. 5. Plot of % extraction *vs.* pH for nitrazepam (curve A), and potassium chlorazepate (curve B), and chlordiazepoxide (curve C).

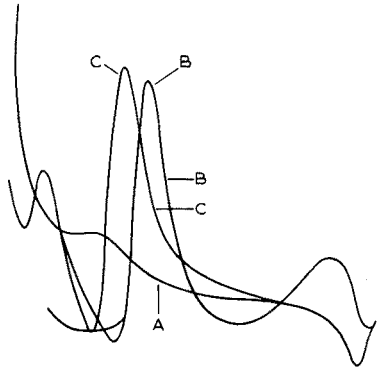

Fig. 6. Cathode ray polarograms (RC derivative circuit, 50 ms). A, urine blank extraction. B, standard potassium chlorazepate ($2 \cdot 10^{-5}$ *M*). C, Potassium chlorazepate after extraction from a spiked ($2 \cdot 10^{-5}$ *M*) urine sample. Current sensitivity $1.5 \cdot 1 \cdot 10$; starting voltage -0.5 V.

ethyl acetate for 10 min followed by centrifugation for 15 min. A blank was treated similarly. The upper layer was then removed, the solvent was evaporated off and the residue was polarographed in Britton–Robinson buffer pH 4 in the range 0 to 0.5 V. This showed the presence of two reduction peaks which were similar in height to those of standard $2 \cdot 10^{-5}$ *M* nitrazepam and chlordiazepoxide and corresponded to the reduction of the $-NO_2$ and $-NO$ groups, respectively. This was repeated several times and gave 95–100% extraction of nitrazepam and chlordiazepoxide at pH 9. The lower layer was then taken, the pH was adjusted to 4 with *M* hydrochloric acid, 2.5 ml of pH 4 Britton–Robinson buffer was added, and this solution was extracted as above. After separation of the layers, the ethyl acetate was evaporated off, and the residue was polarographed in Britton–Robinson buffer pH 4 in the ranges 0 to -0.5 V and -0.5 V to -1.0 V. The former range showed no reduction waves except small rounded peaks which were also present in the blank; the latter range gave one peak which was similar in height to the peak of standard $2 \cdot 10^{-5}$ *M* potassium chlorazepate but was moved about 30 mV to more negative potentials. This is illustrated in Fig. 6. This was repeated several times and gave 90–95% recovery of potassium chlorazepate from the urine samples.

CONCLUSION

The changes in the u.v. spectral bands and polarographic waves of potassium chlorazepate with pH suggest the existence of four species, of which only the

neutral form is extractable into ethyl acetate; extraction is almost quantitative over the narrow pH range 4–5. The behaviour of other therapeutically important benzodiazepines is similar below pH 4 but above pH 4 they continue to be extracted. This provides the basis of an analytical method in that the body fluid containing 'free' benzodiazepine can first be extracted at pH 9 to remove all the benzodiazepines except potassium chlorazepate. Then, by adjustment of the pH to 4, the chlorazepate can be extracted and polarographically determined by means of its azomethine reduction wave in pH 4 Britton–Robinson buffer. This is a specific method for the determination of potassium chlorazepate in the presence of other benzodiazepines.

SUMMARY

U.v. spectroscopy and polarography show that potassium chlorazepate exists in four forms over the pH range 0–14: monoprotonated (pH 0–3.5), neutral (pH 3.5–5.0), monoanionic (pH 5.0–12.0) and dianionic (above pH 12.0). Only the neutral form can be extracted into ethyl acetate from aqueous buffers. Because of differences in extraction profiles above pH 5, potassium chlorazepate can be determined in a mixture of benzodiazepines by extraction and polarography.

REFERENCES

1 N. Holmberg, *Arzneim.-Forsch.*, 22 (1972) 916.
2 K. Chakalampous, *J. Clin. Pharm.*, 13 (1973) 114.
3 B. Cooper, *Brit. J. Psychiat.*, 123 (1973) 475.
4 B. J. Magnus, *Clin. Practice*, 27 (12) (1973) 449.
5 J. M. Clifford and W. Franklin Smyth, *Analyst (London)*, 99 (1974) 241.
6 I. E. Davidson and W. Franklin Smyth, *Proc. Soc. Anal. Chem.*, 9 (1972) 209.
7 J. Barrett, W. Franklin Smyth and J. P. Hart, *J. Pharm. Pharmacol.*, 26 (1974) 9.
8 J. A. Goldsmith, H. A. Jenkins, J. Grant and W. Franklin Smyth, *Anal. Chim. Acta*, 66 (1973) 427.
9 E. Jacobsen and T. V. Jacobsen, *Anal. Chim. Acta*, 55 (1971) 293.
10 S. Halvorsen and E. Jacobsen, *Anal. Chim. Acta*, 59 (1972) 127.
11 J. A. Groves and W. Franklin Smyth, to be published.
12 L. Meites, *Polarographic techniques*, Interscience, 1970.
13 J. M. Clifford and W. Franklin Smyth, *Z. Anal. Chem.*, 264 (1973) 149.
14 J. Barrett, W. Franklin Smyth and I. E. Davidson, *J. Pharm. Pharmacol.*, 25 (1973) 387.

Analytica Chimica Acta, 76 (1975) 299–308

CONTRIBUTION À L'ÉLECTROCHIMIE DES THIOLS ET DISULFURES

PARTIE II: POLAROGRAPHIE D.C., A.C. ET IMPULSIONNELLE DIFFÉRENTIELLE DU GLUTATHION

C. A. MAIRESSE-DUCARMOIS, G. J. PATRIARCHE et J. L. VANDENBALCK

Institut de Pharmacie, Université Libre de Bruxelles, Avenue F-D Roosevelt, 50, 1050 Bruxelles (Belgium)

(Reçu le 1 novembre 1974)

Des travaux antérieurs consacrés, d'une part, à la détermination coulométrique de thiols et disulfures[1] et d'autre part, à l'électrochimie d'acides aminés soufrés tels que la cystéine et la cystine[2] nous ont incités à envisager dans le présent travail d'élucider le comportement d'autres dérivés d'intérêt pharmacologique et parmi ceux-ci le γ-L-glutamyl-L-cystéinylglycine (glutathion, GSH), qui a déjà fait l'objet de plusieurs publications[3–5].

Des techniques telles que les polarographies classiques (d.c.), et à tension sinusoïdale surimposée (a.c.) et la méthode impulsionnelle différentielle (p.p.) nous ont permis de déterminer les caractéristiques électrochimiques de ce dérivé et d'en étudier le mécanisme de réduction.

PARTIE EXPERIMENTALE

Les différentes mesures ont été réalisées à l'aide d'un ensemble polarographique TACUSSEL type PRG 3 et PRG 4. Chaque ensemble a en commun un potentiostat PRT 30–01, un enregistreur EPL 2 équipé d'un tiroir TV 11 GD asservi au tiroir UAP 3 et UAP 4.

Le produit étudié est de qualité analytique, utilisé sans purification préalable.

Les solutions sont préparées extemporanément dans l'électrolyte de support désoxygéné préalablement par un courant d'azote prolongé. Les tampons qui servent à la fois d'électrolytes de support et à l'étude du pH sont du type Clark et Lubs jusqu'à pH 8 et Bates et Bower pour les pH plus alcalins[6].

RESULTATS ET DISCUSSION

L'électrochimie de glutathion (GSH) dont l'instabilité en solution aqueuse est bien connue surtout en milieu alcalin[1,7] a été étudiée en fonction du pH et de la concentration.

Étude en fonction du pH

L'étude du comportement polarographique du GSH est réalisée dans une échelle de pH comprise entre 1,5 et 11,5 à l'aide d'une solution 10^{-3} *M* (Fig. 1). On observe en polarographie conventionnelle une vague anodique et une vague

TABLEAU I

COMPORTEMENT POLAROGRAPHIQUE DU GLUTATHION EN FONCTION DU pH

(Solution 10^{-3} *M* en glutathion)

pH	*D.c.*				*A.c.*	
	$E'_{\frac{1}{2}}$ *(V vs. ECS)*	$E_{\frac{3}{4}}-E_{\frac{1}{4}}$ *(mV)*	$E^2_{\frac{1}{2}}$ *(V vs. ECS)*	$E_{\frac{3}{4}}-E_{\frac{1}{4}}$ *(mV)*	*Sommets du pics A.c. (V vs. ECS)*	
1,54	−0,080	35	−0,255	30	−0,100	−0,250
2,39	−0,130	35	−0,260	30		−0,200
3,53	−0,175	40	−0,295	35	Épaulement	−0,295
5,07	−0,265	45	−0,365	35		−0,365
6,00	−0,340	50	−0,445	45	−0,375	−0,510
7,08	−0,375	55	−0,465	45	−0,422	−0,560
7,53	−0,370	60	−0,565	50	−0,435	−0,565
8,89	−0,455	55	−0,650	45	Épaulement	−0,625
9,85	−0,475	60	−0,680	60		−0,630
10,40	−0,507	65	—	—	−0,615	—
11,58	−0,502	50	—	—	−0,600	—

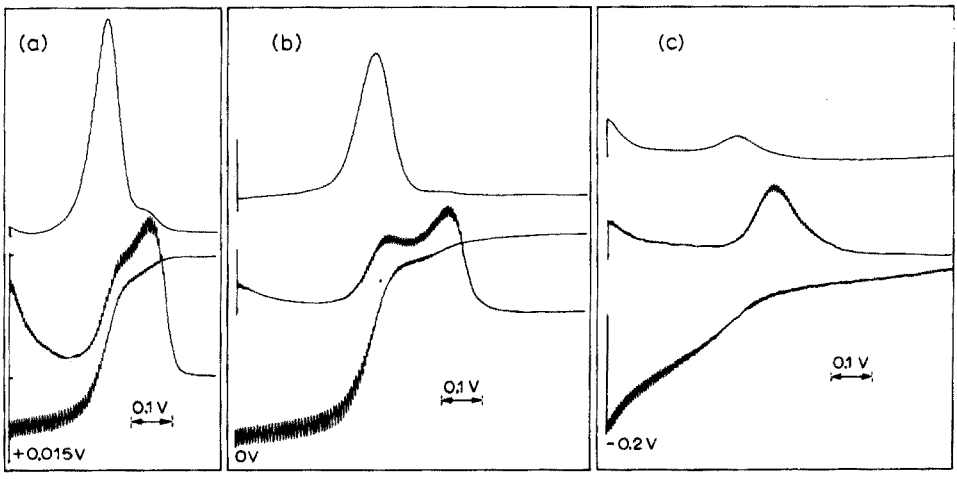

Fig. 1. Polarogrammes d.c., a.c., et p.p. d'une solution 1.10^{-3} *M* en glutathion. *V vs.* ECS. D.c. sensibilité 2,5 μA. A.c. sensibilité 5 μA; temps de chute de gouttes 0.9 s. P.p. sensibilité 2,5 μA, amplitude surimposée 20 mV; durée de l'impulsion 40 ms; temps de chute de gouttes 2 s, retard 1s 8; vitesse de déroulement 2 mV s^{-1}. (a) pH 3,5; (b) pH 6,3; (c) pH 11,3.

cathodique qui sont développées dans toute l'étendue de la zone de pH, mais c'est entre pH 6 et 10 qu'elles sont les mieux séparées comme le montre le Tableau I qui rassemble les valeurs des potentiels de demi-palier. Au dessus de pH 10, le GSH est totalement dissocié sous forme de thiolate et on n'observe plus qu'une seule vague chevauchant les limites des domaines anodiques et cathodiques.

Les mesures effectuées en polarographie a.c. permettent de mettre en évidence l'influence marquée d'une vague d'adsorption, les pics sont déformés entre pH 2 et 5,

ils ont leurs sommets situés au potentiel de $\frac{1}{2}$ palier de la vague cathodique alors que la vague anodique n'apparaît que sous forme d'un épaulement. Entre pH 6 et 7,5, les deux pics se distinguent parfaitement et l'intensité du pic correspondant à la vague d'adsorption va en grandissant.

Au dessus de pH 10 un seul pic se dégage et se déplace vers des valeurs de plus en plus positives à mesure que l'on fait croître le pH (Fig. 1). Comme le montre la Fig. 2, la valeur de la fréquence du signal surimposé à une influence marquante sur la valeur des intensités de pic de la vague d'adsorption. Si nous passons de 90 à 180 Hz à pH 1,5, l'intensité de pic augmente de 0,90 μA à 2,32 μA; ce qui s'observe lors d'un phénomène d'adsorption.

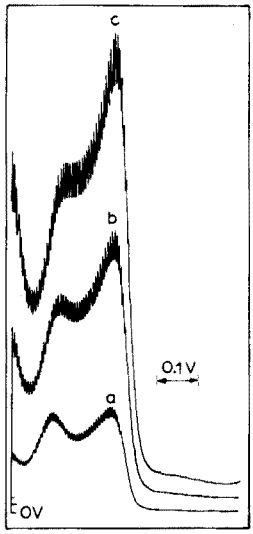

Fig. 2. Influence de la fréquence surimposée sur la courbe a.c. d'une solution 1.10^{-3} M en glutathion (pH 1,5). Sensibilité 5 μA; amplitude surimposée 10 mV; temps de chute de gouttes 0.9 s. Fréquences: (a) 90 Hz; (b) 180 Hz; (c) 270 Hz.

Étude en fonction de la concentration

Les ondes polarographiques varient fortement en fonction de la concentration. C'est ainsi que suivant le pH, la réduction peut se dérouler en une, deux voire trois étapes. Pour des teneurs assez élevées en dépolarisant (comprises entre $1 \cdot 10^{-2}$ et $5 \cdot 10^{-3}$ M), trois vagues sont marquées en polarographie conventionnelle. Deux de celles-ci sont bien développées, l'une est anodique, l'autre est cathodique, la troisième se présentant sous forme d'un maximum du second ordre et se situant à des potentiels plus positifs. L'origine de cette vague est attribuée à la formation d'un composé intermercuriel du type RSHg. Vers des concentrations de l'ordre de $1 \cdot 10^{-3}$ M, les vagues anodiques et cathodiques sont toujours bien séparées ($E_{\frac{1}{2}}$ respectifs de $-0{,}46$ V et 0,65 V *vs.* ECS) tandis que vers $8 \cdot 10^{-4}$ M une fusion s'opère entre les deux vagues et il n'y a plus qu'une seule onde polarographique décelable.

La réversibilité de la réaction change également si l'on en juge par les valeurs

TABLEAU II

COMPORTEMENT POLAROGRAPHIQUE DU GLUTATHION EN FONCTION DE LA CONCENTRATION

(Tampon pH 9,2)

Concentration (M)	*Nombre de vague*	*D.c.*					*A.c.*			
		$E_{\frac{1}{2}}^1$ *(V vs. ECS)*	$E_{\frac{1}{2}}^2$ *(V vs. ECS)*	$E_{\frac{1}{2}}-E_{\frac{1}{4}}$ *(mV)*	$E_{\frac{1}{2}}^3$ *(V vs. ECS)*	$E_{\frac{1}{2}}-E_{\frac{1}{4}}$ *(mV)*	E_p^1 *(V vs. ECS)*	$\omega_{\frac{1}{2}}$ *(mV)*	E_p^2 *(V vs. ECS)*	$\omega_{\frac{1}{2}}$ *(mV)*
10^{-2}	3	−0,345	−0,490	60	−0,727	45	−0,535	95	−0,700	105
$5\cdot10^{-3}$	3	−0,355	−0,485	60	−0,705	45	−0,535	110	−0,685	100
$1\cdot10^{-3}$	2	—	−0,467	45	−0,650	50	−0,545	195	−0,645	—
$5\cdot10^{-4}$	1	—	—	—	−0,620	60	—	—	−0,625	137
$1\cdot10^{-4}$	1	—	—	—	−0,595	60	—	—	−0,620	135

de $E_{\frac{3}{4}} - E_{\frac{1}{4}}$ qui passent de 50 mV à 78 mV si la variation de concentration se situe entre $8 \cdot 10^{-4}$ *M* et 9.10^{-4} *M*. À pH 9,2 (borax 0,05 *M*, nitrate de potassium 0,5 *M*), la mesure de la pente de droite obtenue en portant les log de $(i_d - i)/i$ *vs.* *E* avec une solution 10^{-3} *M* donne une valeur de 63 mV, la droite de régression calculée étant de la forme $y = 0{,}474 - 0{,}063\ x$.

L'observation des tracés obtenus en utilisant la méthode à tension sinusoïdale surimposée correspond parfaitement à ce que l'on avait pu obtenir à l'aide de la méthode conventionnelle. Deux pics distincts séparés de ± 100 mV se développent pour des concentrations de l'ordre de $1 \cdot 10^{-3}$ *M*. Lorsque la teneur en GSH diminue, une fusion des deux pics s'opère et celui-ci devient de plus en plus symétrique. Ces observations sont consignées au Tableau II et au Fig. 3. Les largeurs de pics calculées à mi-hauteur sont respectivement de 105 mV, 100 mV, 195 mV, 137,5 mV et 135 mV.

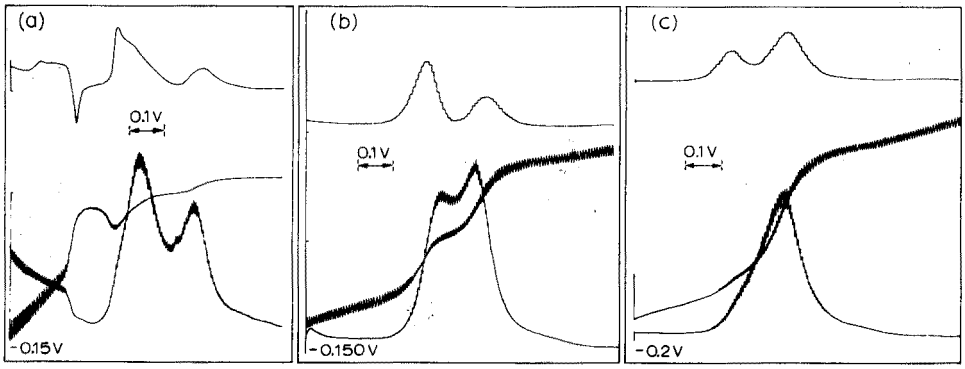

Fig. 3. Polarogrammes d.c., a.c. et p.p. en fonction de la concentration. pH 9,2 *V vs.* ECS. D.c. sensibilité variable. A.c. sensibilité 1.25 μA; temps de chute de gouttes 0.9 s. P.p. sensibilité variable; amplitude surimposée 20 mV, temps de chute de gouttes 2 s, retard 1s 8, durée de l'impulsion 40 ms, vitesse de déroulement 2 mV s^{-1}. (a) $5 \cdot 10^{-3}$ *M* en glutathion; d.c. sensibilité 12,5 μA; p.p. sensibilité 12,5 μA. (b) $1 \cdot 10^{-3}$ *M* en glutathion; d.c. sensibilité 2,5 μA; p.p. sensibilité 2,5 μA. (c) $5 \cdot 10^{-4}$ *M* en glutathion; d.c. sensibilité 1,25 μA; p.p. sensibilité 1,25 μA.

La vague cathodique mesurée pour des concentrations de l'ordre de $1 \cdot 10^{-3}$ *M* reste insensible à une augmentation de concentration. Elle résulte probablement de la formation d'un composé d'adsorption intermercuriel RSHg couplé à un phénomène cinétique que nous avons mis en évidence par des mesures de courbes électrocapillaires qui montrent une adsorption caractéristique à des potentiels correspondants à cette même vague (Fig. 4). Des mesures de courants réalisées en fonction de la hauteur du niveau du mercure montre que la hauteur de l'onde polarographique ne se modifie pas en fonction de ce paramètre.

Comme l'avait déjà souligné Mader *et al.*[7] lors d'une étude consacrée à la cystéine, la solubilité du GSHg adsorbé augmente avec la force ionique de la solution mais ne se modifie pas si la température varie entre 23°C et 30°C.

Quant à la vague anodique qui résulte de l'oxydation du glutathion, elle a les caractéristiques d'une vague de diffusion. Les intensités de courant sont proportionnelles à la concentration et varient linéairement avec la racine carrée de la

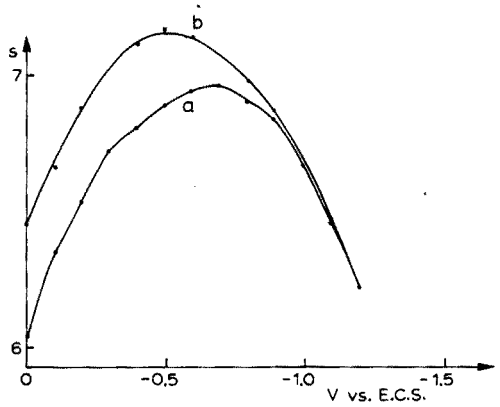

Fig. 4. Courbes électrocapillaires. (a) Electrolyte de support seul (0,05 *M* de borate de sodium, 0,5 *M* KNO_3), (b) électrolyte de support additionné de 10^{-3} *M* de glutathion.

hauteur de la colonne de mercure, le coefficient de température étant égal à $\pm 3\%/°C$. L'oxydation du glutathion se passerait sous la forme du schéma suivant: ou deux électrons interviendraient dans la réaction globale:

$$GSH \rightleftharpoons GS^- + H^+ + e$$

$$2\,GS^- \rightleftharpoons GSSG$$

L'adsorbat se formerait à ce stade sous forme d'un composé intermétallique GSHg.

L'apparition de la vague d'adsorption nous indique que la concentration en thiolate est suffisamment grande à la surface de l'électrode que pour couvrir celle-ci d'une mono-couche de thiolate mercure (I) ou (II) qui freine et inhibe la dissolution du mercure. On pourrait imaginer qu'à de plus grandes concentrations en produits soufrés apparaissent deux voire trois vagues d'adsorption successives qui seraient dues à la formation d'un deuxième et troisième film de thiolate mercurique à l'électrode.

Étude impulsionnelle

L'étude en polarographie impulsionnelle différentielle (p.p.) a été réalisée à pH 3,5 où la vague d'adsorption apparaît faiblement sous forme d'un épaulement du pic correspondant à la vague d'oxydation. À pH 6,5 les deux pics sont nettement plus séparés (Fig. 1 (a), (b)). Pour une teneur de $1 \cdot 10^{-3}$ *M*, les paramètres envisagés sont: l'amplitude de l'impulsion, le temps de chute de gouttes, la vitesse de balayage. Ces paramètres étant fixés nous avons observé l'influence de la variation de la concentration. Toutes les mesures sont effectuées en cellule thermostatisée à $25 \pm 0{,}1°C$.

Influence de l'amplitude à pH 3,5. (Tableau III). Dans les conditions expérimentales, on peut observer que si l'amplitude décroît de 40 à 5 mV, les potentiels de pics sont légèrement déplacés vers des valeurs plus négatives; la largeur à mi-hauteur du pic dû à la vague anodique diminue et son intensité décroît de manière quasi linéaire avec l'amplitude.

Influence du temps de chute de gouttes à pH 3,5. (Tableau IV). L'amplitude de l'impulsion étant fixée à une valeur de 20 mV et les autres paramètres conservant les mêmes valeurs, la diminution du temps de chute affecte plus le premier pic que l'épaulement dû au phénomène d'adsorption: ainsi, la valeur de l'intensité de pic

TABLEAU III

POLAROGRAPHIE IMPULSIONNELLE. INFLUENCE DE L'AMPLITUDE

(Concentration 10^{-3} *M* en glutathion; temps de chute de gouttes 2s; retard à l'impulsion ls 8; durée de l'impulsion 40 ms; vitesse de balayage 2 mV s^{-1}.)

Amplitude (mV)	E_p^1 *(V vs. ECS)*	i_p^1 *(nA)*	$\omega_{\frac{1}{2}}$ *(mV)*	E_p^2 *(V vs. ECS)*	i_p^2 *(nA)*
pH 3,5					
40	−0,175	2170	90	−0,280	140
20	−0,187	1100	72,5	−0,285	80
10	−0,192	510	65	−0,287	40
5	−0,197	242	70	−0,295	16
pH 6,5					
40	−0,330	1660	92,5	−0,475	50
20	−0,335	815	87,5	−0,490	25
10	−0,340	378	90	−0,495	10
5	−0,345	160	85	−0,500	4

TABLEAU IV

POLAROGRAPHIE IMPULSIONNELLE. INFLUENCE DU TEMPS DE CHUTE

(Concentration 10^{-3} *M* en glutathion; sensibilité 2,5 μA.)

Temps de chute	*Pic*			*Épaulement*	
	E_p^1 *(V vs. ECS)*	i_p^1 *(nA)*	$\omega_{\frac{1}{2}}$ *(mV)*	E_p^2 *(V vs. ECS)*	i_p^2 *(nA)*
pH 3,5					
1 gtte. 4 s, ret. 3.8 s	−0,190	1730	70	−0,290	120
3 s, ret. 2.8 s	−0,190	1460	70	−0,285	90
2 s, ret. 1.8 s	−0,187	1100	70	−0,282	80
1 s, ret. 0.8 s	−0,182	640	70	−0,275	70
pH 6,5					
1 gtte. 4 s, ret. 3.8 s	−0,340	1070	87,5	−0,492	30
3 s, ret. 2.8 s	−0,340	920	87,5	−0,492	30
2 s, ret. 1.8 s	−0,335	815	87,5	−0,490	25
1 s, ret. 0.8 s	−0,332	480	90	−0,497	25

n'atteint plus que 37% de sa valeur initiale si le temps de chute passe de 4 s à 1 s; la largeur du pic à mi-hauteur, ne subit aucune fluctuation.

Influence de la vitesse de balayage à pH 3,5 (Tableau V). Si la vitesse de balayage augmente, le pic et son épaulement diminuent d'intensité, la largeur du pic à mi-hauteur augmente forcément et les potentiels de sommet sont légèrement déplacés vers des valeurs plus négatives.

Influence de la concentration à pH 3,5 (Tableau VI). Si la variation de l'intensité de pic dû à la vague anodique est pratiquement linéaire avec la concentration, l'apparition de l'épaulement dû à la vague d'adsorption croît à partir de

TABLEAU V

POLAROGRAPHIE IMPULSIONNELLE. INFLUENCE DE LA VITESSE DE BALAYAGE

(Concentration 10^{-3} *M* en glutathion.)

Vitesse de balayage ($mV\ s^{-1}$)	E_p^1 (*V vs. ECS*)	i_p^1 (*nA*)	$\omega_{\frac{1}{2}}$ (*mV*)	E_p^2 (*V vs. ECS*)	i_p^2 (*nA*)
pH 3,5					
0.5	−0,180	1205	72,5	−0,270	110
1	−0,185	1170	72,5	−0,280	90
2	−0,187	1100	70	−0,285	80
4	−0,195	1000	80	−0,287	80
pH 6,5					
0.5	−0,332	900	85	−0,487	27,5
1	−0,332	870	85	−0,487	27,5
2	−0,335	815	87,5	−0,490	25
4	−0,345	735	87,5	−0,492	25

TABLEAU VI

POLAROGRAPHIE IMPULSIONNELLE. INFLUENCE DE LA CONCENTRATION

Concentration (*M*)	E_p^1 (*V vs. ECS*)	i_p^1 (*nA*)	$\omega_{\frac{1}{2}}$ (*mV*)	*Épaulement*	
				E_p^2 (*V vs. ECS*)	i_p^2 (*nA*)
pH 3,5					
10^{-3}	−0,190	1040	72.5	−0,285	90
$8 \cdot 10^{-4}$	−0,187	815	72.5	−0,280	75
$6 \cdot 10^{-4}$	−0,180	600	72.5	−0,275	95
$4 \cdot 10^{-4}$	−0,175	385	77.5	−0,260	142
$2 \cdot 10^{-4}$	−0,175	162,5	N.mes.	−0,240	150
pH 7,2					
10^{-3}	−0,400	775	90	−0,560	15
$8 \cdot 10^{-4}$	−0,400	650	85	−0,555	20
$6 \cdot 10^{-4}$	−0,395	495	80	−0,550	45
$4 \cdot 10^{-4}$	−0,390	300	72,5	−0,535	50
$2 \cdot 10^{-4}$	−0,385	100	80	−0,520	60

$6 \cdot 10^{-4}$ *M*. Pour une teneur de $2 \cdot 10^{-4}$ *M* les intensités des deux pics sont presque identiques: 162.5 nA et 150 nA si l'amplitude est de 20 mV, mais elles fluctuent avec des changements de celle-ci.

A pH 6,5, les potentiels de pic sont mieux séparés mais toutes les observations mentionnées à pH 3,5 sont également valables pour cet autre pH si l'on en juge par les valeurs qui sont reprises aux Tableaux III–VI.

Ce que l'on peut déduire des phénomènes observés montre qu'à l'opposé des autres méthodes utilisées, le phénomène d'adsorption est relativement peu marqué en polarographie impulsionnelle étant donné que le courant de charge qui passe

durant l'application d'une impulsion de courte durée est insuffisant pour provoquer la formation d'un film organo-mercuriel à la surface de l'électrode. Si l'on veut accentuer le phénomène d'adsorption, il suffirait d'augmenter la concentration en dépolarisant comme l'ont montré Canterford et ses collaborateurs[8,9] lors d'une étude polarographique impulsionnelle directe de l'ion sulfure.

Détermination quantitative du GSH par p.p.

Des quantités aussi faibles que $1 \cdot 10^{-6}$ *M* sont aisément déterminées avec une bonne approximation, ce qui représente 0,3 mg du composé par litre. En dessous de cette concentration, le tracé polarographique devient mal défini et les erreurs de mesure ont tendance à augmenter.

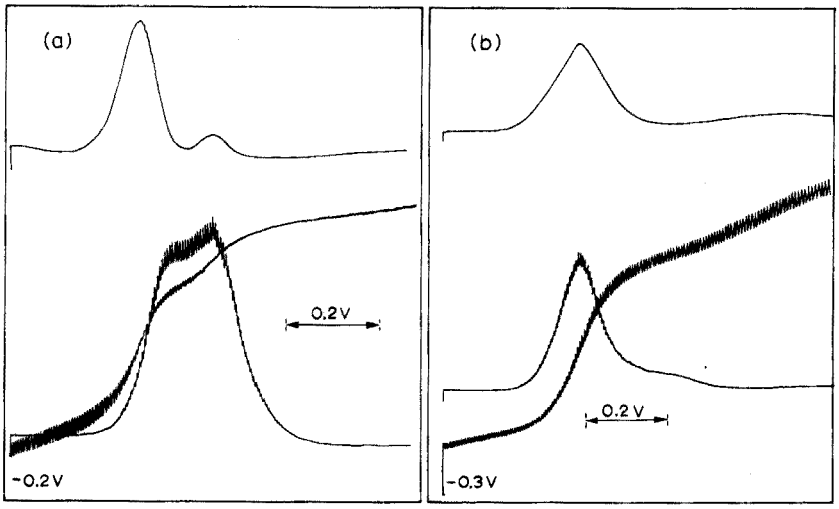

Fig. 5. Polarogrammes d.c., a.c. et p.p. d'une solution $5 \cdot 10^{-4}$ *M* en glutathion (pH 9,2). (a) Au temps zéro. (b) Après 24 h d'oxydation à l'air. D.c. sensibilité 1,25 μA. A.c. sensibilité 1,25 μA; temps de chute de gouttes 0.9 s. P.p. sensibilité 1 μA; amplitude surimposée 20 mV; temps de chute de goutte 2 s; retard 1s 8; durée de l'impulsion 40ms; vitesse de déroulement 2 mV s^{-1}.

TABLEAU VII

DIMINUTION DE LA TENEUR EN GLUTATHION ($5 \cdot 10^{-4}$ *M*) AU COURS DU TEMPS

Temps (h)	*Tampon pH 3,5*		*Tampon pH 9,2*	
	i_d (anodique) (nA)	*Décroissance de teneur (%)*	*i_d (anodique) (nA)*	*Décroissance de la teneur (%)*
0	780	—	645	—
2	700	−10,2	555	−13,9
4	690	−11,5	450	−30,2
6	690	−11,5	295	−54,2
8	670	−14,1	165	−74,4
24	670	−14,1	—	−100,0

Stabilité du glutathion en solution aqueuse

La dégradation de ce thiol, que nous avions déjà signalée dans un précédent travail[1] et plus particulièrement en milieu alcalin, nous montre qu'à pH 9,2, la forme réduite de ce composé disparaît progressivement. C'est ainsi qu'après 6 h de contact avec l'oxygène atmosphérique, la vague d'adsorption se présente sous forme d'un maximum arrondi masquant le développement des autres vagues et l'on voit apparaître à des potentiels plus négatifs une vague cathodique due au disulfure qui se forme progressivement. Après 24 h de contact en milieu alcalin, la forme réduite a totalement disparu pour faire place à la forme oxydée (Fig. 5).

En milieu acide, l'autooxydation est beaucoup moins rapide. La teneur en thiol baisse d'environ 10% endéans les deux premières heures et la décroissance n'est que de 14% après 24 h. Les résultats concernant l'étude de cette dégradation figurent au Tableau VII.

Nos remerciements vont au Fonds National de la Recherche Scientifique pour l'aide apporté à l'un d'entre nous (G.J.P).

RÉSUMÉ

L'étude des caractéristiques électrochimiques du glutathion a été réalisée par les polarographies conventionnelle, alternative et impulsionnelle en fonction du pH et de la concentration. De une à trois vagues polarographiques sont observées et le type de courant a été mis en évidence. Une étude de la stabilité du glutathion a été effectuée à différents pH. La détermination de ce composé par polarographie impulsionnelle différentielle nous a permis de doser des quantités voisines de 0.3 mg l^{-1} ($1 \cdot 10^{-6}$ *M*).

SUMMARY

A study of the electrochemical characteristics of glutathione (GSH) was carried out at various pH values and concentrations by d.c., a.c. and differential pulse polarography. The stability of the compound was also studied at various pH values. Differential pulse polarography made it possible to determine as little as 0.3 mg CSH l^{-1}.

BIBLIOGRAPHIE

1 C. A. Mairesse-Ducarmois, J. L. Vandenbalck et G. J. Patriarche, *J. Pharm. Belg.*, 28 (1973) 300.
2 C. A. Mairesse-Ducarmois, G. J. Patriarche et J. L. Vandenbalck, *Anal. Chim. Acta*, 71 (1974) 165.
3 W. Stricks et I. M. Kolthoff, *J. Amer. Chem. Soc.*, 75 (1953) 5673; 77 (1955) 4733.
4 W. Stricks, I. M. Kolthoff et R. C. Kapoor, *J. Amer. Chem. Soc.*, 77 (1955) 2057.
5 G. Gorin et G. Douchty, *Arch. Biochem. Biophys.*, 126 (1968) 547.
6 L. Meites, *Handbook of Analytical Chemistry*, McGraw Hill, 1963, Sect. 11-6, 11-7.
7 P. Mader, J. Volke et J. Kůta, *Collect. Czech. Chem. Commun.*, 35 (1970) 552.
8 D. R. Canterford and A. S. Buchanan, *J. Electroanal. Chem.*, 44 (1973) 291; 45 (1973) 193.
9 D. R. Canterford, *J. Electroanal. Chem.*, 52 (1974) 144.

Analytica Chimica Acta, 76 (1975) 309–318

POLAROGRAPHIC REDUCTION OF URANYL-BENZENEHEXACARBOXYLATE COMPLEXES IN AQUEOUS AND DIMETHYL SULFOXIDE SOLUTION

TSAI-TEH LAI and CHAUR-SHYONG WEN

Department of Chemical Engineering, Cheng Kung University, Tainan, Taiwan (China)

(Received 18th October 1974)

The outer-sphere complexes of $Cr(NH_3)_5X^{2+}$ with the benzenehexacarboxylate (mellitate) anion have been studied[1]. Yttrium and lanthanum salts of benzenehexacarboxylic acid (mellitic acid) have been prepared[2]. The thermal decomposition of various metal mellitic acid salts has been investigated[3–5].

In the present paper, the polarographic behaviour of uranyl–mellitate complexes in aqueous and in dimethyl sulfoxide (DMSO) solution is reported.

EXPERIMENTAL

Apparatus

The polarograph and techniques used in this work have been described previously[6]. The mercury flow rate and the dropping time of the dropping mercury electrode (DME) at a mercury height of 74.4 cm and an applied potential of −0.40 V *vs.* SCE were: $m=2.03$ mg s^{-1} and $t=4.06$ s/drop measured in aqueous 0.15 *M* $NaClO_4$ solution; and $m=2.01$ mg s^{-1} and $t=3.94$ s/drop measured in 0.15 *M* $NaClO_4$ in 50% (v/v) DMSO solution. All measurements were made at 30 ± 0.1°C.

A Toa Electronics Model CM-IDB electrolytic conductivity meter (cell constant, 2.0) was used for conductimetric titration.

Chemicals

Stock solutions of 0.1 *M* uranyl perchlorate[7] and of 0.2 *M* mellitic acid (H_6A; research grade, Aldrich) in 90% (v/v) DMSO were prepared.

Sodium perchlorate was used as supporting electrolyte, the ionic strength being kept constant at 0.15. Triton X-100 was used as maximum suppressor.

RESULTS AND DISCUSSION

Polarographic waves of mellitic acid

A single well-defined wave was obtained in an aqueous solution of mellitic acid in the pH range 2.3–6.3 but below pH 2.3 there was a double wave (Fig. 1; Table I). The temperature coefficients of the half-wave potential and diffusion current were 0.62 mV/°C and 3.1%/°C, respectively, and the value of $ih^{-\frac{1}{2}}$ was not constant; these data show that the electrode reduction was a reversible

TABLE I

WAVE CHARACTERISTICS OF MELLITIC ACID IN AQUEOUS AND DMSO SOLUTION

(0.15 *M* $NaClO_4$ and 0.002% Triton X-100. $-E_{\frac{1}{2}}$ in *V vs.* SCE; *i* in μA.)

DMSO (% (*v/v*))	$[H_6A]$ (*M*)	*pH*	*Prewave*			*1st wave*			*2nd wave*		
			$-E_{\frac{1}{2}}$	*i*	$E_{\frac{1}{4}}-E_{\frac{3}{4}}$	$-E_{\frac{1}{2}}$	*i*	$E_{\frac{1}{4}}-E_{\frac{3}{4}}$	$-E_{\frac{1}{2}}$	*i*	$E_{\frac{1}{4}}-E_{\frac{3}{4}}$
0	0.01	1.74				0.225	0.63	0.058	0.641	0.35	0.056
		2.25				0.225	0.51	0.061	0.690	0.30	0.059
		3.38	None			0.198	0.53	0.058			
		4.40				0.160	0.33	0.062	None		
		5.40				0.125	0.74	0.065			
		6.31				0.105	0.80	0.059			
50	0.08	1.80							0.631	0.61	0.065
		2.10	None						0.655	0.72	0.082
		2.58	0.112	0.95	0.023	None			0.698	0.73	0.087
		2.75	0.163	0.90	0.018				0.710	0.85	0.089
		3.18	0.260	0.82	0.019				0.733	0.80	0.094

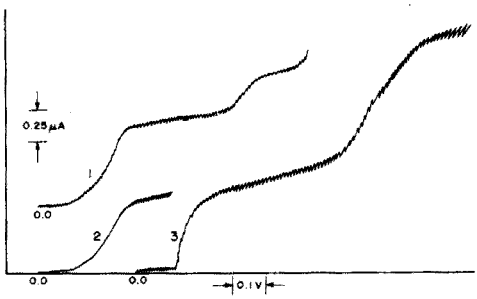

Fig. 1. Polarographic curves of mellitic acid. 0.15 *M* $NaClO_4$, 0.002% Triton X-100 and varying concentrations of mellitic acid and DMSO.

	1	2	3
pH	1.76	3.34	2.77
H_6A, *M*	0.01	0.01	0.08
DMSO, % (v/v)	0	0	50

one-electron reaction and not a diffusion-controlled process. Below pH 2.5, the half-wave potential was independent of pH, indicating that no hydrogen ion took part in the reduction. However, above pH 2.5, the slope of $\Delta E_{\frac{1}{2}}/\Delta pH$ was 0.031 showing that one hydrogen ion was consumed for every two molecules of mellitic acid reduced. As the pH value increased, the half-wave potential shifted to more positive potential (Table I).

Wave characteristics of uranyl–mellitate complexes in aqueous solution

The polarograms of the uranyl–mellitate complexes were influenced greatly by the concentration of mellitic acid and the pH value. In 0.1 *M* mellitic acid, a four-step wave was observed in the pH range 2.5–4.5. Outside this pH range, a two-step wave was obtained, whereas at lower concentrations of mellitic acid, a three-step wave appeared (Figs. 2 and 3). The polarographic characteristics for these waves are listed in Table II.

The first wave was observed in the pH range 1.2–6.2 for mellitic acid concentrations of 0.01–0.1 *M*. The limiting current of the first wave was independent of the concentration of mellitic acid (Fig. 4); it was proportional to h_{corr} and was essentially independent of the temperature (Table III). These data provide evidence for an adsorption wave caused by the adsorption of the reduced product on the electrode surface[8].

If the reduced product is adsorbed on the electrode and the concentration of depolarizer is very high, the excess of depolarizer produces a second wave at a more negative potential, representing the reduction of the depolarizer to the dissolved product.

As shown in Table III, the sum of the heights of the first and second wave was proportional to the square root of the mercury column height; the temperature coefficients of the half-wave potential and diffusion current for the double wave were -0.7 mV/°C and 1.4%/°C, respectively. These results show that the double wave is a reversible diffusion-controlled wave, corresponding to the reduction of the uranium(VI)–mellitate complex to the uranium(V) state.

The third wave was observed in the pH range 2.5–5.0 for the whole concentration range of mellitic acid studied. Its height was very sensitive to

TABLE II

POLAROGRAPHIC CHARACTERISTICS OF THE URANYL–MELLITATE COMPLEX IN AQUEOUS SOLUTION

(1.0 m*M* $UO_2(ClO_4)_2$, 0.15 *M* $NaClO_4$ and 0.002% Triton X-100. $-E_{\frac{1}{4}}$ in *V vs.* SCE; *i* in μA.)

$[H_6A]$ (*M*)	*pH*	*1st wave*			*2nd wave*			*3rd wave*			*4th wave*		
		$-E_{\frac{1}{4}}$	*i*	$E_{\frac{1}{4}}-E_{\frac{3}{4}}$	$-E_{\frac{1}{4}}$	*i*	$E_{\frac{1}{4}}-E_{\frac{3}{4}}$	$-E_{\frac{1}{4}}$	*i*	$E_{\frac{1}{4}}-E_{\frac{3}{4}}$	$-E_{\frac{1}{4}}$	*i*	$E_{\frac{1}{4}}-E_{\frac{3}{4}}$
0.01	2.21	0.178	2.57	0.054	None			None			0.610	2.00	0.120
	3.50	0.257	0.80	0.055	None			0.465	0.95	0.045	0.730	1.20	0.145
	4.01	0.284	0.65	0.064	None			0.474	0.53	0.040	0.822	1.56	0.150
	5.85	0.235	0.70	0.068	None			None			0.951	1.50	0.152
0.05	1.60	0.190	3.85	0.059	None			None			0.589	2.75	0.120
	2.72	0.258	1.77	0.054	None			None			0.665	3.96	0.143
	3.80	0.285	0.76	0.063	None			0.466	0.89	0.034	0.833	2.95	0.132
	5.45	0.201	0.72	0.071	None			None			0.985	1.82	0.142
0.08	2.21	0.258	3.35	0.054	None			None			0.675	3.80	0.107
	3.40	0.275	1.02	0.064	0.410	1.05	0.028	0.510	0.65	0.030	0.782	3.21	0.115
	4.57	0.198	0.75	0.060	None			0.630	0.38	0.042	0.840	2.92	0.128
	5.32	0.175	0.60	0.067	None			None			0.964	2.14	0.135
0.10	2.20	0.265	3.05	0.052	None			None			0.664	4.31	0.090
	3.62	0.280	0.85	0.062	0.432	1.90	0.037	0.630	0.62	0.035	0.830	3.96	0.110
	4.30	0.242	0.75	0.058	0.420	1.90	0.032	0.652	0.49	0.041	0.859	3.88	0.115
	5.50	0.170	0.73	0.065	None			0.678	0.40	0.054	1.045	3.74	0.143

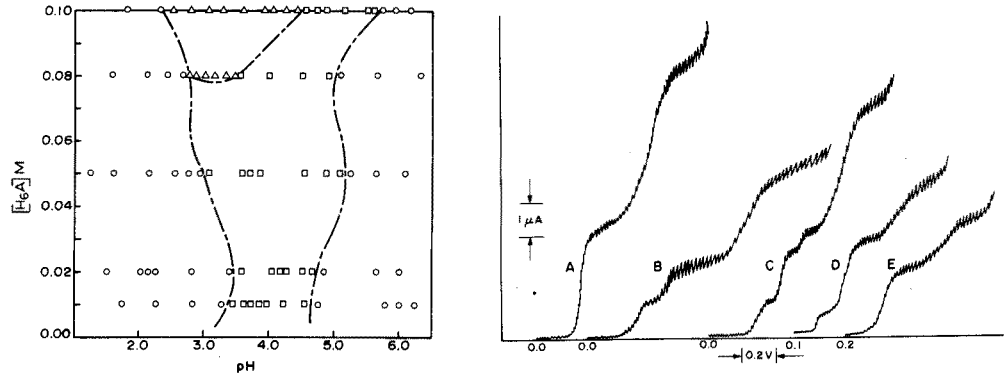

Fig. 2. Waves of uranyl–mellitate complexes in aqueous solution as functions of pH value and ligand concentration. 1.0 m*M* $UO_2(ClO_4)_2$, 0.15 *M* $NaClO_4$, 0.002% Triton X-100. (○) Two-step wave; (□) three-step wave; (△) four-step wave.

Fig. 3. Polarographic curves of uranyl–mellitate complexes in aqueous and DMSO solution. 1.0 m*M* $UO_2(ClO_4)_2$, 0.15 *M* $NaClO_4$, 0.002% Triton X-100 and varying concentrations of mellitic acid and DMSO at various pH.

	A	B	C	D	E
H_6A, *M*	0.1	0.05	0.1	0.08	0.05
DMSO, % (v/v)	0	0	0	50	70
pH	2.2	3.8	3.4	3.1	3.2

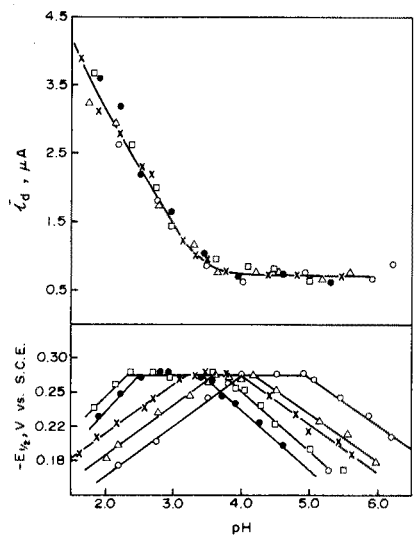

Fig. 4. Effect of pH on the half-wave potential and diffusion current of the first wave of the uranyl–mellitate complex. 1.0 m*M* $UO_2(ClO_4)_2$, 0.15 *M* $NaClO_4$, 0.002% Triton X-100 and various concentrations of mellitic acid: (○) 0.01 *M*; (△) 0.02 *M*; (×) 0.05 *M*; (●) 0.08 *M*; (□) 0.1 *M*.

variation of pH; it decreased with increasing pH and disappeared completely above pH 5.5. In addition, this wave had an abnormally high temperature coefficient for the limiting current (3.9%/°C), and the wave height was independent of $h_{corr.}$. Thus the third wave is a catalytic hydrogen wave caused by the uranyl–mellitate complex.

TABLE III

NATURE OF THE LIMITING CURRENT OF THE FIRST AND SECOND WAVE OF URANYL–MELLITATE COMPLEXES IN AQUEOUS SOLUTION

(1.0 m*M* $UO_2(ClO_4)_2$, 0.15 *M* $NaClO_4$ and 0.002% Triton X-100)

	1st wave	*1st wave + 2nd wave*
Temp. coeff. of $E_{\frac{1}{4}}$ mV/°C (20–45°C)	−0.5	−0.7
Temp. coeff. of %/°C (20–45°C)	0.4	1.4
$i_{l/h}$ (μA cm^{-1})	0.0120 ± 0.0002[a]	
$i_{l/h^{\frac{1}{2}}}$ (μA cm$^{-\frac{1}{2}}$) (h: 64.4–84.4 cm)	0.160 ± 0.003[b]	0.285 ± 0.002[a]

[a] 0.1 *M* mellitic acid at pH 3.0.
[b] 0.05 *M* mellitic acid at pH 3.6.

The fourth wave appeared at half-wave potentials more negative than −0.60 V *vs.* SCE, for ligand concentrations of 0.01–0.1 *M*, in the pH range 1.2–6.3. The value of $ih^{-\frac{1}{2}}$ was 0.424 ± 0.003 and the temperature coefficient of the limiting current was 1.7%/°C, indicating that this wave was diffusion-controlled. The high values of $E_{\frac{1}{4}} - E_{\frac{3}{4}}$ (Table II) and the slope of the $E_{\frac{1}{4}}$ *vs.* pH plots (0.12 V) indicated that the reduction was irreversible and involved hydrogen ions. This fourth wave is an irreversible two-electron wave, corresponding to the reduction of uranium(V) to the uranium(III) state. At lower concentration of mellitic acid, only the first wave exists (Table II). The temperature coefficients of the wave parameters of the first wave (Table III) prove that the reduction of uranyl–mellitate complex is a reversible and diffusion-controlled process.

As shown in Fig. 4, a plot of half-wave potential *vs.* pH has a slope of −0.057 below pH 3.2, zero at pH 3.2–4.0, and +0.057 above pH 4.0 for mellitic acid concentrations of 0.05 *M*. Since the successive pK values of mellitic acid[9] are 1.41, 2.19, 3.31, 4.80, 5.89 and 6.96, respectively, the predominant ligand species must be H_3A^{3-} for the pH ranges investigated in this work. Then, the general equation for the reduction of the uranyl–mellitate complex may be written:

$$UO_2(H_3A)_p^{2-3p} + e \rightleftharpoons UO_2(H_3A)_q^{1-3q} + (p-q)H_3A^{3-} \quad (1)$$

The half-wave potential for reaction (1) can be expressed as

$$(E_{\frac{1}{4}})_c = (E_{\frac{1}{4}})_s - 0.060 \log \frac{K_{oc}}{K_{rc}} - 0.060(p-q)\log[H_6A]$$
$$- 0.060 \log K_1K_2K_3 - 3 \times 0.060(p-q)\log[H^+]$$
$$+ 0.060(p-q)\log\{[H^+]^6 + K_1[H^+]^5 + K_1K_2[H^+]^4 + \ldots + K_1K_2K_3K_4K_5K_6\} \quad (2)$$

where $[H_6A]$ is the total concentration of mellitic acid added.

Since the uranyl chelate suffers hydrolysis above pH 4.0 (ref. 6), the slope of the half-wave potential *vs.* pH value from eqn. (2) should be $-0.060\,(p-q)$ at $pK_2 < pH < pK_3$, zero at $pK_3 < pH < 4.0$, and +0.060 at $4.0 < pH < pK_4$. This

is in good agreement with the experimental data (Fig. 4). Thus, the $(p-q)$ values become one below pH 3.2, and zero above pH 3.2; this was confirmed by the plots of half-wave potential *vs.* ligand concentration in Fig. 5. The p value was shown to be unity by conductimetric titration. Thus, under the conditions used, the predominant chelate species are $UO_2(H_3A)^-$ below pH 4.0 and $UO_2(OH)H_3A^{2-}$ above pH 4.0.

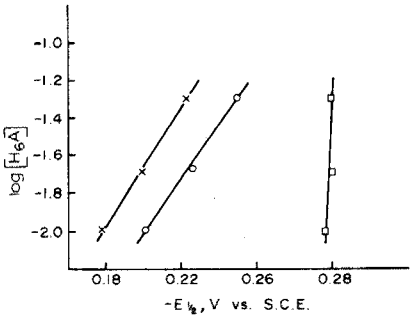

Fig. 5. Effect of ligand concentration on the half-wave potential of the first wave of uranyl-mellitate complex. 1.0 mM $UO_2(ClO_4)_2$, 0.15 M $NaClO_4$ and 0.002% Triton X-100. (×) pH 2.2; (○) pH 2.7; (□) pH 3.8.

Polarographic waves in DMSO solution

In contrast to the complicated nature of the polarographic waves obtained in aqueous solution, only two well-defined waves were obtained in dimethyl sulfoxide solution (Fig. 3); the first wave was reversible but the second was irreversible (Table IV). In 50% (v/v) DMSO a prewave appeared above pH 2.7 (Table IV).

From the data for the half-wave potential and the limiting current, the prewave and the second wave can be attributed to reduction of mellitic acid in the DMSO solution; the first wave is due to reduction of the uranyl–mellitate–DMSO system. This first wave is due to a reversible, one-electron, diffusion-controlled reduction. The number of hydrogen ions involved in the electrode reduction was estimated from the slopes of the $E_{\frac{1}{2}}$ *vs.* pH plots of the data given for the first and second waves in Table IV; the results are shown in Table V.

The electrode reaction for the uranyl–mellitate–DMSO complex can be expressed as

$$UO_2(DMSO)_x(H_3A)_p^{2-3p} + e \rightleftharpoons UO_2(DMSO)_y(H_3A)_q^{1-3q} + (x-y)DMSO + (p-q)H_3A^{3-} \quad (3)$$

The half-wave potential of the complex can be represented by

$$(E_{\frac{1}{2}})_c = (E_{\frac{1}{2}})_s - 0.060 \log \frac{K_{oc}}{K_{rc}} - 0.060(x-y)\log[DMSO] - 0.060(p-q)\log[H_3A^{3-}] \quad (4)$$

The values of $(x-y)$ and $(p-q)$ were obtained from the slopes of $(E_{\frac{1}{2}})_c$ *vs.* $\log[DMSO]$ and $(E_{\frac{1}{2}})_c$ *vs.* $\log[H_6A]$, respectively; the results are shown in Table V.

TABLE IV

POLAROGRAPHIC CHARACTERISTICS OF THE URANYL–MELLITATE COMPLEX WITH VARIOUS CONCENTRATIONS OF DMSO AND MELLITIC ACID

(1.0 m*M* $UO_2(ClO_4)_2$, 0.15 *M* $NaClO_4$, and 0.002% Triton X-100. $-E_{\frac{1}{4}}$ in *V vs.* SCE; *i* in μA.)

Reagent concn.	*pH*	*Prewave*			*1st wave*			*2nd wave*		
		$-E_{\frac{1}{4}}$	*i*	$E_{\frac{1}{4}}-E_{\frac{3}{4}}$	$-E_{\frac{1}{4}}$	*i*	$E_{\frac{1}{4}}-E_{\frac{3}{4}}$	$-E_{\frac{1}{4}}$	*i*	$E_{\frac{1}{4}}-E_{\frac{3}{4}}$
DMSO (%) v/v[a]										
20	1.55	None			0.255	3.70	0.060	0.605	2.42	0.080
	2.05	None			0.265	3.60	0.056	0.647	1.75	0.073
	2.50	None			0.310	3.75	0.054	0.673	1.35	0.072
	3.00	0.240	0.62	0.018	0.365	3.18	0.052	0.715	1.20	0.078
50	1.80	None			0.341	2.60	0.060	0.630	1.80	0.078
	2.20	None			0.350	2.12	0.057	0.665	1.78	0.082
	2.71	0.162	0.53	0.014	0.385	2.29	0.062	0.685	1.55	0.084
	3.05	0.210	0.54	0.015	0.405	1.93	0.054	0.725	1.41	0.086
70	1.98	None			0.377	2.13	0.058	0.705	1.51	0.092
	2.50	None			0.395	2.02	0.056	0.726	1.31	0.103
	3.31	None			0.445	1.81	0.059	0.768	1.45	0.116
	3.65	None			0.460	1.78	0.060	0.785	1.26	0.108
Mellitic acid (M)[b]										
0.01	1.69	None			0.343	2.38	0.057	0.630	1.03	0.098
	2.50	None			0.345	2.01	0.060	0.680	0.98	0.105
	2.82	0.130	0.55	0.028	0.360	2.04	0.058	0.721	0.85	0.110
	3.65	0.223	0.68	0.035	0.412	2.20	0.057	0.795	0.76	0.128
0.02	2.30	None			0.345	2.16	0.055	0.675	1.21	0.083
	2.65	None			0.358	2.06	0.058	0.705	1.02	0.087
	2.91	0.124	0.45	0.025	0.378	2.05	0.056	0.767	1.09	0.094
	3.71	0.254	0.50	0.030	0.426	2.10	0.053	0.810	0.78	0.105
0.05	2.21	None			0.344	2.07	0.059	0.665	1.36	0.082
	2.42	None			0.358	2.15	0.058	0.691	1.48	0.085
	2.80	0.135	0.57	0.027	0.385	2.28	0.060	0.718	1.45	0.087
	3.16	0.240	0.56	0.025	0.410	2.20	0.057	0.747	1.46	0.103

[a] With 0.08 *M* mellitic acid.
[b] In 50% (v/v) DMSO.

TABLE V

NUMBER OF HYDROGEN IONS AND LIGANDS INVOLVED IN THE ELECTRODE REDUCTION

	DMSO < 50%		*DMSO* > 50%	
	pH < 2.2	*pH* > 2.2	*pH* < 2.7	*pH* > 2.7
$(\Delta E_{\frac{1}{4}}/\Delta pH)(H_6A)(DMSO)$	0	0.060	0.031	0.060
H^+ involved	0	1	0.5	1
$(\Delta E_{\frac{1}{4}}/\Delta \log[DMSO])(H_6A)$	0.23	0.11	0.23	0.11
$x-y$	4	2	4	2
$(\Delta E_{\frac{1}{4}}/\Delta \log[H_6A])(DMSO)$	0	0.030	0	0.030
$p-q$	0	0.5	0	0.5

Chelate species

Below pH 2.2, the uranyl–mellitate–DMSO system has essentially the same half-wave potentials as that of uranyl ion in dimethyl sulfoxide solution in the absence of mellitic acid. Thus at these pH values, coordination of dimethyl sulfoxide rather than mellitic acid is favored, and the species involved can be assigned the formula $UO_2(DMSO)_6^{2+}$.

Conductimetric titration showed that uranyl ion and mellitic acid combine in a 1:1 ratio in excess of mellitic acid. Therefore, the species formed in 50% (v/v) dimethyl sulfoxide above pH 2.2 can be formulated as $UO_2(H_3A)(DMSO)_5^{-1}$.

Determination of activation energy of electrode process

If the limiting current of an irreversible process is diffusion-controlled, the activation energy Q_D can be determined[10] from the temperature dependence of log i_d, the slope of the log i_d *vs.* $1/T$ graph being $\frac{1}{2}(Q_D/2.303\ R)$.

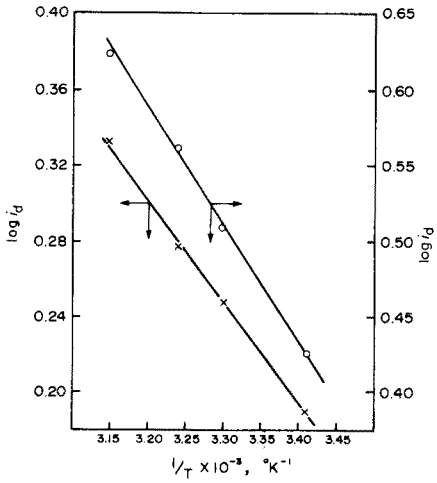

Fig. 6. Effect of temperature on the limiting current. 1.0 m*M* $UO_2(ClO_4)_2$, 0.15 *M* $NaClO_4$, 0.08 *M* mellitic acid and 0.002% Triton X-100. (×) pH 2.20, 50% (v/v) DMSO; (○) pH 3.09, 0% (v/v) DMSO.

TABLE VI

ACTIVATION ENERGY OF THE REDUCTION PROCESS

(1.0 m*M* $UO_2(ClO_4)_2$, 0.15 *M* $NaClO_4$, 0.08 *M* mellitic acid and 0.002% Triton X-100)

pH	*Medium*	*Temp.* *(K)*	$\bar{i}_d$ *(μA)*	*log* $\bar{i}_d$	Q_D *kcal* K^{-1} *mole*$^{-1}$
2.20	DMSO (50 vol.%)	294	1.55	0.190	4.95
		303	1.78	0.247	
		308	1.90	0.278	
		318	2.16	0.334	
3.09	H_2O	294	2.66	0.425	7.43
		303	3.24	0.510	
		308	3.66	0.562	
		318	4.20	0.623	

Figure 6 shows the log i_d *vs.* 1/T plots for the fourth wave in aqueous solution and the second wave in dimethyl sulfoxide solution. The variation of i_d with temperature and the values of Q_D are listed in Table VI. It can be concluded that the activation energy of the reduction of the uranyl–mellitate complex in aqueous solution is larger than that of the complex formed in dimethyl sulfoxide solution.

The authors thank the National Science Council for financial support.

SUMMARY

The reduction of the uranyl–mellitate complex at the dropping mercury electrode has been studied in aqueous and dimethyl sulfoxide solution. In aqueous solution, besides the reduction waves of the uranyl–mellitate complex, corresponding to the reduction of U(VI) to U(V), and of U(V) to U(III), an adsorption wave and a catalytic hydrogen wave were obtained; the species formed below pH 4.0 was $UO_2(H_3A)^-$ and above pH 4.0 was $UO_2(OH)(H_3A)^{2-}$. In dimethyl sulfoxide solution, two well-defined waves were observed; the first wave is due to reduction of a uranyl–mellitate–DMSO complex, and the second to reduction of mellitic acid. The species involved are $UO_2(DMSO)_6^{2+}$ below pH 2.2 and $UO_2(H_3A)(DMSO)_5^{-1}$ above pH 2.2. The activation energies of the reduction process were determined.

REFERENCES

1 K. Cummins and T. P. Jones, *J. Chem. Soc. D*, 11 (1970) 638.
2 K. Eliska, P. Frantisek and H. Bohumil, *Z. Chem.*, 9 (1969) 37.
3 A. K. Galwey, *J. Chem. Soc., London*, October (1965) 5433.
4 A. K. Galwey, *J. Chem. Soc. A*, (1966) 87.
5 R. J. Acheson and A. K. Galwey, *J. Chem. Soc. A*, (1967) 1167.
6 T. T. Lai and C. S. Wen, *J. Electrochem. Soc.*, 117 (1970) 1122.
7 T. T. Lai and B. C. Wang, *Anal. Chem.*, 36 (1964) 26.
8 L. Meites, *Polarographic Techniques*, Interscience, New York, 1967, p. 187.
9 L. F. Fieser and M. Fieser, *Organic Chemistry*, Reinhold, New York, 3rd edn., 1956, p. 668.
10 A. A. Vlcek, *Collect. Czech. Chem. Commun.*, 24 (1959) 3538.

Analytica Chimica Acta, 76 (1975) 319–328

SOME COMPARATIVE STUDIES ON DATA HANDLING IN VARIABLE-TIME KINETIC DETERMINATIONS. MODIFICATION OF MANGANESE(II) CATALYSIS WITH 1,10-PHENANTHROLINE AND SOME ANALOGS

EDWARD W. CHLAPOWSKI* and HORACIO A. MOTTOLA

Department of Chemistry, Oklahoma State University, Stillwater, Oklahoma 74074 (U.S.A.)

(Received 23rd October 1974)

The variable-time kinetic method appears advantageous in the determination of catalytic species (including enzyme activity) in solution[1]. With judicious selection of reference signals, it can be successfully applied even in the presence of induction periods of variable length[2]. The method involves the measurement of the time interval, Δt, required for a monitored species, R, to change from one preset concentration to another. Under controlled experimental conditions, $1/\Delta t$ is directly proportional to the concentration of catalyst in the system.

The simplest, and perhaps commonest, method for obtaining $1/\Delta t$ is to record the signal from the device monitoring, R, with the help of a strip-chart recorder. The time between two reference values of R can then be measured with a ruler or by calibration on the chart along the time axis. Automated "reciprocal time measuring systems" are described in the literature[3–6]. Electromechanical and electronic timers are now widely available and used. Some provide for remote switching by simple interfacing of the signal detection device and timer with a switching analog circuit[7]. This allows a simple and direct measurement of Δt.

This paper describes a new system for the measurement of elapsed time consisting of electronically starting and stopping an electronic clock at two reference potentials. Also reported is a comparison of this system with: (a) an electronic switching network and electromechanical timer[7], and (b) analog recording of signal profiles. In order to evaluate these alternatives for obtaining time intervals, a simulation circuit whose output voltage was logarithmically related to time, was employed. The new method was applied to an evaluation of the modifying effect of 1,10-phenanthroline and some analogs on the manganese(II) catalysis of the malachite green–periodate indicator reaction[7,8].

EXPERIMENTAL

Apparatus

General spectrophotometric equipment. An assembled modular unit was used. High values of radiant power, short- and long-range stability, and the use of as few as possible auxiliary optical units (considering that a high degree of resolution

* Present address: The Dow Chemical Co., U.S.A., B-6201, Freeport, Texas 77566.

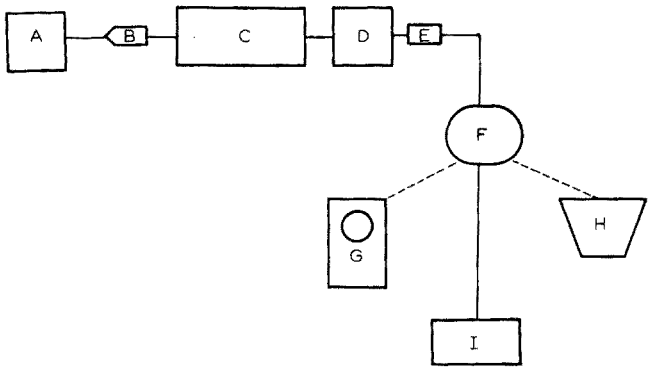

Fig. 1. Block diagram of spectrophotometric arrangement. Operational amplifiers, power supplies, and reference potential sources were modular electronic components from McKee-Pederson Instruments, Danville, Calif. A, MP-1026 regulated power supply. B, MP-1021 6-V light source. C, Jarrell-Ash 0.25 m monochromator. D. Cell holder with a constant-temperature water circulator (Lauda K-2/R) and a stirring control. E, UDI PIN silicone photodiode detector. F, MP-1001 and MP-1002; console with plug-in modules for signal modification, and regulated d.c. power supply. G, Tektronix 564 oscilloscope. H, Sargent SRL chart recorder. I, Heath EU-805 digital voltmeter.

is not critical in rate measurements involving relative changes) were considered desirable in the construction of the unit. A block diagram and description of the different parts is given in Fig. 1. The output of the photodiode was fed into the input of a MP-1031 chopper-stabilized operational amplifier (McKee-Pederson Instruments, Danville, Calif.) with a gain of one ($Z_i = Z_f = 1$ MΩ) to match impedance and isolate the detector from auxiliary circuits. The output of the operational amplifier was then fed into the appropriate circuit for the desired treatment of the signal.

Reference switching potentials were set with a digital voltmeter (Heath EU-805) and found to be constant. The potential from the photodiode was observed to change from day to day for a given absorbance value. The calibration curve (straight line) of potential *vs.* absorbance showed that only the intercept was changing; this facilitated the adjustment of voltage level for a given absorbance.

Simulation circuit. Simulation of the pseudo-first-order rate curves was accomplished by employing a linear voltage ramp coupled with a log ratio amplifier. The major components of the simulation circuit are shown in Fig. 2. The spectrophotometer was used as the potential reference for the initial ramp voltage by adjusting the shutter on the light source until the initial output of the log ratio amplifier was zero. The log ratio amplifier converted the linear voltage ramp (from the integrator) to a first-order plot for output voltage *vs.* time. The ramp voltage was varied by adjusting the variable 10-KΩ resistor until the desired input voltage, E_{in}, was read on the Heath EU-805 operating in the DVM mode. The log ratio amplifier was used in its log A/K mode providing a reference current, I_k, of 10^{-5} A. Adjusting the initial input voltage as -100 mV gave an initial current of 10^{-5} A, thus zero output voltage. Switching the integrator to "run" caused the current, I_A, to increase and gave a negative output voltage logarithmically related to time.

Analog recording set-up. Major components included: a MP-1031 operational amplifier, MP-1008 millivolt sources, and a Sargent SRL recorder with linear gears

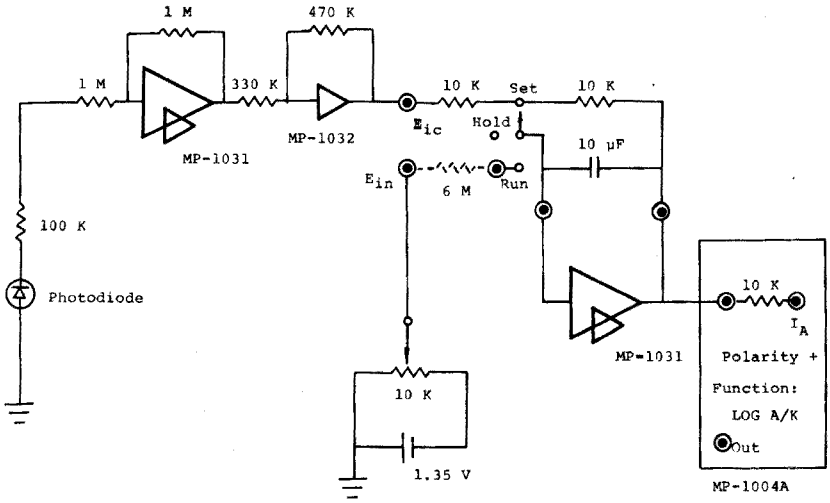

Fig. 2. Simulation circuit. From OUT, the output is fed into the appropriate circuit for treatment.

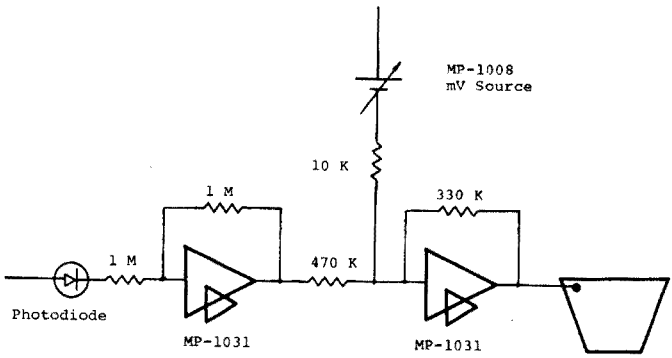

Fig. 3. Spectrophotometer–analog recording system.

(E. H. Sargent and Company, Chicago, Ill.). Figure 3 shows details of the circuits involved. Resistances were chosen to give a gain less than one to accommodate the signal in the 100-mV maximum range of the recorder.

The output voltage from the photodiode was found to be linear with concentration and maximum at zero absorbance. A bucking voltage was used to make the input voltage to the recorder equal to zero at zero absorbance. Span adjustment was performed using as reference a solution of malachite green of known concentration (absorbance).

Electromechanical timer. The circuit components and their function have been reported earlier[7].

The all-electronic timer system. Figure 4 shows a diagram of this system. The operational amplifiers act as polarity switches by operating in the open-loop mode. The Heath EU-805 Universal Digital Instrument, UDI, was used in the "time A–B measurement" mode. The controls on the panel of the UDI were set to switch on a negative slope for both channels with an attenuation setting to

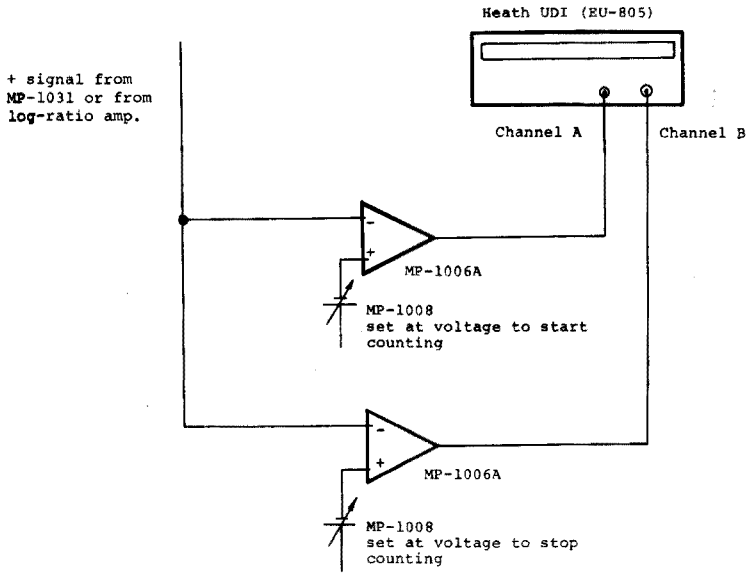

Fig. 4. Switching diagram for the electronic clock system.

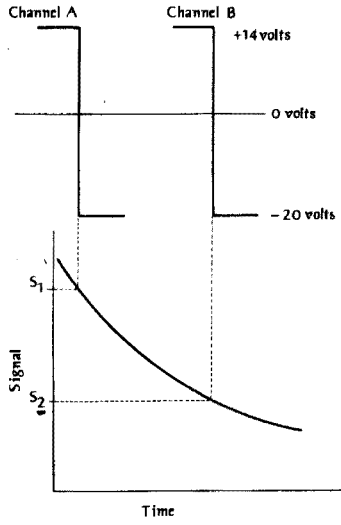

Fig. 5. Voltage levels at channels A and B at switching signals S_1 and S_2 when using the electronic clock system.

accommodate a 20-V d.c. signal, and to switch at the zero level (level control in "auto"). The change in slope at input of channel A started the timer and the change in slope at input of channel B switched the timer off. The time elapsed was then read from the display on the UDI. Figure 5 pictures the "switching signal levels" fed into channels A and B from the MP-1006A operational amplifier. Alternatively, the inputs of the MP-1006A between signal and channel B could be

inverted and channel B made to switch on a positive slope, yielding the measurement of the half-cycle of an asymmetrical "square wave" [10].

Reagents

Malachite green perchlorate was prepared and purified as reported earlier[11]. Reagent-grade 1,10-phenanthroline (Eastman Kodak Co., Rochester, N.Y.), bathocuproinedisulfonic acid (disodium salt), neocuproine hydrochloride monohydrate, and 4,7-diphenyl-1,10-phenanthroline (Aldrich Chemical Co., Milwaukee, Wisconsin) were used. Other reagents were AR grade.

RESULTS AND DISCUSSION

The rationale for the employment of the variable-time kinetic method of determination is discussed in the literature[12,13]. In any event, for catalytically based determinations, the initial concentration of catalyst, $[C]_0$, is directly proportional to the reciprocal of Δt.

$$[C]_0 \propto 1/\Delta t \tag{1}$$

Study with simulated pseudo-first-order rate profiles

The simulated circuit was set up as described under Experimental. The ramp voltages were set by varying the resistance of the 10-KΩ potentiometer (Fig. 2) until the desired voltage was read in the UDI operating in the DVM mode. Seven determinations were made for each ramp setting.

The functioning of the simulating circuit can be explained as follows: a voltage, E, varying linearly with time is given by:

$$E = E_0 + \left(\frac{E_R}{t_i}\right) \cdot t \tag{2}$$

where E_0 refers to the initial voltage of the ramp, and t_i the time for one increment of ramp voltage, E_R. This voltage is introduced into the log ratio amplifier through resistor R_A giving:

$$I_A = \frac{E_0}{R_A} + \left(\frac{E_R}{R_A \cdot t_i}\right) \cdot t \tag{3}$$

The output voltage of the log ratio amplifier is then equal to:

$$E_s = \log(I_A/I_k) \tag{4}$$

where I_k is a constant internal current (reference) of the log ratio unit.

The relationship for the difference in two reference potentials is then given by:

$$E_{s2} - E_{s1} = \log\left[\left(\frac{E_0}{R_A} + \frac{E_R \cdot t_2}{R_A \cdot t_i}\right) I_k\right] - \log\left[\left(\frac{E_0}{R_A} + \frac{E_R \cdot t_1}{R_A \cdot t_i}\right) \Big/ I_k\right] \tag{5}$$

Rearranging eqn. (5) and letting $K = E_R/t_i$, after simplifying and factoring, one obtains:

$$10(E_{s2} - E_{s1}) = K(t_2 - t_1)/I_k R_A \tag{6}$$

For a given set of experimental conditions, $(E_{s1}-E_{s2})$, I_k, R_A, and t_i are all constant. Incorporating these into a new constant, k', gives:

$$k' = E_R(t_2-t_1) \tag{7}$$

which shows the linear relationship between E_R and the inverse of the time necessary to traverse between two reference voltages. This is the same functional relationship with respect to Δt as shown between C_0 and Δt in eqn. (1).

The three methods for obtaining values of Δt for the simulated kinetic runs were evaluated on the basis of the variation of the slope of the working (calibration) line provided by a first-order least-squares treatment of ramp voltages on $1/\Delta t$. The value of the slope of the calibration line was obtained from standard regression analysis formulae[14] for a line of the form $Y=mX+b$, with m equal to:

$$m = \frac{N\Sigma X_i \bar{Y}_i - \Sigma X_i \Sigma \bar{Y}_i}{N\Sigma X_i^2 - (\Sigma X_i)^2} \tag{8}$$

with N = number of points, X_i = voltage ramp (or concentration of 1,10-phenanthroline) and $\bar{Y}_i$ = average Δt value of the seven determinations. The standard error of regression, S_{er}, is given by:

$$S_{er} = (\Sigma(\delta Y_i)^2/(N-2))^{\frac{1}{2}} \tag{9}$$

in which $\delta Y_i = Y_i-(b+mX_i)$. This can be employed to obtain an estimate of the variability of the value of X_i predicted from the least-squares fit by dividing S_{er} by m to yield the standard deviation of X, S_x (ref. 15). The standard deviation of replication for the points on the calibration curve for a method were then pooled[16] by use of:

$$S_p = \left(\frac{\Sigma n_i (S_i)^2}{\Sigma n_i}\right)^{\frac{1}{2}} \tag{10}$$

where n_i = number of degrees of freedom for the standard deviation, S_i.

The switching potentials for the simulated runs were chosen at 14 mV and 25 mV, considering that the curve shapes were very similar to those for actual kinetic runs between these values. Figure 6 shows plots of ramp voltages *vs.* $1/\Delta t$ for the three methods. The lines are those indicated by the least-squares treatment. Table I lists the standard deviations of predicted X_i values and the pooled replication error, S_p. The values for the standard deviation of predicted ramp voltages

TABLE I

VALUES OF S_x AND S_p FOR SIMULATED RATE PROFILES

Method	S_x[a]	S_p[a]
Strip chart	$2.5\cdot10^{-3}$	$1.4\cdot10^{-3}$
Electromechanical	$2.6\cdot10^{-4}$	$2.7\cdot10^{-4}$
Electronic clock	$6.53\cdot10^{-4}$	$8.6\cdot10^{-5}$

[a] See text for definitions

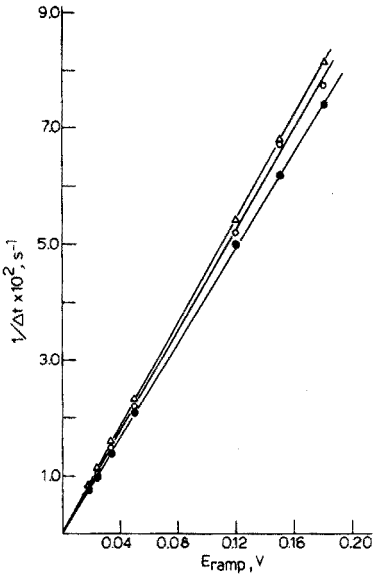

Fig. 6. Working curves from simulated pseudo-first-order rate profiles. (△) Mechanical timer; (○) strip-chart recorder; (●) electronic clock.

indicated that the electromechanical timer system provided the "best line". The pooled standard deviations indicated that the electronic clock system was the method which provided the best reproducibility.

Studies with 1,10-phenanthroline as rate modifier of the manganese(II)-catalyzed oxidation of malachite green by periodate ion

Determinations were carried out in 1-cm quartz cells with magnetic stirring[9]. All reactions were carried out at a malachite green concentration of $1.20 \cdot 10^{-5}$ *M* and in 0.10 *M*, pH 3.5, acetate–phosphate buffer[7]. The reagents were added in the following order: (1) 1.5 ml of purified water; (2) 0.3 ml of 1.0 *M* acetate–phosphate buffer; (3) 0.3 ml of 1,10-phenanthroline solution: (4) 0.3 ml of $1.0 \cdot 10^{-6}$ *M* Mn(II) solution, and (5) 0.3 ml of malachite green solution. The stirrer was set at a constant stirring rate and 0.3 ml of a $5.2 \cdot 10^{-2}$ *M* sodium periodate solution was injected with the aid of a 0.5-ml syringe. Seven determinations were made for each concentration of 1,10-phenanthroline tested.

The switching potentials for the runs were chosen at values of 0.700 and 0.600 for the strip chart (analog) system. The references for the electromechanical timer

TABLE II

VALUES OF S_x AND S_p FOR ACTUAL RUNS WITH 1,10-PHENANTHROLINE

Method	S_x	S_p
Strip chart	$4.7 \cdot 10^{-9}$	$2.2 \cdot 10^{-3}$
Electromechanical	$4.1 \cdot 10^{-10}$	$1.7 \cdot 10^{-3}$
Electronic clock	$1.1 \cdot 10^{-9}$	$7.5 \cdot 10^{-4}$

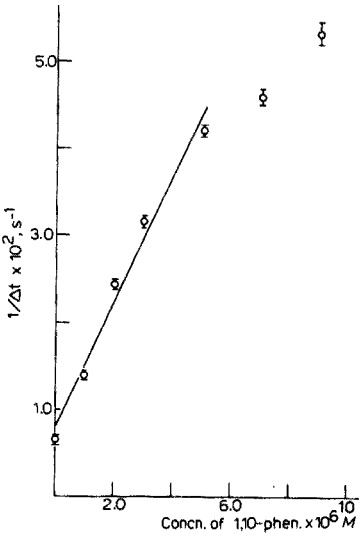

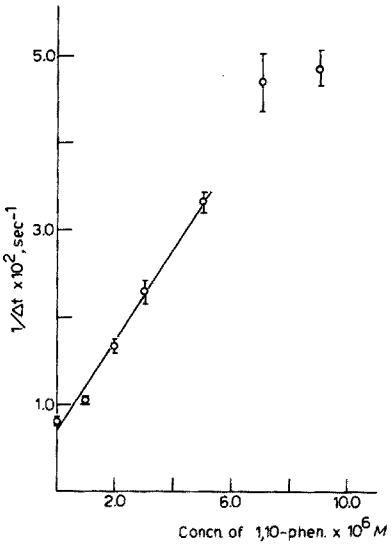

Fig. 7. Working curve for 1,10-phenanthroline with the electronic clock.

Fig. 8. Working curve for 1,10-phenanthroline with the electromechanical timer.

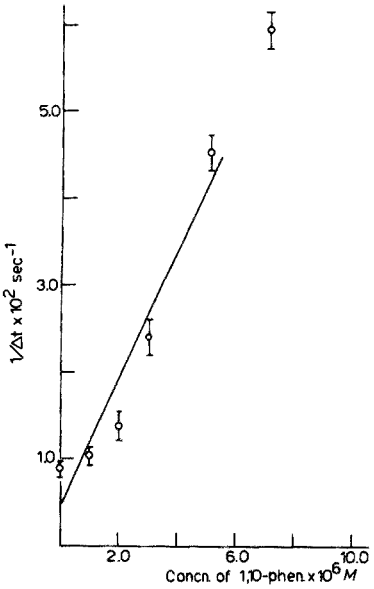

Fig. 9. Working curve for 1,10-phenanthroline with the analog recording system.

and the electronic clock were chosen at 0.667 and 0.597. Working (calibration) curves are shown in Figs. 7–9; the line is that indicated by the least-squares treatment of the first five points. The values of the standard deviations of predicted 1,10-phenanthroline concentrations for the first five points and the pooled standard deviation for the seven data points for each approach are given in Table II.

The values of the standard deviation of predicted 1,10-phenanthroline concentrations indicated that the "best" working curve was, again, provided by the electromechanical timer. The pooled standard deviation was a minimum for the electronic clock system, indicating the best precision for this system. The electromechanical and the electronic clock systems can, however, be considered of comparable precision and accuracy and, as expected, both are definitely superior to the analog recording system for Δt evaluation.

Effect of some analogs of 1,10-phenanthroline on the Mn(II)-catalyzed oxidation of malachite green by periodate ions

Some analogs of 1,10-phenanthroline were tested for their effect on the malachite green–Mn(II)–periodate indicator system, under the same conditions employed for the studies with the parent compound and with the electronic clock and analog recording system. The species included in the comparative study, and the pseudo-first-order rate proportionality constants, k^*, are listed in Table III. The only compound of those tested which enhanced the manganese(II) catalytic effect was 4,7-diphenyl-1,10-phenanthroline. This enhancement was approximately one-half of that exhibited by 1,10-phenanthroline itself.

TABLE III

VALUES OF COMPARATIVE PSEUDO-FIRST-ORDER RATE PROPORTIONALITY CONSTANTS FOR SOME ANALOGS OF 1,10-PHENANTHROLINE

(Analytical concentration of ligands: $1.00 \cdot 10^{-5}$ *M*.)

	k^* (min^{-1})
Blank	0.24
Neocuproine	0.24
Bathocuproinedisulfonic acid	0.24
4,7-Diphenyl-1,10-phenanthroline	0.44
1,10-Phenanthroline	0.74

This work was supported by The National Science Foundation.

SUMMARY

Analog recording and two electronic switching networks have been compared as means of recording the elapsed time in variable-time kinetic determinations. The rate-modifying effect of 1,10-phenanthroline on the magnanese(II)-catalyzed oxidation of malachite green by periodate provided experimental curves for evaluation. Totally simulated rate profiles were also used for comparison purposes. The study was extended to the evaluation of some analogs of 1,10-phenanthroline as modifiers of manganese(II) catalysis.

REFERENCES

1 J. D. Ingle and S. R. Crouch, *Anal. Chem.*, 43 (1971) 697.
2 G. L. Heath, MS Thesis, Oklahoma State University, Stillwater, Oklahoma, 1972; H. A. Mottola,

Anal. Chim. Acta, 71 (1974) 443.
3 H. L. Pardue, C. S. Frings and J. C. Delaney, *Anal. Chem.*, 37 (1965) 1426.
4 R. H. Stehl, D. W. Margerum and J. J. Latterel, *Anal. Chem.*, 39 (1967) 346.
5 G. E. James and H. L. Pardue, *Anal. Chem.*, 40 (1968) 796.
6 S. R. Crouch, *Anal. Chem.*, 41 (1969) 880.
7 H. A. Mottola, *McKee-Pedersen Instrum. Notes*, 6 (1971) 17; H. A. Mottola and G. L. Heath, *Anal. Chem.*, 44 (1972) 2322.
8 A. A. Fernandez, C. Sobel and S. L. Jacobs, *Anal. Chem.*, 35 (1963) 1721.
9 H. Hall, B. E. Simpson and H. A. Mottola, *Anal. Biochem.*, 45 (1972) 453.
10 H. V. Malmstadt and C. G. Enke, *Digital Electronics for Scientists*, W. A. Benjamin, New York, 1969, pp. 384–386.
11 H. A. Mottola and C. R. Harrison, *Talanta*, 18 (1971) 683.
12 H. B. Mark, Jr. and G. A. Rechnitz, *Kinetics in Analytical Chemistry*, Interscience, New York, 1968.
13 H. A. Mottola, *CRC Critical Reviews in Anal. Chem.*, in press.
14 Y. Beers, *Introduction to the Theory of Errors*, Addison-Wesley, Reading, Mass., 1962.
15 F. J. Linnig and J. Mandel, *Anal. Chem.*, 36 (1964) 25A.
16 G. W. Snedecor and W. G. Cochran, *Statistical Methods*, Iowa State University Press, Ames, Iowa, 6th edn., 1967.

Analytica Chimica Acta, 76 (1975) 329–336

DETERMINATION OF MANGANESE IN NATURAL WATERS BY ATOMIC ABSORPTION SPECTROMETRY WITH A CARBON TUBE ATOMIZER

TSUNENOBU SHIGEMATSU, MASAKAZU MATSUI, OSAMU FUJINO and KIYOMI KINOSHITA

The Institute for Chemical Research, Kyoto University, Uji, Kyoto 611 (Japan)

(Received 23rd September 1974)

Recently, flameless atomic absorption spectrometry[1] with carbon filaments[2,3], carbon tubes[4–7], carbon rods[8,9] and tantalum[10–12] or tungsten atomizers[13] has been described. The flameless atomizer heated to a sufficiently high temperature by an electric current, produces a population of ground state atoms more efficiently than the flame atomizer; the method is more sensitive than the flame method and can be applied even to very small volumes of sample solution.

In previous work, the flameless atomic absorption characteristics of manganese with a carbon filament[2] or a tantalum strip[11] have been described, and the direct determination of manganese in sea water with a graphite atomizer has been evaluated[14]. The determination of cadmium[6] or lead[7] by atomic absorption spectrometry with a carbon tube atomizer has been reported. In this paper, the atomic absorption spectrometry of manganese, which is less volatile than cadmium and lead, was studied for a carbon tube atomizer. Experimental parameters have been studied and the method has been applied to the determination of manganese in natural waters.

EXPERIMENTAL

Apparatus and reagents

Atomic absorption measurements were made with a Jarrell-Ash Model AA-1 spectrometer in conjunction with a Jarrell-Ash flameless atomizer; a National spectroscopic electrode was used as the carbon rod. The temperatures of the carbon tube were measured by an optical pyrometer. Radioactivity was measured with a TEN NaI (Tl) (44.5-mm diameter., 50.8 mm depth) well-type scintillation counter, Model EA-14, connected with a Metrodekatron scaler, Model MCL-6B. A Hitachi–Horiba glass electrode pH meter, Model F-5, was used for the pH measurements.

Twice-distilled water was used in the preparation of all solutions. An aqueous 5% solution of sodium diethyldithiocarbamate (DDTC) was prepared daily and was purified by shaking with diisobutyl ketone (DIBK), which had been purified by shaking with 0.1 *M* hydrochloric acid. Standard manganese solution was prepared by dissolving manganese metal (99.99%) with nitric acid and evaporating to dryness, the residue being taken up with 0.1 *M* hydrochloric acid. The radioisotope, manganese-54 (New England Nuclear, Boston, Mass.) was supplied as the chloride in hydrochloric acid solution.

Other chemicals were reagent-grade materials.

Procedure

The atomization chamber has been described previously[6]; it was placed in the position of the burner in the AA-1 spectrometer.

After the sample solution had been introduced into the carbon tube atomizer with a micropipet (5–30 μl), inert gas was passed into the atomization chamber at a constant rate. Then, the carbon tube was heated slowly to about 100–200°C at a voltage of 1–2 V for 1–2 min. After the solvent had completely evaporated, the tube was heated to about 2500°C by applying 6.5 V for 5 s. The peak-absorption signals were measured at 279.5 nm.

RESULTS AND DISCUSSION

Effect of the inner diameter of the carbon tube

Carbon tubes were made by boring carbon rods (length, 70 mm; diameter, 6.35 mm.), the inner diameter ranging from 3.0 mm to 5.0 mm; a hole (3.0-mm diameter) was made at the center of the carbon tube for injecting the sample solution. Although the highest purity grade of carbon rod was selected, a considerable absorption signal was obtained when it was heated. However, after the tube had been heated for 30 s with a voltage of 7.0 V (*ca.* 3000°C), little absorption signal was obtained.

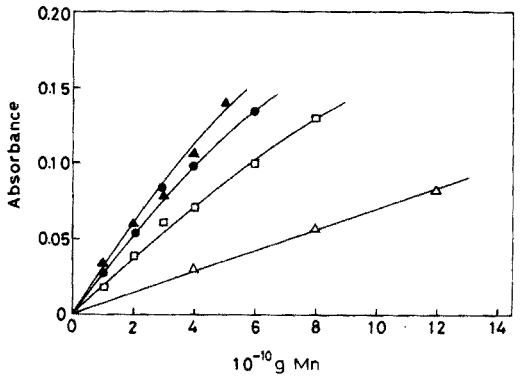

Fig. 1. The effect of the inner diameter of the carbon tube on the sensitivity. Inner diameter (mm): (▲) 3.0; (●) 4.0; (□) 4.5; (△) 5.0. Injection volume 10 μl; Ar, 1.5 l min^{-1}.

The effect of the inner diameter of the carbon tube on the sensitivity of manganese determinations is shown in Fig. 1. These carbon tubes were heated to about 2500°C by voltage adjustments. Smaller bores gave higher sensitivity and a longer life of the tube, but larger bores gave better reproducibility. Manganese behaved like cadmium[6] and lead[7]. In subsequent studies, a carbon tube with an inner diameter of 4.0 mm was used.

Effect of applied voltage

The manganese absorption signal varies with the applied carbon tube voltage. West *et al.*[2] reported that the manganese absorption signal increased with temperature, and as the temperature exceeded the optimum, the sensitivity tended

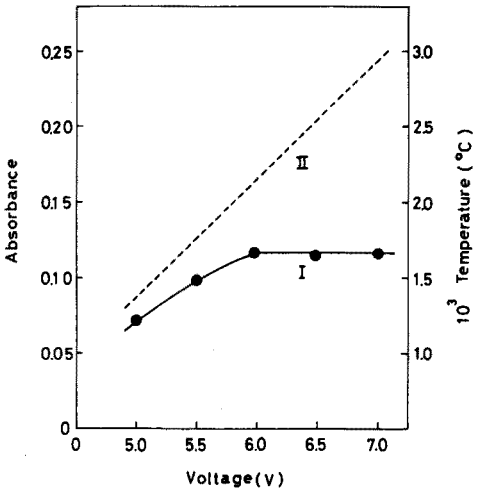

Fig. 2. Variation of absorbance with carbon tube voltage. (I) Mn 25 p.p.b.; injection volume 20 μl; (II) temperature. Carbon tube, 4.0 mm; Ar, 0.7 l min^{-1}.

to decrease in carbon filament atomizers. A similar finding was made by Takeuchi and Yanagisawa[11] in tantalum atomizers. However, as shown in Fig. 2, when the carbon tube voltage was increased beyond 6 V (2200°C), a constant absorption signal was observed. Therefore, in this study, the carbon tube atomizer was heated by a voltage of 6.5 V (2500°C).

Effect of inert gas

The peak absorbance of elements depended on the gas passed through, which protected the carbon tube from atmospheric oxidation at high temperatures. The effect of gases on the peak absorbance of manganese was examined at the 30-p.p.b. level with 20-μl injections of solution. The results are shown in Table I.

TABLE I

EFFECT ON THE PEAK ABSORBANCE OF AN INERT GAS AT 0.7 l min^{-1}

Gas	Ar	N_2	He	CO_2	Air
Absorbance compared to Ar	1.00	1.06	0.62	0.50	0.43

The peak absorbance of manganese in argon was practically the same as that in nitrogen, but in helium it was about 38% lower; this is probably because argon and nitrogen have low thermal conductivity and low specific heat. In air, the life of the carbon tube became very short because of atmospheric oxidation. Argon was used in all further work.

As shown in Fig. 3, the peak absorbance of manganese decreased with increasing flow rate of argon; this is probably caused by the different rates of

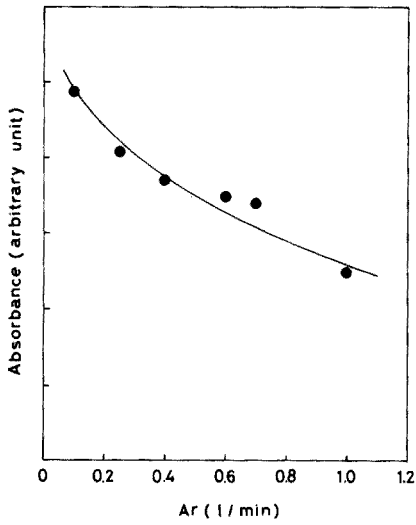

Fig. 3. The effect of argon flow rate. 30 p.p.b. Mn; injection volume, 20 μl Carbon tube 4.0 mm.

diffusion of the manganese atoms from the carbon tube. However, with argon flows exceeding about 0.7 l min^{-1} reproducibility of the peak absorbance was better, and a flow rate of 0.7 l min^{-1} was therefore used.

Calibration curves

In the range $1–6 \cdot 10^{-10}$ g of manganese, calibration curves were constructed for constant volumes (5 μl) of solutions containing 20–120 p.p.b. manganese; different volumes (5–30 μl) of 20 p.p.b. solutions were also used. The results are shown in Fig. 4. A fairly linear calibration curve was obtained when constant

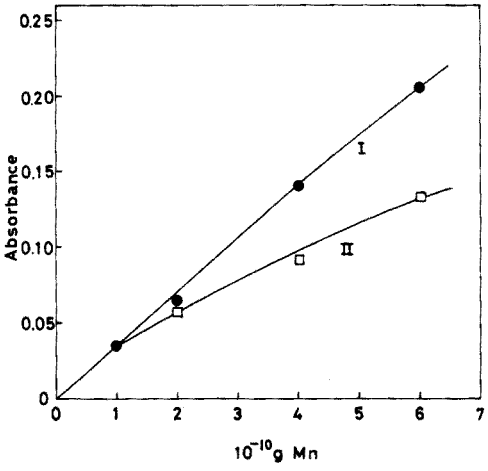

Fig. 4. Calibration curves for manganese, (I) Constant volume (5 μl) of solution at various concentrations; (II) different volumes at a constant concentration (20 p.p.b.). Carbon tube, 4.0 mm; Ar, 0.7 l min^{-1}.

volumes of solutions of different concentration were used. The peak absorbance decreased on increasing the sample volume; the causes have been discussed previously[6,7].

The relative standard deviation calculated from ten measurements at the 20-p.p.b. level, for 5-μl injections was 3.5%. The detection limit (1% absorption) was about $1.5 \cdot 10^{-11}$ g.

Effect of some foreign substances

First, the effect of several inorganic acids at concentrations of 0.05 *M* on the signal for 25 p.p.b. manganese (20-μl injections) was studied. Hydrochloric acid, nitric acid, sulfuric acid and perchloric acid had no similar effect on the peak absorbance. However, phosphoric acid decreased the absorbance by 15% compared to the effects of these acids.

Secondly, the effects of salts on the peak absorbance were studied, with the results shown in Table II. The peak absorbance of manganese was little affected by 40-fold amounts of salts, except that sodium silicate depressed the signal by about 20%. In 400- and 4000-fold amounts, most salts interfered. A particularly interesting finding was the depression by alkali earth metals.

Method for the determination of manganese in sea water

The direct determination of manganese in sea water by atomic absorption

TABLE II

EFFECT OF SOME FOREIGN SUBSTANCES

(25 p.p.b. Mn; 20 μl injected.)

Substance added	*% Effect of*		
	4000 × amount	*400 × amount*	*40 × amount*
None	100	100	100
NaCl	102	102	105
KCl	95	103	101
$MgCl_2$	76	85	97
$CaCl_2$	23	52	97
$SrCl_2$	45	84	92
$BaCl_2$	40	67	98
$FeCl_3$	—	92	97
$CoCl_2$	—	—	105
$NiCl_2$	59	70	95
$CuCl_2$	77	90	96
$ZnCl_2$	86	109	103
$PbCl_2$	79	85	100
$CdCl_2$	81	105	107
$AlCl_3$	—	85	93
$K_2Cr_2O_7$	57	80	104
$(NH_4)_6Mo_7O_{24}$	74	90	98
NH_4VO_3	89	85	95
Na_2SiO_3	62	76	81

spectrometry with carbon tube atomizers is difficult because of the high interference of salts[14] and the low manganese contents in sea water. Therefore, concentration of manganese and separation from interfering elements is needed. In flame atomic absorption spectrometry, sea water samples are usually treated by a separation method such as extraction of trace metal chelates with DDTC into MIBK[15]. However, MIBK is slightly soluble in water, and is therefore unsuitable when the ratio of aqueous to organic phase is high. DIBK was used as extractant in the present work because of its lower solubility in water.

The recovery of manganese from sea water into the DDTC–DIBK extraction system was determined with a radioactive tracer, manganese-54. Extraction times of 30 min were used. When 1 ml of 5% DDTC solution was added to 10 ml of sea water, over 97% of the manganese was extraction into 1 ml of DIBK in the pH range 7.5–9; above pH 9 recoveries decreased. The effect of DDTC concentration was also studied; extraction of manganese at pH 8.0 was complete when 1–2 ml of 5% DDTC was added to 10 ml of sea water. As the volume of sea water phase increased, more DDTC had to be added to maintain a high recovery.

Application to natural water

Natural waters, which had been previously acidified with hydrochloric acid to pH 2 and filtered through a 0.45-μm Millipore filter, were examined. To 1–20 ml of a sample water adjusted to pH 8 with aqueous ammonia, 10 ml of 5% DDTC and 1.0 ml of DIBK were added; the two phases were shaken for 30 min and centrifugally separated, and 10 μl of the organic phase was injected into the carbon tube atomizer for measurement at 279.5 nm.

The instability of the manganese–DDTC complex in MIBK has been reported[16]. However, the absorbance of the complex in DIBK was stable, with about 0.01 absorbance units over the period 0–28 h when solutions containing 80 or 160 p.p.b. were used.

Manganese contents in sea water were measured by both the calibration curve and the standard addition methods. The results (Table III) showed that both methods gave essentially the same results.

By this procedure, 0.50–33.4 p.p.b. of manganese were found in different natural waters (Table IV).

TABLE III

DETERMINATION OF MANGANESE IN SEA WATER BY THE CALIBRATION CURVE AND STANDARD ADDITION METHODS

Sea water (ml)	*Mn added (p.p.b.)*	*Mn found (p.p.b.)*	*Mn in sea water (p.p.b.)*
5	0	9	1.8
10	0	20	2.0
20	0	34	1.7
5	10	19	1.8
5	20	29	1.8
5	40	50	2.0

TABLE IV

MANGANESE CONTENTS IN NATURAL WATER

	Sample no.	*Depth (m)*	*Mn in natural water (p.p.b.)*
Uragami Bay (Wakayama Pref.)			
	I	0	0.76
	II	10	0.50
	III	0	0.61
	IV	10	0.54
Suruga bay (Shizuoka Pref.)			
	I	0	17.8
	II	0	24.8
	III	0	14.0
	IV	0	21.6
	V	5	13.2
Osaka bay (Osaka Pref.)			
	I	0	31.5
Lake Biwa (Shiga Pref.)			
	I	0	12.8
	II	70	33.4
	III	1	17.6

SUMMARY

The atomic absorption spectrometry of manganese was studied with carbon tube atomizers. Various inner diameters of the carbon tubes were studied: small bores gave higher sensitivity, but large bores gave higher reproducibility. A fairly linear calibration curve was obtained in the range of $1–6 \cdot 10^{-10}$ g of manganese with injection volumes of 5 μl. The detection limit was $1.5 \cdot 10^{-11}$ g and the relative standard deviation 3.5%. In 40-fold amounts, few salts interfered, but there were considerable interferences from 400 and 4000-fold amounts. Manganese in natural waters was determined by extracting it into diisobutyl ketone as the diethyldithiocarbamate; the amounts found lay in the range 0.5–33 p.p.b.

REFERENCES

1 G. F. Kirkbright, *Analyst (London)*, 96 (1971) 609.
2 L. Ebdon, G. F. Kirkbright and T. S. West, *Anal. Chim. Acta*, 58 (1972) 39.
3 J. F. Alder and T. S. West, *Anal. Chim. Acta*, 51 (1970) 365.
4 D. J. Johnson and T. S. West, *Anal. Chim. Acta*, 67 (1973) 79.
5 E. Norval and L. R. P. Butter, *Anal. Chim. Acta*, 58 (1972) 47.
6 T. Shigematsu, M. Matsui and O. Fujino, *Jap. Anal.*, 22 (1973) 1162.
7 T. Shigematsu, M. Matsui, O. Fujino and K. Kinoshita, *Nippon Kagaku Kaishi*, 11 (1973) 2123.
8 K. G. Brodie and J. P. Matousek, *Anal. Chem.*, 43 (1971) 1557.
9 M. P. Bratzel, Jr., C. L. Chakrabarti, R. E. Sturgeon, M. W. McIntyre and H. Agemian, *Anal. Chem.*, 44 (1972) 372.
10 J. Y. Hwang, P. A. Ullucci, S. B. Smith, Jr and A. L. Malenfant, *Anal. Chem.*, 43 (1971) 1319.
11 T. Takeuchi and M. Yanagisawa, *Talanta*, 19 (1972) 465.
12 J. Y. Hwang, C. J. Mokeler and P. A. Ullucci, *Anal. Chem.*, 44 (1972) 2018.

13 J. E. Cantle and T. S. West, *Talanta*, 20 (1973) 459.
14 D. A. Segar and J. G. Gonzalez, *Anal. Chim. Acta*, 58 (1972) 7.
15 D. C. Burrell, *Anal. Chim. Acta*, 38 (1967) 447.
16 M. Yanagisawa, M. Suzuki and T. Takeuchi, *Anal. Chim. Acta*, 43 (1968) 500.

Analytica Chimica Acta, 76 (1975) 337–343

THE DETERMINATION OF TOTAL MERCURY AT THE PART PER BILLION LEVEL IN SOILS, ORES, AND ORGANIC MATERIALS

J. W. WIMBERLEY

Analytical Research Section, Research and Development Department, Continental Oil Company, Ponca City, Oklahoma 74601 (U.S.A.)

(Received 1st November 1974)

The determination of mercury at very low levels has become increasingly important in recent years; one primary need is for mercury determinations at the low p.p.b. level in soils. The method described in this paper can be applied successfully to mercury in samples such as soils, ores and coal. One of the main problems concerning this analysis is the liberation and collection of the mercury quantitatively from a sample. Since colorimetric methods do not have the sensitivity required, flameless atomic absorption is usually now selected as the detection system in such analyses. Manning reports a sensitivity of 0.001 μg or lower, whereas that for conventional flame a.a.s. is about 0.5 μg ml^{-1} of sample solution[1].

Many methods are mentioned in the literature for trapping mercury. Woodson[2] filtered solutions containing mercury ions through asbestos pads impregnated with cadmium sulfide; the mercury(II) sulfide formed was subsequently dried and fired in a controlled atmosphere. Pappos and Rosenberg[3] used this procedure for the determination of mercury in wheat, fish, and eggs after oxidizing the samples in a Schöniger combustion flask. A popular method of determining mercury in solution is that of Hatch and Ott[4]. In their method, mercury ions are reduced to the element with tin(II) chloride and swept into a flameless a.a.s. cell with air. Vaughn and McCarthy[5] separated mercury from interfering substances by passing the sample vapors over gold foil; the mercury could later be released by external heating at 500°C. Kalb[6] used a similar method with silver foil in place of gold.

Another scheme used is to deposit the mercury from solution onto a metal wire chemically or electrolytically[8]; the collected mercury could then be released by heating externally (furnace or flame) or by passage of a current through the wire. O'Gorman *et al.*[9] compared three different methods for determination of mercury in some American coals. The three methods were: (1) double gold amalgamation—flameless a.a.s., (2) neutron activation, and (3) combustion and dissolution followed by flameless a.a.s. The conclusions reached from the work were that the double gold amalgamation method was best because it is faster and considerably cheaper than neutron activation. The combustion–dissolution method gave low results.

The method developed here consists of heating the sample to *ca.* 1000°C in an induction furnace, sweeping the liberated mercury through a trap where it is amalgamated with gold, and then desorbing the mercury and sweeping it through a long path-length cell for measurement at 253.7 nm. The heart of the method is the mercury trap described below.

EXPERIMENTAL

Apparatus

The mercury trap consists of a 19-cm long, 1.25-cm diameter Vycor tube containing a 1.8-m 22-gauge hollow, helical shaped Nichrome wire of 6-ohm resistance having on its surface a thin plating (*ca.* 5 g) of pure gold[10]. After amalgamation, a current of 6 A for 8 s releases the mercury so that it can be swept into the absorption cell.

The detection section consists of a 43-cm cell with a single source of 253.7-nm radiation and phototube detectors. The signal from the mercury absorption is amplified by electrometer and read out on a strip chart recorder. Commercial instruments could be used as detectors, if convenient.

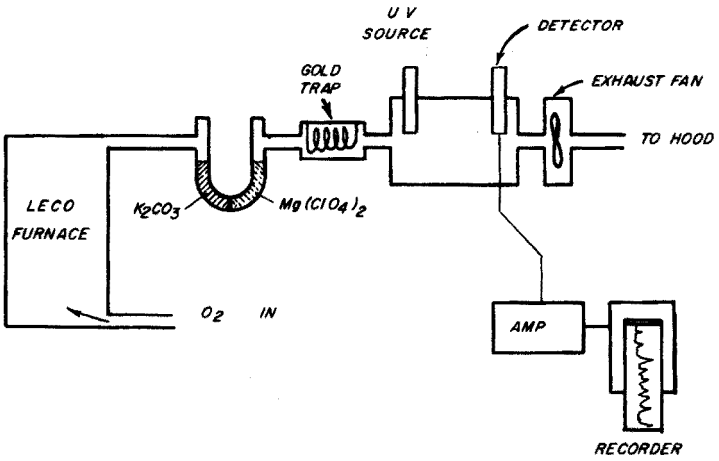

Fig. 1. Diagram of analytical system.

Mercury is liberated from the sample with a Leco (Laboratory Equipment Corporation) induction furnace. Figure 1 shows the system used. The Leco induction furnace heats the sample to *ca.* 1000°C which liberates all mercury from its compounds by thermal decomposition. Oxygen is used as the sweep gas, and a flow rate of about 450 ml min^{-1} is maintained by a Brooks Model 8743 flow controller. The U-tube trap contains potassium carbonate and magnesium perchlorate which absorb water but do not absorb mercury. The mercury vapor is amalgamated with the gold trap. After the sample heating has finished, the mercury is vaporized from the gold-coated coil by passing a current of 6 A for 8 s through the coil. The mercury vapor then passes through the optical cell. The change in absorption is picked up by the detector, amplified, and recorded. The recorded peak height is directly proportional to the mercury concentrations passing through the cell.

Procedure

Turn on the power to the Leco furnace. Set the oxygen tank to a pressure of 5 p.s.i. Turn on the exhaust fan, the recorder power (50 mV setting), and

the electrometer set at 10^{-10} A; the electrometer is left on all the time unless the instrument is not to be used for several days.

Heat the Leco carbon-enclosed-in-quartz crucibles to be used for 5 min to eliminate any mercury contamination. Clean the gold collector by depressing the timer switch. Repeat this procedure every 6–8 min until either no response is attained or a small constant response is found: in the latter case, this response must be subtracted as a blank.

Calibrate the instrument by injecting ahead of the collector 1.0 cm^3 of mercury–air at a known temperature. The mercury–air is taken from a plastic bottle containing a drop of mercury and fitted with a septum. The plastic bottle is surrounded by another plastic bottle filled with water as an insulator and containing a thermometer. After injection, the mercury is flashed off the gold collector and the mercury peak measured. The calibration factor is calculated by dividing the ng of mercury contained in the 1-cm^3 sample by the number of recorder divisions. This usually comes out around 0.5 ng/division when the electrometer is set at 10^{-10} A. Repeat the procedure at least once more. The injections should differ by no more than 1 recorder division.

Weigh the sample into a small ceramic crucible which has been recently heated to 800–1000°C to eliminate contamination, place it into a Leco carbon-enclosed-in-quartz crucible and set into the Leco furnace. Adjust the plate current to the Leco to around 450 mA. After heating for 6 min, flash the mercury off the gold collector and measure the peak height. After 2 min (cooling time for gold coil),

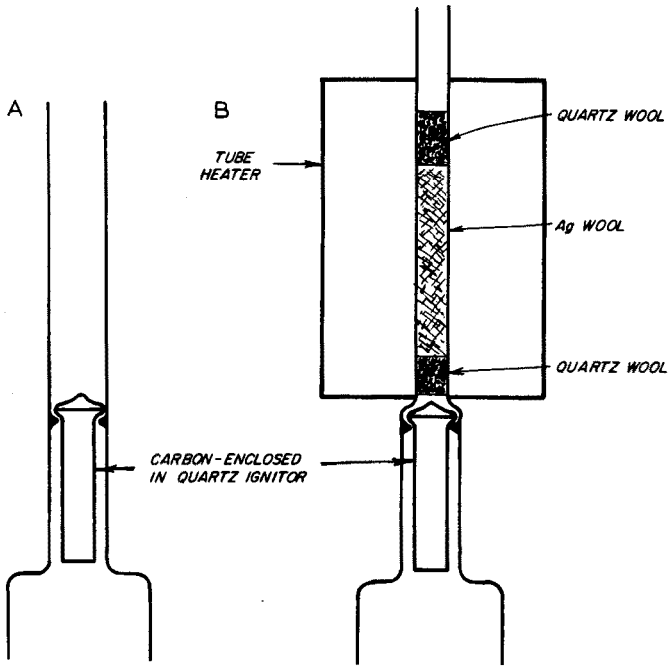

Fig. 2. Leco combustion tubes. A, Regular combustion tube. B, Special combustion tube for organic samples.

another sample can be started (a total of 8 min per sample is required).

It is necessary to cover high sulfide samples with 0.5 g of sodium carbonate before analysis. Doing this eliminates flooding the system with SO_2–SO_3. If the system is flooded with SO_2–SO_3, some of these gases condense in the tubing to form the acids which will trap subsequent mercury vapors, thereby giving low results. For soils and ores containing sulfides, the SO_2–SO_3 gives a large peak, thereby alerting the analyst to the presence of sulfides.

For organic samples, it is necessary to use a specially built combustion tube in the Leco. Figure 2 shows a standard and the specially built combustion tube. A tube furnace fits over the extension containing the silver wool. The temperature is set at 750°C by means of a Variac. The silver wool aids in completing the combustion of any carbonaceous material which was not completely burned in the lower section of the combustion tube. Burning organic samples in the ordinary combustion tube results in coating of the tubing with carbonaceous material, which then traps mercury from subsequent samples.

RESULTS AND DISCUSSION

Linearity of mercury collection and response

Different volumes of mercury–air were passed through the gold collector and flashed through the detector. The mercury–air standard was injected by syringe at a rate of 8 s per injection. Flash time was controlled by a timer and was set at 8 s. Table I illustrates the data collected, which clearly show that the collection and response are linear over the range studied.

TABLE I

REPRODUCIBILITY AND LINEARITY OF RESPONSE

Amount of Hg–air (cm^3)	*Recorder divisions*
0.5	16, 16
1.0	32, 32
1.5	48, 48
2.0	63.2, 65
2.5	79.2, 81

Heating time in the Leco furnace

This study was done in order to determine the length of time necessary to volatilize all of the mercury in a soil sample which had been sieved through an 80-mesh stainless steel sieve. The chemical handbook shows that the most stable mercury compound, mercury(II) fluoride, decomposes at 645°C, so that decomposition of compounds was not a problem. The results indicated that 5 min sufficed at the temperature that was used (1000°C). However, particle size influenced the required time.

Effect of particle size

A short study showed that fine particle size was necessary for good results.

A sample of soil consisting of small pea-sized chunks was analyzed and 8 p.p.b. mercury was determined. When the chunks were ground in a chromic acid-cleaned mortar to a fine powder and rerun, an additional 13 p.p.b. was found. In another experiment, 10 soils were sampled from plastic bags with no attempt made to obtain uniform-sized particles. The soils were then sieved through an 80-mesh sieve and analyzed again. The sieved samples showed higher mercury contents in almost every case; the mercury contents increased by 2–56 p.p.b. for contents in the range 11–130 p.p.b. Consequently, all soil and ore samples were sieved through an 80-mesh sieve before analysis.

The effect of sample size variation

A soil sample was sieved and various weights were analyzed in order to determine any effect of sample size. The results showed that weights in the range 1–3 g (which is all the crucibles hold) caused no problems.

The effect of machine grinding

Machine grinding of core samples may cause mercury losses, owing to the heat generated in the grinding process. Two core samples were chosen for testing; the results (Table II) showed that machine grinding caused losses of mercury, especially in Sample 52-11. The losses probably depend on the form of mercury present; *i.e.*, HgS, $HgCl_2$, etc.[11] and on the friability of the core; very friable cores would generate more heat on grinding than softer ones. In all later tests, core samples were hand ground.

TABLE II

MERCURY LOSSES CAUSED BY MACHINE GRINDING

Description	*p.p.b. Hg*	
	Sample 52-1	*Sample 52-11*
Hand ground	4400, 4300	108, 109
Machine ground	3500, 3300	22, 20

Accuracy and precision

Inorganic materials (soils and ores). Since there are no NBS standard soils or ores of low mercury content, the accuracy was estimated by adding known amounts of mercury(II) solution to a soil which had been found to contain 3 p.p.b. Hg. The solution was prepared from pure mercury(II) oxide dissolved in dilute nitric acid and diluted to a final concentration of 0.2 $\mu g\ ml^{-1}$. The solution was carefully weighed onto the soil, which was then allowed to stand overnight so that most of the water evaporated. In 11 samples, to which 7–23 ng of mercury were added, the recoveries ranged from 10 to 22 ng, and the error did not exceed ± 3 ng, which is quite good considering the very low amounts involved.

A pseudo-standard was prepared by mixing a soil analyzed to contain 4.8 p.p.m. with one containing 5 p.p.b. in proportions such that the mixture calculated to contain 121 p.p.b. mercury. Table III contains the results for this mixture along

TABLE III

PRECISION OF ANALYSIS FOR SAMPLE AND PREPARED STANDARD

	Sample No. LP26	*121 p.p.b. Mixture*
No. of detns.	10	14
Mean	213.8	123.9
s	11.2	4.9
90% Conf. interval	±6.4	±2.3

TABLE IV

ANALYSIS OF SOME U.S.G.S. ROCKS

(Results expressed as p.p.b. Hg)

U.S.G.S. No.	*This method*	*Atomic absorption*[12]	*Neutron activation*[13]
PCC-1	9	10	4
AGV-1	19	15	4
G-2	51	50	39
DTS-1	17	8	4
GSP-1	22	15	21
BCR-1	10	5	7

TABLE V

ANALYSIS OF A COAL STANDARD (NBS No. 1630)

	p.p.m. Hg
No. of detns.	12
Mean	0.125
s	0.01
90% Conf. interval	±0.005

with another soil sample run several times for a precision study. Finally, U.S. Geological Survey rocks were analyzed. The results are shown in Table IV with some other results for comparison purposes. The agreement is reasonably good.

Organic materials. For analysis of organic materials, a certified coal standard (NBS No. 1630) containing 0.13 p.p.m. Hg was obtained. The results are shown in Table V.

SUMMARY

A method has been developed whereby very low levels of mercury can be determined in both inorganic (soils and ores) and organic samples such as coals.

Samples are decomposed in a Leco furnace, and mercury is collected by amalgamation on gold-plated Nichrome wire; it is then flashed off for spectrometric determination at 253.7 nm. Satisfactory results were achieved in the p.p.b. range.

REFERENCES

1 D. C. Manning, *At. Absorption Newslett.*, 9 *(5)* (September–October, 1970).
2 T. T. Woodson, *Rev. Sci. Instrum.*, 10 (1939) 308.
3 E. G. Pappos and L. A. Rosenberg, *J. Ass. Offic. Anal. Chem.*, 49 (1966) 782.
4 W. R. Hatch and W. L. Ott, *Anal. Chem.*, 40 (1968) 2085.
5 W. W. Vaughn and J. H. McCarthy, *U.S. Geol. Survey Prof. Paper 501-D*, (1964) D123.
6 G. W. Kalb, *At. Absorption Newslett.*, 9 (1970) 84.
7 M. E. Hinkle and R. E. Learned, *U.S. Geol. Survey Prof. Paper 650-D*, (1969) D251.
8 H. Brandenberger and H. Bader, *At. Absorption Newslett.*, 6 (1967) 101, 7 (1968) 53.
9 J. V. O'Gorman, N. H. Suhr and P. L. Walker, Jr., *Appl. Spectrosc.*, 26 (1972) 44.
10 P. L. Gant, *U.S. Patent No. 3,693,323*, Continental Oil Company.
11 R. J. Watling, *Trans. Inst. Mining Met., Section B*, 81 (1972) B48–B49.
12 B. Flanagan, *Geochim. Cosmochim. Acta*, 33 (1969) 81.
13 W. D. Ehmann and J. Lovering, *Geochim. Cosmochim. Acta*, 31 (1967) 357.

Analytica Chimica Acta, 76 (1975) 345–354

ÉTUDE DE LA PRÉCONCENTRATION ET SÉPARATION DE TRACES DE MERCURE PAR RÉDUCTION SUR CUIVRE MÉTALLIQUE ET SON DOSAGE PAR SPECTROMÉTRIE D'ABSORPTION ATOMIQUE SANS FLAMME

S. DOĞAN et W. HAERDI

Département de Chimie Minérale et Analytique de l'Université, Sciences II, 1211-Genève 4 (Suisse)

(Reçu le 3 janvier 1975)

ÉTUDE DE LA SÉPARATION PAR RÉDUCTION SUR MICROCOLONNE DE CUIVRE MÉTALLIQUE

La séparation ou la préconcentration de traces de mercure par sa réduction sur cuivre métallique présente, comparée aux autres techniques, certains avantages particuliers lorsqu'on recherche la rapidité, la sensibilité et la simplicité des manipulations.

Le principe de cette méthode a été proposé par divers auteurs[1–3]. Dans ce travail nous décrivons une séparation utilisant des microcolonnes de cuivre. Celles-ci peuvent être utilisées pour la détermination directe du mercure par absorption atomique sans flamme. Dans cette première partie, les différents paramètres régissant la séparation sont étudiés.

Conditions expérimentales

Les rendements de la séparation ont été déterminés par marquage du mercure au moyen de ^{203}Hg ($t_{\frac{1}{2}} = 47$ jours) fourni par CEA France. Les mesures de l'intensité du rayonnement-γ sont effectuées au moyen d'un compteur décadique (précision env. $\pm 5\%$).

Une solution de nitrate de mercure (1–1000 ml, selon les conditions, v. ci-dessous) de molarité et pH connus, contenant le radioélément, est passée à travers un tube en pyrex (dimensions v. Fig. 1) légèrement étiré à l'une des extrémités (afin de retenir la laine de quartz sur laquelle repose le cuivre) et contenant une hauteur active de poudre de cuivre (p.a., Siegfried) de 2–10 mm. Le tube de pyrex est préalablement lavé avec l'acide nitrique (p.a., Merck), chaud (1+1), rincé à l'eau bidistillée et au méthanol (p.a., Merck), séché à l'étuve puis chauffé au four à 500°C pendant 6 h ainsi que la laine de quartz, ceci afin d'éliminer d'éventuelles traces de particules pouvant interférer lors du dosage proprement dit du mercure.

La séparation du mercure de solutions de faible volume (1–10 ml) se fait par injection de celle-ci à travers la colonne au moyen d'une seringue adéquate en polyéthylène (v. Fig. 1, schéma (a)). La préconcentration et séparation du mercure de solutions de grand volume (50–1000 ml) se fait au moyen d'un appareillage approprié (v. Fig. 1, schéma (b)).

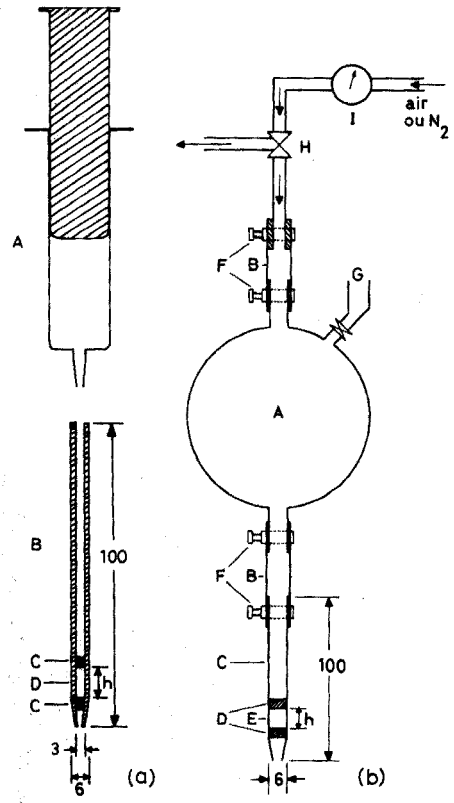

Fig. 1. Système de séparation du mercure sur microcolonne de cuivre. (a) Pour solutions de faible volume: (A) seringue 1–50 ml en polyéthylène, (B) colonne de cuivre, (C) laine de quartz, (D) poudre de cuivre. $h = 2–10$ mm. (b) Pour solutions de grand volume: (A) ballon 50–1000 ml en pyrex, (B) tuyau en polyéthylène, (C) colonne de cuivre, (D) laine de quartz, (E) poudre de cuivre (environ 200 mg), (F) bague de fixation, (G) ouverture pour introduction de la solution, (H) robinet à 3 voies, (I) manomètre.

Le dispositif (a) convient bien pour de faibles volumes et un passage relativement rapide de la solution. Le dispositif (b) convient pour le cas de grands volumes de solution et lorsque le débit doit être contrôlé. Le premier système (a), par exemple, été utilisé pour la détermination de mercure dans le sang après minéralisation. Le second système pour la préconcentration de mercure contenu dans des eaux naturelles à très faible teneur en mercure. Dans ce dernier cas, l'avantage réside dans le fait que l'on évite un traitement préalable de l'échantillon (préconcentration par évaporation, par exemple) ce qui permet d'éviter au maximum des pertes par volatilisation ou entraînement.

Étude des conditions de la séparation

Nous avons étudié divers paramètres régissant cette séparation, soit: importance du volume (ou masse) de cuivre, influence du pH, effet de la vitesse de passage de la solution (débit), rendement en fonction de la concentration en mercure.

Détermination de la masse de cuivre nécessaire. Des essais préliminaires nous

TABLEAU I

RENDEMENT DE L'EXTRACTION DE MERCURE EN FONCTION DE LA HAUTEUR DE CUIVRE (OU DE LA MASSE DE CUIVRE)

(Hg absolu, 100,3 μg)

$h_{colonne}$ (mm)	Masse de cuivre (mg)	Rendement (%)
2	40	99,7
3	60	99,8
5	100	99,7
10	200	99,5

ont montrés qu'en milieu acide (pH $\leqslant$ 3) la séparation était quantitative pour des concentrations en mercure variant entre 10^{-4} et 10^{-8} M. Les résultats du Tableau I ont été obtenus pour une concentration en $[Hg]_t = 10^{-4}$ M, pH = 2,2; débit D = 1,0 ml min^{-1}; volume de la solution $V = 5$ ml.

Nous constatons que pour les conditions choisies, le rendement de la séparation est quantitatif même pour une hauteur de 2 mm (environ 40 mg). Sauf indication contraire, nous avons adopté dans la suite de ce travail une hauteur active de 5 mm (100 mg).

Rendement de la séparation en fonction du pH. La réduction de mercure sur mercure ($E_0 = 0{,}35$ V) dépend évidemment du potentiel du couple Hg^{2+}/Hg^0 ($E_0 = 0{,}85$ V):

$$E = E_0^{Hg} + (RT/nF) \ln a_{Hg} \text{ avec } a_{Hg} \simeq [Hg^{2+}] = [Hg]_t/\alpha_{Hg(L)},$$

ou $\alpha_{Hg(L)}$ est la coefficient de complexation[4]. La concentration de mercure(II) libre dépendra donc du pH auquel on effectue la séparation c'est-à-dire de $\alpha_{Hg(OH)}$:

pH	1	2	3	4	5	6	7	8	9	10	11
$\log \alpha_{Hg(OH)}$	0	0	0,23	1.7	3.7	5,7	7,7	9,7	11,7	13,7	15,7

Il est à prévoir que le potentiel de mercure reste, pour des pH compris entre 0 et 8, supérieur à celui de cuivre; la réduction pourra théoriquement s'effectuer pour des concentrations de $[Hg]_t$ 10^{-15}–10^{-8} M selon le pH. Néanmoins, le rendement de la séparation dépendra de la cinétique de réduction de mercure d'une part et essentiellement de celle régissant la dissociation des complexes hydroxylés de mercure d'autre part. La vitesse de passage de la solution dans la colonne doit donc être contrôlée (v. plus loin: débit). Réaction globale:

$$Hg(OH)_n^{-n+2} \rightleftharpoons Hg_{(aq)}^{2+} + n\,OH^-$$
$$+$$
$$Cu^0 \text{ — } Hg^0(Cu^0) + Cu_{(aq)}^{2+}$$

Théoriquement on détermine que les complexes $HgOH^+$ ($\log \beta_1 = 10{,}3$) et $Hg(OH)_2$ ($\log \beta_2 = 21{,}7$)[4] commence à se former entre pH 2–3. Nous pouvons donc émettre l'hypothèse que c'est à partir de ces valeurs de pH que le rendement de l'extraction peut être affecté. Pratiquement cette hypothèse a été confirmée. La Fig. 2 en rend compte.

La vitesse de passage de la solution sur le cuivre semble donc jouer un rôle important. D'autre part, il serait possible, par cette technique, de séparer le mercure

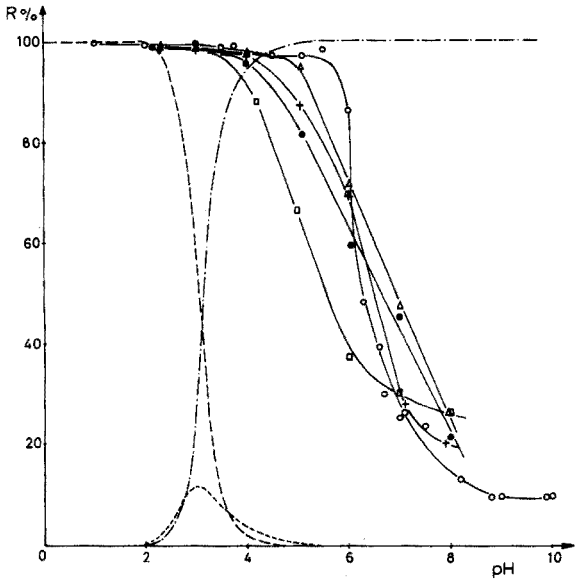

Fig. 2. Rendement de la séparation en fonction du pH pour divers concentrations de $[Hg]_t$: 10^{-4} *M* (○); $5 \cdot 10^{-5}$ *M* (△); $1 \cdot 10^{-5}$ *M* (+); $5 \cdot 10^{-6}$ *M* (●); $1 \cdot 10^{-6}$ *M* (□). Domaine d'existence des divers complexes hydroxylés de Hg: ——— Hg^{2+}; ---- $HgOH^+$; —·—· $Hg(OH)_2$. Débit 1,0 ml min^{-1}. Volume 5 ml. h_{Cu} 5 mm. Système (a).

libre du mercure lié (organomercuriel pare exemple) en jouant sur le débit (*D*) et le pH.

Pratiquement la séparation est quantitative pour $[Hg]_t = 10^{-4} - 10^{-6}$ *M*, jusqu'à pH 3,5 puis, son rendement (*R* %) diminue avec l'augmentation du pH et ceci d'autant plus rapidement que la concentration de mercure diminue.

Influence du débit sur le rendement de la séparation. Afin de vérifier les hypothèses émises dans le paragraphe précédent, nous avons étudié le rendement de la séparation en fonction du temps de contact solution–cuivre en faisant varier le débit de la solution. La Fig. 3 rend compte de *R* (%) en fonction de *D* (ml min^{-1}) pour des pH compris entre 2 et 10. Il semble donc bien que pour des pH $\leqslant 3$ le rendement de la séparation augmente au fur et à mesure que le débit diminue. Toutefois, pour obtenir un rendement appréciable pour nos conditions de travail, le débit devrait être très faible. Afin de pallier à cet inconvénient, nous avons fait des essais d'extraction.

(a) En agitant mécaniquement (méthode statique) 5 ml de la solution de Hg ($|Hg|_t = 10^{-4}$ *M*) de pH 7,2 avec environ 100 mg de poudre de cuivre (équivalent à $h = 5$ mm) dans un tube à centrifuger de 20 ml en polystyrène; le rendement est déjà supérieur à 90% après 10 min d'agitation.

(b) En faisant passer la solution par ittération (passage successifs) sur la microcolonne de cuivre (méthode dynamique) et ceci pour des pH variant entre 4 et 9. La Fig. 4 rend compte des résultats obtenus.

Ces deux techniques permettraient donc une séparation un peu plus rapide de mercure à des pH >3 mais au moyen de manipulations moins aisées. Remarquons que la méthode décrite sous (a) se prête mal à une récupération de la poudre de

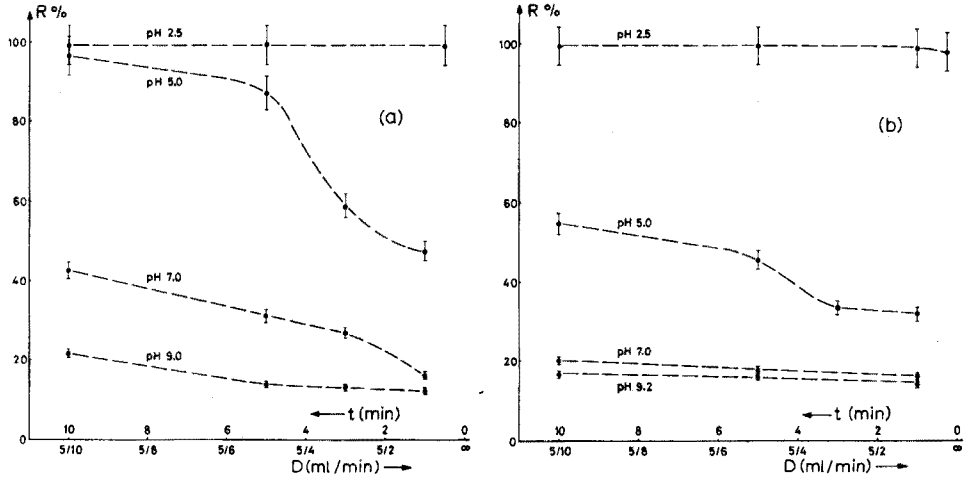

Fig. 3. Rendement de la séparation en fonction du débit à divers pH de la solution. (a) $[Hg]_i = 10^{-5}$ *M*. (b) $[Hg]_i = 5 \cdot 10^{-7}$ *M*. Volume 5 ml.

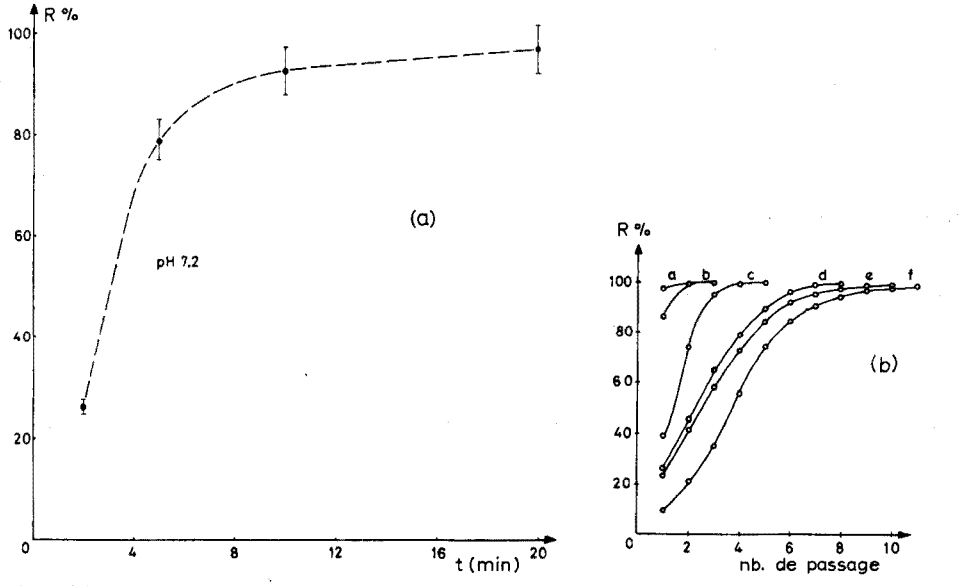

Fig. 4. (a) Rendement de la séparation par agitation mécanique de la solution de mercure en présence de cuivre. (b) Séparation par passages successifs (ittération) de la solution de mercure sur microcolonne de cuivre; pH: (a) 5,5; (b) 6,0; (c) 6,6; (d) 7,1; (e) 7,5; (f) 8,8. Débit de chaque fois 1,0 ml min^{-1}. Volume 5 ml, h_{Cu} 5 mm.

cuivre utilisable directement pour la détermination de mercure par absorption atomique sans flamme.

Étude du rendement en fonction de la concentration de mercure. La Fig. 5 rend compte des rendements de la séparation en fonction de différentes concentrations de mercure.

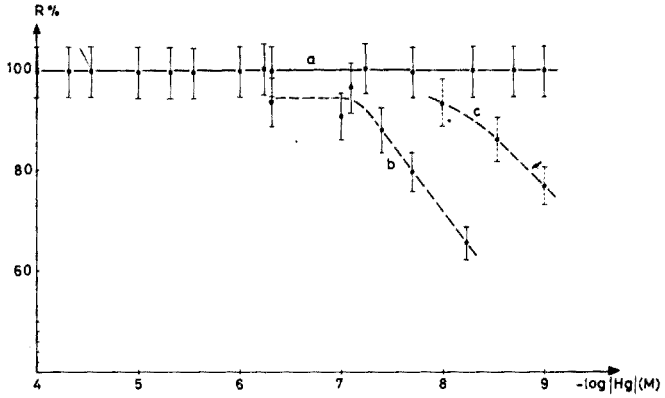

Fig. 5. Rendement de la séparation en fonction de différentes concentrations de mercure. Courbe (a) au moyen du schéma (a) (Fig. 1), volume 5 ml; pH 2,3; D 1,0 ml min^{-1}; conc. 10^{-4} M (Hg total 10^{2} μg) à 10^{-9} M (Hg total 10^{-3} μg). Courbe b au moyen du schéma (b) (Fig. 1), volume 500 ml; h_{Cu} 4 mm; pH 2,0; D 20 ml min^{-1}; conc. 10^{-6} M (Hg total 10^{2} μg) à 10^{-8} M (Hg total 1.0 μg). Courbe (c) comme courbe (b) sauf D 5 ml min^{-1}; conc. 10^{-8} M (Hg total 1 μg) à 10^{-9} M (Hg total 10^{-1} μg).

Les erreurs mentionnées sont de l'ordre de $\pm 5\%$ et dues essentiellement au bas taux de comptage de ^{203}Hg. L'efficacité de la séparation, pour un seul passage de la solution, est donc supérieure à 90% pour des concentrations $\geqslant 10^{-8}$ M.

Phénomène d'absorption et rendement d'extraction

Nous avons pu vérifier que le mercure était facilement adsorbé sur les parois des récipients utilisés pour les préconcentrations. Cet effet commence à affecter la séparation à partir de $|Hg|_t < 10^{-8}$ M. Il est possible d'éviter, dans une certaine mesure, ce phénomène en travaillant en milieu complexant (par exemple Cl^-, EDTA); le Tableau II en rend compte. On constate donc que cette adsorption peut être diminuée par un complexant de mercure(II). Toutefois l'adjonction d'un complexant à la solution doit être contrôlée afin de ne pas faire passer le potentiel redox de mercure en-dessous de celui de cuivre.

TABLEAU II

RENDEMENT DE L'EXTRACTION DE MERCURE EN PRÉSENCE DE COMPLEXANTS

$[Hg]_t = 10\text{–}11$ M; volume 500 ml; autres conditions comme courbe (c), Fig. 5 sauf $\phi_{colonne}$ 3 mm à la place de 6 mm.

pH	*Rendement (%) (Hg total 1 ng/500 ml)*			
	HNO_3	*HCl*	*EDTA 10^{-2} M*	*EDTA 10^{-4} M*
1,0	71,0	91,1	—	—
2,0	76,4	70,8	—	—
4,0	68,6	64,5	93,2	—
7,0	—	—	57,6	45,8

DOSAGE DU MERCURE PAR SPECTROMÉTRIE D'ABSORPTION ATOMIQUE SANS FLAMME

Le dosage de traces de mercure par absorption atomique sans flamme est bien connu[5–7]. Dans cette seconde partie, nous proposons une technique permettant d'utiliser, pour ce faire, directement les microcolonnes de cuivre contenant le mercure amalgamé. Deux modes de dosage sont décrits, l'un basé sur un système statique, l'autre dynamique.

Conditions expérimentales

Le système de cuve est semblable à celui proposé par Brandenberger[6]. Le mercure est vaporisé par chauffage direct de la microcolonne, au moyen d'une résistance *ad hoc*. Les mesures sont effectuées au moyen d'une spectromètre d'absorption atomique Pye Unicam SP 1900 couplé à un enregistreur Philips PM 8100.

Après passage de la solution à analyser sur la microcolonne, celle-ci est lavée 3 à 4 fois par 2–3 ml de méthanol afin d'éliminer les traces d'eau qui peuvent provoquer une interférence par absorption à la longueur d'one 253,7 nm (raie principale de mercure).

Technique de dosage au moyen du système statique

La colonne est coupée de chaque côté à la hauteur de la laine de quartz et est introduite dans la spirale de chauffage (Fig. 6), l'ensemble est rincé au méthanol.

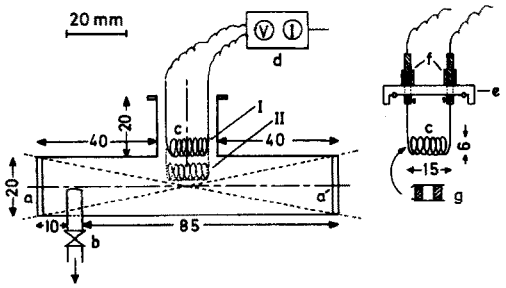

Fig. 6. Cellule de mesure et système d'évaporation de mercure (statique). (a, a') Fenêtres de 2 mm en quartz soudées à la cellule; (b) robinet pour le vide; (c) spirale de chauffage ($R = 1{,}38\ \Omega\ m^{-1}$, $\varnothing = 1{,}0$ mm); (d) source de tension 0–5 A; (e) couvercle en teflon; (f) fiches bananes; (g) microcolonne de cuivre coupée.

Après la mise en place du couvercle, l'excès du méthanol est entraîné sous vide (10 mm de mercure environ), au moyen de robinet (b). Un courant de 1,0 A est appliqué pendant environ 5 min (temp. 65 ± 5°C) jusqu'à pression constante dans la cellule de mesure afin d'éliminer les dernières traces de méthanol. Le robinet (b) est alors formé; en même temps que l'intensité du courant est fixée à 2,5 A (correspondant à 240 ± 5°C) on met en marche l'enregistreur. La mesure terminée, le robinet (b) est ouvert et on augmente l'intensité du courant à 4,5 Å environ, afin de nettoyer la cellule.

Les courbes obtenues sont représentées sur la Fig. 7. Elles présentent toutes, un temps d'induction qui est dû au transfert de chaleur de la spirale au cuivre ainsi

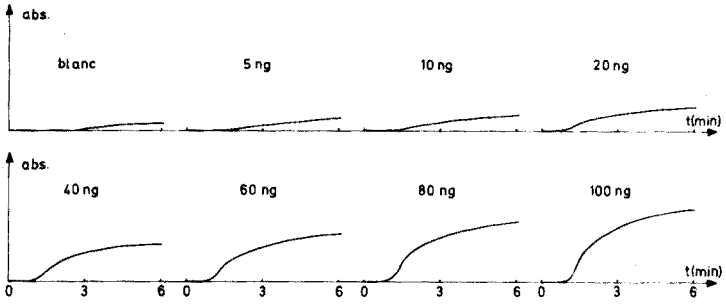

Fig. 7. Courbes d'évaporation du mercure (courant: 2,5 A et position I de la spirale). Temps d'intégration 4 s; échelle d'enregistrement 5 mV; vitesse d'enregistrement 10 mm min^{-1}.

qu'une pente dépendant de la température de la spirale et de la concentration du mercure déposé. La Fig. 8 représente les droites d'étalonnage établies à partir de la mesure des surfaces obtenues après un temps déterminé, que nous avons fixé à 6 min. Ecart type sur 6 mesures: 5 ng $\pm$ 19%, 100 ng $\pm$ 1,5%.

La position de la spirale dans la cellule de mesure, ainsi que sa température, influencent beaucoup la sensibilité du dosage. En effet, lorsque la spirale est placée le plus bas possible (position 2, Fig. 6), la limite de dosage peut être abaissée. Une augmentation de la température a le même effet; toutefois, la valeur du blanc augmente en conséquence.

Technique de dosage au moyen du système dynamique

La microcolonne de cuivre est directement chauffée en la plaçant dans une

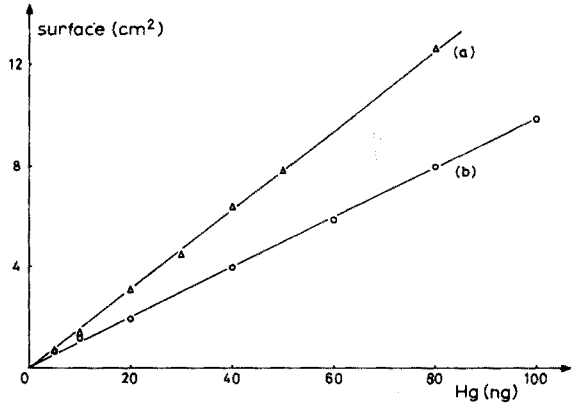

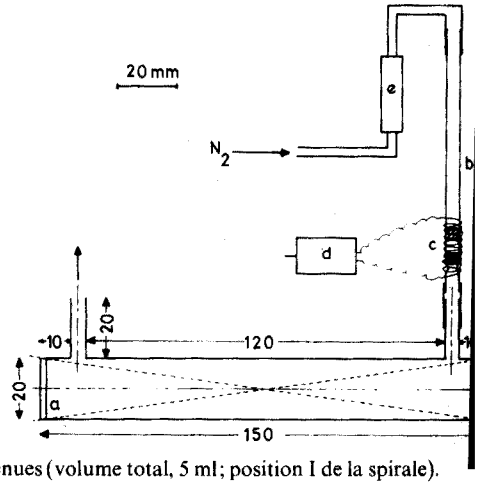

Fig. 8. Droites d'étallonnage en intégrant les surfaces obtenues (volume total, 5 ml; position I de la spirale). (a) $I = 3{,}0$ A (295 ± 5°C), (b) $I = 2{,}5$ A (240 ± 5°C).

Fig. 9. Cellule de mesure et système d'évaporation de mercure (dynamique). (a, a') Fenêtres de 2 mm en quartz; (b) microcolonne de cuivre ($h_{Cu} = 5$ mm $\simeq 100$ mg); (c) spirale de chauffage ($R = 1{,}38\ \Omega\ m^{-1}$, $\varnothing = 1{,}0$ mm); (d) source de tension 0–5 A; (e) débitmètre.

spirale située à l'extérieur de la cellule de mesure (Fig. 9). Les traces de méthanol sont éliminées en appliquant un courant de 1 A (70±5°C) pendant 1 min et un débit d'azote d'environ 300 ml min^{-1}. Puis, l'intensité du courant est portée à 3,5 A (370±5°C), le débit de l'azote fixé à 60 ml min^{-1}. Le pic donnant l'absorbance en fonction du temps est immédiatement enregistré. Les courbes obtenues sont données à la Fig. 10. La droite d'étalonnage obtenue est linéaire de 0 à 50 ng Hg; écart type sur 6 mesures: 1 ng±13%, 50 ng±2%.

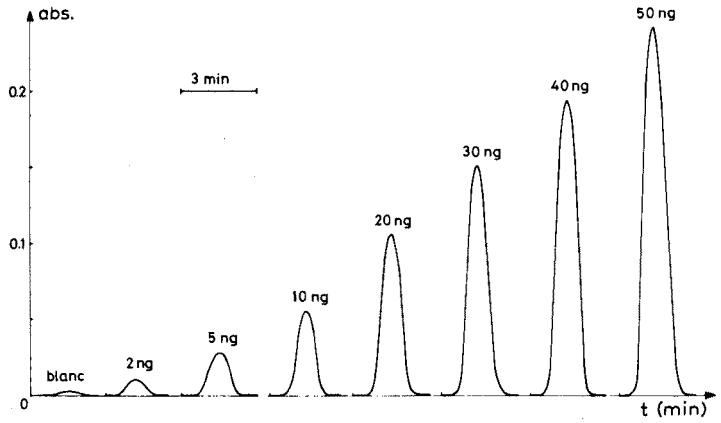

Fig. 10. Pics d'évaporation de mercure. Courant 3,5 A; *D* (azote) 60±5 ml min^{-1}; temps d'intégration 1 s; échelle d'enregistrement 5 mV; vitesse d'enregistrement 10 mm min^{-1}.

Cette technique est plus rapide et plus sensible que la première. Les colonnes peuvent être réutillisées. Cette méthode de dosage a été utilisée pour la détermination de mercure dans le sang et les eaux naturelles.

RÉSUMÉ

Il est montré qu'il est possible de séparer quantitativement, sur micro-colonne de cuivre, moins de 5 ng de mercure de solutions de faible volume. Lorsque le volume de la solution devient relativement grand (500 ml par exemple), la séparation dépend du débit de la solution et des phénomènes d'adsorption de mercure sur les parois des récipients. L'influence de ce dernier facteur peut être diminuée en ajoutant à la solution un complexant de mercure. La détermination du mercure amalgamé sur le cuivre peut se faire directement, par absorption atomique sans flamme. La limite de dosage est 1–2 ng. Cette méthode est plus rapide et plus sélective qu'une préconcentration par électrolyse.

SUMMARY

A micro-column of copper can be used to separate quantitatively as little as 5 ng of mercury from small volumes of solution. For large volumes, *e.g.* 500 ml, separation depends on the flow rate and on adsorption phenomena; the latter effect can be overcome by addition of complexing agents. The mercury amalgamated

on copper is determined directly by non-flame atomic absorption spectrometry. The limit of determination is 1–2 ng. The method is faster and more selective than preconcentration by electrolysis.

BIBLIOGRAPHIE

1 W. Matusiak, M. Cefola et L. dal Cortivo, *Anal. Biochem.*, 8 (1964) 463.
2 J. I. Kim et J. Hoste, *Anal. Chim. Acta*, 35 (1966) 61.
3 J. I. Kim et S. R. Sunoko, *Radioanal. Chem.*, 16 (1973) 257.
4 A. Ringbom, *Les Complexes en Chimie Analytique*, Dunod, Paris, 1967.
5 H. Brandenberger et H. Bader, *Helv. Chim. Acta*, 50 (1967) 1409.
6 H. Brandenberger, *Chimia*, 22 (1968) 449.
7 A. Montiel, *Analusis*, 1 (1972) 66.

Analytica Chimica Acta, 76 (1975) 355–360

BARIUM CARBONATE–BORIC ACID, AN ADVANTAGEOUS FLUX FOR ANALYSIS OF REFRACTORY MATERIALS BY FLAME SPECTROMETRY

D. E. CAMPBELL and W. O. PASSMORE*

Sullivan Park Research and Development Laboratories, Corning Glass Works, Corning, New York-14830 (U.S.A.)

(Received 26th October 1974)

Decomposition for analysis of such materials as corundum, zircon, zirconia and refractories based on these minerals can be a frustrating experience, particularly if analysis for trace levels of the alkali metals is contemplated. In such instances, acid decomposition would be preferable, but such an approach is feasible only by resorting to elevated temperature and pressure[1–3]. Besides requiring special equipment, the pressure decomposition may be hazardous, and in some instances[4] it is not completely effective in putting the sample in solution.

Fusion decomposition, particularly with alkali or calcium borates, can be quite expedient, but for the determination of trace levels of alkali and alkaline earth metals, these fluxes are inapplicable. Moreover, ionization interference by the alkali metals, especially lithium, can be expected in atomic absorption spectrometry[5]. A suitable flux must not only not contain the elements to be determined, but should approach the activity of the alkali borates, have a low flame spectral background, and yet be readily available in sufficient purity. As will be shown, a boric oxide-rich barium tetraborate flux fulfils these requirements quite well. Barium is the least flame-sensitive of the alkaline earths and is rarely encountered (or sought) in the trace analysis of refractory materials. Since both boric acid and barium carbonate are more readily available in a higher state of purity than barium tetra- or metaborate, the flux was generated *in situ*, probably according to the following reaction

$$4\,H_3BO_3 + BaCO_3 \rightarrow BaB_4O_7 + CO_2 + 6\,H_2O$$

EXPERIMENTAL

Flux

Ultrapure or spectrographically pure boric acid and barium carbonate were employed in the flux mixtures. A blend of two parts of boric acid and one part of barium carbonate used in a flux–sample weight ratio of 10:1 was optimal. Although there was a significant excess of boric acid over the amount needed to form barium tetraborate, the fluxing action was efficient and yielded a melt that readily dissolved in dilute acid. A flux mixture of 1 part by weight of barium carbonate to 2 parts by weight of boric acid was used in all further work.

* Present address: Lodi, New York-14860.

One obvious disadvantage in the use of fusion decomposition is the solubility of the melt. This, in conjunction with the flux–sample ratio, can be the limiting factor in determining the lower limits of detection. Hence the solubility was determined for a typical 10:1 flux–sample melt; it proved to be about 2 g of melt per 250 ml. In Table I are compared the solubilities at room temperature (*ca.* 25°C) of other applicable fluxes used in the customary flux–sample weight ratios; some variations in the solubilities will obtain, depending on the sample fluxed. It is apparent, other factors such as purity being equal, that the flux–sample ratio and solubility for the barium carbonate–boric acid mixture are such as to limit the detection of contaminants in the sample to at least an order of magnitude higher than for lithium tetraborate.

TABLE I

SOLUBILITY OF SELECTED FLUXES AT 25°C

Flux	H_3BO_3–$BaCO_3$ (2+1)	$Li_2B_4O_7$	CaB_4O_7	$NaHSO_4$
Flux–sample (wt. ratios)	10:1	3:1	10:1	10 to 20:1
Melt solubility	2.00 g/250 ml	Over 2.00 g/250 ml	2.00 g/100 ml	Over 2.00 g/100 ml

The freedom of the flux mixture from contamination with the elements to be determined was evaluated by carrying the flux mixture through the entire fusion and blank procedure followed by either flame emission (alkali metals) or atomic absorption (alkaline earths). For comparison, lithium tetraborate, calcium tetraborate and sodium hydrogen sulfate (ACS reagent grade or better purity) were similarly evaluated. The results (Table II) clearly indicate that the boric acid–barium carbonate flux is freest of all key contaminants.

TABLE II

CONTAMINATION CALCULATED FROM BLANKS

(Values are given as % by wt. of flux)

	$BaCO_3$–H_3BO_3	$Li_2B_4O_7$	CaB_4O_7	$NaHSO_4$
Rb_2O	<0.0001	—	—	—
K_2O	0.008	0.05	0.005	0.01
Li_2O	<0.0001	—	<0.0001	<0.0001
Na_2O	0.03	0.15	0.05	—
SrO	<0.001	—	—	—
CaO	<0.001	0.05	—	n.d.
MgO	<0.001	0.01	0.05	0.10

Flame emission and absorption spectrometry

Unless otherwise specified, air–acetylene with a single-slot laminar flow burner was used throughout this work.

Spectral background, another important concern, was considered in the case where the flux mixture might be expected to give the most serious problem, *viz.*, the 422.6-nm calcium emission line. From successive scans of the spectral region around 422.6-nm with a Varian Techtron AA-4 flame spectrometer (Fig. 1), it is evident that the background problem is manageable. Also seen in Fig. 1 is the releasing effect of the 0.01 *M* diammonium-EDTA–1000 p.p.m. lanthanum oxide flame buffer[6], which readily overcomes the slight depressing effect of the flux mixture. This background problem, which is similar for all the other elements determined by flame emission (and non-existent for those determined by atomic absorption), is thus readily correctable, provided that an adequate scanning monochromator, such as the 0.5-m Ebert used with the AA-4 spectrometer, is employed.

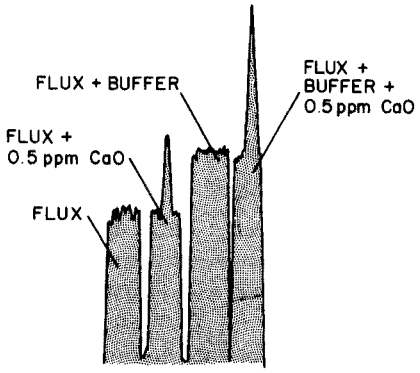

Fig. 1. Spectral emission background for calcium. 0.5 p.p.m. CaO; 8000 p.p.m. $BaCO_3$–H_3BO_3; 0.01 *M* $(NH_4)_4$ EDTA–1000 p.p.m. La_2O_3; Oxyhydrogen flame Beckman burner.

Since the boric acid–barium carbonate flux mixture showed a matrix effect on the calcium emission response, this effect on the other trace elements was investigated. Table III shows the air–acetylene flame responses for each of the elements of interest in the presence and absence of the boric acid–barium carbonate flux mixture; also given are results for calcium tetraborate and lithium tetraborate as well as sodium hydrogensulfate. The enhancement or inhibition effects are least for the boric acid–barium carbonate flux mixture. Of special interest is that the oxygen–hydrogen flame (total consumption burner) significantly reduces the matrix effect for calcium. In any case, these chemical interactional effects are no significant problem with any of the flux systems, particularly the boric acid–barium carbonate flux.

In addition to matrix effects from the flux mixture on the response to the analyte, there is also the effect of the sample matrix itself. As is well known, elements such as aluminum, zirconium and titanium inhibit the flame emission or atomic absorption response of the alkaline earths. The 1000-p.p.m. La_2O_3–0.01 *M* EDTA flame buffer mixture[6] minimizes this effect. Nevertheless, it was found best

TABLE III

MATRIX EFFECT OF FLUX ON THE RESPONSE TO VARIOUS IONS IN AN AIR–ACETYLENE FLAME

(All elements were determined by f.e.s., except magnesium (a.a.s.))

Analyte	*Response ratio of 1 p.p.m. standard + flux to 1 p.p.m. standard*			
	$BaCO_3$–H_3BO_3 8000 p.p.m.	*CaB_4O_7 4000 p.p.m.*	*$Li_2B_4O_7$ 4000 p.p.m.*	*$NaHSO_4$ 4000 p.p.m.*
Rb	2	—	—	—
K	1.5	2	4	10
Na	1.05	1	1	—
Li	1	0.95	—	1
Sr[a]	0.89	—	—	—
Ca[a]	0.59[b]	—	0.80[b]	0.40
Mg[a]	0.95	0.95	0.90	0.95

[a] Run in the presence of EDTA–La_2O_3 buffer.

[b] Use of an oxyhydrogen flame completely eliminates the flux matrix effect.

to utilize matching standards for calibration, to ensure full compensation of both the flux and sample matrix effects.

Decomposition procedure

Grind the sample to pass a 325-mesh nylon sieve. Weigh out 2.0 g of the blended (2+1) H_3BO_3–$BaCO_3$ flux mixture and divide into four equal parts. Transfer one-fourth into a clean agate mortar and another one-fourth into a 30-ml platinum crucible. Weigh 0.2000 g of the sample into the mortar, add another one-fourth portion of flux mixture and triturate, to blend the sample and flux thoroughly. Transfer to the 30-ml platinum crucible. Grind successive small portions of the remaining flux mixture, transferring each portion to the crucible to "rinse" the mortar. Cover the crucible and heat gradually over an air–gas blast burner. With agitation, bring the burner to full heat, and then heat for 0.5–1 h with occasional agitation. Cool and dissolve the melt by digestion with a suitable acid. Nitric or hydrochloric acid is suitable for high alumina, magnesia–zirconia, and titania ceramics. However, for zirconia materials, nitric acid digestion, followed by boiling with EDTA, and ultimately digestion with perchloric or hydrochloric acid, is recommended. If silica is a major constituent, add hydrofluoric acid in addition to the appropriate mineral acid, and fume off the silica and excess of fluoride in the customary manner. Transfer to a volumetric flask and dilute to 250 ml, adding in the case of the alkaline earths, 10 ml of a 0.25 *M* diammonium–EDTA solution[6] containing 25,000 p.p.m. La_2O_3. For calibration, use standards made up to contain the flux mixture at the same concentration as the samples.

RESULTS

Good agreement was found between decomposition with the recommended

TABLE IV

ANALYSIS OF REFRACTORY MATERIALS WITH DIFFERENT FLUXES

Material		*Oxide determined*	*Found (%) using*		
			$BaCO_3$–H_3BO_3	$Li_2B_4O_7$	$NaHSO_4$
Alumina refractory	Sample 1	Na_2O	0.009	<0.01	—
		K_2O	<0.001	<0.01	—
		Li_2O	0.91	—	—
		CaO	<0.01	<0.1	—
	Sample 2	Na_2O	0.034	0.03	—
		K_2O	<0.001	<0.01	—
		Li_2O	0.12	—	—
		CaO	<0.01	<0.1	—
Zirconia refractory	Sample 1	Na_2O	2.25	2.26	
	Sample 2	Na_2O	2.31	2.33	
Magnesia refractory	Sample 1	MgO	81.6		82.3
	Sample 2	MgO	89.0		88.4

TABLE V

COMPARISON OF CALCIUM RESULTS ON HIGH ALUMINA REFRACTORIES BY DIFFERENT METHODS

Sample	*% CaO*	
	Flame ($BaCO_3$–H_3BO_3) flux	*X-ray fluorescence*
A	0.78	0.80
B	1.34	1.38
C	2.49	2.60
D	3.28	3.29
	3.14	

boric acid–barium carbonate flux and lithium tetraborate for each of two different samples of alumina refractory (Table IV). It should be noted that not only can lithium be determined, but lower detection limits for the other elements are achieved with the new flux. Application to other refractory systems is also demonstrated in Table IV; again good agreement was obtained with the results of other flux systems.

Good agreement was also achieved for calcium determinations in high alumina refractories by the recommended flame spectrometric flux decomposition method compared with independent x-ray spectrometric analyses (Table V).

CONCLUSIONS

The (1+2) barium carbonate–boric acid mixture is an especially versatile flux, with an activity approaching the fluxing power of the alkali borates. It offers substantial advantages over other common fluxes, *viz.*, lithium tetraborate, calcium

tetraborate, and sodium hydrogensulfate, for trace analysis of high alumina, zirconia, and high magnesia refractory materials, permitting analysis for all the alkali metals and alkaline earth metals, except barium, on the same sample. Additionally, barium carbonate and boric acid are generally available in a higher state of purity than the constituents of other fluxes.

Examination of the spectral background in the air–acetylene (as well as oxygen–hydrogen for calcium) flame in the regions of the analytical lines for lithium, sodium, potassium, rubidium, strontium, calcium, and magnesium, showed no direct spectral interferences. Such radiation background that is present is easily corrected by recording the spectral scan. Chemical interference by this flux is minimal for lithium, sodium, and magnesium in an air–acetylene flame, but depression of the emission for calcium and strontium is apparent. However, the depression effects can be eliminated by use of a lanthanum–EDTA flame buffer, or, in the case of calcium, by resorting to the oxyhydrogen flame. For rubidium and potassium some enhancement of their emission lines by the barium–boron-containing flux was noted, which introduces no undue complications. Although the 10:1 flux–sample weight ratio restricts the detection limits owing to the solubility of the flux, even in the worst case, trace analysis for sodium down to 100 p.p.m. in the sample is possible. For the other alkali and alkaline earth metals, the limits of detection are significantly better.

Hydrofluoric acid treatment of the fused sample is unnecessary unless the sample contains silica in excess of *ca.* 5% (w/w). Hence direct dissolution of the fused sample in the appropriate acid greatly expedites the flame analysis. Foner[7], who has also identified barium metaborate as a useful flux, advocated separation of the barium by precipitation with sulfuric acid, but the present study shows that this is unnecessary. Not only would it be a liability in terms of occlusion of analyte elements in the precipitate, but there is also the inherent risk of sample contamination owing to the additional reagents and sample handling.

SUMMARY

A (1+2) barium carbonate–boric acid flux mixture used in a 10:1 flux–sample weight ratio is effective in decomposing a wide variety of high alumina, zirconia, and magnesia refractories. Among the advantages demonstrated are its low flame background, minimal matrix effects, freedom from impurities and its capability for use in determination of trace levels (100 p.p.m. or less) of all the alkali and most of the alkaline earth metals.

1 P. B. Adams, *Methods for Emission Spectrochemical Analysis*, ASTM Committee E-2, American Society for Testing and Materials, Philadelphia, 6th Edn., 1971, E-2 SM-10-19, p. 893.
2 K. Lounamaa, *Z. Anal. Chem.*, 146 (1955) 422.
3 F. J. Langmyhr and S. Sveen, *Anal. Chim. Acta*, 32 (1965) 1.
4 F. J. Langmyhr and K. Kringstad, *Anal. Chim. Acta*, 35 (1966) 131.
5 A. M. Bond and D. R. Canterford, *Anal. Chem.*, 43 (1971) 134.
6 P. B. Adams and W. O. Passmore, *Anal. Chem.*, 38 (1966) 630.
7 H. A. Foner, *Israel J. Chem.*, 8 (1970) 541.

Analytica Chimica Acta, 76 (1975) 361–370

THE USE OF A DEMOUNTABLE HOLLOW-CATHODE LAMP SOURCE AND A PIEZOELECTRICALLY SCANNED FABRY–PEROT INTERFEROMETER FOR INVESTIGATION OF THE ISOTOPIC COMPOSITION OF LEAD ORES

D. G. BEVAN and G. F. KIRKBRIGHT

Department of Chemistry, Imperial College, London SW7 2AZ (England)

(Received 28th November 1974)

Modern optical spectroscopic methods for the study of isotope abundance ratios have been employed for a number of elements[1–6]. When atomic emission spectrometry has been applied the high resolution necessary to study small isotope shifts in the atomic line spectra of the element investigated has been provided via a large grating spectrograph used in a high order or by use of a Fabry–Perot interferometer[6]. Recently, several workers have reported the use of atomic absorption spectrometry (a.a.s.), with single isotope sources, for isotope assay; the application of a.a.s. in this way, however, is usually limited to those elements such as lithium[7–10], uranium[11,12] and mercury[13] which exhibit relatively large isotope shifts. In geochronological studies the determination of lead isotope abundance ratios is of increasing importance and rapid reliable methods for this analysis are of interest. Both optical[6,14–16] and mass[17–20] spectrometric techniques have been applied for this purpose. Brody *et al.*[6] used an emission spectrometric method in which a pressure scanning Fabry–Perot interferometer was employed to study the isotopic fine structure of the Pb 405.8-nm line emitted by 3-mg PbO samples contained in an aluminium cathode in a water-cooled Schüler-type hollow-cathode source; these workers determined the isotopic ratios present in normal lead and several enriched samples. In more recent work Kirchhof[15] has described an atomic absorption technique for determination of lead isotopes in ores. In the technique described, hollow-cathode lamps containing the samples and standards of known isotopic composition were used as the radiation sources. The ^{208}Pb (or ^{206}Pb) content in the sample was determined by measuring the absorbance of the source radiation by lead vapour (in a second cathode) known to contain only ^{208}Pb (or ^{206}Pb). The elemental lead used in the sample cathode was obtained from the lead ores examined by dissolution in nitric acid, reduction to the element in an atmosphere of hydrogen and vacuum evaporation onto the inner wall of the aluminium cathode.

Jardy and Rosset[16] investigated the isotopic composition of lead uranothorianite by an emission spectrometric method in which lead was separated from the sample by anodic electrodeposition as lead dioxide followed by cathodic deposition as elemental lead onto an aluminium cathode. This electrode, containing 10–20 mg of deposited lead, was then employed as the cathode of a hollow-cathode discharge lamp. The isotopic analysis was effected by observation

of the hyperfine structure of the lead 405.8-nm line with a pressure scanning Fabry–Perot interferometer. Several workers[18–20] have utilized similar electrodeposition methods for the separation of lead from rocks and minerals before determination of its isotopic composition by mass spectrometry. In a recent paper, Arden and Gale[20] have described a low blank method of this type for the separation of lead from a variety of matrices, especially complex natural silicates, which is suitable as a separative step before mass spectrometry and can be used for samples containing greater than 10 ng of lead.

This paper describes a rapid method for the determination of the isotopic composition of small amounts of lead separated from minerals and ores. In the method described, lead is separated from interfering matrix elements by a sequential anodic and cathodic electrodeposition; a small amount of the lead in the sample (100–150 μg) is deposited onto a platinum foil cathode which is then inserted into the hollow stainless steel cathode of a commercially available hollow-cathode lamp source. A piezoelectrically scanning Fabry–Perot interferometer assembly is then employed to determine the relative intensities of the isotopic hyperfine structure components present in the emission from the 405.8-nm line of lead. The rapidity and simplicity of operation of the method compared to previously reported procedures accrues from the use of a rapid scanning interferometer with a signal-averaging facility, a hollow-cathode lamp source with easily interchangeable cathodes, and the requirement for the final deposition of only small amounts of elemental lead to form the spectroscopic cathode.

EXPERIMENTAL

Apparatus

A detailed description of the assembly and performance characteristics of the piezo-electrically scanned Fabry–Perot interferometer has been published elsewhere[21,22]. The optical arrangement employed was also similar and the demountable hollow-cathode lamp was positioned to replace the various atomic line sources examined in the earlier work.

The interferometer plates used in this work were of vitreous silica (25 mm diameter); the central region of each plate was flat to $\lambda/150$ at 546.1 nm and the dielectric plate coating gave 96% reflectance and an absorption of not more than 1%. A plate separation of 9.16 mm giving a Free Spectral Range of $8.8 \cdot 10^{-3}$ nm was used. In the fast scan mode (5 Hz) employed with the time-averaging computer, a finesse of 21 was recorded with these plates at the lead 405.8-nm line. In the slow scan mode, a finesse of 31 was achieved. The time averaging computer employed (Model DL 102, 200 point averager, Data Laboratories Mitcham, U.K.) was used to improve signal-to-noise ratios in the line emission profiles at 405.8 nm when only small amounts of lead were deposited into the cathode of the hollow-cathode lamp. Line profiles were displayed on a potentiometric chart recorder or on an oscilloscope.

A Miniglow demountable hollow-cathode lamp (Spectrogram Corp, New Haven, Connecticut) was employed as the atomic line source. The construction and general operation of this source for atomic absorption spectrometry has recently been described elsewhere[23]. In the applications to emission spectrometry reported

here, the water-cooled lamp was operated with a continuous purge of helium filler gas at a pressure of 8 torr and a d.c. operating current of between 3 and 10 mA depending on the sample requirements. A stainless steel hollow cathode (length 25 mm, 4 mm i.d., 6 mm o.d.) was employed. A platinum foil rectangle (length 24 mm, width 12.5 mm, thickness 0.025 mm) bearing the electrodeposited lead from the samples was bent into cylindrical form and inserted into the steel cathode.

The sequential cathodic and anodic electrodeposition of lead from samples was done with a simple BTL Electrolyte Analysis Apparatus (Baird and Tatlock Ltd., London) with the platinum foil electrodes. A standard calomel electrode and a digital voltmeter was used to monitor the potential of the working electrode *vs.* SCE.

Experimental method with lead samples

Samples of native lead, lead sulphide and silicate ores were reduced to a fine powder in an agate mortar. Samples (0.5–1 g) containing native lead or lead sulphide were treated with warm hydrochloric acid (1 + 1; 5 ml) and heated to dryness. The residue was dissolved in a second 5-ml aliquot of hydrochloric acid (1 + 1) and the solution was diluted to 20 ml with distilled water. Samples of silicate ores (0.5–1 g) were heated with hydrofluoric acid (48%; 5 ml) in a Teflon beaker on a hotplate for 2 h. The resulting solution was evaporated to dryness, 2 ml of concentrated hydrochloric acid was added, and the solution was again taken to dryness. The residue was heated with hydrochloric acid (1 + 1; 10 ml) for 1 h and the supernatant solution decanted. The residue was treated with a second aliquot of hydrochloric acid (1 + 1) and the supernatant solution decanted; the two extracts were then combined.

Hydrazinium chloride solution (2 ml, 1% w/v) was added to each sample solution before electrolysis; any iron(III) present was thus reduced to iron(II) to prevent the reduction occurring at the cathode during electrolysis in preference to the reduction of lead(II). Each sample solution was electrolysed for 30 min; two platinum foil electrodes were used and the cathode was maintained at −0.65 V *vs.* SCE. The cathode was then removed and washed by dipping into distilled water several times, and the deposited material was dissolved in a small volume of hot nitric acid (1 + 1; 0.5–2.5 ml depending on lead content of the sample). Excess of copper nitrate solution (10% w/v; 1 ml) and 1 ml of 0.4 *M* nitric acid was then added and the solution was diluted to 10 ml with distilled water. The electrolysis with platinum electrodes was then repeated for 45 min, the anode being maintained at +1.8 V *vs.* SCE. The anode foil carrying the deposited lead dioxide was then washed free of copper by dipping into distilled water several times. The foil anode was bent into cylindrical form for insertion into the steel cathode of the hollow cathode discharge lamp. For each sample, the lamp was pumped down and flushed twice with helium before final pumping and initiation of the hollow-cathode discharge. The helium pressure in the discharge lamp was set to 8 torr and the operating current was adjusted to produce sufficient intensity at the Pb 405.8-nm line. In order to allow the lamp to stabilize the discharge was operated for 5 min before the scanning Fabry–Perot interferometer was used to obtain the profile of the lead 405.8-nm line.

RESULTS AND DISCUSSION

Choice of analytical line

Blaise[24] has studied the hyperfine structure of a number of atomic lines of lead which lie between 400 and 650 nm. An examination of these shows that hyperfine structures of the lead 520.1-nm and 434.0-nm lines are simple, each line showing only two components rather than three because of nuclear hyperfine splitting in the lead 207 isotope, and that the individual components are well-spaced and separate on the wavelength scale. In addition, Blaise[24] has reported that the lead 520.1-nm line is relatively unaffected by self-absorption effects. In the hollow-cathode discharge used in this work, however, the relatively weak Pb 520.1 and 434.0-nm lines were not observed, probably because of the low transmittance of the interferometer at these wavelengths. The intense Pb 405.8-nm line, corresponding to the transition $7s^3P_1^0$–$6p^2\ ^3p_2$ lies at a wavelength at which high reflectivity was obtained with the Fabry–Perot etalon plates available here, so that good finesse was available at this line; additionally, as the 405.8-nm line originates from a level 1.32 eV above the ground state, its use should give rise to only a small degree of self-absorption when the source operating conditions are chosen judiciously. The hyperfine structure of the Pb 405.8-nm line has been used by other workers in studies of lead isotope composition for similar reasons. The structure of the Pb 405.8-nm line is shown in Fig. 1(a). The line consists of six components over a total width of *ca.* $7 \cdot 10^{-3}$ nm. These components comprise single lines from each of the three isotopes of even numbers (^{204}Pb, ^{206}Pb, ^{208}Pb), where there is no nuclear hyperfine splitting, and three lines resulting from this splitting in the ^{207}Pb isotope. These three lines are designated 207s, 207m and 207w (strong, medium and weak) in Fig. 1. The theoretical intensities may be calculated, using the sum rule for intensities, as 9:5:1 for 207s:207m:207w. It is apparent that only small wavelength displacements are expected in the hyperfine structure of the Pb 405.8-nm line in lead samples; thus the separation of the ^{208}Pb and ^{206}Pb components is only $1.4 \cdot 10^{-3}$ nm and for the ^{208}Pb and ^{207}Pb$_s$ lines is only *ca.* $0.18 \cdot 10^{-3}$ nm. Clearly the highest possible instrumental resolution available from the spectrometer is required, and the narrowest possible source line widths, to minimize overlap of components, are desirable. It is thus important to establish carefully the optimal source operating conditions to minimize line broadening effects on the lead 405.8-nm emission.

Optimization of discharge lamp operating conditions

Filler gas. The filler gas for the discharge lamp was chosen to provide efficient sputtering action while maintaining freedom from spectral interference from atomic line emission of the filler gas itself. Argon and neon exhibit line emission, at 405.5 nm and 406.3 nm, respectively, which interferes at the Pb 405.8-nm line with the broad auxiliary monochromator band-pass employed (1 nm half-width) in this work. Helium was therefore chosen as filler gas.

Cathode material. The platinum foil bearing the lead dioxide electrodeposited from samples was inserted into a hollow cathode in the discharge source. No spectral interference was encountered from platinum, but care must be taken in the choice of the material of the hollow cathode itself. The available cathode materials were copper, brass, graphite and stainless steel. The use of either copper or brass

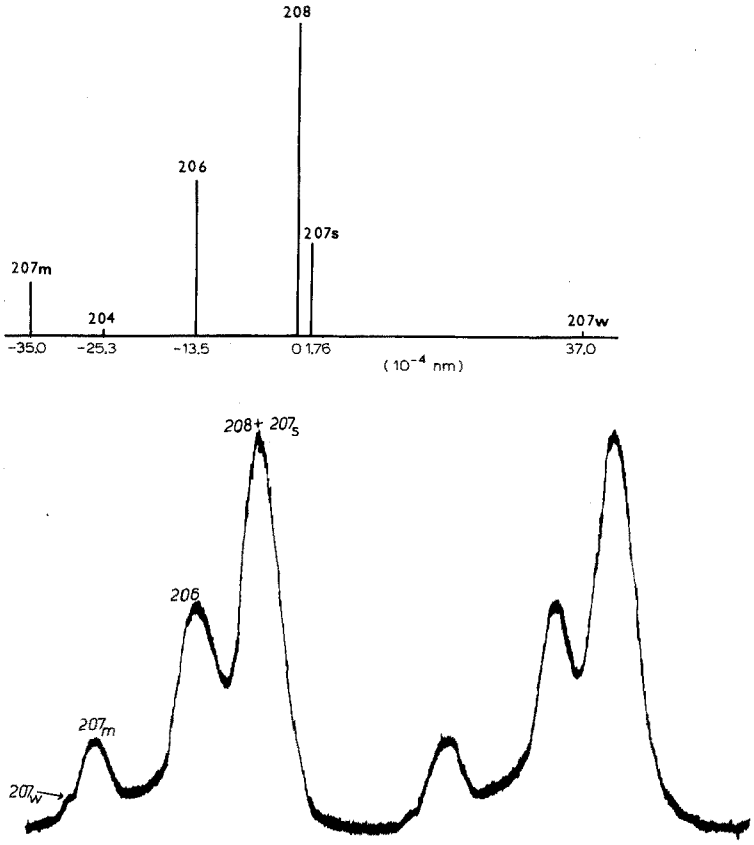

Fig. 1. (a) Hyperfine structure of the Pb 405.78-nm line. Displacement of components from central wavelength of ^{208}Pb shown in nanometres·10^4. (b) Typical recorder tracing observed for Pb 405.8-nm line from natural lead sample with the interferometer in the slow scan mode. Two orders scanned.

resulted in interference with the Pb 405.8-nm emission by the Cu 406.3-nm line. The graphite cathodes available exhibited weak line emission at 406.4 nm; in addition, graphite is a poor conductor of heat and its use gave rise to less efficient water-cooling. Stainless steel cathodes did not cause spectral interference and these were employed for all further studies.

Operating current and filler gas pressure. The discharge lamp current and helium filler gas pressure were chosen to provide (a) adequate line intensity and an acceptable signal: noise ratio, (b) freedom from self-absorption which causes broadening and increases the overlap of the components of the Pb 405.8-nm line, and (c) sufficient operating lifetime with the small amounts of lead dioxide electrodeposited onto the platinum foil within the hollow cathode. As the lamp was continuously purged with helium, the tendency of lead vapour to persist in front of the cathode at low operating currents was minimized; this effect therefore minimized self-absorption broadening. When high operating currents ($>ca.$ 20 mA) were employed, the intensity of the Pb 405.8-nm line decreased rapidly, presumably owing

to rapid depletion of the lead dioxide deposit at the increased sputtering rate attained. For all electrodeposited samples of lead studied in this work the optimal helium pressure was found to be 8 torr. The operating current was maintained at a value which varied between 3 and 10 mA depending on the amount of lead present in the cathode. In order to produce adequate emission intensity at 405.8 nm for a period of 1 h, a current of 3 mA could be used when more than 200 μg of lead was present in the cathode, whereas for smaller amounts a higher current was required to produce sufficient intensity. Under the latter conditions, lamp operating lifetime was usually restricted to 30–40 min.

Determination of isotope concentrations

Figure 1(b) shows a typical record from a natural lead sample of the structure of the Pb 405.8-nm line observed from the demountable hollow-cathode source with slow scanning of the Fabry–Perot interferometer. It is apparent that the hyperfine structure of the line is only partly resolved. As the free spectral range used for the interferometer was $8.8 \cdot 10^{-3}$ nm and the finesse attainable in the slow scan mode was 31, the instrumental contribution to the half-width of each component was only $0.29 \cdot 10^{-3}$ nm; the relatively broad line-widths observed, therefore, were the result of the broadening effects within the source rather than a reflection of the instrumental band-pass of the spectrometer.

It can be seen by a comparison of Figs. 1(a) and (b) that the strongest of the three ^{207}Pb components ($^{207}Pb_s$) could not be resolved from the ^{208}Pb line (the central wavelengths being only $0.18 \cdot 10^{-3}$ nm apart) and that the ^{206}Pb component was also not completely resolved from the ^{208}Pb line. The ^{204}Pb line, and the weakest ^{207}Pb component ($^{207}Pb_w$), each contributed only *ca.* 1% to the total observed line intensity at 405.8 nm and were too weak to be measured. Owing to the incomplete resolution of the components of the 405.8-nm line it was necessary to correct the observed intensities of the ^{208}Pb, ^{206}Pb and the calculated intensity of the $^{207}Pb_s$ component to compensate for their mutual overlap. This was accomplished by establishing correction factors. The spectrum of an isotopically pure ^{208}Pb sample was obtained at 405.8 nm when the same free spectral range as that employed for the mixed isotope samples was used. A single symmetrical line was obtained. The percentage contributions to this line of the ^{208}Pb intensity at the wavelengths of the ^{206}Pb and $^{207}Pb_s$ lines were calculated and used to correct measurements at these wavelengths. It may be assumed that a similar line profile to that for ^{208}Pb could be obtained for the single ^{206}Pb line and the $^{207}Pb_s$ component; the correction factor for overlap between the ^{206}Pb and $^{207}Pb_s$ lines could therefore be determined similarly. The validity of the latter correction was also checked by generation of the 405.8-nm line spectrum for an isotopically pure sample of ^{206}Pb. The overlap factors established, as a percentage contribution of intensity of one line to that of its overlapping neighbour, were: 208–207s, 90%; 208–206; 6%; 206–207s, 4%.

The intensity of the $^{207}Pb_s$ component was not established by direct measurement but by measurement of the intensity of the resolved $^{207}Pb_m$ component. As stated earlier, it is known that in the absence of self-absorption the theoretical intensities of $^{207}Pb_s$; $^{207}Pb_m$:$^{207}Pb_w$ are in the ratio 9:5:1. As the intensity of $^{207}Pb_m$ may be measured without overlap by other components, the

intensity of the $^{207}Pb_s$ component may be obtained by multiplying the $^{207}Pb_m$ intensity by 9/5. The theoretical intensity ratio of 9:5:1 for the components of the ^{207}Pb line would only be obtained under conditions where self-absorption may be neglected. The spectrum obtained for isotopically pure ^{207}Pb deposited as lead dioxide into the hollow-cathode source, which was operated under the established optimal conditions, is shown in Fig. 2. It is apparent that within the limits of experimental error, the theoretically expected intensity ratio was obtained.

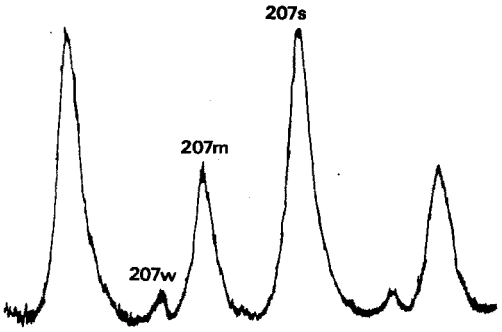

Fig. 2. Hyperfine structure observed for pure ^{207}Pb deposited as PbO_2 into hollow-cathode source operated under conditions employed for analysis of samples. Two orders scanned.

The percentages of each isotope in a particular sample were determined from the measurement of the intensities of the components as follows. If the measured intensities are represented as:

$$^{208}Pb = A,\ ^{206}Pb = B, \text{ and } ^{207}Pb_m = C,$$

then $^{207}Pb_s = (9/5)\ C$. When A and B are corrected for $^{207}Pb_s$ overlap, then:

$$^{208}Pb = [A - 0.9 \times (9/5) C]$$

$$^{206}Pb = [B - 0.04 \times (9/5) C]$$

Correction for mutual overlap between ^{208}Pb and ^{206}Pb then gives:

$$^{208}Pb_{true} = [A - 0.9 \times (9/5) C] - [0.06 \times {}^{206}Pb_{true}]$$

$$^{206}Pb_{true} = [B - 0.04 \times (9/5) C] - [0.06 \times {}^{208}Pb_{true}]$$

These two simultaneous equations may be solved for $^{208}Pb_{true}$ and $^{206}Pb_{true}$. The $^{207}Pb_{true}$ value was obtained from the relationship $^{207}Pb_{true} = (15/5) C$. The percentage of each isotope was then simply obtained from the three corrected intensities measured for each.

Accuracy and precision

The concentration of each of the principal lead isotopes in a natural lead sample and a lead sulphide mineral was determined by the method developed. The results are shown in Table I and compared to those reported for mass spectrometric and atomic absorption methods with the same samples by Kirchhof[15]. In order to provide a further test of the accuracy of the method, the lead sulphide sample was "spiked" with pure ^{206}Pb or ^{207}Pb to produce different abundance ratios in the

TABLE I

RESULTS OBTAINED FOR ISOTOPIC COMPOSITION IN SAMPLES EXAMINED

Sample	*Mass spectrometry results*[15] *and values for synthetic samples (%)*			*A.a.s. method*[15] *(%)*		*This work (%)*		
	^{206}Pb	^{207}Pb	^{208}Pb	^{206}Pb	^{208}Pb	^{206}Pb	^{207}Pb	^{208}Pb
Old Joplin (PbS)	27.58(MS)	—	51.17(MS)	28.3	50.4	27.2±0.5	22.0±0.7	50.8±0.7
Langbau (native Pb)	23.32(MS)	—	52.24(MS)	24.5	53.3	23.4±0.5	24.2±0.7	52.0±0.7
Old Joplin (^{206}Pb enriched)	42.6	16.8	40.5	—	—	42.6±0.7	17.8±1.0	39.6±1.0
Old Joplin (^{207}Pb enriched)1	15.5	56.0	28.6	—	—	16.0±0.7	55.7±1.0	28.3±1.0
Old Joplin (^{207}Pb enriched)2	11.9	65.9	22.1	—	—	13.6±0.7	64.4±1.0	22.0±1.0

sample. The results for these samples are also shown in Table I. The standard deviation values shown were obtained from eight analyses conducted on each sample.

The principal source of error in the procedure resulted from random error associated with the measurement of the intensity of the $^{207}Pb_m$ component in each spectrum. It is difficult to measure this intensity to better than 3%, which caused errors in the ^{207}Pb value. As this measurement was used to correct the combined $[^{208}Pb + ^{207}Pb_s]$ intensity measurement for the contribution from $^{207}Pb_s$ the error in measurement of the $^{207}Pb_m$ intensity was also reflected in the value obtained for ^{208}Pb. Similar considerations apply to the value obtained for the true ^{206}Pb intensity, which was obtained after correction for the contribution from $^{207}Pb_s$; the extent of the overlap was smaller in this case, however. It was not possible in any of the studies reported here to determine the concentration of ^{204}Pb in samples. This isotope is present at only *ca.* 1% concentration in natural lead samples; the single ^{204}Pb component is thus of very low intensity and is located between the $^{207}Pb_m$ and ^{206}Pb components and overlapped by them. The ^{204}Pb intensity may thus be determined only by calculating the contributions of the $^{207}Pb_m$ and ^{206}Pb components at the central wavelength of the ^{204}Pb component and subtracting these from the total intensity observed at this wavelength. The low signal:noise ratio obtained at the low intensity observed at this wavelength, however, precludes evaluation of the ^{204}Pb concentration.

Conclusion

The procedure developed for the determination of ^{206}Pb, ^{207}Pb and ^{208}Pb is sensitive; relatively low concentrations of lead in mineral samples may be determined by the electrolytic separation and preconcentration procedure employed. Only 50–100 μg of lead are required within the hollow-cathode source in order to undertake the analysis. The electrolytic separation procedure ensures that high selectivity is obtained in the determination. The only common element which is carried through the cathodic and anodic deposition procedure is bismuth; fortunately, bismuth does not cause spectral interference at 405.8 nm. The precision of the method developed with the instrumentation available is adequate for the rapid examination of approximate isotopic abundance ratios. As mentioned above, the precision is limited by the attainable resolution of the hyperfine components with the source employed and the signal:noise ratio obtained at the relatively low operating currents used to prevent rapid depletion of the sample deposited in the hollow cathode. It is possible that the use of a liquid nitrogen-cooled hollow-cathode source would result in better resolution of the hyperfine components of the Pb 405.8-nm line; this advantage would be offset, however, by loss of the operational simplicity of the demountable hollow-cathode lamp employed in this study.

SUMMARY

The intensities of the hyperfine and isotope components of the Pb 405.8-nm atomic line emission from a demountable hollow-cathode discharge lamp have been measured with a piezoelectric scanning Fabry–Perot interferometer. A simple method has been developed for the determination of the isotopic composition of lead ores and minerals. Lead is separated by a sequential cathodic and anodic electrodeposition

procedure with platinum electrodes and the foil electrode bearing the final deposit of lead dioxide is used as the spectroscopic electrode (cathode) within the demountable hollow-cathode lamp. The method has been applied successfully to a number of ore and mineral samples.

REFERENCES

1 J. K. Brody, *Argonne National Laboratory, Report, ANL-4359*, 1949, p. 94.
2 H. P. Broida and J. W. Moyer, *J. Opt. Soc. Amer.*, 42 (1952) 37.
3 J. K. Brody, M. Fred and F. S. Tomkins, *Spectrochim. Acta*, 6 (1954) 383.
4 G. K. Werner, D. D. Smith, S. J. Ovenshine, O. B. Rudolph and J. R. McNally, Jr., *J. Opt. Soc. Amer.*, 45 (1955) 203.
5 J. K. Brody, *J. Opt. Soc. Amer.*, 42 (1952) 408.
6 J. K. Brody, F. S. Tomkins and M. Fred, *Spectrochim. Acta*, 8 (1957) 329.
7 A. N. Zaidel and E. P. Korennoi, *Opt. Spectrosk.*, 10 (1961) 570.
8 A. N. Zaidel and E. P. Korennoi, *Zavod. Lab.*, 29 (1963) 1449.
9 D. C. Manning and W. Slavin, *At. Absorption Newslett.*, 1 (1962) 39.
10 J. A. Goleb and Y. Yokoyama, *Anal. Chim. Acta*, 30 (1964) 213.
11 J. A. Goleb, *Anal. Chem.*, 35 (1963) 1978.
12 J. A. Goleb, *Anal. Chim. Acta*, 34 (1966) 135.
13 K. R. Osborn and H. E. Gunning, *J. Opt. Soc. Amer.*, 45 (1955) 552.
14 M. S. Kashtan and T. N. Khlopina, *Opt. Spectrosc. (USSR)*, 266 (1961) 10.
15 H. Kirchhof, *Spectrochim. Acta, Part B*, 24 (1969) 235.
16 A. Jardy and R. Rosset, *Bull. Soc. Chim. Fr.*, 11 (1970) 4173.
17 F. Tera and G. J. Wasserburg, *Earth Planet. Sci. Lett.*, 13 (1972) 457.
18 W. Shields, *Nat. Bur. Stand. (US), Tech. Note*, 546 (1969–70) 36.
19 M. Tatsumoto, *Earth Planet. Sci. Lett.*, 9 (1970) 193.
20 J. W. Arden and N. H. Gale, *Anal. Chem.*, 46 (1974) 2.
21 G. F. Kirkbright and M. Sargent, *Spectrochim. Acta, Part B*, 25 (1970) 577.
22 G. F. Kirkbright, O. E. Troccoli and S. Vetter, *Spectrochim. Acta, Part B*, 28 (1973) 1.
23 G. F. Kirkbright and P. J. Wilson, *Anal. Chem.*, 46 (1974) 1414.
24 J. Blaise, *Ann. Phys.*, 3 (1958) 1019.
25 *Massachusetts Institute of Technology Wavelength Tables*, Technology Press, 1939.

Analytica Chimica Acta, 76 (1975) 371–376

RÖNTGENSPEKTROMETRISCHE BESTIMMUNG VON BLEI IN AUTOMATENSTAHL

TEIL I. BRIKETT-VERFAHREN

O. G. KOCH

Chemisches Laboratorium, Neunkircher Eisenwerk AG, D-668 Neunkirchen/Saar (B.R.D.)

(Eingegangen den 16. Dezember 1974)

Die laufende Bestimmung des Bleigehaltes in grossen Probenserien ist ein wichtiger Bestandteil der Produktionskontrolle von Automatenstählen. Zur Lösung dieser Aufgabe ist der Einsatz einfacher, sicherer und rationeller Analysenverfahren notwendig. Eine hierzu geeignete Methode für unlegierten und legierten Automatenstahl wurde vom Autor bereits früher veröffentlicht[1–4], bei der das Blei als Bleijodid photometrisch bestimmt wird. Gegenüber anderen bekannten Bestimmungsmethoden erwies sich diese photometrische Methode als vorteilhafter wegen ihrer Einfachheit, des geringen apparativen Aufwandes und des vergleichsweise niedrigen Zeitbedarfes von 45 min. Sie weist aber einen noch relativ hohen Zeit- und Arbeitsaufwand auf, wenn man sie mit den in der Stahlanalyse in der Regel eingesetzten, automatischen Spektrometern vergleicht.

Im Rahmen der Arbeiten zur weiteren Rationalisierung der Arbeitsabläufe des Laboratoriums wurden auch die Möglichkeiten für eine Verbesserung des Verfahrens zur Bestimmung von Blei in Automatenstahl untersucht. Als Ergebnis zahlreicher Versuche wurden zwei Methoden zur röntgenspektrometrischen Bestimmung von Blei in unlegierten und legierten Automatenstählen ausgearbeitet, über die nachfolgend berichtet wird.

EXPERIMENTELLER TEIL

Wegen der besonderen Produktionstechnik bei Automatenstahl ist es nicht möglich, den Bleigehalt in der bei Stahl sonst üblichen Giessprobe zu bestimmen. Die Bestimmung des Bleigehaltes erfolgt deshalb im Halbzeug, den sogenannten Walz- und Knüppelproben mit einem Querschnitt von etwa 85 × 85 mm bis 150 × 150 mm, die während der Walzung entnommen werden. Schliesslich muss noch der Bleigehalt der Fertigprodukte bestimmt werden im Rahmen der Ausgangskontrolle.

Probenvorbereitung

Zuerst wurde versucht, das Blei in kompakten Stahlproben spektrometrisch zu bestimmen. Hierzu wurden Scheiben von *ca.* 20 mm Dicke über den Querschnitt der Walz- und Knüppelproben abgesägt, auf der Tellerschleifmaschine mit Korundschleifpapier (Körnung 40 oder 60) geschliffen und der Emission- und Röntgen-

spektrometeranalyse unterzogen. Die Spektrometeranalyse erfolgte an mehreren, ausgewählten Punkten der geschliffenen Probenfläche, wonach die Messwerte auf Streuung und Richtigkeit geprüft wurden. Ihre Auswertung zeigte eine zu grosse Streuung der Analysenergebnisse, die auf zwei Ursachen zurückzuführen ist: (a) die Inhomogenität der Stahlprobe, (b) die Behandlung der Stahlprobenoberfläche.

Homogenität der Stahlprobe. Die für die starke Analysenstreuung erkannte erste Ursache ist die inhomogene Verteilung des Bleies in der Stahlprobe, die auch durch Messung an mehreren Punkten der Probenoberfläche und Mittelung der Messwerte[5,6] nicht ausgeglichen werden kann. Die empfohlene[6] Anwendung besonderer Anregungsbedingungen bei der Emissionspektrometeranalyse zur Homogenisierung der Probe und damit zur Verbesserung von Reproduzierbarkeit und Genauigkeit der Analysen brachte ebenfalls keine befriedigenden Ergebnisse. Das zur Verbesserung der Bleiverteilung vereinzelt angewandte Ausschmieden der Stahlprobe wurde wegen des erheblichen Arbeits- und Zeitaufwandes nicht näher untersucht.

Drei weitere Möglichkeiten für eine Homogenisierung der Stahlproben sind: (i) das Zerspanen der Stahlprobe und Umschmelzen der Stahlspäne im Lichtbogenofen[7–12] oder Hochfrequenzofen[13,14], (ii) das Zerspanen der Stahlprobe und Brikettieren der Stahlspäne[15–21], (iii) das Zerspanen der Stahlprobe und Auflösen der Stahlspäne in Mineralsäure.

(i) *Umschmelzen.* Hier wird die Stahlprobe über den Querschnitt zerspant, die Späne umgeschmolzen und die so erhaltene Stahl-Knopfprobe für die Messung verwendet. Wie theoretisch zu erwarten war und experimentell bestätigt werden konnte, verdampft das Blei vollständig bei den notwendigen Schmelztemperaturen, weshalb das Umschmelzen hier nicht angewandt werden kann.

(ii) *Zerspanen und Brikettieren.* Hier wird die Stahlprobe über den Querschnitt zerspant, die Späne zu einem Brikett verpresst und das so erhaltene Stahlspäne-Brikett für die Messung verwendet. Diese Homogenisierungsmethode erwies sich für unseren Zweck als brauchbar und findet deshalb in der unten beschriebenen Analysenmethode Anwendung. Die verwendeten Späne sollen möglichst fein sein. Von den möglichen Spanarten Sägespäne, Hobelspäne, Frässpäne mit in der angegebenen Reihenfolge zunehmender Spangrösse sind deshalb die Sägespäne am geeignetsten. Bohrspäne sind dagegen ungeeignet, da die Späne über den gesamten Querschnitt der Stahlprobe genommen werden müssen. Deshalb werden hauptsächlich Sägespäne in unserem Laboratorium verwendet. Fräs- und Hobelspäne können auch für die Analyse verwendet werden, sie weisen aber gegenüber Sägespänen eine grössere Analysenstreuung auf. Auch muss für jede Spanart eine eigene Eichkurve benutzt werden, worauf noch in *Ergebnisse* eingegangen wird. Bei der einmal gewählten Spanform muss streng darauf geachtet werden, dass die Späne mit befriedigender Reproduzierbarkeit stets dieselbe Spangrösse und -form aufweisen.

(iii) *Zerspanen und Auflösen.* Hier wird die Spanprobe über den Querschnitt zerspant, die Späne in Mineralsäure gelöst und die so erhaltene Probelösung für die anschliessende Messung entsprechend weiter behandelt. Gegenüber den unter (i) und (ii) genannten Methoden erzielt man mit dieser Methode den grössten Homogenisierungseffekt. Über ihre Anwendung wird in Teil II[22] berichtet.

Behandlung der Probenoberfläche. Die für die starke Analysenstreuung erkannte zweite Ursache ist das Schleifen der Proben mit Korundschleifpapier. In-

folge eines Schmiereffektes wird das Blei durch das Schleifen über die Stahlprobenoberfläche verschmiert, wobei das Ausmass der Bleiverteilung auf der Probenoberfläche je nach Bleigehalt und Stahlqualität unterschiedlich und nicht reproduzierbar ist. Dies hat zu grosse Analysenstreuungen, Ausreisser und unbrauchbare Eichkurven zur Folge. Diese Schwierigkeit tritt sowohl bei kompakten Stahlproben als auch bei Stahlspäne-Briketts auf. Aus diesem Grunde werden die Brikett-Proben in der vorliegenden Analysenmethode nicht geschliffen.

Auswahl der Messmethode

Zum Vergleich wurden die Messungen bei allen Versuchen sowohl emissionspektrometrisch mit Hilfe des ARL-Vakuumspektrometers 31000 als auch röntgenspektrometrisch mit Hilfe des ARL-Mehrkanalröntgenspektrometers 72000 durchgeführt. Die Messergebnisse des Röntgenspektrometers wiesen dabei stets die geringere Streuung auf, weshalb die Messung in der vorliegenden Analysenmethode röntgenspektrometrisch durchgeführt wird.

Arbeitsvorschrift

Apparatur. Mehrkanalröntgenspektrometer 72000 von Applied Research Laboratories (Ecublens, Schweiz) mit angeschlossenem Digitalrechner Mincal 4 N (Dietz, Mülheim).

Messbedingungen. Pt/Rh-Röhre, 50 kV, 40 mA; gekrümmter ($r = 11$-in.) LiF-Kristall; Linie: Pb $L\alpha_1$, 1,175 Å; Messzeit: 20 s; Probe gedreht.

Presswerkzeug. Das für die Herstellung des Stahlspäne-Briketts verwendete Presswerkzeug ist aus Stahl hergestellt und besteht aus folgenden Teilen: Stempel (29,8 mm Dia. und 55 mm hoch), Ring (Matrize) (30,0 mm innen-Dia., 50 mm aussen-Dia. und 40 mm hoch) und Bodenplatte (65 mm Dia. und 20 mm dick). Stempel und Bodenplatte sind aus gehärtetem Stahl (z.B. Qualität X 210 Cr 12: 2,10% C, 0,3% Si, 0,3% Mn, 12,0% Cr), der Ring aus gewöhnlichem Stahl (z.B. Qualität St 33: 0,08% C, 0,40% Mn, 0,070% P, 0,050% S). Die Oberfläche der Bodenplatte, auf die der Ring mit den Spänen aufgesetzt wird, ist plangeschliffen und poliert.

Probenvorbereitung und Messung. Vor jedem Pressvorgang wird die obere, dem Späne-Brikett zugewandte Fläche der Presswerkzeug-Bodenplatte mit feinem Korund-Schleifpapier (Körnung 240 oder 320) von Hand abgeschliffen, um anhaftende Probenreste (besonders Blei!) vom vorhergehenden Pressvorgang zu entfernen und damit eine Verunreinigung der Brikettoberfläche zu vermeiden. Anschliessend wird der Presswerkzeug-Ring auf die Presswerkzeug-Bodenplatte gesetzt, mit einem Strichmass (Löffel) *ca.* 15 g Sägespäne abgemessen und in das Presswerkzeug gegeben. Mit einem Stab verteilt man die Späne auf gleiche Schütthöhe über die gesamte Oberfläche und verpresst sie mit Hilfe einer elektrohydraulischen Presse mit 90 t Druck zu einem Brikett von 30 mm Dia. Die Oberfläche des Briketts wird nicht geschliffen. Man belässt das Brikett im Ring des Presswerkzeuges, setzt es mit diesem in den Probenhalter ein, fährt dann die Probe in das Röntgenspektrometer ein, misst die Pb-Strahlung doppelt und verwendet den Mittelwert für die Auswertung.

ERGEBNISSE UND DISKUSSION

Trotz des hohen Pressdruckes weist das Stahlspäne-Brikett im Vergleich zur

kompakten Stahlprobe eine gewisse Porosität auf, die mit zunehmender Feinheit der Späne in der Reihenfolge Frässpäne (grob)—Hobelspäne (mittel)—Sägespäne (fein) abnimmt, während gleichzeitig der Messwert zunimmt. Gegenüber dem Sägespäne-Brikett beträgt die Zunahme der Porosität bzw. die Abnahme des Messwertes: beim Hobelspäne-Brikett 4,7% und beim Frässpäne-Brikett 13,3%. Für jede Spanart muss deshalb eine eigene Eichkurve verwendet werden (s. Tabelle I). Die Eichkurve ist im Bereich von 0,05–0,5% Pb linear.

TABELLE I

MESSWERTE DER EICHKURVEN

% Pb	Messwerte (mV)		
	Sägespäne	*Hobelspäne*	*Frässpäne*
0,05	316	301	274
0,10	632	602	548
0,20	1264	1205	1096
0,30	1896	1807	1644
0,40	2528	2409	2192

Wegen des Einflusses der Porosität auf das Analysenergebnis muss auch beim Verpressen der Stahlspäne beachtet werden, dass die Späne im Presswerkzeug über die gesamte Fläche die gleiche Schütthöhe aufweisen, um eine gleichmässige Kompaktheit bzw. Porosität über die gesamte Brikettoberfläche zu erreichen. Weiterhin ist sowohl bei der Wahl und Einhaltung konstanter Arbeitsbedingungen als auch bei der Beurteilung der Analysenergebnisse zu berücksichtigen, dass Ungleichmässigkeiten bei der Herstellung der Späne (Schwankungen der Spangrösse, Entmischungen der Späneproben) und die ungleichmässige Verteilung des Bleies im Stahl einen Einfluss auf die Analysenstreuung haben.

Mit zunehmender Feinheit der Späne nimmt die Analysenstreuung ab, weshalb die Verwendung von Sägespänen am zweckmässigsten ist. Die wiederholte Messung an einem Sägespäne-Brikett mit einem Gehalt von 0,243% Pb zeigte eine Messstreuung des Röntgenspektrometers von $s = \pm 0{,}0014\%$ Pb. Die Messung von 10 Briketts, die von einer Sägespäne-Probe mit einem Gehalt von 0,244% Pb hergestellt wurden, ergab eine Reproduzierbarkeit der Methode von $s = \pm 0{,}0036\%$ Pb. Vergleicht man die Analysenwerte der hier beschriebenen röntgenspektrometrischen Brikett-Methode mit jenen der nasschemischen photometrischen Methode[1–4] (Genauigkeit: in der Annahme, dass die photometrischen Werte richtig sind), so weist die Brikett-Methode für eine statistische Sicherheit von $S = 95\%$ ein Toleranzintervall bzw. einen Streubereich[1] von $T = \pm 0{,}010$–$0{,}015\%$ Pb auf.

Die beschriebene Methode eignet sich zur Bestimmung von 0,05–0,5% Pb in unlegiertem und niedrig legiertem Automatenstahl. Der Zeitbedarf für eine Einzelbestimmung (Herstellung eines Stahlspäne-Briketts *ca.* 45 s und Doppelmessung mit Auswertung *ca.* 105 s) beträgt 2,5 min. Im Vergleich zur photometrischen Methode[1–4] ermöglicht die vorliegende röntgenspektrometrische Methode eine erhebliche Verminderung des Zeit- und Arbeitsaufwandes. Die Bestimmungsgrenze[1]

($L_Q = 10\sigma$) des Verfahrens liegt unter den gewählten Arbeitsbedingungen bei $L_Q =$ 0,05% Pb, lässt sich aber bei Bedarf noch senken.

Die Methode wird in unserem Laboratorium seit fünf Jahren mit befriedigendem Erfolg eingesetzt, wobei täglich etwa 100–200 Bleibestimmungen durchgeführt werden.

Herrn K. H. Bohrer danke ich für die sorgfältige Durchführung zahlreicher Versuche bei der Entwicklung des Analysenverfahrens.

ZUSAMMENFASSUNG

Es wird eine Methode zur röntgenspektrometrischen Bestimmung von 0,05–0,5% Pb in Automatenstählen beschrieben. Die Stahlspäne werden brikettiert und das Brikett für die Analyse im Röntgenspektrometer verwendet. Die Methode weist eine Reproduzierbarkeit von $s = \pm 0{,}004\%$ Pb und eine Genauigkeit innerhalb $\pm 0{,}010$–$0{,}015\%$ Pb auf. Der Zeitbedarf für eine Einzelbestimmung beträgt 2,5 min.

SUMMARY

A method is described for the x-ray spectrometric determination of 0.05–0.5% Pb in free-cutting steels. Steel chips are briquetted and the briquette is used for analysis in the x-ray spectrometer. The method shows a reproducibility of $s = \pm 0.004\%$ Pb and an accuracy within ± 0.010–0.015% Pb. One determination requires 2.5 min.

LITERATUR

1 O. G. Koch und G. A. Koch-Dedic, *Handbuch der Spurenanalyse*, Springer, Berlin, 2 Aufl., 1974.
2 S. Meyer und O. G. Koch, *Arch. Eisenhütten.*, 29 (1958) 677.
3 *Handbuch für das Eisenhüttenlaboratorium, Bd. 2, Stahleisen*, Chemikerausschuss des Vereins Deutscher Eisenhüttenleute, Düsseldorf, 1966.
4 O. G. Koch, *Anal. Chim. Acta*, 62 (1972) 462.
5 K. Ohls, K. H. Koch und G. Becker, *Z. Anal. Chem.*, 250 (1970) 369.
6 K. Slickers und J. P. Vorpe, *Arch. Eisenhütten.*, 43 (1972) 819.
7 M. Humbert, *VIII. Colloquium Spectroscopicum Internationale Luzern (1959)*, Sauerländer und Co., Aarau, 1959, p. 140; *IX. Colloquium Spectroscopicum Internationale Lyon (1961), Tome 2*, Publications G.A.M.S., Paris 1961, p. 413.
8 W. A. Fahlbush, *Appl. Spectrosc.*, 17 (1963) 72.
9 P. Höller, *Z. Anal. Chem.*, 209 (1965) 259; *Arch. Eisenhütten.*, 37 (1966) 483.
10 L. A. Prince, A. J. Ellgren und T. J. DeGlopper, *Appl. Spectros.*, 20 (1966) 372.
11 P. König, K. H. Schmitz und P. Jaensch, *Arch. Eisenhütten.*, 40 (1969) 993.
12 P. Höller, K. Slickers und H. Mattner, *Stahl Eisen*, 89 (1969) 948.
13 N. Kemp. *Z. Anal. Chem.*, 240 (1968) 303.
14 J. Bruch und A. Wutschel, *Arch. Eisenhütten.*, 41 (1970) 433.
15 N. Stoll und A. Wagner, *C.N.R.M. Met. Rep.*, 5 (1965) 73.
16 S. Eckhard, *Z. Anal. Chem.*, 208 (1965) 241, 401.
17 S. Eckhard und R. Marotz, *Z. Anal. Chem.*, 215 (1966) 355; *XII. Colloquium Spectroscopicum Internationale, Exeter (1965)*, Hilger and Watts, London, 1965, p. 484.
18 W. Ramsden und D. F. Sermin, *XII. Colloquium Spectroscopicum Internationale, Exeter (1965)* Hilger and Watts, London, 1965, p. 489.

19 K. H. Koch und G. Becker, *Z. Anal. Chem.*, 231 (1967) 173.
20 K. H. Koch, L. Schmitz und W. Loose, *Hoesch Berichte aus Forschung und Entwicklung*, 3 (1968) 51.
21 H. Mayer, *Z. Anal. Chem.*, 249 (1970) 375.
22 O. G. Koch, submitted to *Anal. Chim. Acta.*

Analytica Chimica Acta, 76 (1975) 377–391

DISTRIBUTION COEFFICIENTS AND CATION-EXCHANGE BEHAVIOUR OF ELEMENTS IN HYDROBROMIC ACID–ACETONE MEDIA

F. W. E. STRELOW, M. D. HANEKOM, A. H. VICTOR and CYNTHIA ELOFF
National Chemical Research Laboratory, P.O. Box 395, Pretoria 0001 (South Africa)
(Received 7th November 1974)

The first systematic investigation of cation-exchange separations in aqueous hydrobromic acid probably is that published by Fritz and Garralda[1]. A considerably more complete survey of the aqueous hydrobromic acid system was later published by Nelson and Michelson[2]. The presence of organic solvents either decreases adsorption by enhancing complex formation or may increase adsorption by selective destruction of the hydration cloud of the cation in the external phase, thus preferentially facilitating entry of a certain cation into the resin phase. Organic solvents therefore add another dimension to ion-exchange separations. Korkisch and Klakl[3] have investigated the cation-exchange behaviour of 19 elements in hydrobromic acid with 8 different organic solvents. Unfortunately, the region of low acid and acetone concentration has not been covered, and no coefficients were determined at acid concentrations above 0.9 *M*. With acetone as the solvent, a considerably more complete survey including 54 cations and covering hydrobromic acid and acetone concentrations ranging from 0.1 to 3.0 *M* and from 0 to 95% respectively, has been carried out in this laboratory. The results are presented below. The elution behaviour and favourable conditions for some separations are selected out of the wealth of possible ones, for detailed discussion.

EXPERIMENTAL

Apparatus

A Perkin-Elmer 303 and a Zeiss PMQII instrument were used for atomic absorption and for spectrophotometric measurements, respectively. Borosilicate glass tubes of 20 mm i.d., with fused-in glass sinters of No. 2 porosity and a burette tap at the bottom and a B19 ground-glass joint at the top were used as columns.

Reagents

The resin used was the AG50W-X8 sulphonated polystyrene cation exchanger (Bio-Rad Laboratories, Richmond, California). Resin of 100–200-mesh particle size was used for batch equilibrations and of 200–400 mesh for column work.

Analytical-reagent grade chemicals were used whenever possible. Many of the rarer chemicals such as compounds of the platinum metals, germanium gallium, indium, scandium and niobium were obtained from Fluka A.G., Switzerland.

Standard solutions containing 5 exchange milliequivalents of the element per

10 ml of 2.50 *M* or 5 *M* hydrobromic acid were prepared by dissolving the bromides or the oxides. Sometimes the chlorides or nitrates were converted into the bromides by an ion-exchange process. Solutions of V(V), Mo(VI), W(VI), Se(IV), As(III) and As(V) were prepared by passing aqueous solutions of the ammonium or sodium salts through a cation-exchange column and washing with water. Hydrogen peroxide (1%) was added to solutions containing V(V), Mo(VI) and W(VI) and hydrobromic acid (2.5 *M*) to those of Se(IV), As(III) and As(V). Solutions of Sb(III) and Te(IV) were prepared by passing solutions of the sodium salts in 1 *M* hydrobromic acid through a long cation-exchange column and making the standard solution up to 2.5 *M* hydrobromic acid. Standard solutions of gold(III), the platinum metals and niobium(V) were prepared directly from the chlorides by dissolution in 2.5 *M* hydrobromic acid, and the niobium(V) solution also contained 1% hydrogen peroxide for stabilization. Standards of titanium(IV) were prepared from titanium(III) chloride solutions by oxidation with hydrogen peroxide. Solutions of lead were made up by dissoving the nitrate in distilled water and contained only 0.1 millimole of lead per 10 ml because of the limited solubility of lead bromide. Solutions of bismuth were prepared from the nitrate in 2.5 *M* hydrobromic acid and contained 0.5 millimole of bismuth per 10 ml. The presence of small amounts of chloride or nitrate in the equilibria of these elements was found to have only negligible effects on their adsorption.

Distribution coefficients

The coefficients were determined by equilibrating 250 ml of a solution containing 5-meq amounts of the elements with 2,500 g of AG50W-X8 resin in the hydrogen form, which had been dried at 60°C in a vacuum pistol with phosphorus pentoxide as drying agent. In the cases of W(VI), Mo(VI), Nb(V) and V(V), the equilibrium mixtures also contained 2.5 ml of 30% hydrogen peroxide. In a few cases, marked in the Tables, smaller amounts of the elements were used because of limited solubilities; in other cases a shorter equilibration time was used to reduce reaction of hydrogen peroxide with other components of the equilibrium mixtures. As given, 1 *M* hydrobromic acid containing 80% acetone means 50 ml of 5 *M* hydrobromic acid mixed with 200 ml of acetone. Volume changes on mixing were disregarded.

After equilibration for 24 h in a mechanical shaker at 25°C, the resin was separated from the aqueous phase by filtration, and the amounts of the elements in both phases were determined by appropriate analytical methods. From the results, weight equilibrium distribution coefficients

$$D = \frac{\text{amount of element in resin}}{\text{amount of element in solution}} \times \frac{\text{ml of solution}}{\text{grams dry resin}}$$

were calculated.

Distribution coefficients in 0.10, 0.20, 0.50, 1.00, 2.00 and 3.00 *M* HBr are presented in Tables I–VI, respectively. Coefficients for solutions containing no acetone are included for the sake of completeness because most of these coefficients are not available in the literature. When an element was already only very weakly absorbed from low acid concentrations, coefficients at higher acid concentrations were not determined except in a few very special cases such as gold(III).

TABLE I

DISTRIBUTION COEFFICIENTS IN 0.10 *M* HBr WITH VARIOUS AMOUNTS OF ACETONE

Element	*Percentage acetone*						
	0	*20*	*40*	*60*	*80*	*90*	*95*
Zr	$>10^4$	$>10^4$	$>10^4$	$>10^4$	>10	5.1	3.6
Th	$>10^4$	$>10^4$	$>10^4$	$>10^4$	$>10^4$	$>10^4$	$>10^4$
Hf	$>10^4$	$>10^4$	4100	111	61	23.8	22.9
La	$>10^4$	$>10^4$	$>10^4$	$>10^4$	$>10^4$	$>10^4$	$>10^4$
Ce(III)	$>10^4$	$>10^4$	$>10^4$	$>10^4$	$>10^4$	$>10^4$	$>10^4$
Gd	$>10^4$	$>10^4$	$>10^4$	$>10^4$	$>10^4$	$>10^4$	$>10^4$
Y	$>10^4$	$>10^4$	$>10^4$	$>10^4$	$>10^4$	$>10^4$	$>10^4$
Yb	$>10^4$	$>10^4$	$>10^4$	$>10^4$	$>10^4$	$>10^4$	$>10^4$
Sc	$>10^4$	$>10^4$	$>10^4$	$>10^4$	$>10^4$	$>10^4$	$>10^4$
Ga	$>10^4$	$>10^4$	$>10^4$	$>10^4$	$>10^4$	1037	5.9
Fe(III)	$>10^4$	$>10^4$	$>10^4$	$>10^4$	1620	27.7	3.6
Al	$>10^4$	$>10^4$	$>10^4$	$>10^4$	$>10^4$	9800	5700
Ba	5530	8630	$>10^4$	$>10^4$	$>10^4$	$>10^4$	$>10^4$
Pb[a]	6600	5260	4770	3470	11.7	6.1	3.0
Sr	2440	4210	9400	$>10^4$	$>10^4$	$>10^4$	$>10^4$
In(III)	2110	2750	2630	1050	10.1	1.8	2.0
Ca	1900	2970	6910	$>10^4$	$>10^4$	$>10^4$	$>10^4$
Co(II)	987	1820	4120	$>10^4$	$>10^4$	$>10^4$	429
Zn	933	1530	2690	974	24.1	2.5	2.0
Fe(II)	927	1330	3170	7280	3660	144	14.4
Mn(II)	917	1340	2790	4980	9200	5240	385
Ni(II)	877	1004	1260	2210	4130	4980	2720
Cu(II)	869	1475	3200	4480	186	2.2	1.4
Mg	825	1180	2530	6560	9900	8370	4900
V(IV)	583	973	2260	7300	$>10^4$	8840	2290
Be	577	631	1100	2090	2340	1770	1150
Ti(IV)[b]	573	1100	2260	5100	9800	$>10^4$	$>10^4$
Te(IV)	352	1280	Prec.	Prec.	93	2.1	1.5
Cr(III)	337	404	565	967	1380	1660	709
Cs	225	291	481	1120	2430	3030	2430
Cd	125	142	69	7.1	1.2	1.0	0.9
Rb	118	149	238	461	1070	1220	1080
K	95	124	216	437	885	1220	1060
Na	46.8	62	105	229	392	401	413
Li	29.9	35.4	56	86	160	236	260
Sn(IV)	Prec.	Prec.	Prec.	Prec.	13.2	2.3	1.5
Bi(III)[c]	Prec.	Prec.	8.3	1.1	0.8	0.6	0.6
Mo(VI)[b,d]	7.6	6.6	3.3	0.6	0.5	0.5	5.0
Au(III)	1.7	0.7	0.7	0.8	0.9	1.0	1.1
Ir(III)[d] (IV)	0.9	0.6	0.4	0.5	0.6	0.7	0.3
Rh(III)	0.8	0.9	0.9	0.7	0.7	0.6	0.6
Pt(IV)	0.6	0.6	0.6	0.6	0.6	0.5	0.5
Ge(IV)	0.4	0.4	0.4	0.4	0.5	5.7	11.2
W(VI)[b,d]	0.4	0.4	0.5	0.4	0.5	0.5	0.9
Tl(III)	0.3	0.4	0.3	0.2	0.3	0.3	0.3
Pd(II)	0.2	0.2	0.2	0.2	0.1	0.2	0.1
Hg(II)	<0.5	<0.5	<0.5	<0.5	<0.5	<0.5	(2.1)
As(III), As(V), Se(IV), Se(VI)	<0.5	<0.5	<0.5	<0.5	<0.5	<0.5	<0.5
Sb(III)	Prec.	Prec.	Prec.	Prec.	Prec.	<0.5	<0.5
V(V)[b,d]	Not reproducible because of partial reduction						

[a] 0.1 millimole. [b] 1 ml 30% H_2O_2 present. [c] 0.5 millimole. [d] 2-h equilibration.

TABLE II

DISTRIBUTION COEFFICIENTS IN 0.20 *M* HBr WITH VARIOUS AMOUNTS OF ACETONE

Element	*Percentage acetone*						
	0	*20*	*40*	*60*	*80*	*90*	*95*
Zr	$>10^4$	$>10^4$	$>10^4$	$>10^4$	9700	14.2	13.0
Th	$>10^4$	$>10^4$	$>10^4$	$>10^4$	$>10^4$	$>10^4$	$>10^4$
Hf	$>10^4$	$>10^4$	7530	6350	95	112	83
La, Ce(III), Gd, Y, Yb, Sc	$>10^4$	$>10^4$	$>10^4$	$>10^4$	$>10^4$	$>10^4$	$>10^4$
Ga	8840	$>10^4$	$>10^4$	$>10^4$	$>10^4$	124	3.5
Fe(III)	3720	5050	9460	$>10^4$	251	2.5	1.4
Al	3360	4220	8540	$>10^4$	$>10^4$	10^4	—
Ba	1980	2730	6000	$>10^4$	$>10^4$	$>10^4$	—
Pb(II)[a]	8840[e]	5860[e]	4020[e]	103	4.3	3.7	3.2
Sr	848	1300	3310	9800	$>10^4$	$>10^4$	$>10^4$
Ca	581	843	1860	4360	8820	6910	—
Co(II)	354	503	1010	2730	4160	2250	43.2
Zn	342	465	701	198	3.5	1.6	1.2
Mn(II)	336	458	859	1880	3160	2490	—
Cu(II)	334	500	996	1230	106	4.0	1.7
Fe(II)	314	472	858	1930	1470	91	—
Ni(II)	310	398	759	1490	2440	2020	776
In(II)	298	274	241	98	1.5	1.5	1.4
Mg	287	392	776	1790	3740	2600	—
Ti(IV)[b]	216	324	668	1460	3150	$>10^4$	$>10^4$
Be	212	253	371	599	823	584	—
V(IV)	197	265	488	1020	1940	1220	—
Cr(III)	120	147	262	507	880	458	—
Cs	113	142	239	522	1050	1040	972
Rb	70	93	144	362	495	679	542
K	54	70	122	228	488	468	463
Sn(IV)	Prec.	Prec.	Prec.	3930	1.9	1.5	1.3
Cd	35.4	13.3	5.3	1.7	1.0	0.9	0.8
Na	29.9	35.1	61	154	259	301	369
Te(IV)	21.7	56	Prec.	Prec.	2.5	2.2	1.7
Li	17.9	21.7	33.5	59	103	124	—
Mo(VI)[b,d]	17.3	14.9	6.5	1.6	0.6	4.9	8.7
Bi(III)[c]	4.0	1.5	0.9	0.7	0.7	0.6	0.6

[a–d] Footnotes as for Table I.

[e] Values probably too high because of precipitation.

Elution curves

Three multicomponent elution curves (Figs. 1–3) indicate how the systematic information contained in the Tables can be applied to develop analytical separation procedures. When possible, conditions were selected under which the distribution coefficient of the eluted element was less than 5 while those for the retained ones were above 50. It should be pointed out that a correction of about +1% acetone has to be applied to the coefficients in the Tables to make them applicable to column conditions, the reason being that the dry resin in a batch experiment takes up water from the external solution and lowers its water concentration by about 1%. A column is already in equilibrium with water.

TABLE III

DISTRIBUTION COEFFICIENTS IN 0.50 *M* HBr WITH VARIOUS AMOUNTS OF ACETONE

Element	*Percentage acetone*					
	0	*20*	*40*	*60*	*80*	*90*
Zr	$>10^4$	$>10^4$	$>10^4$	7800	102	33.3
Hf	$>10^4$	$>10^4$	$>10^4$	$>10^4$	$>10^4$	173
Th	$>10^4$	$>10^4$	$>10^4$	$>10^4$	$>10^4$	$>10^4$
La	1950	3120	9900	$>10^4$	$>10^4$	$>10^4$
Ce(III)	1850	2980	9600	$>10^4$	$>10^4$	$>10^4$
Gd	1390	2200	6290	$>10^4$	$>10^4$	$>10^4$
Sc	1050	1880	4320	$>10^4$	$>10^4$	$>10^4$
Yb	848	1380	3610	$>10^4$	$>10^4$	$>10^4$
Y	841	1350	3500	$>10^4$	$>10^4$	$>10^4$
Fe(III)	385	517	929	1440	5.7	1.9
Ba(II)	378	635	1460	5270	9660	$>10^4$
Al	375	522	1080	3100	5660	3050
Ga	368	508	1250	2440	67	4.0
Sr	207	248	584	1610	4520	$>10^4$
Ca	127	180	344	826	1990	3530
Co(II)	79	113	206	448	605	30.1
U(VI)	76	101	179	370	504	486
Mn(II)	76	100	173	349	485	99
Cu(II)	76	98	153	140	2.6	1.5
Zn	76	91	83	8.8	1.8	1.3
Fe(II)	74	102	176	371	217	2.0
Ni(II)	72	102	185	408	535	279
Mg	67	87	156	319	521	375
Be	47.9	55	82	129	151	116
Ti(IV)[b]	46.7	61	104	324	1850	3500
V(IV)	46.3	59	96	184	274	196
Cs	41.6	53	91	164	388	381
Pb(II)	40.5	30.5	10.7	8.7	5.7	5.3
Sn(IV)	36.6	967	31.6	2.4	1.4	1.2
Rb	32.2	39.3	69	122	245	230
K	27.6	34.0	53	101	193	198
Cr(III)	25.9	28.6	45.3	94	147	89
In	24.8	21.8	18.6	3.6	1.3	1.1
Na	13.9	15.0	25.7	43.9	78	90
Li	7.7	9.8	14.0	24.6	44.4	57
Mo(VI)[b,d]	6.2	7.5	8.8	7.3	4.6	0.9
Te(IV)	5.4	8.5	7.8	5.7	1.3	0.8
Cd	1.9	1.3	1.1	1.0	0.8	0.8
Au(III)	1.3	0.9	0.8	0.6	0.4	0.4
Bi(III)[c], Tl(III), Hg(II), Rh(III), Pd(II), Ir(III), Pt(IV), Se(IV), Se(VI), Ge(IV), As(III), As(V), Sb(III), W(VI)[b,d]	<1.0	<1.0	<1.0	<1.0	<1.0	<1.0
V(V)[b]	Not reproducible because of partial reduction					

[a–d] Footnotes as for Table I.

TABLE IV

DISTRIBUTION COEFFICIENTS IN 1.0 *M* HBr WITH VARIOUS AMOUNTS OF ACETONE

Element	*Percentage acetone*				
	0	*20*	*40*	*60*	*80*
Zr	$>10^4$	$>10^4$	$>10^4$	$>10^4$	129
Hf	5480	$>10^4$	$>10^4$	$>10^4$	$>10^4$
Th	2410	4120	$>10^4$	$>10^4$	$>10^4$
La	289	427	994	3610	$>10^4$
Ce(III)	278	414	975	3480	$>10^4$
Gd	220	312	729	2420	7290
Sc	170	284	687	2820	$>10^4$
Yb	161	231	464	1390	2930
Y	155	214	448	1340	3860
Ba	111	186	429	1500	5270
Ga	80	94	190	553	3.3
Fe(III)	75	89	137	113	3.6
Al	63	97	163	385	671
Sr	57	84	165	428	1620
Ca	40.8	57	107	242	812
Co(II)	26.6	35.5	53	101	71
U(VI)	26.1	38.0	64	130	65
Mn(II)	23.3	29.0	49.8	95	103
Fe(II)	21.5	31.3	52	90	5.1
Cu(II)	20.9	26.6	37.0	37.0	1.6
Ni(II)	20.4	27.0	51	104	124
Zn	20.3	20.2	6.4	1.9	1.5
Mg	20.0	24.6	64	102	135
Cs	19.5	25.1	39.9	71	131
Rb	14.8	18.7	32.2	55	109
V(IV)	13.9	17.4	26.0	54	77
K	13.7	16.4	28.2	50	98
Be	13.5	15.0	21.8	34.8	42.1
Ti(IV)	13.2	15.6	32.4	159	751
Cr(III)	7.9	10.7	16.9	30.6	43.8
Na	6.9	8.5	14.2	25.7	41.3
Pb(II)[a]	5.9	9.1	7.1	6.0	5.1
Li	3.8	4.6	6.6	11.4	20.6
In(III)	3.8	3.5	3.1	1.9	1.1
Te(IV)	1.5	2.6	2.1	1.3	0.6

[a] 0.1 millimole.

Hg(II), Cd(II), In(III), Zn(II), Cu(II), and Co(II). A solution containing about 0.5 mmole of each element in about 50 ml of 0.1 *M* nitric acid was passed through a column (2.0 × 19 cm) of 60 ml of AG50W-X8 resin (200–400 mesh, hydrogen form). The elements were washed onto the resin with 0.1 *M* nitric acid and then eluted with the following sequence of reagents: 200 ml of 0.10 *M* HBr for Hg(II); 200 ml of 0.20 *M* HBr in 50% acetone for Cd; 250 ml of 0.80 *M* HBr in 20% for In; 250 ml of 0.20 *M* HBr in 80% acetone for Zn; 200 ml of 0.50 *M* HBr in 85% acetone for Cu(II); and 250 ml of 2.00 *M* HCl for Co(II). The solution was always allowed to drain to the level of the resin bed before the eluting agents were

TABLE V

DISTRIBUTION COEFFICIENTS IN 2.0 *M* HBr WITH VARIOUS AMOUNTS OF ACETONE

Element	*Percentage acetone*				
	0	*20*	*40*	*60*	*70*
Zr	661	1350	4240	6690	146
Th	341	460	1560	$>10^4$	$>10^4$
Hf	295	710	2790	10^4	$>10^4$
La	55	80	171	597	1900
Ce(III)	53	77	161	563	1610
Gd	39.8	55	119	430	977
Ba	35.0	61	157	655	1450
Sc	34.8	63	141	639	2520
Y	29.1	39.5	80	238	487
Yb	27.8	38.9	72	214	394
Sr	17.3	21.7	49.6	162	740
Ga	14.2	18.4	33.7	10.3	5.3
Al	12.8	15.5	26.9	60	94
Ca	12.5	16.8	32.4	79	186
Fe(III)	11.9	15.5	15.4	5.6	3.2
U(VI)	9.4	13.1	25.2	49.6	51
Co(II)	9.2	12.2	17.8	25.0	13.9
Ni(II)	7.6	8.6	13.4	20.0	25.4
Cs	7.3	8.4	12.8	22.0	26.8
Rb	6.9	8.8	13.9	26.5	28.6
Mn(II)	6.8	8.4	12.3	17.8	22.6
K	6.5	8.6	12.3	21.8	33.0
Fe(II)	6.3	7.6	11.7	15.5	4.5
Cu(II)	5.7	5.9	3.4	1.2	1.0
Mg	5.5	7.0	11.1	20.9	27.1
V(IV)	4.9	5.9	8.8	16.1	22.4
Zn	3.9	2.0	1.3	1.2	1.2
Be	3.6	4.7	6.5	11.0	13.2
Cr(III)	3.2	4.2	5.5	9.2	12.7
Ti(IV)	3.0	3.7	8.4	39.4	103
Na	2.8	3.4	4.4	8.1	13.9
Li	2.0	2.3	3.1	5.3	7.7

changed. The maximum flow rate attainable by gravity flow with a solution head of about 25–30 cm was maintained throughout, provided that it was not faster than about 3.5 ml min^{-1}. At low acetone concentrations, flow rates were considerably slower, about 1.5–2.0 ml min^{-1} (0.5–0.7 ml min^{-1} per cm^2), while at high acetone concentrations the flow rate had to be controlled by the stopcock. Aliquots of 25 ml were taken with an automatic fractionator, and the amounts of the elements in the fractions were determined by appropriate analytical methods. The experimental curve is presented in Fig. 1.

Bi(III), Pb(II), Zn(II), Fe(III) and Mn(II). These elements were adsorbed from a solution containing about 0.5 millimole of each element in 50 ml of 0.2 *M* nitric acid containing 30% of acetone. The column was of the size and type described above, but had been equilibrated with 50 ml of 0.2 *M* nitric acid containing 30%

TABLE VI

DISTRIBUTION COEFFICIENTS IN 3.0 *M* HBr WITH VARIOUS AMOUNTS OF ACETONE

Element	*Percentage acetone*			
	0	*20*	*40*	*60*
Zr	159	232	751	81
Th	151	230	1760	5780
Hf	36.3	97	482	3210
La	22.4	33.9	81	395
Ce(III)	20.6	31.5	77	371
Ba	19.5	36.8	120	530
Sc	16.0	32.6	97	799
Gd	14.8	22.7	56	253
Y	10.9	15.6	36.4	126
Yb	10.4	13.5	29.2	98
Sr	9.6	14.1	25.6	82
Ca	7.0	9.1	16.8	66
Ga	6.1	9.0	12.1	6.8
Al	6.0	6.4	10.9	23.1
Rb	4.6	5.5	7.0	10.5
K	4.2	5.4	8.7	13.1
Cs	4.1	4.7	6.8	10.8
Ci(II)	3.9	5.0	7.1	12.6
Mn(II)	3.8	4.2	5.9	8.1
Tl(I)	3.6	Prec.	Prec.	0.5
Fe(III)	3.4	4.0	4.9	2.9
Fe(II)	3.4	3.9	5.3	6.9
Ni(II)	3.3	3.6	5.0	7.6
Cu(II)	3.1	2.0	0.8	0.7
Au(III)	3.1	0.3	0.2	0.2
Mg	2.9	3.5	5.4	7.2
V(IV)	2.8	3.5	5.3	9.7
Be	2.2	2.4	2.9	3.9
Cr(III)	1.7	2.3	3.3	6.0
Na	1.7	2.2	2.7	5.1
Ti(IV)	1.6	2.3	3.9	29.6
Li	1.6	1.8	2.4	4.7
Zn	1.2	1.1	1.0	0.9

of acetone. The following sequence of reagents was used for the elution of the elements: 200 ml of 0.20 *M* HBr in 40% acetone for Bi(III); 350 ml of 0.50 *M* HBr in 40% acetone for Pb(II); 300 ml of 0.50 *M* HBr in 65% acetone for Zn; 300 ml of 0.50 *M* HBr in 90% acetone for Fe(III); and 250 ml of 2.00 *M* HBr for Mn(II). The flow rates were as described above. The experimental elution curve is presented in Fig. 2.

Au(III), Cd(II), In(III), Ga(III), Al(III) and Sc(III). A solution containing about 0.5 mmole of each element in 25 ml of 0.1 *M* HBr was passed through a column of the size and type described above and equilibrated with 50 ml of 0.1 *M* HBr. The eluate was taken from the beginning of the adsorption step, and the following sequence was used for the elution of the elements: 200 ml of 0.10 *M* HBr

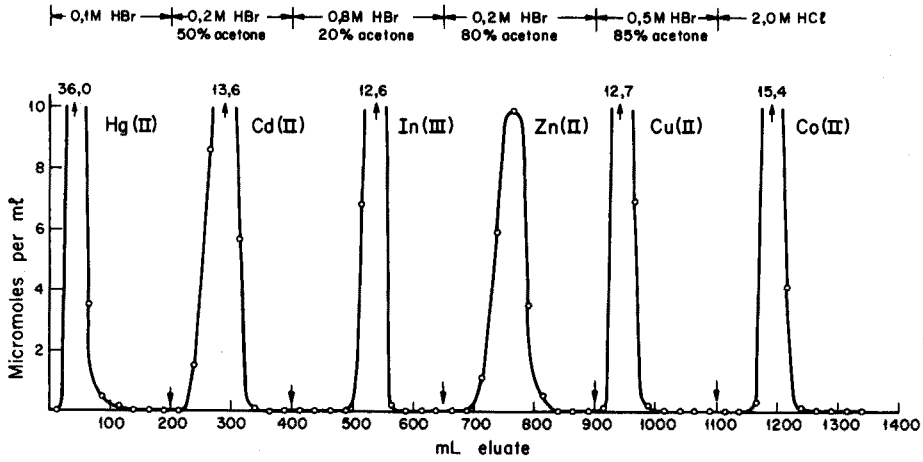

Fig. 1. Elution curve for Hg(II)–Cd–In–Zn–Cu(II)–Co(II). Column of 60 ml (19 × 2.0 cm) AG50W-X8 resin, 200–400 mesh, H^+-form. Flow rate 2.0±0.5 ml min^{-1} for Cd and In; 3.0±0.5 ml min^{-1} for other elements.

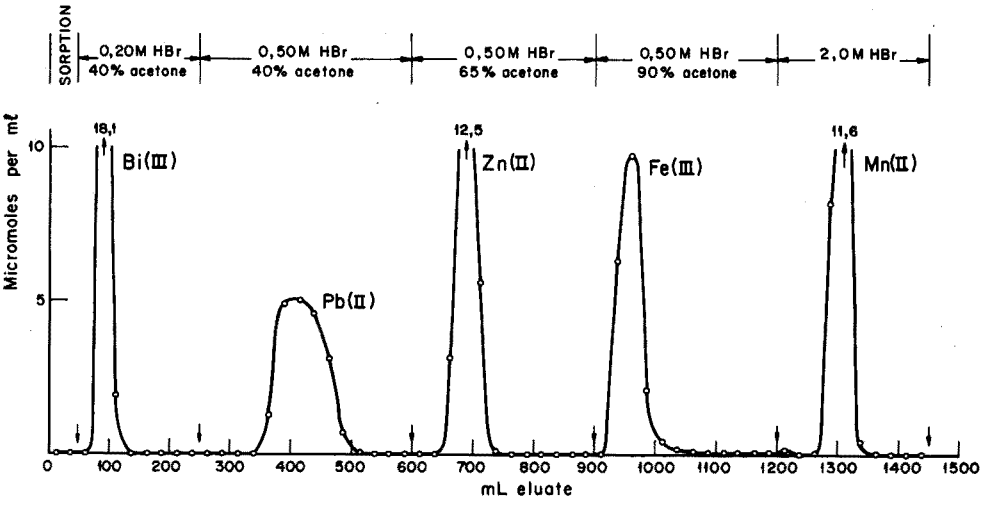

Fig. 2. Elution curve for Bi(III)–Pb(II)–Zn(III)–Fe(III)–Mn(II). Column of 60 ml (19 × 2.0 cm) AG50W-X8 resin, 200–400 mesh, H^+-form. Flow rate 2.0±0.5 ml min^{-1} for Bi(III) and Pb(II); 3.0±0.5 ml min^{-1} for other elements.

for Au(III); 200 ml of 0.20 *M* HBr in 50% acetone for Cd; 200 ml of 0.50 *M* HBr in 60% acetone for In; 250 ml of 0.50 *M* HBr in 90% acetone for Ga; 300 ml of 3.00 *M* HBr in 30% acetone for Al; 300 ml of 4.00 *M* HCl for Sc. The experimental elution curve is presented in Fig. 3.

RESULTS AND DISCUSSION

In accordance with the mass action law, the cation-exchange distribution

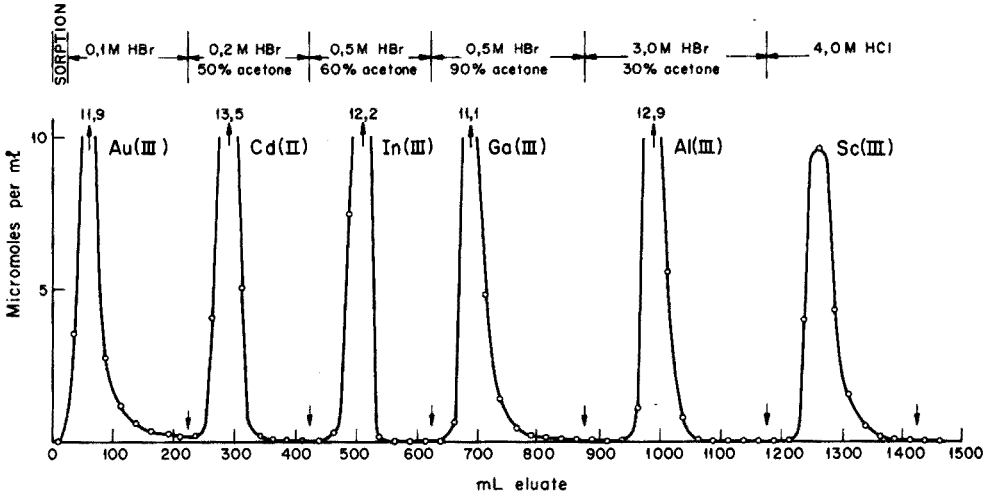

Fig. 3. Elution curve for Au(III)–Cd–In–Ga–Al–Sc. Column of 60 ml (19 × 2.0 cm) AG50W-X8 resin, 200–400 mesh, H^+-form. Flow rate 2.0±0.5 ml min^{-1} for Cd, In and Al: 3.0±0.5 ml min^{-1} for other elements.

coefficients decrease with increasing hydrogen ion concentration in the region 0.10–3.00 *M* hydrobromic acid. They increase with increasing acetone concentration until the hydration field around the cation is weakened enough to allow replacement of the water ligands in the co-ordination shell by bromide anions. This causes a sudden decrease in the values of the coefficients, often very much below their value in pure aqueous acid. In hydrobromic acid some elements such as Cd and Pb(II) show this sudden decrease at a lower acetone concentration than in the corresponding solutions of hydrochloric acid[4]; others such as In, Zn, Co(II) and U(VI) show it at a higher acetone concentration. Ion pairs such as Cd–In[5] (see Fig. 1), Pb(II)–Zn (see Fig. 2) and Cu(II)–U(VI)[6], which have very similar distribution coefficients and cannot be separated in hydrochloric acid–acetone mixtures, are easily separated in hydrobromic acid–acetone.

Alkali metals

Distribution coefficients increase with acetone concentrations but considerably less than in corresponding HCl–acetone[4] and HCl–ethanol[7] mixtures. Separation factors for the Na/Li pair are less favourable than in hydrochloric acid–acetone, but reasonable separations with a separation factor of 2.2 are still possible by using 1.0 *M* hydrobromic acid in 60 or 65% acetone as eluting agent. The best separation for this pair on a sulphonated polystyrene resin seems to be that using 1.0 *M* hydrochloric acid in 80% methanol as eluting agent[8]. The separation factor in this case is 5.3, and the column kinetics are very good.

The alkali metals as a group can easily be separated from Cu(II), Zn, Cd, In, Ga, Sn(IV), Pb(II), Au(III), Hg(II) and several other elements, by eluting these elements with 0.50 *M* hydrobromic acid in 90% acetone, while the alkali metals are retained. Iron(III) is also eluted but shows considerable tailing. Mn(II), Co(II) and U(VI), which can be eluted and separated from the alkalies in hydrochloric acid–

acetone mixtures[4] and also Ni(II), Al, Ti(IV), the alkaline earths, Zr, Hf, Th, Sc, Y and the lanthanides, accompany the alkali metals, but can be separated by eluting the alkali metals with 0.50 *M* nitric acid[9,10].

Alkaline earths

The separation of calcium from Mg, Be, Fe(III), Mn(II), Cu(II), Ni(II), Zn, Cd, In, Ga and some other elements in 3.0 *M* hydrobromic acid containing 60% acetone is as good as in the corresponding HCl–ethanol[11] and HCl–acetone[4] mixtures. The heavy alkali metals are eluted more easily and their separation from calcium is improved in 3.0 *M* hydrobromic acid containing 60% acetone, but separation of Al and Ti(IV) from calcium requires a lower acetone concentration (about 50%) and has lower separation factors. Barium can be separated from Sr, Ca, Mg, Al, Fe(III), Ti(IV) and most other elements in 3.0 *M* hydrobromic acid containing 20% acetone, but separation factors for the most critical elements are also slightly lower than in the corresponding HCl–ethanol[12] and HCl–acetone[4] mixtures, though the separations are still quite satisfactory.

Cd, In

These elements have very similar distribution coefficients in hydrochloric acid–acetone, and no separation is possible[4,5]. In hydrobromic acid–acetone the coefficients for cadmium are considerably lower and those for indium considerably higher than in the corresponding HCl–acetone mixtures. Excellent separations with a separation factor of about 60 can be carried out by eluting cadmium with 0.2 *M* hydrobromic acid in 50% acetone[5]. Elements such as Bi(III), Hg(II), Au(III) and the platinum metals accompany cadmium. Indium can then be eluted selectively with 0.5 *M* hydrochloric acid in 30% acetone, while Zn, Pb(II), Ga, Fe(III), Cu(II) and many other elements are still retained[13].

Pb, Zn

These elements also have very similar cation-exchange behaviour in hydrochloric acid–acetone and cannot be separated, while in hydrobromic acid–acetone a good separation is possible by eluting lead with 0.5 *M* hydrobromic acid in 40% acetone while zinc is retained (Fig. 2). The separation factor is about 8 and considerably higher than that in aqueous hydrobromic acid. Zinc can then be eluted with 0.5 *M* hydrobromic acid in 65% acetone (Fig. 2), while Fe(III), Ga, Cu(II), Ni(II), V(IV), Mg and many other elements are still strongly retained.

Al, Ga, In, Tl(III)

In comparison with hydrochloric acid–acetone mixtures, In and Ga are still absorbed at higher acetone concentrations in hydrobromic acid. Quite satisfactory separations are obtained by the elution sequence: 0.10 *M* HBr in 60% acetone for Tl(III); 0.5 *M* HBr in 60% acetone for In; 0.5 *M* HBr in 90% acetone for Ga, and 3.0 *M* HBr in 30% acetone for Al. Gallium shows some tailing and requires a fairly large elution volume for complete recovery, but the peaks of Tl(III) and In are very sharp and that of Al is also quite satisfactory. Elution with 0.10 *M* hydrobromic acid in 60% acetone can also be used for the separation of Tl(III) from Pb(II), Zn, Cu(II), Co(II) and many other elements. Only Hg(II), Cd, Bi(III),

Au(III), the platinum metals and elements such as W(VI) which do form oxy-anions accompany Tl(III). Indium together with Cd, Sn(IV) and Pb(II) can be eluted with 0.5 *M* hydrobromic acid in 60% acetone and separated from Cu(II), Co(II), Mn(II), Fe(III) and many other elements which are retained. Furthermore, aluminium can be separated from Be, Cu(II), Ga, In, Zn, Cd, Hg(II), Sn(IV), Bi(III) and some other elements by eluting these elements with 2.0 *M* hydrobromic acid in 70% acetone.

Au(III), Pt(IV), Pd(II), Rh(III), Ir(III+IV)

Gold(III) shows very strong tailing when eluted with aqueous 0.1 *M* hydrobromic acid but can be very effectively eluted with 0.1 *M* hydrobromic acid containing 80 or 90% acetone. The other elements can be eluted with aqueous 0.1 *M* hydrobromic acid or with HBr–acetone mixtures and separated from most other elements.

Cu(II), U(VI)

The distribution coefficients of these elements are very similar in hydrochloric acid–acetone mixtures. In 0.5 *M* hydrobromic acid with 85% acetone, copper(II) can be eluted and separated from uranium(VI) with a separation factor larger than 200, because the distribution coefficients of uranium(VI) show almost no signs of complex formation and with increasing acetone concentration follow a pattern similar to that of Mg or Ni(II). By combining and alternating HCl–acetone and HBr–acetone elution steps, very selective separations of either copper(II)[6] or uranium(VI) from practically all other elements of the periodic table can be obtained, excepting only those which form precipitates or hydrolyse in the eluting agent. For the separation of uranium(VI) from others, a 4% cross-linked resin has to be used in order to eliminate the fairly strong tailing[14].

Zn, Cd, Hg(II)

These elements can be separated by the elution sequence: 0.1 *M* HBr in 20% acetone for Hg(II); 0.2 *M* HBr in 50% acetone for Cd; and 0.5 *M* HBr in 65% acetone for Zn. Elements such as Cu(II), Co(II), Mn(II), Ni(II), Fe(III), U(VI), V(IV), Ga, Be, Mg, Ca, Sr, Ba, Al, the alkali metals, Sc, Y, the lanthanides, Zr, Hf, Ti(IV) and Th are still retained by the column and can be separated from zinc. Indium accompanies zinc.

Bi(III), Sn(IV)

Tin(IV) has considerably higher coefficients in 0.5 *M* hydrobromic acid containing acetone than in the corresponding HCl–acetone mixtures. Separation can be obtained by eluting bismuth(III) with 0.5 *M* hydrobromic acid in 20% acetone while tin(IV) is retained. Tin can be eluted with 0.5 *M* hydrobromic acid in 60% acetone, while Fe(III), Cu(II), Ni(II), Co(II), Mn(II) and many other elements are retained, but elution of tin(IV) with HCl–acetone mixtures is more effective. Bismuth can also be eluted quickly and effectively with 0.2 *M* hydrobromic acid in 40% acetone and separated from lead(II) with a very large separation factor (Fig. 2). Almost all other elements are retained together with lead(II), but cadmium accompanies bismuth(III). With 0.1 *M* hydrobromic acid in 45% acetone, elution of bismuth(III) is considerably slower, but separation from cadmium is possible.

Zr, Hf, Th, Sc, Y and the lanthanides

Distribution coefficients of these elements are comparable to those in HCl–acetone mixtures[4], and separations can be obtained under similar conditions. Zr and Hf show a sharp decrease in the values of their coefficients at the highest acetone concentrations probably because of hydrolysis. All the above elements can be separated as a group from Al(III), Ti(IV), Fe(III), Mg, Mg, Be, Cu(II) and many other elements by eluting these elements with 3.0 *M* hydrobromic acid in 40% or 45% acetone, while zirconium etc. are retained. Because aluminium shows some tailing and some other elements also have slow exchange rates, the separations are considerably improved by using resin of small particle size and the application of slow flow rates. Ca, Sr and Ba accompany the zirconium group partially or completely.

Fe(III)

Iron(III) has a favourable distribution coefficient for elution in 0.5 *M* hydrobromic acid containing 90% acetone, but shows very heavy tailing (Fig. 2). Hydrobromic acid–acetone mixtures at low concentrations of acid seem to be much less suitable for eluting iron(III) than HCl–acetone mixtures, and iron(III) can spread over several elution fractions when its strong tendency to tailing in hydrobromic acid–acetone is not taken into account when planning a separation procedure.

Ge(IV), Se(IV), Te(IV), As(III), Sb(III), Nb(V), Ta(V)

Ge(IV), Se(IV) and As can be eluted with 0.1 *M* aqueous hydrobromic acid and separated from most other elements. Only Au(III), Hg(II) and the platinum metals are quantitatively eluted; Mo(VI), W(VI), V(V) and Bi(III), depending on the amounts present, can be partially or quantitatively eluted. Ta(V) and Sb(III) tend to form insoluble compounds in aqueous 0.1 *M* hydrobromic acid and also in its mixtures with acetone, but antimony(III) can be eluted with 0.1 *M* hydrobromic acid in 90% acetone or with 0.5 *M* hydrobromic acid in 80% acetone. Tellurium(IV) is strongly adsorbed from aqueous 0.1 *M* hydrobromic acid and 0.1 *M* hydrobromic acid in acetone up to 80%, but can be eluted with 0.2 *M* hydrobromic acid in 90% acetone. Niobium(V) tends to precipitate in hydrobromic acid solutions containing acetone and elution with aqueous 0.1 *M* hydrobromic acid containing hydrogen peroxide is very prolonged. Aqueous 0.5 *M* hydrobromic acid containing peroxide is unstable. A reasonably fast elution can be obtained with aqueous 0.25 *M* sulphuric acid containing hydrogen peroxide.

V(V), Mo(VI), W(VI)

Vanadium(V) is unstable in hydrobromic acid–acetone solutions containing hydrogen peroxide and reduction to V(IV) takes place at a much faster rate than in HCl–acetone solutions. Distribution coefficients and column behaviour are not reproducible. Molybdenum(VI) solutions in hydrobromic acid–acetone containing hydrogen peroxide also show a time-dependent behaviour. Distribution coefficients increase slowly and are not easily reproducible. Elution is possible with fresh solutions of 0.1 *M* hydrobromic acid in 80 or 90% acetone containing hydrogen peroxide. Tungsten(VI) can be eluted with fresh solutions of 0.1 *M* hydrobromic acid containing hydrogen peroxide at all acetone concentrations. Generally all hydrobromic acid

solutions containing peroxide are considerably less stable than the corresponding hydrochloric acid solutions.

Co(II), Mn(II), Ni(II), V(IV)

All four elements show trends in their distribution coefficients similar to those of magnesium; indications of complex formation at high acetone concentration, as shown very distinctly in HCl–acetone[4], by Co(II) and Mn(II), are only minimal. Copper(II) can easily be separated by elution with 0.5 *M* hydrobromic acid in 85% acetone while the above elements are retained. The separation factor for the Cu/Co pair is about 200 as compared with a factor of about 18 in HCl–acetone[15]. Many other elements such as Zn, Pb(II), Cd, Hg(II), Sn(II) and In are eluted together with copper(II).

Pb(II)

Distribution coefficients of lead(II) in hydrobromic acid or hydrobromic acid–acetone mixtures are considerably lower than those in hydrochloric acid–acetone mixtures. Though the amounts of lead which can be separated are limited by the limited solubility of lead bromide, good separations are possible. Lead(II) can be eluted with 0.5 *M* hydrobromic acid in 40% acetone (Fig. 2) and separated from elements such as Zn, Cu(II), Fe(III), Ga, Co(II), Mn(II), Mg, Ca and others which are retained.

Ti(IV)

The distribution coefficient pattern of titanium(IV) is very similar to that in hydrochloric acid–acetone mixtures[4]. Excellent separations are possible from bromide complex forming elements such as Cu(II), Zn, Pb(II), Cd, In, Sn(IV) and Bi(III) by eluting these with 1.0 *M* hydrobromic acid in 60% acetone while titanium(IV) is retained. Titanium(IV) can be eluted with 1.25 *M* hydrobromic acid in 20% acetone and separated from elements such as Al, Ga, Fe(III), Ca, Sr, Ba, Sc, Y, the lanthanides, Zr, Hf and Th, which are retained. Separation of titanium(IV) from most of these elements, except Sc, Zr and Hf, is better when titanium(IV) is eluted with 0.5 *M* sulphuric acid containing hydrogen peroxide[16].

Cr(III)

The behaviour of this element is similar to that described for hydrochloric acid–ethanol solution[7], but the overall distribution coefficients are considerably lower than those in HCl–ethanol[7] or HCl–acetone[4]. Apparently chromium is present in the equilibrium mixtures preferentially as the $[CrBr_2(H_2O)_4]^+$ species and this is about as strongly adsorbed as an alkali metal.

Conclusions

The hydrobromic acid–acetone system offers a large number of attractive possibilities for separations. Some of these cannot be carried out in mixtures of hydrochloric acid with acetone or with other organic solvents. Examples are the Pb(II)–Zn, Cd–In and Cu(II)–U(VI) ion pairs, which can be separated very well in hydrobromic acid–acetone. Especially useful for obtaining very selective separations for special elements is a procedure combining alternate elution with hydro-

bromic acid–acetone and hydrochloric acid–acetone in cases where the elements to be separated have different places in the selectivity sequence in the two eluting agents. Such cases have been described for the selective separation of uranium(VI)[14] and of copper(II)[6] from other elements. General elution behaviour, advantages and disadvantages of hydrobromic acid–acetone eluting agent are very similar to those described for hydrochloric acid–acetone[4]. The major difference is that hydrobromic acid at higher concentrations is much more easily oxidized to bromine by reagents such as peroxide or nitrate. This has to be taken into account in planning separation procedures.

SUMMARY

Cation-exchange distribution coefficients with Bio-Rad AG50W-X8, a sulphonated polystyrene cross-linked with divinylbenzene are presented for 54 cations in hydrobromic acid–acetone media, ranging from 0.1 to 3.0 *M* acid and 0 to 95% acetone. The elements are arbitrarily arranged according to their coefficients in aqueous hydrobromic acid. Some possible separations are pointed out and aspects of the elution behaviour of various elements are discussed. The versatility of hydrobromic acid–acetone mixtures as eluting agents for cation-exchange separations are demonstrated by sequential elution of the mixtures Hg(II), Cd, In, Zn, Cu(II) and Co(II); Bi(III), Pb, Zn, Fe(III) and Mn(II); and Au(III), Cd, In, Ga, Al and Sc.

REFERENCES

1 J. S. Fritz and B. B. Garralda, *Anal. Chem.*, 34 (1962) 102.
2 F. Nelson and D. C. Michelson, *J. Chromatogr.*, 25 (1966) 414.
3 J. Korkisch and E. Klakl, *Talanta*, 16 (1969) 377.
4 F. W. E. Strelow, A. H. Victor, C. R. van Zyl and Cynthia Eloff, *Anal. Chem.*, 43 (1971) 870.
5 F. W. E. Strelow, A. H. Victor and C. H. S. W. Weinert, *Anal. Chim. Acta*, 69 (1974) 105.
6 F. W. E. Strelow, C. H. S. W. Weinert and M. D. Boshoff, *J. S. Afr. Chem. Inst.*, 26 (1973) 118.
7 F. W. E. Strelow, C. R. van Zyl and C. J. C. Bothma, *Anal. Chim. Acta*, 45 (1969) 81.
8 F. W. E. Strelow, C. H. S. W. Weinert and T. N. van der Walt, *Anal. Chim. Acta*, 71 (1974) 123.
9 F. W. E. Strelow, J. H. J. Coetzee and C. R. van Zyl, *Anal. Chem.*, 40 (1968) 196.
10 F. W. E. Strelow, F. von S. Toerien and C. H. S. W. Weinert, *Anal. Chim. Acta*, 50 (1970) 399.
11 F. W. E. Strelow and C. R. van Zyl, *Anal. Chim. Acta*, 41 (1968) 529.
12 F. W. E. Strelow, *Anal. Chem.*, 40 (1968) 929.
13 F. W. E. Strelow, C. H. S. W. Weinert and T. N. van der Walt, *Talanta*, 21 (1974) 1183.
14 F. W. E. Strelow and C. H. S. W. Weinert, *Talanta*, 20 (1973) 1127.
15 F. W. E. Strelow and A. H. Victor, *Anal. Chim. Acta*, 59 (1972) 389.
16 F. W. E. Strelow, *Anal. Chem.*, 35 (1963) 1279.

Analytica Chimica Acta, 76 (1975) 393–399

DETERMINATION OF CADMIUM, COPPER AND LEAD IN NATURAL WATERS AFTER ANION-EXCHANGE SEPARATION

J. KORKISCH and A. SORIO

Institute for Analytical Chemistry, Analysis of Nuclear Raw Materials Division, University of Vienna, Währingerstrasse 38, A-1090 Vienna (Austria)

(Received 16th December 1974)

In connection with environmental studies concerning the distribution of trace constituents in natural waters, it is frequently necessary to determine very low concentrations of elements (in the p.p.b. range) such as cadmium, lead and copper. For this purpose, methods based on atomic absorption spectrometry are most useful, especially when employed after preliminary enrichment and separation of the trace elements from the water.

Most of the techniques which are currently used to preconcentrate cadmium, lead and copper are based on liquid–liquid extraction of suitable complexes of these elements; after their extraction the atomic absorption measurements are carried out directly in the organic extracts[1–8].

Improved detection limits and accuracy in the determination of cadmium, lead and copper by atomic absorption spectrometry can also be achieved by the preliminary application of anion-exchange resin procedures as a means to enrich these elements. In this paper, a combination of these methods is described.

EXPERIMENTAL

Solutions and reagents

Ion-exchange resin. The strongly basic anion-exchange resin Dowex 1 (Bio-Rad AG 1-X8; 100–200 mesh; chloride form) was used. Slurry the resin (4 g) with a few ml of 6 *M* hydrochloric acid, and after 30 min, pour into an ion-exchange column. Subsequently wash the resin bed, in the following order, with 20 ml of water, 50 ml of 1 *M* nitric acid, 10 ml of water, 50 ml of 1.5 *M* and 30 ml of 0.15 *M* hydrobromic acid. The same method of pretreatment was employed before application of the strongly basic anion-exchange resin Lewatit M5080 (100–200 mesh; chloride form).

Standard solutions. Dilute aliquots of stock solutions containing 500 μg Cd(II) (as nitrate), 500 μg Cu(II) (as sulphate) and 500 μg Pb(II) (as nitrate) per ml of 6 *M* hydrochloric acid with 0.15 *M* hydrobromic acid to obtain standard solutions containing 5–50 p.p.m. of cadmium, copper and lead respectively.

Methanolic-hydrobromic acid. Prepare a mixture of 90% (v/v) methanol and 10% (v/v) 1.5 *M* hydrobromic acid.

Apparatus and operating conditions

A Perkin-Elmer atomic absorption spectrophotometer 303 (equipped with a

Hitachi–Perkin-Elmer Recorder 56 connected to a read-out accessory) was used. The appropriate hollow-cathode lamps were used as sources. In all cases, slit 4 (1 mm; 0.7-nm bandpass) and the u.v. grating were used with the standard burner head (flat), an acetylene pressure of 8 p.s.i.g. (7.0 on flow meter) and an air pressure of 30 p.s.i.g. (9.0 on flow meter). The other instrumental settings were as follows:

	Cd	Cu	Pb
Wavelength	228.8 nm	324.7 nm	283.3 nm
Scale expansion	up to 3 ×	up to 3 ×	up to 10 ×
Lamp current	8 mA	15 mA	8 mA
Noise suppression	up to 4	up to 4	up to 5

When the methanolic hydrobromic acid solution was used, the following sensitivities for 1% absorption were obtained: Cd = 0.033 p.p.m.; Cu = 0.04 p.p.m.; Pb = 0.28 p.p.m.

The separations of cadmium, copper and lead were performed in ion-exchange columns of the same type and dimensions as described earlier[9].

Determination of distribution coefficients

The weight distribution coefficients (K_d values) of cadmium, copper and lead were determined by the batch method[10].

Ion-exchange procedure

Acidify 500 ml of the water sample with 8.7 ml of concentrated hydrobromic acid. (If a larger or smaller volume of sample is required for analysis, the amounts of reagents to be added have to be varied accordingly.). Filter through a dense filter and to the filtrate add 2.5 g of ascorbic acid. Mix thoroughly until this reductant has dissolved, and pass the mixture (sorption solution) through an ion-exchange column containing 4 g of the pretreated anion-exchange resin at a flow rate which corresponds to the back-pressure of the resin bed (about 50 ml h^{-1}). Afterwards, wash the resin bed with 20 ml of 0.15 *M* hydrobromic acid and subsequently elute cadmium, copper and lead with 60 ml of 1 *M* nitric acid (eluate).

Determination of Cd, Cu and Pb

Evaporate the eluate (see above) to dryness under an infrared lamp and dissolve the residue in 25 ml of methanolic hydrobromic acid solution. Aspirate the solution into the air–acetylene flame. Construct calibration curves by aspirating suitable cadmium, copper and lead standard solutions (prepared in exactly the same way as the samples) before and after each batch of samples.

In the determination of extremely small quantities of cadmium, copper and lead, it is necessary to run a reagent blank through the whole procedure (starting with the addition of concentrated hydrobromic acid; see above) and finally to deduct its concentrations of cadmium, copper and lead from those contents measured in the water samples.

RESULTS AND DISCUSSION

Anion-exchange separation of Cd, Cu and Pb

Previous investigations[11] have shown that cadmium(II) and lead(II) ions are strongly retained by the strong base anion-exchange resin Dowex 1 from 0.15–0.9 *M* hydrobromic acid solutions, while practically all other elements including copper(II) are not adsorbed on the exchanger. Batch equilibrium studies which were carried out in 0.15 *M* hydrobromic acid in the presence of ascorbic acid showed, however, that copper is also strongly adsorbed on this resin. From the results of these investigations (Table I), copper is only adsorbable in the presence of ascorbic acid, a fact which suggests the formation of an anionic copper(I)–bromo complex. In the absence of ascorbic acid, copper is present in the divalent oxidation state which does not react with bromide ion to form a negatively charged complex; hence copper(II) is not retained by Dowex 1 ($K_d = <1$; see Table I). Therefore, in the presence of ascorbic acid, cadmium, copper and lead which are elements of great interest with respect to environmental studies, can be concentrated simultaneously on a column of the anion-exchange resin from 0.15 *M* hydrobromic acid. This separation principle is the basis of the present paper.

TABLE I

DISTRIBUTION COEFFICIENTS IN 0.15 *M* HYDROBROMIC ACID

(1 g DOWEX 1; 1 mg load)

Ion	*In presence of ascorbic acid (5 g l^{-1})*	*In absence of ascorbic acid*
Cd(II)	$9.1 \cdot 10^3$	$9.1 \cdot 10^3$
Cu(I; II)	$3.3 \cdot 10^3$	<1
Pb(II)	$1.4 \cdot 10^3$	$1.4 \cdot 10^3$

To investigate the effect of the volume of water sample on the recovery and accuracy of the determinations of cadmium, copper and lead, varying volumes of tap water were analysed for these three elements. The results are shown in Table II. It can be seen that the volume of water has no effect provided that it does not exceed 500 ml. If larger volumes of the water sample are passed through the anion-exchange column, the adsorption of copper and lead decreases with increasing volume. That is because of the salt effect, *i.e.* the displacement of the anionic bromo complexes of these metals by sulphate and bromide ions contained in the water (bromides of calcium and magnesium are formed from the carbonates on acidification of the water sample with hydrobromic acid; see ion-exchange procedure). With respect to the accuracy of the determinations of copper and lead, the volume has practically no influence (in the range of 0.1–0.5 l). It is impossible, however, to determine cadmium in Vienna tap water when only 100–500 ml of the sample is used; in this case, at least 1 l of the sample has to be

TABLE II

EFFECT OF THE VOLUME OF WATER SAMPLE ON THE DETERMINATION OF Cd, Cu AND Pb IN VIENNA TAP WATER AFTER SEPARATION BY ANION-EXCHANGE

Volume of tap water taken (l)	*Date taken*	*Contents found ($\mu g\ l^{-1}$)*		
		Cd	*Cu*	*Pb*
0.2	19.9.1974	—	4.20	13.6
0.5	19.9.1974	—	4.10	13.5
1.0	19.9.1974	—	3.70	13.0
2.0	19.9.1974	—	3.30	12.2
5.0	19.9.1974	—	2.10	4.9
0.2	25.9.1974	~0.1[a]	4.90	17.6
0.5	25.9.1974	~0.1[a]	4.80	17.5
1.0	25.9.1974	0.1[a]	4.00	17.3
2.0	25.9.1974	0.1[a]	3.00	15.6
5.0	25.9.1974	0.1[a]	1.75	5.9
0.1	1.10.1974	—[b]	6.20[b]	16.9[b]
0.2	1.10.1974	—[b]	6.30[b]	16.8[b]
0.3	1.10.1974	~0.1[b]	6.18[b]	16.8[b]
0.4	1.10.1974	~0.1[b]	6.10[b]	16.8[b]
0.5	1.10.1974	~0.1[b]	6.05[b]	16.6[b]
0.6	1.10.1974	~0.1[b]	5.80[b]	16.4[b]
0.7	1.10.1974	~0.1[b]	5.60[b]	16.6[b]
0.8	1.10.1974	~0.1[b]	5.40[b]	16.6[b]
0.9	1.10.1974	~0.1[b]	5.30[b]	16.0[b]
1.0	1.10.1974	~0.1[b]	5.05[b]	15.9[b]

[a] Cadmium content after deduction of 5 μg of cadmium which was added as a spike before the anion-exchange separation.

[b] Contents of cadmium, copper and lead after deduction of 5-μg amounts of these elements, which were added as spikes before the anion-exchange separation.

passed through the anion-exchange column to obtain an eluate which contains sufficient cadmium to be measurable with some accuracy. Therefore, relatively large volumes of water have to be processed in order to obtain reliable cadmium values for Vienna tap water; this cadmium concentration of 0.1 p.p.b. was obtained after deduction of 5 μg of cadmium which was added as a spike before the anion-exchange separation (see Table II). Because of the very high distribution coefficient of cadmium (Table I), no effect of the volume of water sample on the recovery of cadmium was observed in the range of 0.1–5.0 l (Table II).

Effects of other metal ions

Since the main constituents of natural waters, *i.e.* calcium, magnesium, the alkali metals and iron, are not retained on Dowex 1 from 0.15 *M* hydrobromic acid, the effect of metal ions on the anion-exchange separation of cadmium, copper and lead was studied with respect to the behaviour of some trace elements only. The results of these investigations are shown in Table III; it can be seen that 1 mg amounts of all the elements listed did not affect the recoveries of cadmium, copper and lead. Among these foreign metal ions, only zinc may be present in

TABLE III

EFFECT OF FOREIGN METAL IONS ON ANION-EXCHANGE SEPARATION OF CADMIUM, COPPER AND LEAD

(The metal ions (1000 μg) were added as the bromides to 0.5 l of tap water which was 0.15 *M* in hydrobromic acid and contained 2.5 g of ascorbic acid.)

Metal tested	*Contents found (μg l^{-1})*		
	Cd[a]	*Cu*	*Pb*
Zn	~0.1	6.05	15.15
Hg	~0.1	6.00	15.62
Bi	~0.1	6.03	15.30
Sn	~0.1	6.28	15.10
Tl	~0.1	6.30	15.15
Mo	~0.1	6.05	15.62
Ag	~0.1	6.30	15.70
—	~0.1	6.18	15.60

[a] Cadmium content after deduction of 5 μg of cadmium which was added as a spike before the anion-exchange separation.

natural waters to any larger extent but even then it would not interfere because zinc is not retained by the resin from 0.15 *M* hydrobromic acid ($K_d=3$)[11].

Effect of concentration

Experiments with respect to the effect of the concentrations of cadmium, copper and lead on their recovery from 0.5-l samples of tap water gave the results presented in Table IV; it can be seen that not only p.p.b. but also p.p.m. quantities of these elements can be separated quantitatively. Therefore, the applicability of the method is not restricted to the analysis of natural non-saline waters but may also be used to isolate cadmium, copper and lead from industrial effluents.

Application to natural waters

Table V shows the results of determinations of cadmium, copper and lead

TABLE IV

EFFECT OF CONCENTRATION ON THE RECOVERY OF CADMIUM, COPPER AND LEAD

Amounts (μg) of Cd, Cu and Pb added to 0.5 l tap water[a]	*Contents found (μg l^{-1})*[b]		
	Cd	*Cu*	*Pb*
10	10.2	10.1	10.2
50	49.8	50.3	50
100	101	99.7	103
1000	958	975	1020

[a] In each case equal amounts of all three elements were added to the water sample.
[b] Contents of cadmium, copper and lead after deduction of the average natural contents (shown in Table III).

TABLE V

RESULTS OF DETERMINATIONS OF CADMIUM, COPPER AND LEAD IN SAMPLES OF AUSTRIAN WATERS

(A, Direct atomic-absorption determination without preliminary separation by anion-exchange. B, Determination after preliminary isolation by anion-exchange on Dowex 1. C, Results obtained after preliminary isolation by anion-exchange on Dowex 1 and deduction of known amounts of cadmium, copper and lead which were added as spikes before the separations. The number in parentheses gives the amount of spike used. D, Results obtained after preliminary isolation by anion-exchange on Lewatit 5080. N.d., Not detectable.)

Sample no, geographical origin and sampling date	*Cd content ($\mu g\ l^{-1}$)*				*Cu content ($\mu g\ l^{-1}$)*				*Pb content ($\mu g\ l^{-1}$)*			
	A	*B*	*C*	*D*	*A*	*B*	*C*	*D*	*A*	*B*	*C*	*D*
1 Gailitz at Arnoldstein, Carinthia; 12.10.1974	N.d.	0.8	0.95 (0.5)	0.9	17.4	16.7	16.1 (40)	17.7	N.d.	146	152 (200)	142
2 Gail at Müllern, Carinthia; 12.10.1974	N.d.	3.5	3.4 (5.0)	3.6	20.6	20.4	20.0 (40)	21.1	N.d.	148	155 (200)	145
3 Drau at Villach-North, Carinthia; 12.10.1974	N.d.	0.3	0.4 (0.5)	0.3	11.8	11.7	11.4 (40)	13.3	N.d.	35.5	33.0 (100)	39.0
4 Afritzerbach at St. Ruprecht, Carinthia; 12.10.1974	N.d.	0.4	0.4 (0.5)	0.4	11.9	12.0	12.1 (40)	13.6	N.d.	39.5	39.4 (100)	35.0
5 Obere Tibl at Feldkirchen, Carinthia; 12.10.1974	N.d.	0.4	0.5 (0.5)	0.4	20.6	20.0	19.6 (40)	20.2	N.d.	51.5	58.5 (100)	54.0
6 Glan at St. Veit-South, Carinthia; 12.10.1974	N.d.	0.4	0.4 (0.5)	0.5	13.5	12.9	13.2 (40)	12.7	N.d.	33.5	33.0 (100)	38.0
7 Mürz at Mürzzuschlag, Styria; 12.10.1974	N.d.	0.5	0.5 (0.5)	0.6	22.5	20.1	20.7 (40)	19.5	N.d.	60.6	65.2 (100)	58.4
8 Danube at Nussdorf, Vienna; 28.10.1974	N.d.	0.3	0.3 (0.5)	0.3	19.4	18.5	18.5 (40)	18.5	N.d.	5.0	6.5 (20)	5.6
9 Danube at oil port, Vienna; 27.10.1974	N.d.	0.4	0.4 (0.5)	0.3	18.8	16.3	16.3 (40)	19.6	N.d.	19.0	23.0 (20)	19.6
10 Ground water taken at Neufeldersee-Siedlung, Burgenland; 7.10.1974	N.d.	0.3	0.4 (0.5)	0.4	24.1	22.5	22.2 (40)	20.7	N.d.	3.7	3.6 (20)	3.6

in Austrian waters by the recommended procedure. These results clearly indicate that cadmium and lead cannot be determined in these waters without preliminary isolation by the anion-exchange method (see columns A of Table V), although the copper contents can be measured by direct application of atomic absorption spectrometry (see column A of Table V). Table V also includes results which were obtained after adsorption of cadmium, copper and lead on the strongly basic anion-exchanger Lewatit 5080. These experiments (see columns D of Table V) show that with this resin practically the same results were obtained as on application of Dowex 1 (see columns B and C of Table V).

Because the anion-exchange separation can be performed more or less automatically, numerous samples can be analysed simultaneously, *i.e.* the procedure is well suited for the routine determination of cadmium, copper and lead in natural waters.

This research was sponsored by the Fonds zur Förderung der wissenschaftlichen Forschung, Vienna, Austria. The generous support from this Fund is gratefully acknowledged.

SUMMARY

A method is described for the determination of cadmium, copper and lead in samples of natural non-saline waters. After acidification with hydrobromic acid, the water sample is filtered and, following the addition of ascorbic acid, passed through a column of the strongly basic anion-exchange resin Dowex 1-X8 (bromide form). On this exchanger cadmium(II), copper(I) and lead(II) are adsorbed as anionic bromide complexes. After elution of these elements with 1 *M* nitric acid, the determinations by atomic absorption spectrometry are carried out in a medium consisting of 90% (v/v) methanol and 10% (v/v) 1.5 *M* hydrobromic acid. The procedure was used for the routine determination of cadmium, copper and lead in water samples collected in Austria.

REFERENCES

1 J. L. Robinson, R. G. Barnekow and P. F. Lott, *At. Absorption Newslett.*, 8 (1969) 60.
2 G. Kisfaludi, C. Henry and J. L. Jourdain, *Chim. Anal. (Paris)*, 53 (1971) 388.
3 P. M. Holroyd and D. J. Snodin, *J. Ass. Pub. Anal.*, 10 (1972) 110.
4 K. H. Schaller, K. Lindner and G. Lehnert, *Arch. Hyg. Bakteriol.*, 152 (1968) 298.
5 D. L. Tsalev, I. P. Alimarin and S. I. Neiman, *Zh. Anal. Khim.*, 27 (1972) 1223.
6 A. Zlatkis, W. Bruening and E. Beyer, *Anal. Chem.*, 42 (1970) 1201.
7 R. J. Magee and A. K. Matior Rahman, *Talanta*, 12 (1965) 409.
8 R. R. Brooks, B. J. Presley and I. R. Kaplan, *Anal. Chim. Acta*, 38 (1967) 321.
9 W. Koch and J. Korkisch, *Mikrochim. Acta*, (1972) 687.
10 J. Korkisch, *Modern Methods for the Separation of Rarer Metal Ions*, Pergamon, Oxford, 1969.
11 E. Klakl and J. Korkisch, *Talanta*, 16 (1969) 1177.

Analytica Chimica Acta, 76 (1975) 401–408

THE EXTRACTION OF TITANIUM(IV) AND ALUMINIUM(III) FROM SULPHURIC ACID SOLUTIONS BY DI-(2-ETHYLHEXYL)-PHOSPHORIC ACID

TAICHI SATO and TAKATO NAKAMURA

Department of Applied Chemistry, Faculty of Engineering, Shizuoka University, Hamamatsu (Japan)

(Received 13th September 1974)

The extraction of aluminium(III) from sulphuric acid solutions by di-(2-ethylhexyl)-phosphoric acid (DEHPA) was first demonstrated by Blake *et al.*[1]. The extraction of some other trivalent and tetravalent metals from sulphuric acid solutions by DEPHA has also been reported[2–4]. This study extends the work to the extraction of titanium(IV) and aluminium(III).

EXPERIMENTAL

The DEHPA (Union Carbide Corp.) was the same as used previously[5], and was diluted with purified kerosene[2] or other organic solvents. Aqueous solutions of titanium or aluminium were prepared by dissolving the corresponding sulphate in sulphuric acid of the required concentration. Other chemicals were of analytical-reagent grade.

The distribution coefficients were determined as described previously[6], except that titanium and aluminium were stripped with aqueous 1 *M* solutions of sodium hydroxide and hydrochloric acid, respectively. Equilibrium between the organic and aqueous phases was complete in 15 min for the extraction of titanium(IV), but was markedly dependent on temperature for the extraction of aluminium(III) from its solution (0.0029 *M*) in 0.005 *M* sulphuric acid by 0.05 *M* DEHPA in kerosene (Fig. 1). The concentrations of titanium and aluminium in the aqueous

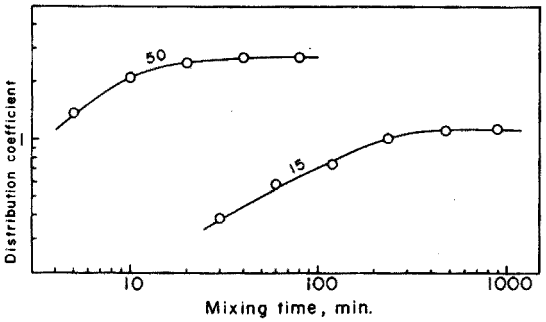

Fig. 1. Effect of mixing time by mechanical agitation on the extraction of aluminium(III) from 0.005 *M* sulphuric acid solutions by 0.05 *M* DEHPA in kerosene (numerals on curves are temperatures of extraction, °C).

solutions were determined by adding excess of EDTA and back-titrating with zinc sulphate solution at pH 7 to an eriochrome black T end-point[7], and at pH 5.3 to a xylenol orange end-point[8], respectively. The water content of the organic phase was determined by Karl Fischer titration and the sulphate concentration by EDTA titration[9].

The infrared spectra of the samples, prepared by evaporating the organic phases from extraction with DEHPA in n-hexane, and the nuclear magnetic resonance spectra of the organic, from the extraction with carbon tetrachloride as diluent, were obtained as described previously[10].

RESULTS AND DISCUSSION

Dependence on concentrations of acid, solvent and metal

The extraction of titanium(IV) from its solution (0.0042 *M*) in sulphuric acid at various concentrations by DEHPA in kerosene at 20°C gave the results shown in Fig. 2. The distribution coefficient for titanium(IV) decreases with increasing aqueous acidity below about 5 *M*, but above this acidity the extraction curve

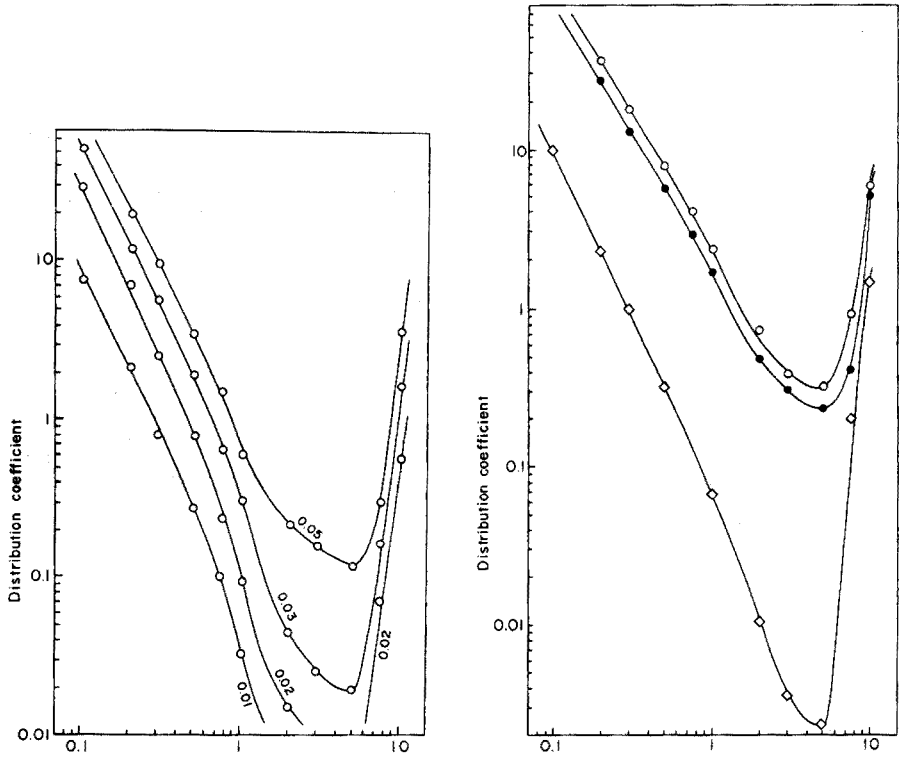

Fig. 2. Extraction of titanium(IV) from sulphuric acid solutions by DEHPA in kerosene at 20°C (numerals on curves are DEHPA concentrations, *M*).

Fig. 3. Extraction of titanium(IV) from sulphuric acid solutions by 0.1 *M* DEHPA in kerosene (○), n-hexane (●) and benzene (◇) at 20°C.

rises. This tendency is not greatly influenced by varying the nature of the diluent (Fig. 3), although the extraction efficiency decreases in the order kerosene > n-hexane > benzene[2,11]. Although a similar phenomenon is often observed in extractions from hydrochloric and nitric acid solutions[3,5,11,12], examples for the extraction from sulphuric acid solution are few except for hafnium(IV)[13] and some rare earth elements[14]. Accordingly, the variation of the distribution coefficient is interpreted as follows: at low acidity of the aqueous phase, titanium is extracted by a cation-exchange reaction in which hydrogen is liberated, and at high acidity by a solvating reaction similar to that with non-ionic reactions.

There is no simple aquated titanium(IV) ion because of the extremely high charge-to-radius ratio; in aqueous solutions, hydrolyzed species occur and basic oxo salts or hydrated oxides may precipitate. Moreover, a titanyl ion, TiO^{2+}, does not appear to exist in either solutions or in crystalline salts. As the species $[Ti(OH)_2(H_2O)_4]^{2+}$ is generally considered to be the prevailing species in dilute aqueous solutions of titanium salts[15], the initial decrease in the distribution coefficient is probably governed by an ion-exchange reaction:

$$Ti(OH)_2^{2+}(a) + 2\,(HX)_2(o) \rightleftarrows TiOX_4H_2(o) + 2\,H^+(a) + H_2O(a) \qquad (1)$$

in which X represents the anion $(C_8H_{17}O)_2PO_2^-$, $(HX)_2$ refers to the dimeric reagent, and (a) and (o) indicate the aqueous and organic phases, respectively. The following relationship should then hold:

$$\log 4E_a^o = \log K + 2\log(C_S - 4C_{Ti})/C_H \qquad (2)$$

where E_a^o is the distribution coefficient, K the equilibrium constant, C_S the total DEHPA concentration, C_{Ti} the titanium concentration of the organic phase, and C_H the acidity of the aqueous phase. However, log–log plots of E_a^o *vs.* $(C_S - 4C_{Ti})/C_H$ at constant acidity indicated that eqn. (2) was not satisfied at sulphuric acid concentrations below 0.75 *M*, hence it is postulated that the extraction involves the formation of a polymeric species:

$$TiOX_4H_2(o) + Ti(OH)_2^{2+}(a) + (HX)_2(o) \rightleftarrows (TiO)_2X_6H_2(o) + 2\,H^+(a) + \\ + H_2O(a) \qquad (3)$$

The overall reaction

$$2Ti(OH)_2^{2+}(a) + 3\,(HX)_2(o) \rightleftarrows (TiO)_2X_6H_2(o) + 4\,H^+(a) + 2\,H_2O(a) \qquad (4)$$

leads to the relationship

$$\log 4\,E_a^o = \log K_1 + 2\log(C_S - 2\,C_{Ti})/C_H \qquad (5)$$

in which K_1 is a constant. Log–log plots of E_a^o *vs.* $(C_S - 2\,C_{Ti})/C_H$ showed that eqn. (5) was satisfied at sulphuric acid concentrations below 0.75 *M*. Accordingly, it appears that the increase in the titanium concentration in the organic phase involves the formation of polymeric titanium(IV)–DEHPA complex. Hence the following general equation, expressed as an ion-exchange reaction involving the formation of polymeric species, describes the extraction of titanium(IV) from sulphuric acid solutions at low acidities by DEHPA:

$$n\,\mathrm{Ti(OH)_2^{2+}(a)} + (n+1)(\mathrm{HX})_2(\mathrm{o}) \rightleftarrows (\mathrm{TiO})_n\mathrm{X}_{2(n+1)}\mathrm{H}_2(\mathrm{o}) + 2n\,\mathrm{H^+(a)} + n\,\mathrm{H_2O(a)} \quad (6)$$

where $n \geqslant 1$. If eqn. (6) is correct, the distribution coefficient should be inversely dependent on $[H^+]^2$. In Fig. 2, the slopes of log–log plots of the distribution coefficient for titanium(IV) *vs.* the initial aqueous acid concentration at low acidity approach a limiting value of -2 with increasing DEHPA concentration.

At high acidity of the aqueous phase, species such as $Ti(OH)_3HSO_4$ and $Ti(OH)_2HSO_4^+$ exist[15]; if it is assumed that extraction involves the combination of m molecules of DEHPA dimer $(HX)_2$, which is bonded as monomer units with the titanium species by the solvating reaction:

$$\mathrm{Ti(OH)_2HSO_4^+(a)} + \mathrm{HSO_4^-(a)} + m(\mathrm{HX})_2(\mathrm{o}) \rightleftarrows \mathrm{Ti(OH)_2(HSO_4)_2\cdot 2}m\,\mathrm{HX(o)} \quad (7)$$

then

$$\log 2^m E_a^\circ = \log K_2 + 2m \log(C_S - 2m\,C_{Ti}) \quad (8)$$

where K_2 is a constant. Log–log plots of E_a° *vs.* $(C_s - 2mC_{Ti})$ in 7.5 and 10 M H_2SO_4 gave slopes of 1.6 and 2 for $2m = 1$–4, respectively. It is therefore expected that $m = 1$ in eqn. (7). Chemical analysis and infrared spectroscopy supported the suggestion that the complex, $Ti(OH)_2(HSO_4)_2\cdot 2HX$, is formed in the extraction at high acidities.

When the molar ratios of DEHPA concentration and water content to the titanium concentration in the organic phase as a function of initial aqueous titanium concentration at 0.3 M sulphuric acid were determined with 0.01 M DEHPA in kerosene at 20°C, it was found that the former approached a limiting value of two and the latter decreases to zero. This suggests that a complex containing titanium: DEHPA in the molar ratio 1:2 but no coordinated water is formed at higher titanium concentrations. Additionally, at the same sulphuric acid concentration, the variation in the titanium concentration in the organic phase as a function of the initial aqueous titanium concentration at a fixed total concentration of $[Ti] + [HX] = 0.075$ M was followed by the method of continuous variations; it was found that a maximum occurred at a molar ratio $[HX]/[Ti] = \sim 2$, implying the formation of the polymeric species $TiOX_2$.

The extraction of aluminium(III) from its solution (0.0029 M) in sulphuric acid at various concentrations by DEHPA in kerosene at 15°C is illustrated in Fig. 4. As the distribution coefficient for aluminium(III) decreases monotonically with the aqueous acidity, it seems that the extraction of aluminium is principally dominated by an ion-exchange reaction. From the dependence of the distribution coefficient on the concentrations of DEHPA and the acidity of the aqueous phase, it is suggested that the following equation, which is analogous to those for extractions of some trivalent metals[3,4,5] holds for the extraction of aluminium-(III) from sulphuric acid solutions:

$$\mathrm{Al^{3+}(a)} + 3(\mathrm{HX})_2(\mathrm{o}) \rightleftarrows \mathrm{AlX_6H_3(o)} + 3\,\mathrm{H^+(a)} \quad (9)$$

although aluminium(III) is less extractable than titanium(IV). However, when the variation in the molar ratio of DEHPA concentration to the aluminium concentration of the organic phase as a function of initial aqueous aluminium

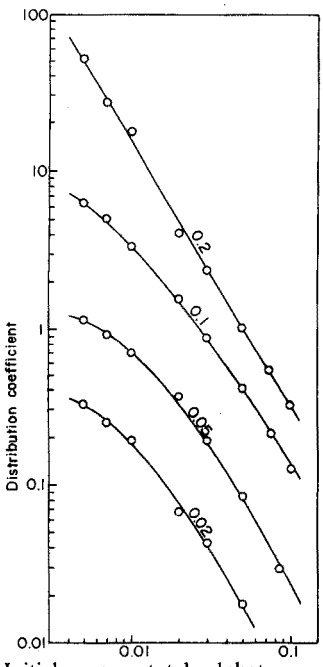

Fig. 4. Extraction of aluminium(III) from sulphuric acid solutions by DEHPA in kerosene at 15°C (numerals on curves are DEHPA concentrations, M).

concentration in 0.005 M sulphuric acid was examined with 0.1 M DEHPA in kerosene at 15°C, its ratio approached a limiting value of nearly three, indicating the formation of the species AlX_3. Accordingly, the extraction of aluminium(III) may be also expressed by the general equation involving the formation of polymeric species:

$$q\,Al^{3+}(a)+(2q+1)(HX)_2(o) \rightleftarrows Al_qX_{2(2q+1)}H_{q+2}(o)+3q\,H^+(a) \qquad (10)$$

where $q \geqslant 1$.

Extraction in the presence of sodium sulphate

Extractions of titanium(IV) and aluminium(III) from their solutions (0.0042 and 0.0029 M, respectively) in sulphuric acid and sodium sulphate by DEHPA in kerosene showed that the distribution coefficients were not appreciably influenced by sulphate ion concentrations below 1 M, but decreased with increasing hydrogen ion concentration (Fig. 5). It is therefore thought that species containing sulphate ion are inextractable at low acidities. This was confirmed by the fact that the infrared spectra of extracted organic species did not exhibit an absorption band from the sulphate group; chemical analysis showed no sulphate in the organic phase.

Temperature effect

Extractions of titanium(IV) and aluminium(III) (0.0042 and 0.0029 M, respectively) in sulphuric acid with DEHPA in kerosene at temperatures between 10 and 50°C gave the results presented in Table I. The distribution coefficients

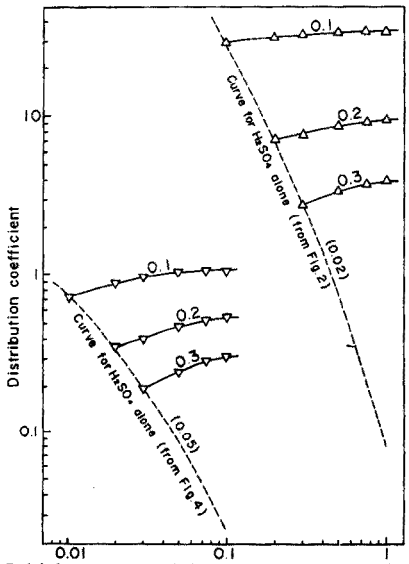

Fig. 5. Extraction of titanium(IV) and aluminium(III) from sulphuric acid solutions containing sodium sulphate by DEHPA in kerosene (numerals on curves are initial aqueous sulphuric acid concentrations, M; figures in parentheses indicate DEHPA concentration, M; continuous and broken lines represent extraction from mixed H_2SO_4/Na_2SO_4 solutions and from H_2SO_4 solutions, respectively; (△) Ti at 20°C, (▽) Al at 15°C).

TABLE I

TEMPERATURE DEPENDENCE OF DISTRIBUTION COEFFICIENT FOR THE EXTRACTION OF TITANIUM(IV) AND ALUMINIUM(III) FROM SULPHURIC ACID SOLUTIONS BY DEHPA IN KEROSENE

Metal	*[DEHPA] (M)*	*Initial aqueous $[H_2SO_4]$ (M)*	*Distribution coefficient*					
			10°C[a]	*15°C*[a]	*20°C*[a]	*30°C*[a]	*40°C*[a]	*50°C*[a]
Ti(IV)	0.02	0.1	28.0	—	30.4	33.1	35.3	38.2
	0.02	10.0	0.629	—	0.596	0.506	0.384	0.313
Al(III)	0.05	0.005	—	1.16	—	1.76	2.20	2.82

[a] Temperature of extraction.

for titanium(IV) at high acidity decreased with increasing temperature, but at low acidities, the distribution coefficients for both titanium(IV) and aluminium(III) increased with temperature. The values of the heat of reaction (change in enthalpy, $-\Delta H$, kcal mole^{-1}) for eqns. (6), (7, $m=1$) and (10) were estimated to be as follows: for titanium(IV) with 0.02 M DEHPA -1.45 in 0.1 M H_2SO_4 and 4.08 in 10 M H_2SO_4; for aluminium(III) with 0.05 M DEHPA, -4.46 in 0.005 M H_2SO_4.

Infrared and n.m.r. spectra

The organic extracts from aqueous solutions containing 0.0084, 0.0168,

0.0252, 0.0336 and 0.042 *M* titanium(IV) in 0.3 *M* sulphuric acid with 0.01 *M* DEHPA, and the extracts from 0.021, 0.042, 0.063, 0.084 and 0.105 *M* titanium(IV) in 10 *M* sulphuric acid with 0.02 *M* DEHPA in n-hexane at 20°C were examined by i.r. spectroscopy. Extracts from solutions containing 0.0145, 0.029, 0.0725, 0.145, 0.290 and 0.435 *M* aluminium(III) in 0.005 *M* sulphuric acid with 0.1 *M* DEHPA in n-hexane at 15°C were also examined.

The infrared spectrum of DEHPA shows P→O stretching bands at 1230 cm^{-1}, OH stretching bands at 2680 and 2350 cm^{-1}, arising from the hydrogen bond in the formation of the dimer, the OH bending band at 1690 cm^{-1}, the (P–O)–C stretching band at 1030 cm^{-1}, and the broad band centered around 585–455 cm^{-1}, assigned to the (O–P–O) which has the nature of coupling with other modes[16,17]. In the spectra of the extracts from solutions of low acidity, as the concentration of titanium increased, the intensities of the OH bands decreased, and the P→O absorption band bonded to the metal ion shifted to lower frequencies at 1185 cm^{-1}, while the intensity of the free P→O band decreased. Simultaneously, the band at 850 cm^{-1}, which probably results from the Ti–O–Ti bridging bond[18–20] formed according to eqn. (6), appeared; the absorptions at 1085, 1060 and 990 cm^{-1}, ascribed to the polymeric species[21], were observed as shallow shoulders of the peak at 1030 cm^{-1}.

The extracts from solutions of high acidity, however, showed absorption at 1145 cm^{-1}, from the POO^- asymmetric frequency of the X^- group[3], in addition to the P→O band at 1230 cm^{-1}, the OH stretching bands at 3460 and 3240 (shoulder) cm^{-1}, and the OH bending bands at 1725 (shoulder) and 1635 cm^{-1}, although the absorption band at 855 cm^{-1} did not appear. Additionally, the absorptions assigned to the hydrogen sulphate group (point group C_{3v} symmetry)[22] appeared at 1050 cm^{-1}, in the overlap to the (P–O)–C stretching vibration at 1030 cm^{-1}, and at 630 and 420 cm^{-1} as very shallow shoulders to the (O–P–O) band of DEHPA at 585–455 cm^{-1}; this suggests that the extraction proceeds according to eqn. (7). This was also supported by the fact that the organic solution saturated with titanium in the extraction from 10 *M* sulphuric acid contained titanium, DEHPA, sulphate and water in the molar ratio 1:2:2:2. Further, the extracts at low and high acidities showed the Ti–O stretching band[23] at 332 and 275 cm^{-1}, respectively.

In contrast, the spectra of the organic extracts from aluminium sulphate solutions showed that the Al–O stretching band at 373 cm^{-1} and the POO^- assymmetric vibration at 1145 cm^{-1} progressively increased in intensity as the aluminium concentration in the organic phase increased, although the P→O absorption band at 1230 cm^{-1} was little influenced. The infrared results confirm that titanium and aluminium extracted into DEHPA either by cation-exchange or by solvation are bonded to the phosphoryl oxygen atom.

The organic phases from the extraction of aluminium sulphate solutions (0.0145, 0.0725, 0.145, 0.290 and 0.435 *M*) containing 0.005 *M* sulphuric acid with 0.2 *M* DEHPA in carbon tetrachloride at 15°C were examined by n.m.r. spectroscopy. The spectrum of water-saturated DEHPA showed a sharp peak at $\tau = 0.91$ in a doublet caused by methyl protons, a strong peak at 0.67 assigned to the methylenic protons, a triplet at 6.12 arising from methylenic protons attached to the carbon atoms immediately adjacent to oxygen atoms, and a hydroxyl proton

band at −0.40. In the organic extracts, however, the water proton signals shifted to higher field at 0.1, 0.6 and 0.85, for initial aqueous aluminium sulphate concentrations of 0.0145, 0.0725 and 0.145 *M*, respectively; simultaneously, their intensities decreased and then the resonances disappeared for aluminium concentrations of 0.290 and 0.435 *M*, in agreement with the infrared result.

SUMMARY

The distributions of titanium(IV) and aluminium(III) between sulphuric acid solutions and solutions of di-(2-ethylhexyl)-phosphoric acid (DEHPA) in organic solvents were investigated under different conditions. Aluminium is extracted by a cation-exchange reaction; titanium is extracted by a cation-exchange process at low aqueous acidity and by a solvating reaction at high acidity. The organic phases were also studied by i.r. and n.m.r. spectroscopy. The mechanisms of the extractions are discussed.

REFERENCES

1 C. A. Blake, Jr., C. F. Baes, Jr., K. B. Brown, C. F. Coleman and J. C. White, *Proc. 2nd Int. Conf. Peaceful Uses of Atomic Energy, Geneva, 1958, Vol. 28*, United Nations, 1958, p. 289.
2 T. Sato, *J. Inorg. Nucl. Chem.*, 27 (1965) 1395.
3 T. Sato and T. Nakamura, *J. Inorg. Nucl. Chem.*, 33 (1971) 1081; *Proc. Int. Solvent Extraction Conf., The Hague, 1971, Vol. 1*, Soc. Chem. Ind., London, 1971, p. 238.
4 T. Sato and T. Takeda, *J. Inorg. Nucl. Chem.*, 32 (1970) 3387.
5 T. Sato and M. Ueda, *J. Inorg. Nucl. Chem.*, 35 (1973) 1003.
6 T. Sato, *J. Inorg. Nucl. Chem.*, 24 (1962) 699.
7 Z. Sir and R. Pribil, *Collect. Czech. Chem. Commun.*, 21 (1956) 866; *Chem. Listy*, 50 (1956) 221.
8 J. Kinnunen and B. Wennerstrand, *Chemist–Analyst*, 46 (1957) 92.
9 K. F. Sporek, *Anal. Chem.*, 30 (1958) 1032.
10 T. Sato and K. Adachi, *J. Inorg. Nucl. Chem.*, 31 (1969) 1395; T. Sato, S. Kotani and M. L. Good, *J. Inorg. Nucl. Chem.*, 35 (1973) 2547.
T. Sato, *J. Inorg. Nucl. Chem.*, 27 (1965) 1853; 29 (1967) 555; *Z. Anorg. Allg. Chem.*, 367 (1111969) 303.
12 T. Sato, *J. Inorg. Nucl. Chem.*, 25 (1963) 109; *Z. Anorg. Allg. Chem.*, 358 (1968) 296; *Anal. Chim. Acta*, 52 (1970) 183.
13 O. Navriatil, *J. Inorg. Nucl. Chem.*, 31 (1969) 855.
14 O. B. Michelsen and M. Smutz, *Proc. Int. Solvent Extraction Conf., The Hague, 1971, Vol. 2*, Soc. Chem. Ind., London, 1971, p. 939.
15 F. A. Cotton and G. Wilkinson, *Advanced Inorganic Chemistry*, Interscience, New York, 2nd edn., 1966, p. 803.
16 K. Nakamoto, *Infrared Spectra of Inorganic and Coordination Compounds*, Wiley–Interscience, New York, 2nd. edn., 1970, pp. 117 and 174.
17 L. E. Smythe and T. L. Whaleley, *J. Inorg. Nucl. Chem.*, 30 (1968) 1553.
18 R. S. Nyholm, J. Lewis and C. G. Barrachough, *J. Chem. Soc., London*, (1964) 3552.
19 M. Cox, J. Lewis and R. S. Nyholm, *J. Chem. Soc., London*, (1965) 2840.
20 G. H. Dahland and B. P. Block, *Inorg. Chem.*, 6 (1967) 1439.
21 T. Sato, *J. Inorg. Nucl. Chem.*, 26 (1964) 311.
22 G. E. Walrafen and D. M. Dodd, *Trans. Faraday Soc.*, 57 (1961) 1286.
23 J. R. Ferraro, *Low-Frequency Vibrations of Inorganic and Coordination Compounds*, Plenum Press, New York, 1971, pp. 65–109.

Analytica Chimica Acta, 76 (1975) 409–415

THE SPECIFIC FLUORIMETRIC DETERMINATION OF DIGOXIN

ADAM Z. BRITTEN and EFRAIM NJAU

Department of Pharmacy, University of Aston in Birmingham, Gosta Green, Birmingham B4 7ET (England)

(Received 13th November 1974)

Analytical studies on cardiac glycosides have so far shown that specific reactions for each glycoside cannot be expected from the sugar or cardenolide moiety. Specificity may only be expected from a reaction taking place somewhere in the steroid ring system which may contain up to several hydroxyl groups according to the glycoside, as shown in Fig. 1. Position 14 hydroxyl is common to all the glycosides and so is a trisaccharide sugar residue at position 3. The sugar may be of several types (cymarose, digitoxose, glucose, galactose, rhamnose, sarmantose and xylose).

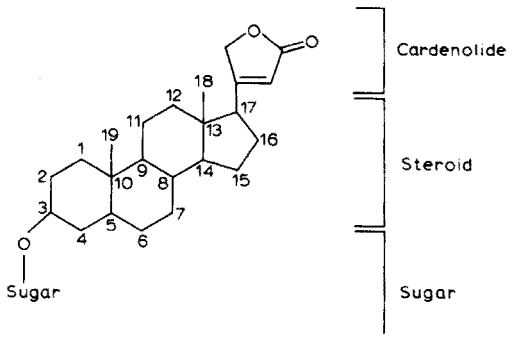

Name	OH position
Digoxin	14,12
Digitoxin	14
Gitoxin	14,16
Ouabain	14,1,5,11,19

Fig. 1. The structure of some cardiac glycosides.

Most analytical methods reported for the determination of digoxin are colorimetric[1–3], fluorimetric[4–8], or radioimmunoassay[9]. None of the colorimetric procedures exhibits the necessary sensitivity or selectivity for the estimation or detection of digoxin at sub-microgram levels. As a result fluorimetric procedures have been investigated. Wells *et al.*[6] described a modification of Jensen's method[4] for the assay of cardiac glycosides based on the fluorescence induced by concentrated hydrochloric acid; the effects of time, temperature and reagent concentrations, on the excitation and emission properties of the glycosides, and on the mechanism of fluorescence formation were described in detail. Difficulties were encountered in their attempt to apply this method to extracts of the glycosides from biological fluids.

It has been suggested[8] that a mixture of chloramine-T and trichloroacetic acid produces stable fluorescent products with cardiac glycosides on thin-layer plates. In the present work, this reagent was applied to a wide range of other

steroids to obtain a rapid indication of its selectivity and approximate sensitivity. The use of this reagent for the determination of digoxin and other steroid substances in solution has not previously been reported; a quantitative method based on a modified reagent is described below.

EXPERIMENTAL

Reagents

Glycosides and aglycones. Digoxin, pure B.P., and digitoxin (Koch-Light), ouabain and gitoxin (Fluka) digoxigenin, digitoxigenin and gitoxigenin (Aldrich) were used. These materials were all checked for homogeneity by thin-layer chromatography and used without further purification.

Steroids. All the steroids used (Koch-Light; pure grade) were chromatographically homogeneous.

Ethanol. Absolute ethanol (B.P. 99.9%) was doubly distilled and diluted with similarly distilled water to produce 80% ethanol which was used for all the fluorescence studies.

Trichloroacetic acid. A 10% (w/v) solution of analytical-grade reagent (BDH) in 80% ethanol was freshly prepared each week and used as required.

Equipment

Glassware was normally soaked in chromic acid overnight, washed thoroughly with warm water and then finally rinsed with distilled water before being dried for use.

Fluorescence spectra were obtained with an Aminco–Bowman Spectrophotofluorimeter equipped with a Hanovia 200 W mercury/xenon lamp and a Hewlett–Packard X/Y recorder. The recommended slit arrangement No. 3 (3233232) was used throughout with the sensitivity setting at maximum. Stoppered 1-cm quartz cells were used. A 1% (w/v) solution of sodium nitrite in a 1-cm quartz cell at a fixed position in the secondary path was used to eliminate the Raman scatter peak for ethanol.

Calibration procedure

Dissolve a weighed sample of digoxin B.P. (1 mg) in ethanol to make 100 ml of solution. After serial dilution, pipette 1-ml aliquots containing 0.1–2.0 μg of digoxin into 5-ml volumetric flasks. To each flask add 1 ml of the 10% trichloroacetic acid reagent making a reaction mixture of 2 ml. Prepare a reagent blank similarly. Transfer the flasks to an oil bath maintained at 130+1°C and heat for 40 min. Cool to 4°C and dilute with ethanol to 5 ml. Measure the solutions in the fluorimeter within 20 min of being made up to volume. There is, however, no significant change in intensity on recording the fluorescence of these solutions after 24 h.

Determination of digoxin in tablets

Place a tablet containing approximately 250 μg of digoxin in a 250-ml volumetric flask, pulverize with a glass rod and add 50 ml of ethanol. Stopper the flask and shake mechanically for 30 min. Filter through a sintered glass filter,

wash several times with alcohol, and dilute to 250 ml. Treat 1 ml of this solution as described above.

For tablets containing 62.5 μg of digoxin, shake up with 5 ml of ethanol and dilute the filtrate and washings to 50 ml. Measure the solutions on the fluorimeter and read the amount of digoxin present in $\mu g\ ml^{-1}$ of solution from the standard curve.

RESULTS AND DISCUSSION

Mechanism of the reaction

The determination is based on the formation of a fluorophor upon heating digoxin with trichloroacetic acid in ethanol under specified conditions. Excitation and emission spectra of the fluorophor in ethanol are shown in Fig. 2. Maximum excitation occurs at 340 nm and emission at 420 nm. The mechanism of the reaction is not clear but work is under way to isolate and characterize the fluorophor. It is, however, known that the treatment of digoxigenin with hydrochloric acid yields two anhydro derivatives[10] which have been reported to be fluorescent[6].

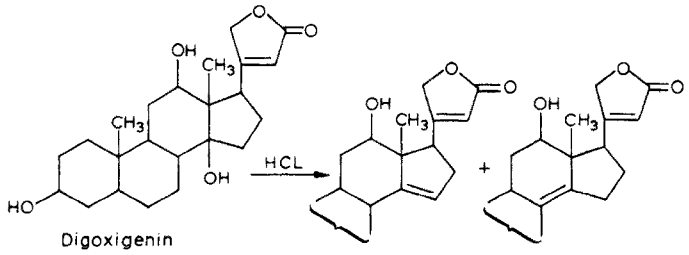

The excitation (350 nm) and emission (490 nm) properties of these products are different from those observed for the digoxin–trichloroacetic acid reaction. Therefore, the formation of the fluorophor in the reaction described here may well involve a more complex reaction than a mere dehydration.

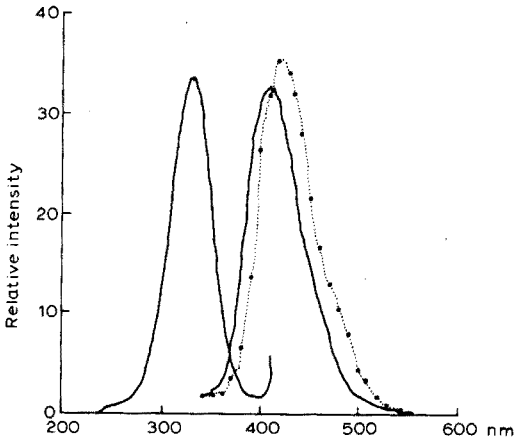

Fig. 2. The excitation and emission spectra of digoxin fluorophor in ethanol.

Reactions of steroids with moderately strong organic acids are not well documented in the literature. Reactions with mineral acids are largely non-specific and tend to produce a wide range of products most of which are difficult to isolate[11]. In the course of this investigation on steroid reactions with organic acids, it was observed that trichloroacetic acid in ethanolic solution reacts, on heating under controlled conditions, with 4-androsten-17α-methyl-17β-ol-3-one (methyltestosterone) to afford a C-aromatic ring product as the major product.

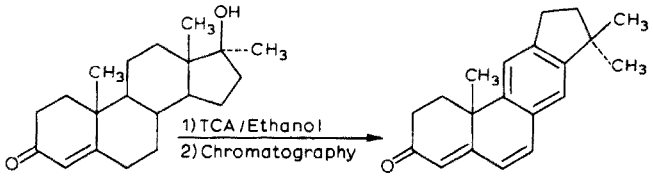

This pale yellow crystalline material, which was isolated by column chromatography on neutral alumina, has been assigned the structure shown on the basis of i.r., u.v., n.m.r., mass spectrum and elemental analysis, which will be reported elsewhere. The observed specific reaction of digoxin with trichloroacetic acid could be equally remarkable.

Optimal reaction conditions for the assay

The reaction takes about 3 h to be completed when carried out on a steam bath at 98–100°C. At lower temperatures, there is no significant reaction. Raising the reaction temperature to 130°C enables the maximum fluorescence to be attained in only 30 min. Prolonged heating leads to a gradual decay of fluorescence with time (Fig. 3). A reaction time of 30–45 min is optimal under the conditions described for the assay.

The concentration of trichloroacetic acid in the reaction mixture influences

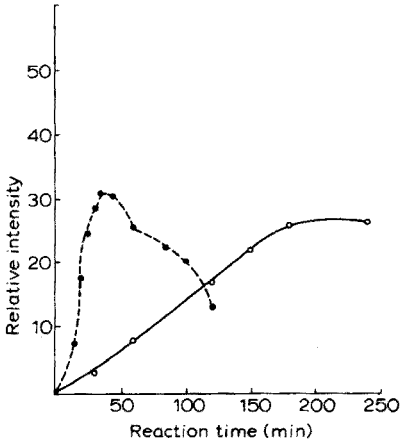

Fig. 3. Effect of temperature and reaction time on the intensity of fluorescence of digoxin (0.4 μg ml^{-1}) in solution. (○) 98–100°C, (●) 130 ± 1°C. Other conditions as in procedure.

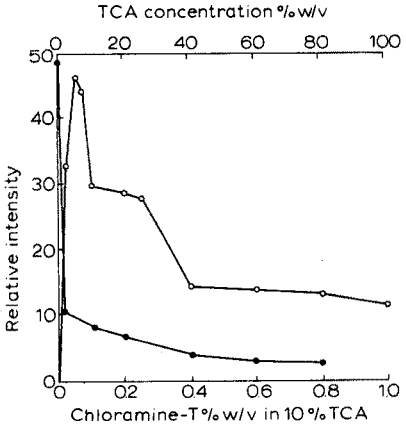

Fig. 4. Effect of trichloroacetic acid and of chloramine-T concentrations on the development of fluorescence, 0.4 μg of digoxin per ml. (○) Trichloroacetic acid, (●) chloramine-T in trichloroacetic acid. Other conditions as in procedure.

the development of fluorescence remarkably (Fig. 4). Though the fluorescence intensity obtained with concentrations of trichloroacetic acid below 10% was large, it was not possible to obtain reproducible results for assay purposes. There was little change in intensity between 10% and 25% concentrations and reproducible results were easily obtained. Between 25% and 40% concentrations, the intensity dropped by a factor of about 2 and then gradually levelled off. A concentration of 10–25% was chosen for the reagent on the basis of sensitivity and reproducibility.

A direct application of the chloramine-T–trichloroacetic acid reagent reported by Frerejacques and de Graeve[8] to the determination of digoxin in solution was attempted. The fluorophor was readily produced in the same manner as described except that the emission occurred at a slightly longer wavelength (430 nm), the excitation wavelength remaining the same (340 nm); the fluorescence intensity was reduced by a factor of about 5.0 compared with the digoxin–trichloroacetic acid reaction. The role of chloramine-T in the reaction was therefore investigated. It was demonstrated that chloramine-T, even when present in concentrations as little as 0.01%, partly quenched the fluorescence of the digoxin fluorophor (Fig. 4). Although it seems feasible to use this reagent to assay digoxin in solution, chloramine-T appears to serve no useful purpose in the reaction and only reduces the sensitivity.

Sensitivity and reproducibility of the fluorimetric determination

The determination of the precise amount of digoxin in tablets is of obvious interest to the pharmaceutical industry, as these tablets are of low dosage (50–250 μg per tablet) and high potency. As such, they require unit dose analysis as a control on the homogeneity of the product. Clinically, digoxin is normally given in oral doses of 50–1500 μg daily. Since the therapeutic dose is very close to the toxic dose, methods of high sensitivity are required for the study of the pharmacokinetic behaviour of this drug. One such method has already been described by Oliver *et al.*[9] on the radioimmunoassay for digoxin, but it suffers from the drawback that a whole working day is needed to complete the assay. On the basis of the sensitivity,

rapidity and specificity of the method described here, it seems feasible to investigate its application to direct analysis of digoxin extracts from urine and other biological fluids.

The concentration range of digoxin showing linearity with fluorescence was 0.02–1.0 $\mu g\ ml^{-1}$ and the lowest limit of detection was 0.008 $\mu g\ ml^{-1}$. A secondary filter of sodium nitrite solution (1% w/v) at a fixed position in the path was chosen to eliminate the Raman scatter peak for ethanol which appeared at about 410 nm, distorting the emission spectrum. Loss of intensity caused by the filter was about 5%.

Three samples of 250-μg tablets and one of 62.5-μg were obtained from three different manufacturers and assayed as described. Their digoxin content ranged from 98.6–101% of the labelled amount. The standard deviation of duplicate determinations within one assay was $\pm 0.361\%$, indicating good reproducibility.

Selectivity

The fluorophor is produced as a result of a reaction specific to the steroid ring, as the aglycone gives identical results to digoxin, taking into account the difference in molecular weights. The reaction is characterized by a u.v. absorption maximum in ethanol at 290 nm with a shoulder at 320 nm. Reaction products of digitoxin and gitoxin have u.v. absorption maxima at 280 nm and 335 nm, respectively. Their genins exhibit similar absorption characteristics. Ouabain octahydrate, however, exhibits no u.v. absorption above 250 nm after the reaction with trichloroacetic acid. Under the conditions described here for the determination, digitoxin, gitoxin and ouabain do not interfere with digoxin estimation when present in similar quantities (Table I). Other steroids, including estrogens and some androgens were also found not to interfere: 4-androsten-17β-ol,3-one, 4-androsten-17α-methyl, 17β-ol,3-one, 5-androsten-17α-methyl,17β-ol,3-one, 4-pregnen-17α,21-diol,3,11,20-trione, 1,3,5(10)-estratriene-3-ol,17-one, 1,3,5(10)-estratriene-3,17β-diol, 1,3,5(10)-estratriene-3,16,17-triol, and 1,3,5(10)-estratriene-17α-ethyl-3,17β-diol-3-methyl ether at the 4.0 $\mu g\ ml^{-1}$ level gave no fluorescence at all.

TABLE I

SELECTIVITY OF THE DIGOXIN ASSAY METHOD

Steroids and glycosides	*Concentration ($\mu g\ ml^{-1}$)*	*Fluorescence intensity*	*Relative intensity (%)*
Digoxin	0.4	16.0	100.0
	4.0	189.0	100.0
Gitoxin	0.4	0.7	4.4
	4.0	1.0	0.6
Digitoxin	0.4	0.8	5.0
	4.0	2.5	1.3
Ouabain	0.4	0	0
	4.0	0	0

E. Njau wishes to acknowledge the Tanzanian Government and Professor M. R. W. Brown of the Pharmacy Department, University of Aston, for financial support.

SUMMARY

A simple, specific and sensitive fluorimetric determination of digoxin, and its application to tablet preparations, is described. Digoxin can be determined in the presence of digitoxin, gitoxin and also ouabain. The reaction is based on the formation of a fluorophor on heating digoxin with ethanolic trichloroacetic acid. The fluorescence emission occurs at 420 nm on excitation at 340 nm. The reaction is complete within 40 min and as little as 20 ng ml^{-1} can be determined. The linear range of the method is 0.02–1.0 μg ml^{-1}. For tablet analysis, the standard deviation is about 0.4%.

REFERENCES

1 H. Kiliani, *Arch. Pharm. (Weinheim)*, 234 (1896) 273.
2 F. K. Bell and A. C. Krantz, Jr., *J. Amer. Pharm. Ass., Sci. Ed.*, 37 (1948) 297.
3 M. Kimura, *J. Pharm. Soc. Jap.*, 71 (1951) 991.
4 K. B. Jensen, *Acta Pharmacol. Toxicol.*, 8 (1952) 101.
5 I. M. Jakovljevic, *Anal. Chem.*, 35 (1963) 1513.
6 D. Wells, B. Katzung and F. H. Meyers, *J. Pharm. Pharmacol.*, 13 (1961) 389.
7 R. W. Jelliffe, *J. Chromatogr.*, 27 (1967) 172.
8 M. Frerejacques and P. de Graeve, *Ann. Pharm. Fr.*, 21 (1963) 509.
9 G. C. Oliver, B. M. Parker and C. W. Parker, *Amer. J. Med.*, 51 (1971) 186.
10 S. Smith, *J. Chem. Soc. London*, (1935) 1050; (1936) 354.
11 M. Kimura, K. Akimaya, K. Harita, T. Miura and M. Kawata, *Tetrahedron Lett.*, 5 (1970) 377.

Analytica Chimica Acta, 76 (1975) 417–422

SPECTROPHOTOMETRIC DETERMINATION OF MOLYBDENUM AS A MIXED THIOCYANATE–MONOOCTYL α-ANILINOBENZYLPHOSPHONATE COMPLEX

B. TAMHINA, M. J. HERAK and V. JAGODIĆ

Laboratory of Analytical Chemistry, Faculty of Science, University of Zagreb and Institute "Ruder Bošković", 41000 Zagreb (Yugoslavia)

(Received 18th October 1974)

The spectrophotometric determination of microgram amounts of molybdenum has been frequently investigated[1–4]. Probably the most widely applied reagent for molybdenum is thiocyanate[1,5,6]. When thiocyanate is used, there are numerous interferences and measurements tend to lack reproducibility. To remove interfering elements, various precipitation[7], ion-exchange[8] or extraction procedures[6] have been applied. The stability of the molybdenum thiocyanate complex can be enhanced by adding a second ligand to form a new mixed complex which can be extracted into an organic solvent; several such methods have been reported in the literature[9]. Since molybdenum(V) gives a more intense color with thiocyanate than molybdenum(VI), various reducing agents have also been studied to reduce molybdenum(VI).

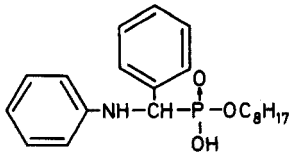

The method described here involves ascorbic acid as a reducing agent. The molybdenum thiocyanate complex is formed and is then extracted with monooctyl α-anilinobenzylphosphonate (I; MOABP) dissolved[10] in chloroform. The method allows determination of less than 0.7 μg Mo ml^{-1}; it is rapid and reproducible, and the color of the complex is stable for at least 24 h. The composition of the extracted Mo:SCN:MOABP complex has been established spectrophotometrically.

EXPERIMENTAL

Reagents

Standard molybdenum solution (0.01 M). Dissolve 1.7657 g of ammonium molybdate in 1 l of water. The solution was standardized gravimetrically with 8-hydroxyquinoline[11]. Working solutions of molybdenum were prepared by dilution.

MOABP solution (0.02 M). Dissolve 0.7509 g of MOABP in 100 ml of chloroform. All the chemicals used were of analytical purity.

Apparatus

A Beckman DU 2 spectrophotometer with 1-cm quartz cells was used.

Procedure

In a separatory funnel, place a solution containing 7–280 μg of molybdenum, and add 3 ml of 10 *M* hydrochloric acid, 2 ml of 30% (w/v) potassium thiocyanate solution, 1 ml of 10% (w/v) ascorbic acid solution and water to bring the total volume to about 10 ml. Allow this solution to stand at room temperature for 10 min. Add 5 ml of 0.02 *M* MOABP in chloroform and shake for 2 min. Transfer the chloroform layer to a 10-ml volumetric flask and extract the aqueous solution twice with 2-ml portions of chloroform. Combine the chloroform extracts in the same volumetric flask and dilute to the mark with chloroform. Measure the absorbance at 470 nm against a reagent blank.

RESULTS AND DISCUSSION

Development of the molybdenum thiocyanate color

Reduction of Mo(VI) to Mo(V) was studied in hydrochloric acid solution with tin(II) chloride in the presence of iron(III) chloride and, in another series of experiments, with ascorbic acid. After addition of the reducing agent, potassium thiocyanate was introduced and the complex formed was extracted with MOABP in chloroform. The effects of the concentrations of hydrochloric acid, reducing agent, potassium thiocyanate and MOABP were studied. When tin(II) chloride was used as the reducing agent, the maximal molybdenum thiocyanate color and reproducible results were obtained only within a narrow concentration range of the reagents. With ascorbic acid, a definite excess of the reagent was necessary to obtain maximal color, but any further increase in the concentration did not affect the absorbance readings in hydrochloric acid media. In sulfuric acid media, the absorbance reached a maximum, and then decreased with increasing acidity (Fig. 1). Therefore all the experiments were carried out in hydrochloric acid

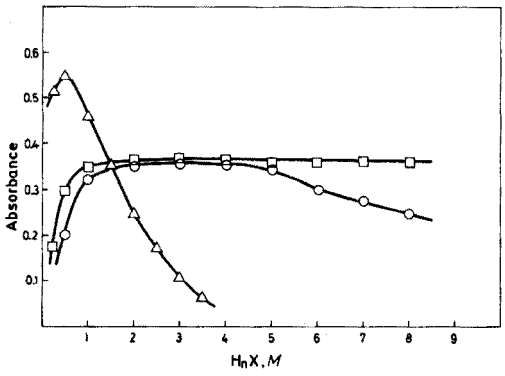

Fig. 1. Dependence of absorbance of molybdenum complex on acid concentration. (△) HCl varied; 0.5% $SnCl_2$+0.15% $FeCl_3$, 6% SCN, $1 \cdot 10^{-5}$ *M* Mo(VI), $1 \cdot 10^{-2}$ *M* MOABP in $CHCl_3$. (□) HCl varied, (○) H_2SO_4 varied; 2% ascorbic acid, 6% KSCN, $7 \cdot 10^{-5}$ *M* Mo(VI), $1 \cdot 10^{-2}$ *M* MOABP in $CHCl_3$.

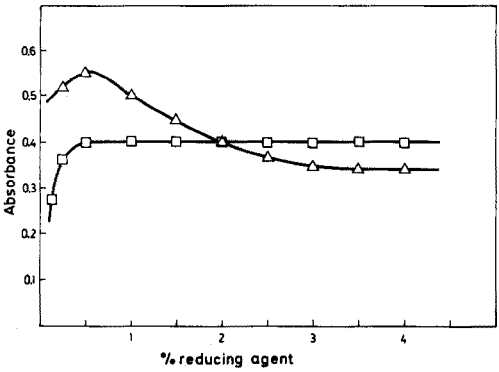

Fig. 2. Dependence of absorbance of molybdenum complex on reducing agent. (△) $SnCl_2$ varied; 0.5 *M* HCl. (□) Ascorbic acid varied; 3 *M* HCl. 6% KSCN, $7 \cdot 10^{-5}$ *M* Mo(VI), $1 \cdot 10^{-2}$ *M* MOABP in $CHCl_3$ in all tests.

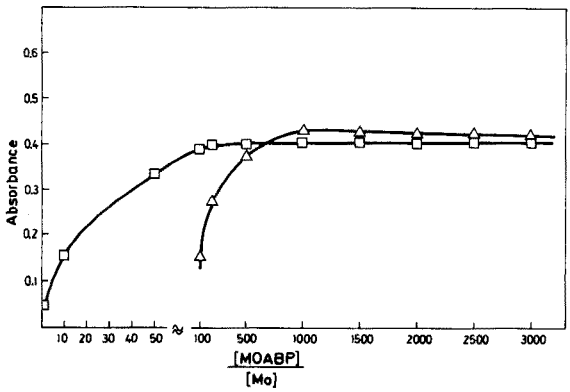

Fig. 3. Dependence of absorbance of molybdenum complex on MOABP concentration. (△) 0.5% $SnCl_2$+0.15% $FeCl_3$. 0.5 *M* HCl, 6% KSCN, $7 \cdot 10^{-5}$ *M* Mo(VI). (□) 1% Ascorbic acid, 3 *M* HCl, 6% KSCN, $1 \cdot 10^{-5}$ *M* Mo(VI).

solutions. Figure 2 shows that the ascorbic acid was a more reliable reductant than tin(II). The amount of potassium thiocyanate added did not affect the results, provided that at least 3% (w/v) was present. The effect of varying the MOABP concentration is shown in Fig. 3.

These results showed that the optimal concentrations for the determination were 3 *M* hydrochloric acid, 1% (w/v) ascorbic acid, 6% (w/v) potassium thiocyanate and 0.01 *M* MOABP dissolved in chloroform. Under these conditions it was possible to determine 0.7–28 μg Mo ml^{-1}. The absorbance of the complex at 470 nm obeyed Beer's law over this range. The molar absorptivity was 5858 l $mole^{-1}$ cm^{-1}. The photometric sensitivity, as defined by Sandell[1], was 0.0175 μg Mo cm^{-2}. The reproducibility of the measurements, expressed as standard deviation, was 0.3–2%, depending on the molybdenum concentration.

Influence of diverse ions

Fluoride, chloride, bromide, iodide, nitrate, perchlorate, sulfate, phosphate,

acetate, citrate, oxalate, tartrate and cyanide did not interfere in 10000-fold amounts. Ammonium, potassium, sodium, magnesium, calcium, barium, zinc, cadmium, aluminum, gallium, chromium(III), manganese(II), cobalt(II) and nickel(II) were also tolerated in 10000-fold amounts. Mercury(II), tin(II), lead(II), vanadium(V), antimony(V) and tungsten(VI) could be present in 1000-fold amounts, and bismuth(III), tantalum(V) and palladium(II) in 100-fold amounts.

Interfering cations are listed in Table I. Copper and zirconium decrease, and titanium, thorium, niobium, uranyl ion and iron increase, the absorbance. If these elements are present in amounts higher than tolerated, they must be separated previously. When the procedure described above is used, up to 300-fold amounts of iron(III) do not interfere; as shown in Table I, 1000-fold amounts of iron can be tolerated if enough ascorbic acid is added to reduce it completely.

TABLE I

INTERFERING CATIONS

($7 \cdot 10^{-5}$ *M* MOLYBDENUM(VI), $1 \cdot 10^{-2}$ *M* MOABP, 1% ascorbic acid, 3 *M* HCl, 6% KSCN)

Cation	*Cation: Mo molar ratio*	*Absorbance*	*Cation*	*Cation: Mo molar ratio*	*Absorbance*
—	—	0.410	Thorium(IV)	100	0.460
Copper(II)	100	0.340		10	0.410
	50	0.365	Niobium(V)	1000	0.440
	10	0.405		100	0.415
Titanium(IV)	1000	0.412[a]		10	0.410
	100	0.403[b]	Iron(III)	1000	0.570[c]
	10	0.400[b]		1000	0.415[d]
	1	0.408[b]		300	0.415
Zirconium(IV)	600	0.295	Uranium(VI)	200	0.500
	100	0.370		100	0.430
	10	0.400		10	0.410
	1	0.405			

[a] 1.0 *M* fluoride present. See text.
[b] 0.1 *M* fluoride present.
[c] 5% ascorbic acid present.
[d] 10% ascorbic acid present.

Although titanium interferes strongly, causing positive errors, it can be retained in the aqueous phase by complexing with fluoride[1], so that molybdenum can be determined even in the presence of a 1000-fold amount of titanium. Copper forms a precipitate in the aqueous phase; the observed decrease in absorbance readings probably occurs because of molybdenum coprecipitation. Large amounts of copper can be removed by precipitation with hydrogen sulphide. The other interfering elements listed in Table I can be removed by extraction with TBP[6], but iron, vanadium and tungsten are difficult to remove in this way[6].

Besides the higher selectivity and sensitivity of the proposed method in comparison with many other spectrophotometric methods for molybdenum, an advantage of the procedure described here is that relatively high concentrations of iron, vanadium and tungsten can be tolerated, since they are reduced with

ascorbic acid in hydrochloric acid solution[4], *i.e.* under the conditions applied for the molybdenum determination. If the amounts of iron, vanadium and tungsten exceed the permitted level, only an excess of ascorbic acid need be added. Figure 2 shows that a large excess of ascorbic acid does not affect the determination.

Determination of composition of Mo:SCN:MOABP complex

The ratio of molybdenum to the thiocyanate and MOABP ligand, was determined by Job's method of continuous variations and by the slope–ratio method[12]. Since the extractable complex consists of three components, two series of experiments were carried out. In one experiment, the concentrations of molybdenum and thiocyanate were varied while the concentration of MOABP was kept constant and in excess. In the second experiment, the concentrations of molybdenum and MOABP were varied, and a constant concentration of thiocyanate, in large excess, was added. The results obtained (Figs. 4 and 5) indicate

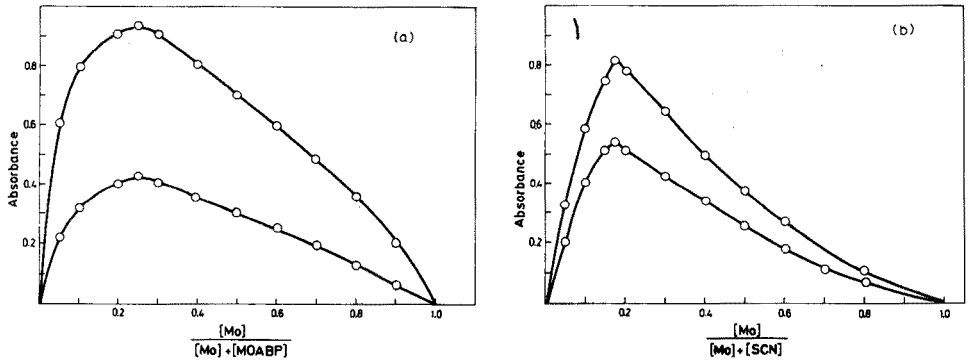

Fig. 4. Determination of complex composition by Job's method. 1% Ascorbic acid, 3 *M* HCl, 6% KSCN. (a) (●) [Mo]+[MOABP]=$2\cdot10^{-4}$ *M*; (○) [Mo]+[MOABP]=$4\cdot10^{-4}$ *M*. (b) $1\cdot10^{-2}$ *M* MOABP. (●) [Mo]+[SCN]=$2.5\cdot10^{-3}$ *M*; (○) [Mo]+[SCN]=$5\cdot10^{-3}$ *M*.

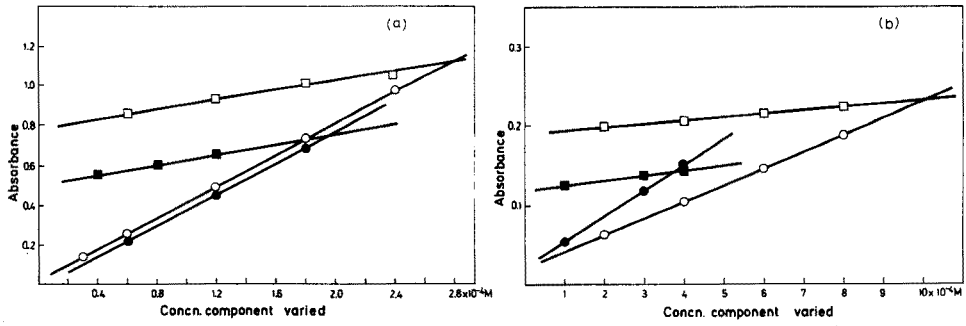

Fig. 5. Determination of complex composition by slope–ratio method. 1% Ascorbic acid, 3 *M* HCl. (a) 6% KSCN. (■) $2\cdot10^{-4}$ *M* MOABP, [Mo] varied; (●) [MOABP] varied, $2\cdot10^{-4}$ *M* Mo; (□) $3\cdot10^{-4}$ *M* MOABP, [Mo] varied; (○) [MOABP] varied, $3\cdot10^{-4}$ *M* Mo. (b) $1\cdot10^{-2}$ *M* MOABP. (■) $5\cdot10^{-4}$ *M* SCN^-, [Mo] varied; (●) [SCN^-] varied, $5\cdot10^{-4}$ *M* Mo; (□) $1\cdot10^{-3}$ *M* SCN^-, [Mo] varied; (○) [SCN^-] varied, $1\cdot10^{-3}$ *M* Mo.

that the molar ratio of Mo:SCN:MOABP is 1:5:3. Extraction of molybdenum can thus be presented by the equation:

$$Mo(VI)_{(aq)} + 5\ SCN^-_{(aq)} + 1.5(HA)_{2\,(org)} \xrightarrow{\text{Ascorbic acid}} Mo(SCN)_5 \cdot 3\ HA_{(org)}$$

where $(HA)_2$ denotes the dimeric form of MOABP in the chloroform solution[13,14].

SUMMARY

A sensitive method for the spectrophotometric determination of molybdenum is described. Molybdenum is reduced with ascorbic acid in hydrochloric acid solution, and complexed with thiocyanate ions, and the complex formed is extracted with monooctyl α-anilinobenzylphosphonate (MOABP) in chloroform. The molar absorptivity of the method is 5858 l mole^{-1} cm^{-1} at 470 nm. Beer's law is obeyed in the range 0.7–28 μg Mo ml^{-1}. Few metals interfere; the separation of the interfering elements is discussed. The composition of the extracted complex is $Mo(SCN)_5 \cdot 3$ MOABP.

REFERENCES

1 E. B. Sandell, *Colorimetric Determination of Traces of Metals*, Interscience, New York, 3rd edn., 1959.
2 J. Bankovskii, E. Suares and A. Levins, *Zh. Anal. Khim.*, 14 (1959) 313.
3 A. I. Busev and F. Chang, *Zh. Anal. Khim.*, 16 (1961) 39.
4 A. K. Chakrabarti and S. P. Bag, *Talanta*, 19 (1972) 1187.
5 C. P. Savariar, M. K. Arunachalam and T. R. Hariharan, *Anal. Chim. Acta*, 69 (1974) 305.
6 E. G. Lillie and L. P. Greenland, *Anal. Chim. Acta*, 69 (1974) 313.
7 K. M. Chan and J. P. Riley, *Anal. Chim. Acta*, 36 (1966) 220.
8 K. Kawabuchi and R. Kuroda, *Talanta*, 17 (1970) 67.
9 O. G. Koch and G. A. Koch-Dedic, *Handbuch der Spurenanalyse*, Springer-Verlag, Berlin, 1974, p. 835.
10 V. Jagodić, *Chem. Ber.*, 93 (1960) 2308.
11 A. I. Vogel, *A Text-book of Quantitative Inorganic Analysis*, Longmans and Green, London, 3rd edn., 1961, p. 508.
12 A. E. Harvey, Jr. and D. L. Manning, *J. Amer. Chem. Soc.*, 72 (1950) 4488.
13 V. Jagodić and M. J. Herak, *J. Inorg. Nucl. Chem.*, 32 (1970) 1323.
14 M. J. Herak and V. Jagodić, *J. Inorg. Nucl. Chem.*, 35 (1973) 995.

Analytica Chimica Acta, 76 (1975) 423–431

AUTOMATIC CLASSIFICATION OF CHEMICAL BEHAVIOR BY SEQUENTIAL HYPOTHESIZATION AND MULTIPARAMETRIC CURVE-FITTING

PART II. THE FULLY AUTOMATED ELUCIDATION OF DATA OBTAINED IN ACIDIMETRIC POTENTIOMETRIC TITRATIONS OF THE ANIONS OF LONG-CHAIN ACIDS

LOUIS MEITES and EGON MATIJEVIĆ

Department of Chemistry and Institute of Colloid and Surface Science, Clarkson College of Technology, Potsdam, New York 13676 (U.S.A.)

(Received 7th January 1975)

Acidimetric potentiometric titrations of laurate, myristate, and other anions of long-chain acids yield titration curves having complex shapes that vary with the initial concentration of the anion and other experimental conditions. This is because they can involve several different chemical processes. If the initial concentration of the anion, S^-, is very low, the free acid HS formed during the titration may remain dissolved; the curve then resembles one for the titration of an ordinary monofunctional weak base like acetate ion. With a higher initial concentration of S^-, the solubility product of HS may be reached at some point, after which HS precipitates on further addition of acid and the curve begins to obey the familiar equations that describe isovalent ion-combination titrations, in which the activity of the product is invariant. Especially in the presence of a high concentration of an alkali-metal cation M^+, such as sodium or potassium ion, an acid soap MHS_2 may precipitate[1], only to disappear as more acid is added and the equilibrium $MHS_2(s)+H^+ = M^+ + 2\,HS(aq\ or\ s)$ is driven to the right. With very high initial concentrations of S^-, micelle formation may occur, and if it does it will persist until enough acid has been added to decrease the concentration of unneutralized S^- below the critical concentration for micelle formation.

Feinstein and Rosano[2] showed that these processes accounted for the shapes of experimental titration curves for laurate and myristate ions under various conditions. In doing so, they employed values of the relevant parameters that had been obtained by Lucassen and others. It has since been shown[3] that the titration data can be used to evaluate these parameters by multiparametric curve-fitting[4], a technique involving brute-force non-linear regression to the theoretical equations that describe the processes known to occur. In the present paper, it is shown that multiparametric curve-fitting can also be employed to effect fully computerized decisions about which processes did and did not occur in a particular experiment.

This is the second of a series of papers dealing with machine-made decisions based on multiparametric curve-fitting to experimental data. Its predecessor[5] dealt with the problem of evaluating the functionality of an unknown base from data obtained in a potentiometric titration with a strong acid. That was a "linear" classifi-

cation problem in the sense that successive hypotheses (monofunctional, difunctional, ..., etc.) could be arranged in an *a priori* order and tested in a predetermined sequence. It was solved by beginning with the hypothesis that the base was monofunctional, obtaining the best fit to the equations describing that hypothesis, using the resulting values of the appropriate parameters to compute the deviation of each successive point, and searching for a cluster of large systematic deviations such as would be obtained with a di- or higher-functional base. If no such cluster could be found the monofunctional hypothesis was accepted; if one was, a test of the difunctional hypothesis was begun, and so on.

The present problem, in contrast, involves a triple binary classification: there are three distinct phases that can exist, and each of them may or may not have separated during the titration being considered. A completely different logical structure is therefore required.

Automatic decision-making is common both to the procedures described in this series, and to pattern recognition, whose chemical applications have been the subject of much recent attention[6], but the kinds of data and the bases for the decisions are very different. In pattern recognition, the independent variable is usually constrained to assume only certain discrete values, such as the integral values of m/e on a low-resolution mass spectrum or the wavelengths at the midpoints of a limited number of intervals on an infrared spectrum, while the dependent variable is usually expressed as either a binary (absent/present) or ternary (absent/weak/strong) number. Such constraints are needed to make the dimensionality of the classification space low enough to be tractable. In the techniques considered here, both the dependent variable and the independent one are continuous rather than discrete: the former may, for example, be pH, absorbance, concentration, or temperature, while the latter may be time or volume of a reagent. Another fundamental difference is that the present techniques are based on established theoretical relationships, one for each hypothesis to be considered, between the dependent and independent variables, whereas no such relationship is known or conceivable in most applications of pattern recognition.

EXPERIMENTAL

The data that were employed, and the conditions under which they were obtained, have been described previously[3]. The number of data points in the region chosen for analysis varied between 10 and 22 in different titrations.

THEORY

Three binary decisions must be made and the initial hypothesis is that all are affirmative—that is, that each of the three possible non-aqueous phases did separate at some stage of the titration. Four numerical parameters are entailed; they are defined by the equations:

$$K_a = [H^+][S^-][HS(aq)] \quad (1)$$

$$S_{HS} = [HS(aq)] \quad (2)$$

$$K_{MHS_2} = [M^+][H^+][S^-]^2 \quad (3)$$

and, on the basis of the phase-separation model[7],

$$C = [S^-] \tag{4}$$

where C represents the critical concentration for micelle formation and is assumed to be equal to a concentration of S^- that is invariant in the aqueous phase when micelles are present. Because all of these parameters are written as concentration or conditional constants, the measurements must be so carried out as to obviate variations of activity coefficients during the titration. This is most conveniently done by adding appropriate large concentrations of MCl both to the solution of MS titrated and to the solution of strong acid used as the reagent. Since this had been done in obtaining all of the data used in this work, it was possible to simplify the equations by neglecting changes in $[M^+]$ brought about by the precipitation of MHS_2 at some points. Constancy of temperature and liquid-junction potential, the absence of adventitious acids and bases such as carbon dioxide or free alkali-metal hydroxide, and the attainment of equilibrium at every experimental point must be assumed as well, and must be ensured in designing titrations from which the data are to be processed in this way.

Two kinds of initial input are required. One consists of the experimental data and includes the total number of points obtained and their coordinates. The other deals with the experimental conditions, and for the present purpose includes the volume V_b^0 and concentration C_b^0 of the soap solution titrated, the concentration C_a of the acid used as the titrant, and the concentrations $C_{MX,b}$ and $C_{MX,a}$ of the alkali-metal salt MX in these solutions.

The titration-curve equations that are employed describe only the portion of the curve that precedes the equivalence point, where one mole of acid has been added for each mole of soap initially present. This is chiefly because pH values in the presence of excess of acid are so little dependent on the values of S_{HS}, K_{MHS_2}, and C that data obtained after the equivalence point would be of little use in the computations. Points very near the start of the titration or close to the equivalence point are also of little use, because they may be unduly affected by small uncertainties in the purity of the soap or in the concentration of the acid, by adsorption onto a solid phase if one is present, or by supersaturation with respect to one of the precipitates, and such points are therefore automatically rejected. The average ionic strength, taken as the ionic strength at the point where half as much acid has been added as at the last point accepted, is computed, and values of the mean ionic activity coefficients of hydrochloric acid and potassium chloride at that ionic strength are requested from the user. They are combined to obtain an estimate of the apparent single-ion molarity activity coefficient of hydrogen ion from the approximate relation

$$y_{H^+} = \gamma_{\pm,HCl}^2 / \gamma_{\pm,KCl} \tag{5}$$

which resembles the Guggenheim assumption but ignores the difference between molarity and molality activity coefficients. Though this is crude, a more accurate value of y_{H^+} is not required, for the sole effect of changing y_{H^+} is to shift the entire curve with respect to the pH-axis without changing its shape, and consequently an error in y_{H^+} cannot alter the classification even though it may affect the values of the parameters obtained. In principle, it should be possible to treat y_{H^+} as

another parameter to be evaluated, but this would be wasteful of computer time.

No other information is required of the user, and execution proceeds from this point without human intervention.

Initial estimates of the parameters are needed and are obtained directly from the data. It is essential that they be so chosen as to make it appear that each of the possible processes occurs at some, but not all, of the experimental points. Too low an initial estimate of S_{HS}, for example, might make it appear that solid HS was present at every experimental point, and the hypothesis that it was not might not receive a fair test before an incorrect decision had been based on a mistaken appearance. The initial estimate $K_a = 1.5 \cdot 10^{-5}$ is appropriate for all but a very few uncommon monocarboxylic acids[8]. Initial estimates of S_{HS}, K_{MHS_2}, and C are made in such a way that S_{HS} is satisfied at a point two-thirds of the way through the titration, K_{MHS_2} is satisfied at one a third of the way through the titration, and C is equal to one-third of the initial concentration of the soap. Adjustments of these estimates by the curve-fitting portion of the program not only alter the pH values computed for the experimental points but also affect the number of points at which each of these processes appears to occur.

The initial estimates are used to compute a pH value at each point. The deviations of these computed values from the measured ones are squared and summed, and the values of the parameters are adjusted so as to minimize the sum of the squares of the deviations. The portion of the program by which these adjustments were effected was transcribed without change from a program[3] designed to evaluate the parameters after classification had been made by the user; that program in turn was only slightly modified from a general one that has been described elsewhere[9] and employed for many other purposes.

The subroutine used to compute the pH values resembles the one previously described[3], but differs from it in one important way. The first step in that subroutine was to calculate test values of $[S^-]$, [HS(aq)], and $[H^+]$ from equations that were equivalent to supposing that only simple homogeneous neutralization had occurred, and that neither free acid, acid soap, nor micelles had separated. Then, if $[S^-]$ exceeded C, if [HS(aq)] exceeded S_{HS}, or if $[M^+][H^+][S^-]^2$ exceeded K_{MHS_2}, further computation was undertaken to obtain the pH value corresponding to the currently assumed values of all the parameters. There is one situation in which the test values indicate that all three phases have separated at the point being considered. When the classification is known *a priori*, it is appropriate to sort this situation out into any of the five real possibilities that may give rise to it, and to apply a small error to the previously calculated pH value only if none of these five possibilities is found to be applicable. Thus the error surface is artificially steepened in ways that discourage such apparent violations of the phase rule.

Here, however, it was found to be advantageous to apply such an error at once when the test values indicated that C, S_{HS}, and K_{MHS_2} were all exceeded. The procedure finally adopted was to allow twelve cycles of normal computation to bring the original crude estimates into reasonably good conformity with the data, and thereafter to inflict immediate punishment of apparent infractions of the phase rule. This both ensured and speeded rejection of processes that did not actually take place. If, at the end of the fit, none of the possible processes had been rejected, the values attained after twelve cycles were retrieved and the fit was completed in the

ordinary way to ensure that the final results were not affected by this deliberately erroneous procedure. The effect is to prevent the retention of parameters that may give a better numerical fit but that are not actually involved in the titration.

Like its antecedents[3,9], the present program tests three values of each parameter on each cycle of computation. One of the three is the initial estimate or the result of prior adjustment of the initial estimate. When, as is true here, only positive values of the parameters are permitted, the other two are obtained from the first by division and multiplication by a factor $(1+D)$. The value of D is arbitrarily chosen at first and is subsequently adjusted along with the value of the parameter to which it pertains.

When one of the three processes considered—say, micelle formation—does not occur during a titration, the value of the parameter characterizing that process is steadily increased through a number of cycles of computation. Eventually it becomes so large that the process does not appear to occur at any point. It then becomes immaterial whether the critical concentration is assumed to have the then current value C or a still larger one $(1+D)C$. In most applications of multiparametric curve-fitting, failure of the sum of the squares of the deviations to depend on the value of any one parameter signifies that the minimum on the multidimensional error surface is so far away from the value being tested that the surface is virtually flat in the region being inspected. When this occurs it is appropriate to increase D considerably so that that region will be wider on the next cycle.

This is the basis of the decision-making machinery employed here. When the value of D for any one parameter has been increased in this way so many times that it exceeds about 100, it is concluded that the process represented by that parameter does not occur. Then the number of parameters remaining to be evaluated is decreased by 1, the surviving ones are relabelled if necessary, a message is provided to inform the operator of the decision that has been made, and the fit is continued.

Eventually an acceptable fit is found, and the identities and values of the parameters that remain are printed out. They are used to compute the pH values at the experimental points for one last time, and as this is done a tally is kept of the number of points for which each parameter is employed. If C or K_{MHS_2} is used in computing the pH values at only four or fewer points, its value is identified as being doubtful, for a reliable value cannot be expected from so little pertinent information. If S_{HS} is not unused for at least four points (meaning that solid HS appears to have precipitated at almost every point), its value is automatically combined with that of K_a to give the solubility product of the acid, and this is given on the final printout instead of the separate values of K_a and S_{HS}, which have no independent meaning in these circumstances. The choice of four in these criteria was arbitrary; it yielded messages indicating doubt when doubt seemed appropriate, and is surely preferable to either a much larger number or a much smaller one, but there were no firm grounds for this particular choice.

Computations

All of the computations were performed with a PDP8/I minicomputer operated in a multiuser configuration under the manufacturer's EDUSystem 25 BASIC, which provided 4096 words of core memory as the user area for this work. Partly because of the complexity of the subroutine needed to compute the pH

values at the individual points, and partly because of the number of print commands required, the entire program was too long to be stored and executed in this user area, and it was therefore divided into four chained parts. The first contains the initial interactive dialogue, selects the points to be used, calculates and identifies the initial estimates of the parameters, and otherwise initializes the computation. The second performs the fit to the equations that describe the current hypothesis, contains the decision-making steps, and makes provision for continuing the calculation after a possible product has been rejected. The third, which comes into play only when none of the possible products is rejected by the second, resumes

```
READY
RUN

TITRATION OF A SOAP WITH A STRONG ACID

CONDITIONS:
  SOAP SOLN.
    VOLUME,CC.=? 100
    CONCN.,M=? 7E-4
    MX CONCN.,M=? 0.05
  ACID SOLN.
    CONCN.,M=? 0.01
    MX CONCN.,M=? 0.04
NO. OF DATA POINTS ACCEPTED= 12 , LAST ONE AT 6 CC.
AVERAGE IONIC STRENGTH= .05038835 M; MEAN IONIC ACTIVITY COEFFICIENTS
  OF HCL AND KCL AT THAT IONIC STRENGTH=? 0.830,0.816
INTERMEDIATE DIAGNOSTIC PRINTOUT: 0=NO, 1=YES? 0

FIRST ASSUMPTION IS THAT MICELLES MAY FORM AND BOTH ACID
  SOAP AND FREE ACID MAY PRECIPITATE

MICELLES DO NOT FORM; NEXT ASSUMPTION IS THAT BOTH ACID
  SOAP AND FREE ACID MAY PRECIPITATE

 ACID SOAP DOES NOT PRECIPITATE;
  NEXT ASSUMPTION IS THAT FREE ACID MAY PRECIPITATE


PRECIPITATION BEGAN SO EARLY THAT K(A) AND S FOR HS CANNOT
  BE EVALUATED SEPARATELY; ITS SOLUBILITY PRODUCT= 2.086777E-10

X              Y,MEAS.       Y,CALC.       DIFF.,M-C     DIFF./STD.DEV
 .5             6.627         6.564813       .06218696     1.340283
 1              6.552         6.527896       .02410436      .5195085
 1.5            6.5           6.487962       .01203764      .2594408
 2              6.425         6.444436      -.01943547     -.4188824
 2.5            6.341         6.396554      -.05555427     -1.197332
 3              6.26          6.343288      -.08328825     -1.795068
 3.5            6.228         6.283193      -.05519307     -1.189547
 4              6.216         6.214153       1.846671E-3    .03980033
 4.5            6.16          6.132889       .02711099      .584309
 5              6.072         6.033906       .0380941       .8210222
 5.5            5.94          5.906904       .03309613      .7133036
 6              5.743         5.728759       .0142411       .3069309

SUM(DEV.)↑2= .021528I ,   STD.DEV.=  .04639838

READY
```

Fig. 1. Initial dialogue, rejection messages, and final printout for the data obtained in a typical titration. The final classification given is the one known to be correct.

the fit from the twelfth cycle without the artificial distortion of the error surface introduced at that stage in the original fit. The fourth, which follows the second if any product has been rejected, or the third if micelles, acid soap, and solid free acid have all been judged to be present, provides the final printout. Figure 1 shows the input (excluding the coordinates of the data points, which are entered separately before execution begins) and output for a typical run. In the worst case, which is the one in which the third part of the program is used, the total execution time was about 10 min on a PDP8/I dedicated to the calculation and operated in POLYBASIC*.

RESULTS AND DISCUSSION

The program was tested with data from all of the titrations described previously[3] as well as with those from a few others performed subsequently. The solubility of lauric acid in water is so low that it was not feasible to obtain data under conditions such that none of the possible processes occurred, and these were therefore counterfeited by employing data obtained[10] in titrations of 0.1, 0.025, and 0.0062 *M* acetate with hydrochloric acid. There were 33 titrations in all.

Twenty nine of the 33 titrations were correctly classified. There was one definite error, in which a titration of 0.0125 *M* laurate known to have involved micelle formation as well as precipitation of both of the possible solid phases was judged to involve only precipitation of the acid soap and free acid. The other three misclassifications consisted of retaining processes that were not believed to have occurred, but each such retention was based on so few points for the parameter incorrectly retained that the occurrence of the process and the value of the parameter describing it were identified as doubtful on the final printout. Depending on how much charity one is willing to extend to these expressions of doubt, the program might be said to be between 87 and 97% correct.

When one of us attempted to classify the same titrations on the basis of the same data, but without knowing the initial conditions, the percentage of success was well below 70. There are some ideal cases that are easily recognized visually. If phase separation does not occur, as in the titrations of acetate, the curve is symmetrical around its midpoint, and its first half is concave upward while its second half is concave downward. If only the free acid precipitates, the curve is smooth and everywhere concave downward when the initial concentration of laurate greatly exceeds the solubility of the acid. Visual differentiation of even these two simple cases would be much more difficult if the acid were much more soluble than lauric acid or if the anion were much more dilute than it was in the present titrations, and would be almost impossible if the first precipitate of free acid did not appear until after the halfway point had been passed. If precipitation of the acid soap is extensive, the first portion of the curve is shifted toward higher pH values and becomes steeper,

* A briefly annotated hard-copy listing of the program in BASIC may be obtained by remitting $25.00 to the Computing Laboratory of the Department of Chemistry, Clarkson College of Technology, Potsdam, New York 13676. Listings of the general multiparametric curve-fitting program CFT3 from which it was derived, in several languages including FORTRAN-IV, together with a 170-page manual of documentation, explanation, and instruction, may be obtained at the same time for a total remittance of $45.00.

and a break halfway to the equivalence point is followed by a region in which the acid soap and solid free acid coexist and the pH is almost constant, though because of variations in the concentration of the alkali-metal ion it may not be perfectly so. If micelle formation is also extensive, there is another region of nearly constant pH near the beginning of the titration.

Marginal cases are much more difficult to recognize and identify than these descriptions might suggest, and even a fairly simple one may be misinterpreted if a region of constancy is represented by only one of the data points or has been skipped altogether. None of the three cases in which the machine produced a doubtful classification could be correctly classified by a human operator who did not have *a priori* knowledge of the situation.

It was interesting to note that various different paths could be followed en route to the final conclusion. For six of the eight titrations in which only lauric acid precipitated, micelle formation was rejected before the precipitation of acid soap, but for the other two this order was reversed. For two of the three titrations of acetate, micelle formation was rejected first, then precipitation of acid soap, and finally precipitation of free acid, but for the third it was the precipitation of free acid that was rejected first.

Conclusions

Although several procedures have been described for effecting machine decisions of chemical and other scientific questions[11] by applying techniques like multivariate analysis[12] and principal component analysis[13] to a group of response curves obtained with different samples or under different conditions, there is scant precedent for the demonstrations in this series that such decisions can be based on individual curves. Many, and perhaps even most, of the human-made decisions in chemical research are founded on individual curves. Thus a reaction may be classified as pseudo-first-order on the basis of a single concentration–time curve or an appropriate plot derived therefrom; a half-reaction may be classified as reversible on the basis of a single triangular-wave voltammogram; and an electrolyte may be classified as strong or weak on the basis of a plot of equivalent (or molar) conductance against concentration. Other curves may certainly be scrutinized to confirm the correctness of the classification or to define the range of conditions over which it is valid, but this is merely repetition of classification on the basis of individual curves.

These considerations suggest that machine-decision procedures will become extremely valuable in chemical research. By performing qualitative as well as numerical interpretation of the data obtained they should enable the chemist to devote his full attention to the selection of problems and experimental conditions that will repay investigation and to the design and improvement of techniques of measurement that will yield more accurate and reliable data.

This work was supported in part by Unilever Research Laboratory, Port Sunlight, England, and by grant number GP-10325 from the National Science Foundation. Thanks are expressed to the Eastman Kodak Company and the National Science Foundation for Departmental grants that made possible the purchase and maintenance of the computer system employed.

SUMMARY

This paper describes the logic and structure of a computer program for classifying the potentiometric titration curve obtained when a solution of a long-chain carboxylate ion, such as laurate, is titrated with a strong acid in the presence of excess of alkali-metal ion. During such a titration either the free carboxylic acid or an acid soap, or both, may precipitate and micelle formation may occur. From the coordinates of the data points and other information about the experimental conditions, the program decides which of these processes occurred, provides the best values of the numerical parameters characterizing those that did, and achieves a higher percentage of success than a human chemist.

REFERENCES

1 J. Lucassen, *J. Phys. Chem.*, 70 (1966) 1824.
2 M. E. Feinstein and H. L. Rosano, *J. Phys. Chem.*, 73 (1969) 601.
3 S. L. Young, E. Matijević and L. Meites, *J. Phys. Chem.*, 78 (1974) 2626.
4 T. Meites and L. Meites, *Talanta*, 19 (1972) 1131.
5 L. Meites, *Talanta*, 21 (1974) 393.
6 T. L. Isenhour, B. R. Kowalski and P. C. Jurs, *Crit. Revs. Anal. Chem.*, 4 (1974) 1.
7 G. Stainsby and A. E. Alexander, *Trans. Faraday Soc.*, 46 (1950) 587.
8 G. Kortüm, W. Vogel and K. Andrussow, *Dissociation Constants of Organic Acids in Aqueous Solution*, IUPAC–Butterworths, London, 1961.
9 L. Meites, *The General Multiparametric Curve-Fitting Program CFT3*, Computing Laboratory, Department of Chemistry, Clarkson College of Technology, Potsdam, N.Y., 2nd edn., 1974.
10 D. M. Barry, M. S. Thesis, Clarkson College of Technology, 1974.
11 See, *e.g.*, W. H. Lawton and E. A. Sylvestre, *Self-Modeling Curve Resolution*, Management Systems Development Department, Eastman Kodak Co., Rochester, N.Y., undated.
12 T. W. Anderson, *Introduction to Multivariate Analysis*, Wiley, New York, 1958.
13 C. R. Rao, *The Use and Interpretation of Principal Component Analysis in Applied Research*, Technical Report No. 9, Department of Statistics, Stanford University, 1964.

Analytica Chimica Acta, 76 (1975) 433–442

COULOMETRIC TITRATION OF IODIDE AND IODINE WITH ELECTROLYTICALLY GENERATED HYPOBROMITE

JÁN MOCÁK and DUŠAN I. BUSTIN

Department of Analytical Chemistry, Slovak Technical University, 880 37 Bratislava (Czechoslovakia)

JARMILA KMEŤOVÁ

State Drug Research Institute, 801 00 Bratislava (Czechoslovakia)

(Received 2nd November 1974)

The possibilities of the determination of iodide by coulometric titration have been studied by several authors. Most of these methods are based on the reaction of iodide with silver(I)[1–3] or mercury(I)[4,5] ions, with electrolytic oxidation of electrode material for generation of the titrant. The oxidation of iodide to iodine in acidic solution has been applied in titrations with electrolytically generated cerium(IV)[6] and manganese(III)[7]; oxidation to iodine bromide with electrolytically generated bromine[8] has also been used.

Iodine has been used in coulometric titrations mainly as a titrant, and very few papers have been concerned with coulometric determination of iodine; only electrolytically generated iron(II)–EDTA[9] and tin(II)[10–13] have been used.

Because of the instability of hypobromite solutions[14], this strong oxidant is particularly suitable for applications in coulometric titrations. Its generation under weakly basic conditions has 100% current efficiency[15]. The work described here is an application of its reactions with iodide and iodine for determinations of these substances.

Oxidation in solutions at *ca.* pH 9 offers new possibilities for the determination of iodide in the presence of oxidants (mainly oxy anions) which do not react with iodide under the conditions used. Moreover, successful coulometric titration of iodide with hypobromite assumes that bromide does not interfere with the analysis even at high bromide–iodide ratios, so that this method is preferable to argentometric or mercurimetric titrations.

The titration of iodine with hypobromite ion is a suitable oxidation method for its determination. Because of the large change in oxidation state (iodate is the assumed reaction product), high sensitivity can be expected. This, together with the fact that large amounts of bromide (and chloride) do not interfere makes the method particularly advantageous.

EXPERIMENTAL

Chemicals and solutions

All chemicals, unless otherwise stated, were of reagent-grade purity. Potassium iodide and arsenic trioxide used as standards were dried at 110°C to constant weight[16]; potassium iodate and sodium iodate were dried[16] at 150°C. The solutions

of iodide were; as a rule, prepared in such concentrations that 1 ml of the solution could be pipetted for the determination. The potassium iodide standard, tested by classical potentiometric titration with iodate[16], was shown to be 100% pure.

Solutions of iodine were made by dissolving resublimated iodine in methanol. The very dilute solutions of iodine were prepared by dilution of the methanolic solution with distilled water.

Solutions of arsenite were prepared immediately before use by dissolving arsenic trioxide in 10 ml of warm 1 *M* sodium hydroxide; after dilution with distilled water the solution was adjusted to pH 7 with hydrochloric acid; a little sodium hydrogencarbonate was added to the solution, which was then diluted to the desired volume with distilled water. The purity of the standard arsenic trioxide was verified coulometrically by titration with electrolytically generated iodine (for the conditions, see below).

Coulometric titrations with hypobromite were done with solution A, containing 2 g of borax and 100 g of potassium bromide per 1 l of distilled water. The required pH was adjusted with HCl or NaOH. Unless otherwise stated, all titrations were done at pH 8.7.

Iodimetric coulometric titrations were done with freshly prepared solution B, containing 0.2 *M* sodium hydrogencarbonate and 0.1 *M* potassium iodide.

Apparatus

A universal coulometric analyzer OH-404 (Radelkis, Budapest) was used. The chosen constant current was maintained by the galvanostatic unit of the instrument. The titration agent was generated continuously. The amount of electricity consumed was measured with an integrator. The equivalence point was determined biamperometrically, by means of the control unit of the analyzer, the titration being stopped automatically at a preselected current.

An electrolytic vessel (OH-930; Radelkis) was used. A platinum foil (area, 5.5 cm^2) wound round a glass rod (OH-935; Radelkis) served as the working electrode. The auxiliary electrode was a platinum foil (OH-934) with an area of 5.4 cm^2, and was separated from the electrolyzed solution by a fine glass sinter. The working electrode was cleaned (after about 100 runs) by cathodization in dilute (1+2) nitric acid.

A pair of platinum wires (OH-938) served as the indicator electrodes (area of each wire, 0.06 cm^2). When not in use, the electrodes were short-circuited and immersed in distilled water. Any potential difference between the electrodes was eliminated by their intermittent cathodization and anodization in a dilute (1+2) solution of nitric acid. The potential difference between the indicating electrodes was 150 mV in the hypobromite titrations and 50 mV in iodimetric titrations.

Procedures

Titrations with electrogenerated hypobromite. Solution A (110 ml) was placed in the coulometric vessel and a pre-electrolysis was done. Then the sample (1 ml) was added and titrated. The result of the first addition was not taken into account; only the determinations of subsequent 1-ml samples were considered. The highest concentrations were determined in series of 4 additions, in order to

avoid change of pH after larger numbers of titrations. For more dilute samples up to 10 additions of the sample were made successively to the same base electrolyte. Blanks were run for each generating value and preset indicator current separately in a similar manner. The blank value for methanol was much higher than that for 1 ml of water, hence samples with low contents of iodine were analyzed in solutions containing 10, 3 and 1% methanol in water as a solvent, so that with a decreased amount of iodine in the sample, the blank value also decreased.

Titrations with electrogenerated iodine. Solution B (110 ml) was used. Pre-electrolysis was followed by addition of 1 ml of the iodine sample together with 1 ml of a standard solution of arsenic containing about 100–150% excess of arsenic(III). The excess of arsenic(III) was then back-titrated with electrolytically generated iodine.

All measurements were done at 25°C. The statistical evaluations and the test results were calculated for 95% probability (significance level $\alpha = 0.05$)[17].

RESULTS

Determination of iodide

The coulometric titrations showed that the oxidation of iodide in weakly basic solutions proceeded according to the reaction:

$$I^- + 3\,BrO^- \rightarrow IO_3^- + 3\,Br^- \qquad (1)$$

All titrations were therefore evaluated on this basis. Table I summarizes the results obtained under different titration conditions of generating and indicating currents as well as concentration of iodide.

A change in the shape of the titration curve with changes in the generating current indicated a relatively slow rate for the overall oxidation reaction (1). Therefore, small generating currents had to be used to obtain quantitative results (Table I). At a potential difference of 150 mV between the indicator electrodes, there was only a slight initial increase and then a decrease in the indicating current, with a minimum at the equivalence point; the titration curve was not symmetrical, having a maximum at 30% of the titration. After the equivalence point, the indicating current increased sharply because of the formation of the reversible redox system of the titrant.

The results of coulometric determinations of iodide at different pH values and in the presence of a large amount of chloride or iodate are also included in Table I. The influence of large amounts of iodate on the results was tested by Student's t-test[17]. Application of the Fisher–Snedeckor F-test[17] showed that the difference in variances of results with and without iodate was not statistically significant; checking the mean values by the t-test showed that there was no significant difference between them, even at high concentrations of iodate (Table I, note b). Similarly, the standard deviations and averages of the results in the presence of chloride showed that chloride did not interfere.

It was found that the most accurate and precise results were obtained in solutions with pH 8.7 or 9.0. At pH 10 the results were higher (statistically significant by a t-test), and at pH 8 the variance of the results was higher (F-test) than in solutions of pH 8.7–9.0.

TABLE I

DETERMINATION OF IODIDE BY ELECTROLYTICALLY GENERATED HYPOBROMITE AT pH 8.7

Iodide taken (μg)	*Iodide found (μg)*	*n*	*s (μg)*	*Reliability interval (μg)*	*Current*		*Conditions*
					Generating (mA)	*Indicating (μA)*	
2115	2109	8	12.62	±11	15.0	0.5	
634.0	631.0	8	3.45	± 2.9	8.0	0.25	
634.0	632.2	8	1.67	± 1.4	4.0	0.25	
422.8	420.2	8	2.62	± 2.2	8.0	0.25	
422.8	422.7	8	2.14	± 1.8	4.0	0.25	
211.4	210.3	8	1.13	± 0.95	3.0	0.1	
126.9	126.8	9	2.26	± 1.7	2.0	0.1	pH 8.0[a]
126.9	126.5	9	0.88	± 0.68	2.0	0.1	pH 8.7[a]
126.9	126.6	9	0.91	± 0.70	2.0	0.1	pH 9.0[a]
126.9	129.2	9	0.83	± 0.64	2.0	0.1	pH 10.0[a]
97.00	97.14	8	0.52	± 0.44	2.0	0.1	[b]
97.00	97.26	8	0.58	± 0.49	2.0	0.1	0.1 *M* NaCl[c]
97.00	97.56	8	0.71	± 0.60	2.0	0.1	0.05 *M* KIO_3[b,c]
63.45	63.39	9	0.54	± 0.42	2.0	0.06	
63.45	63.51	10	0.61	± 0.44	1.5	0.06	
25.38	25.64	9	0.49	± 0.38	1.2	0.04	
9.50	9.74	9	0.38	± 0.29	1.0	0.04	

[a] pH adjusted by HCl or NaOH addition.

[b] $(s^2_{IO_3^-}/s^2_A) = (0.71^2/0.52^2) = 1.86 < F_{7,7,0.05}$ (according to Eckschlager[17], $F_{7,7,0.05} = 3.79$); $t = 1.35 < t_{12,0.05}$ (according to Eckschlager[17], $t_{12,0.05} = 2.1788$).

[c] Base electrolyte contained also salt indicated in column *Conditions*; resulting pH = 8.7.

As shown above, the presence of large amounts of iodate (weight ratio of iodate/iodide up to $3.2 \cdot 10^5$) did not affect the determination; this fact together with the great sensitivity makes this method very suitable for the determination of iodide in iodates. Table II shows the results of the determination of iodide in three samples of iodates (Lachema, Czechoslovakia); the iodide content in all three samples was lower than limit allowed by the Czechoslovak standard[18].

TABLE II

DETERMINATION OF IODIDE IN IODATES BY ELECTROLYTICALLY GENERATED HYPOBROMITE

(5 ml of 0.25 *M* iodate solution was used. 8 determinations were done in each case in two series of 4 determinations.)

Sample	*Iodide found (μg)*	*s (μg)*	*Reliability interval (μg)*	*% iodide*	*Permitted limit*[18] *(%)*
$NaIO_3$, pure	21.95	0.50	±0.42	$8.87 \cdot 10^{-3}$	$50 \cdot 10^{-3}$
$NaIO_3$, R.G.	6.21	0.25	±0.21	$2.51 \cdot 10^{-3}$	$10 \cdot 10^{-3}$
KIO_3, pure	10.40	0.38	±0.32	$3.89 \cdot 10^{-3}$	$5 \cdot 10^{-3}$

Determination of iodine

Since very dilute standard solutions of iodine are difficult to prepare, the determination of iodine by coulometric titration with hypobromite was compared with the results of iodimetric titrations in which an excess of standard arsenite solution was added to the iodine sample, and the solution was back-titrated coulometrically with iodine. This was very convenient for small amounts of iodine; for larger amounts of iodine, volumetric and coulometric back-titrations were done, and results were identical in all cases.

The results showed that under slightly alkaline conditions (pH 8.7), iodine was oxidized with hypobromite according to the overall equation:

$$I_2 + 5\,BrO^- + 2\,OH^- \rightarrow 2\,IO_3^- + 5\,Br^- + H_2O \qquad (2)$$

The results were therefore evaluated on this basis. The indicating current was similar to that observed in the analogous titrations of iodide. Similarly, it was found that the overall reaction (2) was relatively slow so that small currents were suitable for continuous generation of hypobromite.

Table III summarizes the results obtained over a wide range of iodine concentrations at optimal values of the generating and preset indicating currents; the calculated values of the F- and t-tests and the corresponding critical values[17] are also given. The fact that the average results obtained by the two methods are in agreement (the calculated values of the t-test were in all cases lower than the critical value) indicates that the results of the determinations are correct. The variance of the results for small amounts of iodine (24–80 μg) was significantly smaller in the hypobromite titrations than in the iodimetric titrations. For larger amounts of iodine, the calculated F-values were smaller than the critical values, but the difference was not large. The standard deviations were always smaller in the hypobromite titrations. It can be concluded that the coulometric titration

TABLE III

COMPARISON OF RESULTS FOR IODINE BY ELECTROLYTICALLY GENERATED HYPOBROMITE AND BY COULOMETRIC BACK-TITRATION

Hypobromite titration						*Iodimetric back-titration*[1]						*Statistical criteria*			
I_2 found (μg)	*n*	*s (μg)*	*Reliab. interval (μg)*	*Current*		*I_2 found (μg)*	*n*	*s (μg)*	*Reliab. interval (μg)*	*Current*		*F*	*Critical value $F_{\nu_1,\nu_2,\alpha/2}$*	*t*	*Critical value $t_{\nu,\alpha}$ resp. K*
				Gen. (mA)	*Ind.[j] (μA)*					*Gen. (mA)*	*Ind.[k] (μA)*				
3311[a]	7	12.7	±11.7	15	0.50	3303	7	19.6	±18.0	5.0	0.20	2.38	4.28	0.91	2.179
2496[a,h]	7	10.7	± 9.8	20	0.10	2494	7	17.4	±16.0	10	0.10	2.64	4.28	0.26	2.179
2498[a,h]	7	11.9	±11.0	12	0.50	2499	7	18.2	±16.7	4.0	0.10	2.34	4.28	0.12	2.179
716.3[a]	9	2.99	± 2.30	10	0.10	718.0	8	5.23	± 4.40	2.0	0.10	3.06	3.50	0.84	2.132
217.7[b]	8	1.33	± 1.12	4.0	0.10	216.7	9	2.29	± 1.76	1.5	0.06	2.97	3.73	1.08	2.132
80.09[c]	8	0.58	± 0.49	1.5	0.06	79.63	9	1.16	± 0.89	1.0	0.04	4.00	3.73	1.05	2.319
24.26[d]	9	0.47	± 0.36	1.0	0.04	24.60	9	1.01	± 0.78	1.0	0.04	4.62	3.44	0.92	2.306
61.93[c,i]	8	0.51	± 0.43	1.5	0.08										
62.37[c,e,i]	8	0.70	± 0.59	1.5	0.08							1.88	3.79	1.44	2.145
61.57[c,f,i]	8	0.63	± 0.53	1.5	0.08							1.53	3.79	1.26	2.145
61.97[c,g,i]	8	0.67	± 0.56	1.5	0.08							1.73	3.79	0.13	2.145

[a] Sample prepared in R.G. methanol. [b] Sample prepared in 10% methanol. [c] Sample prepared in 3% methanol. [d] Sample prepared in 1% methanol. [e] Base electrolyte contained also 0.01 *M* KIO_3. [f] Base electrolyte contained also 0.05 *M* $KBrO_3$. [g] Base electrolyte contained also 0.05 *M* K_2CrO_4; F- and t-values calculated for hypobromite titration with and without added salt. [h] The same sample. [i] The same sample. [j] 150 mV between indicating electrodes. [k] 50 mV between indicating electrodes. [l] 150–200% excess of As(III) used.

of iodine with hypobromite is a more precise method, especially when small amounts of iodine are to be determined.

The presence of a large amount of iodate in the base electrolyte (iodate/iodine ratios up to $3.1 \cdot 10^3$) did not influence the precision or the accuracy of the hypobromite method. Similarly, there was no interference from large amounts of bromate (bromate/iodine ratios up to $1.1 \cdot 10^4$) or chromate (chromate/iodine ratios up to $1.0 \cdot 10^4$).

DISCUSSION

The variation of the indicating current of the coulometric determination of iodide and iodine with hypobromite, together with the relatively slow rate of reactions (1) and (2) and the large number of electrons necessary for the oxidation of 1 mole of the titrated substance, shows that the overall oxidation is a complex process. The iodine determined (as well as the iodine formed by oxidation of iodide) undergoes a disproportionation reaction in weakly basic solutions:

$$I_2 + OH^- \overset{K_3}{\rightleftharpoons} HIO + H_2O \qquad (3)$$

the equilibrium constant[19] of which $K_3 = [IO^-][I^-]/[I_2][OH^-]^2 = 30$. Reaction (3) is fast[20] ($k_3 = (0.5\text{–}1) \cdot 10^{10}$ l mol^{-1} s^{-1}). The hypoiodite formed at room temperature immediately reacts further[19]:

$$3\,IO^- \overset{K_4}{\rightleftharpoons} 2\,I^- + IO_3^- \qquad (4)$$

The equilibrium constant $K_4 = 10^{20}$ favours iodide and iodate formation[19]. At a high concentration of bromide, the stability of the monopositive iodine oxidation state is considerably higher, and the concentration of IBr becomes real. However, the concentration of I^+ is negligible in the absence of bromide (at *ca.* pH 9 the predominant form of I^+ would be HIO with a pK_a value[19] of 11). As a result of reaction (4) the equilibrium of the reaction:

$$IBr + OH^- \rightleftharpoons Br^- + HIO \qquad (5)$$

is shifted to the right.

According to a number of authors, electrochemical oxidation of iodide in acidic, neutral and slightly alkaline solutions proceeds in maximally three oxidation steps[20–22]. The first step corresponds to the oxidation of iodide to iodine and the second to the further oxidation to hypoiodite. In a solution of pH 7–9 the kinetic nature of the second step alters gradually, and the wave is shifted to more negative values with increasing pH. At pH 9 it coincides with the first step, which is unaffected by pH, having an $E_{\frac{1}{2}}$ value of +0.5 V *vs.* SCE; the total wave is diffusion-controlled. Based on these observations, the second step probably proceeds as follows:

$$2(I_2 + H_2O \rightleftharpoons HIO + H^+ + I^-) \qquad (6a)$$

(a chemical reaction below pH 9 determining the rate of the overall electrode oxidation)

$$2\,I^- - 2\,e \Rightarrow I_2 \qquad (6b)$$

(a fast electrode reaction proper)

The overall electrode reaction is the sum of (6a) and (6b):

$$I_2 + 2\ H_2O - 2\ e \rightleftharpoons 2\ HIO + 2\ H^+ \qquad (6c)$$

The third oxidation step produces iodate[20–22] and at *ca.* pH 9 proceeds at potentials 500 mV more positive than does the second oxidation step[20].

From the relatively low positive potential of the electrode oxidation of iodide to the second step, it can be assumed that even in the coulometric titration of iodide and iodine with electrolytically generated hypobromite, the oxidation proceeds directly at the generating electrode with formation of IBr. The oxidation mechanism is probably the same in the coulometric determinations of iodide and iodine, because at about pH 9 the solution of iodine always contains iodide (eqn. 3) which is oxidized directly at the electrode; this suggestion is supported by the similar shape of the biamperometric titration curves in both cases. Hence, the redox system controlling the indicating current is the system I_3^-/I_2, and the indicating current is relatively small because the concentration of at least one component of this system is low during the analysis.

The direct oxidation effect of the electrode in the partial oxidation process most probably accounts for the sufficiently high rate of the overall oxidation reaction in the coulometric determination; the direct volumetric titration of iodide is slow and cannot be accomplished unless special precautions are taken[23,24].

Best results for the coulometric determination of iodide and iodine with hypobromite can be obtained when small (submilligram) amounts of iodide or iodine are present. When larger quantities are present, the pH of the solution changes after several runs. The pH 8.7 found to be optimal here agrees with the pH values for determinations of other reducing substances with electrolytically generated hypobromite: pH 8.5–8.9 for the determination of ammonia[25–27]; pH 8.2 for peroxide[28]; pH 8.5 for thiocyanate and β-mercaptocarboxylic acids[29]; pH 8.9 for cyanide[30]; and pH 8.3–11 in a study of the current efficiency for the generation of hypobromite[15].

The proposed coulometric determinations of iodide and iodine have several advantages. They are simple; no special preparation of the working electrode is necessary, unlike the determination of iodide with electrolytically generated mercury(I). The determination, in contrast to the determination of iodine with electrolytically generated tin(II), does not require an inert atmosphere. The methods are considerably more sensitive than the procedures based on silver(I)[1–3], cerium(IV)[6] or manganese(III)[7] for iodide, or the tin(II) method[10–13] for iodine. The sensitivity is similar to that of coulometric titrations of iodide in acidic solutions with mercury(II)[4,5] or bromine[8].

The accuracy and the precision of the results is ensured by the practically 100% current efficiency of hypobromite generation under optimal conditions[15]. In contrast, the current efficiency of the generation of tin(II) observed in the determination of iodine is lower[11,12]. The biamperometric indication used, with a preselected level of indicating current, makes the method suitable for routine analyses and automation.

The presence of Cl^-, Br^-, IO_3^-, BrO_3^-, and CrO_4^{2-} ions, even in high concentrations, does not interfere. This again is in contrast to the other coulometric methods mentioned above where halides or oxidizing agents interfere.

The proposed method was successfully applied to the determination of iodide in commercial samples of potassium iodate, sodium iodate and iodized salt. The procedure was simpler in the last case (the amount of iodide in 2-ml samples containing 4 *M* sodium chloride was determined), and was more sensitive than, for instance, the polarographic method[31].

Although the coulometric oxidation involved in the iodimetric determination of iodine by back-titration of a standard arsenic(III) solution was found to be more complicated and less accurate than the method based on hypobromite, it can be used and combined with the determination with hypobromite when a mixture of iodide and iodine has to be analyzed. The titration with hypobromite provides the sum of iodide and iodine and the amount of iodine is determined in a separate run by iodimetry.

SUMMARY

Conditions for the quantitative coulometric titration of iodide and iodine with electrolytically generated hypobromite in the presence of borax buffer have been established. Iodide and iodine are oxidized to iodate. The method, with biamperometric indication of the equivalence point, was successfully applied for a wide range of iodide concentrations (6.21–2115 μg with reliability intervals of ± 0.21–± 11 μg) and iodine concentrations (24.26–3311 μg with reliability intervals of ± 0.36–± 11.7 μg). The determinations are accurate and sensitive even in the presence of large amounts of bromides and chlorides ($Br^-/I^- = 1.2 \cdot 10^6$ and $Cl^-/I^- = 4.0 \cdot 10^3$), as well as in the presence of oxidizing agents such as IO_3^-, BrO_3^- and CrO_4^{2-} ($IO_3^-/I^- = 3.2 \cdot 10^5$, $IO_3^-/I_2 = 3.1 \cdot 10^3$, $BrO_3^-/I_2 = 1.1 \cdot 10^4$ and $CrO_4^{2-}/I_2 = 1.0 \cdot 10^4$), as was confirmed by statistical tests. The oxidation mechanism under the conditions of coulometric titrations is discussed.

REFERENCES

1 J. J. Lingane, *Anal. Chem.*, 26 (1954) 622.
2 R. L. Kowalkowski, J. H. Kennedy and P. S. Farrington, *Anal. Chem.*, 26 (1954) 626.
3 P. S. Tutundzić, J. Doroslovački and O. Tatić, *Anal. Chim. Acta*, 12 (1955) 481.
4 E. P. Przybylowicz and L. B. Rogers, *Anal. Chem.*, 28 (1956) 799.
5 D. D. De Ford and H. Horn, *Anal. Chem.*, 28 (1956) 797.
6 J. J. Lingane, C. H. Langford and F. C. Anson, *Anal. Chim. Acta*, 16 (1957) 165.
7 P. S. Tutundzić, N. M. Paunović and M. M. Paunović, *Anal. Chim. Acta*, 22 (1960) 345.
8 W. S. Wooster, P. S. Farrington and E. H. Swift, *Anal. Chem.*, 21 (1949) 1457.
9 H. H. Stein, *Dissert. Abstr.*, 16 (1956) 2326; *Chem. Abstr.*, 51 (1957) 8576c.
10 A. J. Bard and J. J. Lingane, *Anal. Chim. Acta*, 20 (1959) 463.
11 T. Takahashi and H. Sakurai, *Talanta*, 9 (1962) 74.
12 H. Sakurai, J. Chem. Soc. *Jap., Ind. Chem. Sect.*, 64 (1961) 2121.
13 S. Suzuki, J. Chem. Soc. *Jap., Ind. Chem. Sect.*, 64 (1961) 2112.
14 H. A. Laitinen, *Chemical Analysis*, Chimiya, Moscow, 1966, p. 475.
15 L. B. Agasyan, E. P. Nikolaeva and P. K. Agasyan, *Vestn. Mosk. Goss. Inst., Ser. Khim.*, 5 (1966) 96.
16 J. Čihalík, *Potenciometrie*, Publishing House of the Czechoslovak Academy of Sciences, Prague, 1961.
17 K. Eckschlager, *Chyby chemických rozborů (Errors in Chemical Analysis)*, SNTL, Prague, 1971.
18 *Czechoslovak State Standard 684917* (for KIO_3); *684918* (for $NaIO_3$).
19 F. A. Cotton and G. Wilkinson, *Advanced Inorganic Chemistry*, Czech Edn., Academia. Prague, 1973, pp. 554, 555.

20 M. Eigen and K. Kustin, *J. Amer. Chem. Soc.*, 84 (1962) 1355.
21 G. Dryhurst and P. J. Elving, *Anal. Chem.*, 39 (1967) 606.
22 F. J. Miller and H. E. Zittel, *J. Electroanal. Chem.*, 11 (1966) 85.
23 H. H. Willard and F. Fenwick, *J. Amer. Chem. Soc.*, 45 (1923) 623.
24 O. Tomíček and P. Filipovič, *Chem. Listy*, 32 (1938) 410; *Collect. Czech. Chem. Commun.*, 10 (1938) 340.
25 G. M. Arcand and E. H. Swift, *Anal. Chem.*, 28 (1956) 440.
26 A. F. Krivis, G. S. Supp and E. S. Gazda, *Anal. Chem.*, 35 (1963) 2216.
27 G. D. Christian, E. C. Knoblock and W. C. Purdy, *Anal. Chem.*, 35 (1963) 2217.
28 F. J. Feldman and R. E. Bosshart, *Anal. Chem.*, 38 (1966) 1400.
29 R. J. Palma, H. K. L. Gupta and D. F. Boltz, *Anal. Lett.*, 4 (1971) 277.
30 J. Mocák, D. I. Bustin and M.Žiaková, *Chem. Zvesti*, 26 (1972) 126.
31 J. V. A. Novák in J. Heyrovský and P. Zuman, *Introduction to Practical Polarography*, Czech Edn., Publishing House of the Czechoslovak Academy of Sciences, Prague, 1953, p. 146; *Collect. Czech. Chem. Commun.*, 19 (1954) 177.

Analytica Chimica Acta, 76 (1975) 443–451

COMPLEXIMETRIC BACK-TITRATIONS BASED ON 1:2 METAL–LIGAND COMPLEX FORMATION

G. J. VAN ROSSUM and G. DEN BOEF

Laboratory for Analytical Chemistry, University of Amsterdam, Nieuwe Achtergracht 166, Amsterdam (The Netherlands)

(Received 12th November 1974)

In a previous paper[1], a qualitative explanation and also some examples were given of back-titrations of metal ions involving 1:2 metal–ligand complex formation, with linear end-point indication. In the present paper a mathematical treatment is given for the determination of a metal N with a ligand L by back-titration with a metal M, involving the formation of NL, NL_2, ML and ML_2 and making use of linear end-point indication. Back-titrations have advantages over direct titrations when the reaction between N and L is slow, and when the end-point of this reaction cannot be indicated or can only be indicated at large concentrations.

Linear indication is indispensable for titrations based on 1:2 complex formation, as logarithmic methods, such as potentiometry or the use of metallochromic indicators, seldom give good results in such cases.

MATHEMATICAL EXPRESSIONS

The symbols used are the same as in previous papers[1,2] on this subject.

It is assumed that the volume does not change during the titration. For the mathematical treatment it is also assumed that all reactions are sufficiently rapid for equilibrium to be attained within a reasonable time.

The analytical concentration of the metal ions M and N and of the ligand L are c_M, c_N and c_L. The conditional stability constants of the stepwise complex formation processes are: K'_{NL}, K'_{NL_2}, K'_{ML} and K'_{ML_2}. To facilitate the mathematical treatment, the following dimensionless quantities are introduced:

(a) relative concentrations

$$l = [L]/c_L;\ m = [M]/c_L;\ ml = [ML]/c_L;\ ml_2 = [ML_2]/c_L$$

$$n = [N]/c_N;\ nl = [NL]/c_N;\ nl_2 = [NL_2]/c_N$$

(b) $$Z_{NL} = K'_{NL}c_L = nl/n \cdot l \quad (1)$$

$$Z_{NL_2} = K'_{NL_2}c_L = nl_2/n \cdot l \quad (2)$$

$$Z_{ML} = K'_{ML}c_L = ml/m \cdot l \quad (3)$$

$$Z_{ML_2} = K'_{ML_2}c_L = ml/ml \cdot l \quad (4)$$

(c) the titration parameter $f = c_M/c_L$.

The following mass balances hold:

$$l+ml+2ml_2+[(nl+2nl_2)c_N/c_L]=1 \tag{5}$$

$$n+nl+nl_2=1 \tag{6}$$

$$m+ml+ml_2=c_M/c_L=f \tag{7}$$

The equations (1)–(7) are the seven basic equations from which the dependence of the relative concentrations on the titration parameter can be found.

The most convenient way to represent the relationship between the titration parameter f and the relative concentrations is by means of a parameter representation, with l as the parameter. This results in:

$$f=\left[1-l-\frac{c_N}{c_L}\left(\frac{Z_{NL_2}l+2lZ_{NL}Z_{NL_2}l^2}{1+Z_{NL}l+Z_{NL}Z_{NL_2}l^2}\right)\right]\left[\frac{1+Z_{ML}l+Z_{ML}Z_{ML_2}l^2}{Z_{ML}l+2Z_{ML}Z_{ML_2}l^2}\right] \tag{8}$$

$$m=\frac{1}{1+Z_{ML}l+Z_{ML}Z_{ML_2}l^2}f \tag{9}$$

$$ml=\frac{Z_{ML}l}{1+Z_{ML}l+Z_{ML}Z_{ML_2}l^2}f \tag{10}$$

$$ml_2=\frac{Z_{ML}Z_{ML_2}l^2}{1+Z_{ML}l+Z_{ML}Z_{ML_2}l^2}f \tag{11}$$

$$n=\frac{1}{1+Z_{NL}l+Z_{NL}Z_{NL_2}l^2} \tag{12}$$

$$nl=\frac{Z_{NL}l}{1+Z_{NL}l+Z_{NL}Z_{NL_2}l^2} \tag{13}$$

$$nl_2=\frac{Z_{NL}Z_{NL_2}l^2}{1+Z_{NL}l+Z_{NL}Z_{NL_2}l^2} \tag{14}$$

The quantities which determine the shapes of the titration curve are Z_{ML}, Z_{ML_2}, Z_{NL}, Z_{NL_2} and c_N/c_L. Therefore it is useful to classify the different types of titration curves with respect to the relative magnitude of the Z values involved. The large number of types of titration curves which then theoretically follows from eqns. (8)–(14), is very much reduced by taking into account that, for 1:2 complex formation, $Z_1 > Z_2$ generally[3].

In the present case of compleximetric back-titration involving 1:2 complex formation, this results in only 13 possibilities for the relative magnitude of the Z values. These are given in Table I. Without the restriction $Z_1 > Z_2$, the number of possibilities would be 75. This illustrates the importance of this general property of consecutive complex formation for the simplification of the treatment of these complicated titration procedures.

Figure 1 presents an example of each of the six cases mentioned in Table I for which all Z values differ at least one order of magnitude. A minimal value for Z_{ML_2} of 100 has to be adopted, as this is a requirement for good end-points in 1:2 complex formation titrations[1] by means of ML_2. All titration curves were

TABLE I

POSSIBLE RELATIVE MAGNITUDES OF Z VALUES[a]

1.	$Z_{NL} > Z_{NL_2} > Z_{ML} > Z_{ML_2}$	8.	$Z_{NL} > Z_{ML} > Z_{NL_2} \simeq Z_{ML_2}$
2.	$Z_{NL} > Z_{ML} > Z_{NL_2} > Z_{ML_2}$	9.	$Z_{NL} \simeq Z_{ML} > Z_{NL_2} > Z_{ML_2}$
3.	$Z_{NL} > Z_{ML} > Z_{ML_2} > Z_{NL_2}$	10.	$Z_{NL} \simeq Z_{ML} > Z_{NL_2} \simeq Z_{ML_2}$
4.	$Z_{ML} > Z_{NL} > Z_{ML_2} > Z_{NL_2}$	11.	$Z_{ML} > Z_{NL} > Z_{NL_2} \simeq Z_{ML_2}$
5.	$Z_{ML} > Z_{NL} > Z_{NL_2} > Z_{ML_2}$	12.	$Z_{NL} \simeq Z_{ML} > Z_{ML_2} > Z_{NL_2}$
6.	$Z_{ML} > Z_{ML_2} > Z_{NL} > Z_{NL_2}$	13.	$Z_{ML} > Z_{NL} \simeq Z_{ML_2} > Z_{NL_2}$
7.	$Z_{NL} > Z_{NL_2} \simeq Z_{ML} > Z_{ML_2}$		

[a] For practical use, > means a difference of at least one order of magnitude, which is usually the case for K_1 and K_2 in stepwise complex formation; $\simeq$ means the same order of magnitude.

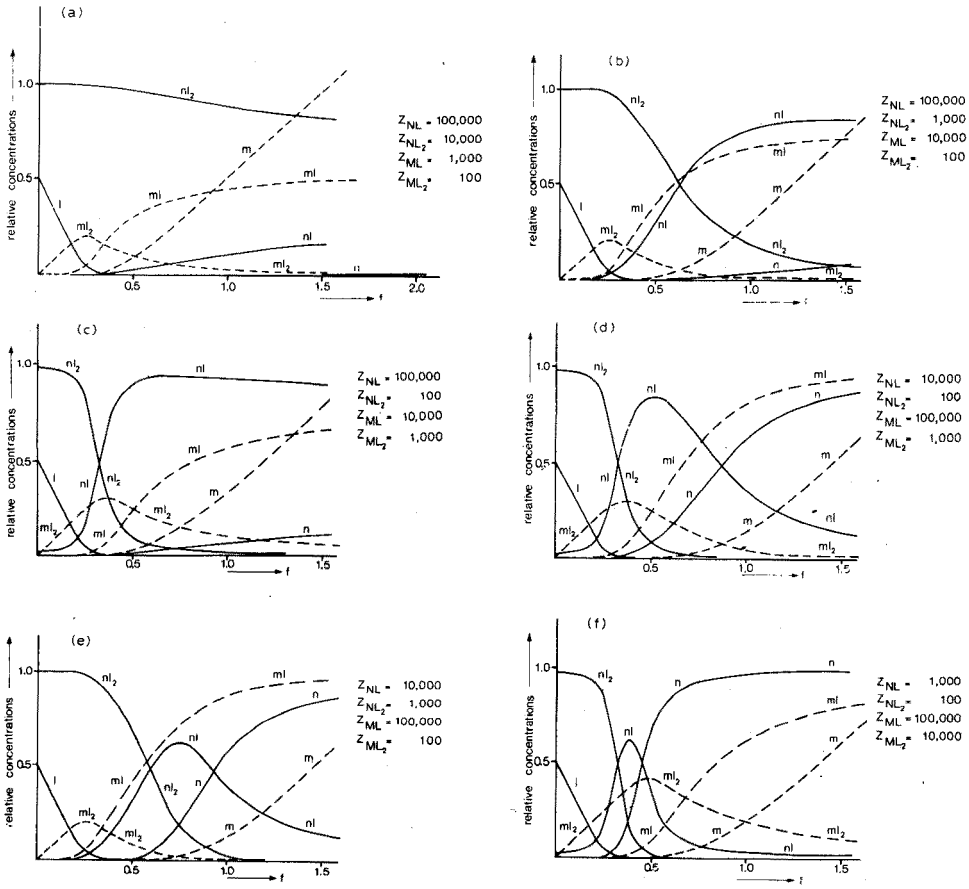

Fig. 1. Theoretical titration curves, f *vs.* reduced concentrations, when all Z values differ by at least one order of magnitude. Figs. a–f refer to cases 1–6 in Table I; $c_N/c_L = 0.25$.

calculated from eqns. (8)–(14) by means of a desk computer. Indication of the end-point by means of NL or NL_2 need not be taken into consideration as a direct titration procedure would then be simpler. The indication by means of L might be

interesting analytically when the complex formation of N with L is slow, but then the curves mentioned in Fig. 1 cannot be used because in the back-titration the reaction mixture will not attain equilibrium. Therefore the discussion will be restricted to linear indication by means of M, ML and ML_2. An exact treatment of the titration curves is very cumbersome, hence only a few cases will be discussed, in which certain conditions for the Z values are fulfilled.

The f–ml_2 curve

Any f–ml_2 curve can be constructed by means of eqns. (8) and (11). It consists of a rising part before the first end-point and a descending branch after the first end-point. Under certain circumstances a second end-point occurs at the intersection of the descending branch and the horizontal branch for larger f values. This second end-point will not be considered.

The f value at which the first end-point occurs depends on the relative magnitude of the Z values.

The concentration of L at the start of the back-titration is $c_L - 2c_N$, provided that NL_2 is completely formed. The addition of M will then result in the formation of ML_2 until all free L is consumed. Then the value of f is

$$f = \frac{1}{2} - \frac{c_N}{c_L}$$

The solution then consists approximately, of a mixture of ML_2 and NL_2. What happens on further addition of M will depend on the several values of Z. A few cases will be treated in more detail.

$Z_{NL_2} \geqslant Z_{ML_2}$. When $Z_{NL_2} \gg Z_{ML_2}$ further addition of M will break up ML_2 according to

$$M + ML_2 \rightleftarrows 2\ ML$$

resulting in a sharp decrease of ML_2. An end-point occurs at $f = 1/2 - c_N/c_L$. When Z_{NL_2} and Z_{ML_2} have about the same value, the corresponding compounds will be broken up simultaneously, which also results in a break in the f–ml_2 curve, though less sharp. So an end-point again occurs at $f = 1/2 - c_N/c_L$.

$Z_{ML_2} \gg Z_{NL_2}$. In this case NL_2 will be broken up first. It is obvious to consider first the reaction

$$M + NL_2 \rightleftarrows ML + NL \qquad (a)$$

The equilibrium constant of this reaction is K_{ML}/K_{NL_2}. This constant is very large as K_{ML_2} is already supposed to be much larger than K_{NL_2} and $K_{ML} > K_{ML_2}$. So reaction (a) proceeds to the right-hand side. It will however be followed by

$$ML + NL_2 \rightleftarrows ML_2 + NL \qquad (b)$$

the equilibrium constant of this reaction being K_{ML_2}/K_{NL_2} which is supposed to be very large. So the net reaction occurring after $f = 1/2 - c_N/c_L$ will be

$$M + 2\ NL_2 \rightarrow ML_2 + 2\ NL \qquad (c)$$

The result is a further increase of the concentration of ML_2 at least until reaction (c) is completed, which is at $f = 1/2(1 - c_N/c_L)$. The reaction mixture then consists of

ML_2 and NL. Further addition of M will break up the weaker of these complexes. When the reaction

$$M + ML_2 \rightleftarrows 2ML \qquad (d)$$

is considered first, it is obvious that the equilibrium is to the right-hand side, as the equilibrium constant of (d) is K_{ML}/K_{ML_2}. The question, however, is whether ML can break up NL by

$$ML + NL \rightleftarrows ML_2 + N \qquad (e)$$

The equilibrium constant of this reaction is K_{ML_2}/K_{NL}. So when $K_{ML_2} > K_{NL}$, reaction (e) will proceed to the right, resulting in the net reaction after $f = 1/2\text{-}(1 - c_N/c_L)$

$$M + 2NL \rightleftarrows ML_2 + 2N \qquad (g)$$

This reaction is completed at $f = 1/2$. Then a solution containing ML_2 and N results. Further addition of M breaks up ML_2 resulting in an end-point at $f = 1/2$, which in fact has no analytical relevance as it does not allow the determination of c_N. When, however, $K_{NL} > K_{ML_2}$ the equilibrium (e) lies to the left and the net reaction after $f = 1/2(1 - c_N/c_L)$ is reaction (d) to the right-hand side. This results in a decrease in the concentration of ML_2 and an analytically useful end-point at this value of f. When K_{NL} and K_{ML_2} have approximately the same value, an ill-defined break may occur at this same value of f, as ML_2 will hardly change on further addition of M.

The results of this section are summarized in Table II.

TABLE II

CONDITIONS FOR SHARP END-POINTS WITH LINEAR INDICATION BY ML_2

Condition	*Type*	*End-point*
$Z_{NL_2} \geqslant Z_{ML_2}$	1	$f = \frac{1}{2} - \frac{c_N}{c_L}$
$Z_{NL} \geqslant Z_{ML_2} > Z_{NL_2}$	2	$f = \frac{1}{2}\left(1 - \frac{c_N}{c_L}\right)$
$Z_{ML_2} > Z_{NL}$	3	$f = \frac{1}{2}$(irrelevant)

Notes. In practice, the titration curves will be rounded off near the end-points. The larger the ratios of the different Z values, the sharper the break-points will be.

When Z_{NL_2} is very small, so that NL_2 is incompletely formed even when L is present in excess, the end-point at $f = 1/2(1 - c_N/c_L)$ still occurs provided again that $Z_{NL} > Z_{ML_2}$. This can easily be confirmed according to the same reasoning. An illustration of this case will be given in the Results section. It must be repeated however that under all circumstances Z_{ML_2} should be at least 100.

The f–ml curve

Any *f–ml* curve can be constructed by means of eqns. (8) and (10). It consists of a horizontal part coinciding with the *f*-axis before the end-point and a rising branch after the end-point. It can be seen easily that the conditions for sharp end-points by linear indication by ML are exactly those mentioned in Table II for ML_2.

The f–m curve

The *f–m* curve can be constructed by means of eqns. (8) and (9). It consists of a horizontal part coinciding with the *f*-axis before and a rising part after a possible end-point. Linear indication by means of M will only be of practical significance in these complicated systems. In most cases, photometric or fluorimetric indication will be applied, making use of signals caused by the ligand or its complexes. Furthermore, the conditions necessary for a successful linear indication by means of M are rarely fulfilled. In any case, M should not be able to break up NL, which means that Z_{NL} should be larger than Z_{ML}. Moreover, only $Z_{ML} \gg Z_{ML_2}$ results in sharp end-points. Because of its lack of analytical usefulness, this case will not be considered further.

EXPERIMENTAL

In order to illustrate the theoretical considerations, some photometric back-titrations were carried out of metal ions with pyridine-2,6-dicarboxylic acid (DPA) as the ligand. The reactions are fast and the complexes of certain metal ions exhibit very suitable absorbances for photometric indication.

Titration curves were recorded semi-automatically with a Zeiss PMQ II spectrophotometer provided with a MM 12 monochromator, a titration cell of 2-cm path length and a Telsec recorder. The Metrohm E457 burette was equipped with a stepping motor and an electronic device for synchronizing the burette and the recorder, as developed by Poppe[4].

Analytical-grade reagents and deionized water were used throughout the experiments.

The stability constants of the complexes of the ligand DPA with some metal ions, taken from the literature[5], are given in Table III. Other stability constants necessary for the calculations of side-reaction coefficients were also taken from the literature[5].

TABLE III

STABILITY CONSTANTS OF METAL ION COMPLEXES OF DPA

Metal ion	$\log \beta_1$	$\log \beta_2$
Cd(II)	6.75	11.15
Co(II)	6.65	12.70
Cu(II)	9.14	16.52
Pb(II)	8.70	11.60
Zn(II)	6.35	11.88
H^+	4.68	6.78

All the experiments were carried out in a 0.1 M acetate buffer of pH 5.3. At this pH value, side reactions of the metal ions and the ligand occur only to a slight extent, which allows the determination of the lowest possible concentrations of metal ions with this ligand. In all examples a 100% excess of the ligand was added with respect to the formation of NL_2 and the change in absorbance during the back-titration was about 0.05. With the available equipment, results near the limit of determination are then obtained.

RESULTS

The examples follow the three cases mentioned in Table II.

$Z_{NL_2} \geq Z_{ML_2}$ (*Type 1*)

Figure 2 illustrates the photometric titration at 360 nm and pH 5.3 of $2.5 \cdot 10^{-5}$ M copper(II) with cobalt(II) as the back-titrant; $c_L = 10^{-4}$ M. Under the experimental conditions $Z_{CuL} = 12{,}600$, $Z_{CuL_2} = 1{,}950$, $Z_{CoL} = 160$ and $Z_{CoL_2} = 90$, the value of Z_{ML_2} is just large enough to allow an end-point determination. At 360 nm the light absorption by CoL_2 prevails over the other compounds present in the solution. The equivalence point should theoretically occur at $f = 1/2 - c_N/c_L = 0.250$. Figure 2(a) gives the seven theoretical curves, f *vs.* reduced concentrations, and Fig. 2(b) gives the experimental titration curve, which closely corresponds to the theoretically expected curve.

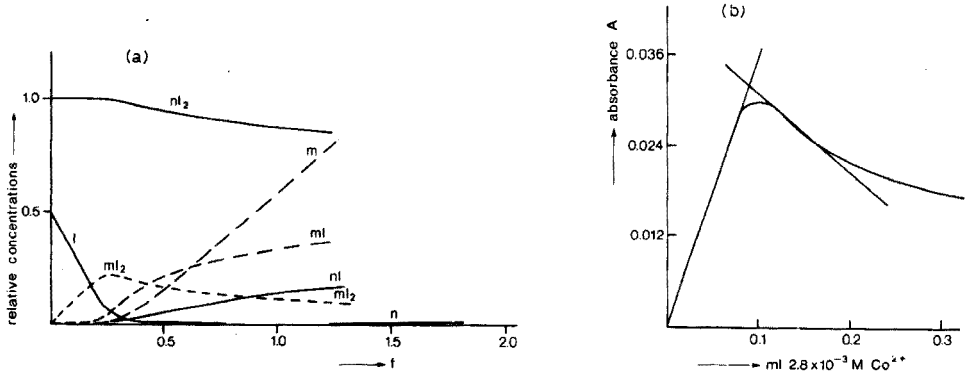

Fig. 2. Theoretical titration curves (a) and experimental photometric titration curve (b) for back-titration of $2.5 \cdot 10^{-5}$ M copper(II) (N). Back-titrant cobalt(II) (M). pH 5.3; $c_L = 10^{-4}$ M; $Z_{CuL} = 12{,}600$; $Z_{CuL_2} = 1950$; $Z_{CoL} = 160$; $Z_{CoL_2} = 90$. Wavelength 360 nm.

$Z_{NL} \geq Z_{ML_2} > Z_{NL_2}$ (*Type 2*)

Figure 3 gives the photometric titration at 360 nm and pH 5.3 of $2.5 \cdot 10^{-5}$ M lead(II) with cobalt(II) as the back-titrant; $c_L = 10^{-4}$ M. Under the experimental conditions $Z_{PbL} = 2000$, $Z_{PbL_2} = 0.06$, $Z_{CoL} = 160$ and $Z_{CoL_2} = 90$. Again, absorption by CoL_2 prevails. The equivalence point is to be expected at $f = 1/2(1 - c_N/c_L) = 0.375$. Figure 3(a) gives the theoretical curves and Fig. 3(b) gives the photometric titration curve obtained experimentally. It closely agrees with theory.

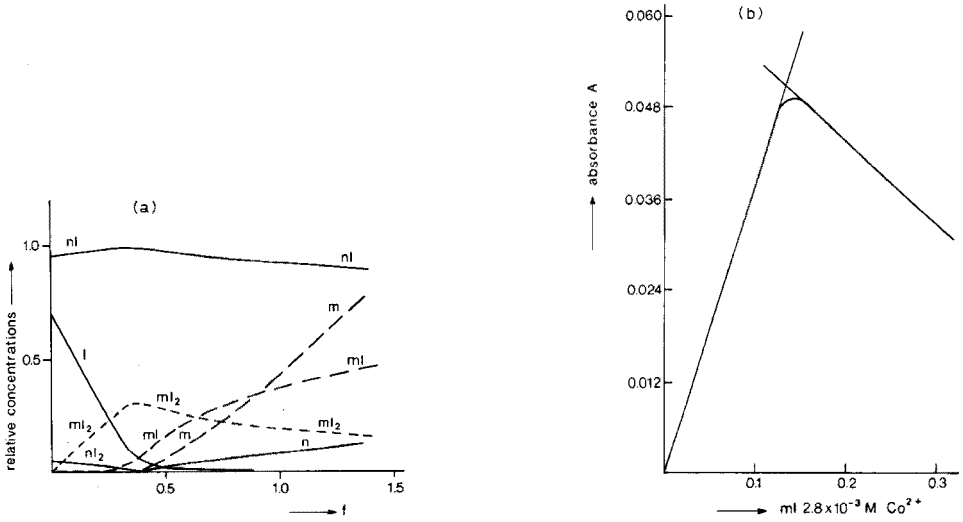

Fig. 3. Theoretical titration curves (a) and experimental photometric titration curve (b) for back-titration of $2.5 \cdot 10^{-5}$ M lead(II) (N). Back-titrant cobalt(II) (M). pH 5.3; $c_L = 10^{-4}$ M; $Z_{PbL} = 2000$; $Z_{PbL_2} = 0.06$; $Z_{CoL} = 160$; $Z_{CoL_2} = 90$. Wavelength 360 nm.

$Z_{ML_2} > Z_{NL}$ *(Type 3)*

Figure 4 gives the photometric titration at 1100 nm and pH 5.3 of $2.8 \cdot 10^{-4}$ M cobalt(II) with copper(II) as the back-titrant; $c_L = 10^{-3}$ M. The Z values are $Z_{CoL} = 1620$, $Z_{CoL_2} = 900$, $Z_{CuL_2} = 126{,}000$ and $Z_{CuL} = 19{,}500$. At 1100 nm, absorption by CuL_2 prevails. Theory and experiment give an end-point at $f = 1/2$ which is, as mentioned before, unsuitable for the determination of cobalt(II). (In a previous

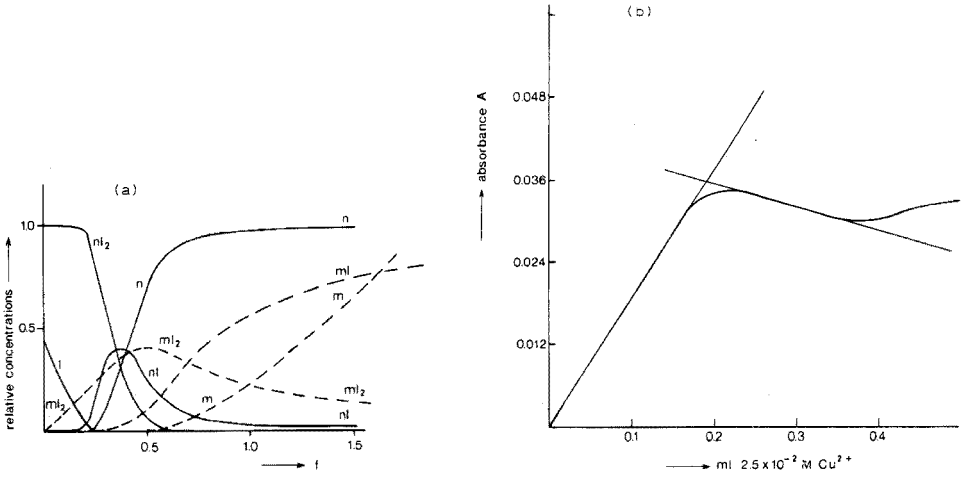

Fig. 4. Theoretical titration curves (a) and experimental photometric titration curve (b) for back-titration of $2.8 \cdot 10^{-4}$ M cobalt(II) (N). Back-titrant copper(II) (M). pH 5.3; $c_L = 10^{-3}$ M; $Z_{CoL} = 1600$; $Z_{CoL_2} = 900$; $Z_{CuL} = 126{,}000$; $Z_{CuL_2} = 19{,}500$. Wavelength 1100 nm.

paper[1], the photometric titration curve of this third example was given at 360 nm, where absorption by CoL_2 prevails.) Then an end-point at $f=1/2(1-c_N/c_L)$ is observed, which would produce the unknown concentration of cobalt(II). However, from an analytical point of view this is not very relevant either, as it would be obvious to carry out a direct determination when indication by means of CoL_2 is used.

Some other determinations with DPA were tested under similar conditions. The determination of cadmium(II) appeared to be possible by the Type 2 method with cobalt(II) as the back-titrant, again at 360 nm where absorption by CoL_2 prevails. This is in agreement with theory. The corresponding titration curve for zinc(II) appeared to be of Type 1, which does not agree with the conclusions drawn from Tables II and III. Side reactions of the metal ions or ternary complex formation obviously change the order of the different Z values.

DISCUSSION

These compleximetric back-titrations based on 1:2 metal–ligand complex formation may be of practical importance for a couple of reasons.

First, the number of ligands forming 1:2 complexes with metal ions is much larger than that of the commonly used ligands in titrimetry which give complexes of the 1:1 type. Secondly, among the known ligands of the 1:2 complex-forming type, many give intensely coloured or highly fluorescing complexes which are very suitable for photometric or fluorimetric end-point indication of titrations. The back-titration has the advantage that metal ions incapable of forming absorbing or fluorescing complexes can be tackled.

SUMMARY

Compleximetric back-titrations involving the formation of 1:2 metal–ligand complexes are discussed theoretically. The end-point indication depends not only on the magnitude of the concentration of the metal ion to be determined and the conditional stability constants of the various complexes but also on the relative magnitude of these constants. A number of cases can be distinguished, which are all illustrated experimentally.

REFERENCES

1 G. den Boef, G. J. van Rossum and F. Freese, *Anal. Chim. Acta*, 61 (1972) 297.
2 F. Freese, G. den Boef and G. J. van Rossum, *Anal. Chim. Acta*, 58 (1972) 429.
3 G. J. van Rossum and G. den Boef, *Anal. Chim. Acta*, 76 (1975) 000.
4 H. Poppe, unpublished results.
5 L. G. Sillen and A. E. Martell, *Stability Constants, Special Publication no. 17*, The Chemical Society, London, 1964; *Supplement no. 1, Special Publication no. 25*, The Chemical Society, London, 1971.

Analytica Chimica Acta, 76 (1975) 452–455

SHORT COMMUNICATION

Determination of chloride in some yttrium compounds containing silicon with a chloride-selective electrode*

N. SHIBATA, K. OSHIMA and H. KOJIMA

Central Research Laboratory, Hitachi Ltd., Kokubunji, Tokyo (Japan)

(Received 2nd October 1974)

Methods for the determination of some cations or anions are frequently facilitated by the use of ion-selective electrodes. Recently, rapid and precise methods for determining fluoride and/or chloride in some inorganic materials have been proposed[1–4]. For example, Bruton[1] reported that fluoride and chloride in calcium halophosphate could be determined simultaneously by means of known addition technique; these halides have also been determined in a calcium halophosphate phosphor which contained slightly soluble compounds[2]. In these methods[1,3,4] the sample is usually dissolved at or near room temperature to avoid volatilization of hydrogen chloride.

In this paper, a technique for the determination of chloride in slightly soluble samples such as yttrium compounds containing silicon is proposed. Some yttrium silicate compounds containing chloride were recently prepared as phosphor matrices[5]; the accurate determination of chloride in these compounds was important because they are believed to be new series of yttrium and lanthanide compounds. One of the related compounds, $Yb_3(SiO_4)_2Cl$, was reported recently[6].

Yttrium chlorosilicates are only slightly soluble in several acids near roon temperature, but were found to be soluble in phosphoric acid at 160–180°C with simultaneous evolution of hydrogen chloride. To date, there have been only a few studies on the separation of chloride by volatilization or distillation. For example, after decomposition of organic compounds by the oxygen flask method, hydrogen chloride can be evolved from 80% sulfuric acid solution at 80°C and detgrmined conductimetrically[7].

In contrast to the lack of interest in this means of separating chloride, the separation of fluoride by volatilization and/or distillation has often been studied[8]. The presence of gelatinous silica is known to retard the volatilization of fluoride[8], and it was found here that gelatinous silica also prevents volatilization of chloride. In order to solve this problem, the silicate sample was dissolved in phosphoric acid and heated to 280°C in a nitrogen atmosphere. At this temperature, some phosphate escaped into the distillate, however it actually had no effect on the determination of chloride (or fluoride (TISAB)) when ion-selective electrodes were used.

* Presented at the Pittsburgh Conference on Analytical Chemistry and Applied Spectroscopy, 4–8 March 1974, Cleveland Convention Center, Cleveland, Ohio, U.S.A.

Experimental

Apparatus. For the separation of chloride, the steam-distillation apparatus shown in Fig. 1 was used. The nitrogen stream was controlled so as to avoid spattering any silicic acid deposits on the glass walls.

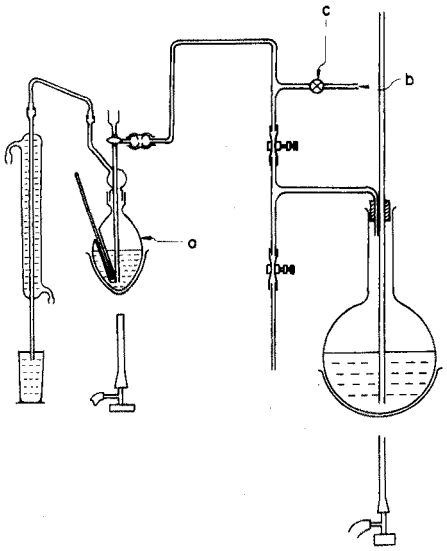

Fig. 1. Steam-distillation apparatus; (a) quartz flask; (b) nitrogen inlet; (c) needle valve.

Potentials between a Corning No. 476126 solid-state chloride electrode and a silver–silver chloride reference electrode (Corning No. 476029), thermostatted at 25.0±0.2°C, were measured on a Corning Model 12 expanded scale pH meter. As a double junction, a potassium nitrate-saturated agar-agar bridge was used. Chloride sample solutions were placed in 50-ml Teflon beakers and stirred rapidly, but without bubbles, with a small Teflon-encapsulated stirring bar positioned close to the electrode membrane.

Reagents. All the reagents used were of guaranteed grade. Elving's prescription[9] was used for the preparation of constant ionic strength buffer solution, but potassium nitrate was used in place of sodium chloride.

The sodium chloride standard solutions were prepared from a 1000 p.p.m. chloride stock solution. The chloride test solutions were made up by diluting to 200 ml after 20 ml of the constant ionic strength buffer solution had been added to some distillates. The pH value and the ionic strength of the solutions were 3 and 0.2 *M* respectively. A series of chloride standard solutions was made up in the same way.

Procedure. Transfer 50 mg of sample to the quartz flask. Add 20 ml of concentrated phosphoric acid, and heat the solution. After the sample has dissolved completely, pass a nitrogen stream through the solution as gently as possible (about 50 ml min^{-1}). Raise the temperature of the solution to 280°C and maintain this temperature until water drops can hardly be observed on the upper

part of the condenser. Cool to 120°C, and steam-distil at 180°C. Collect 150 ml of the distillate, add 20 ml of the buffer solution, and dilute the solution to 200 ml exactly. Transfer an aliquot of the solution to the Teflon beaker. Insert the electrodes and when they have reached equilibrium, read the potential in mV.

Minor changes in pH and ionic strength had no effect on the electrode potentials when Elving's constant ionic strength buffer solution was used; this contained a large quantity of phosphate ions[2]. During the distillation of chloride a considerable amount of phosphate escaped into the distillate, but its effect on the electrode potential was negligible.

About 2 h were required for each determination.

Results

Recovery of chloride by steam distillation. In preliminary tests, 50 mg of yttrium silicate was dissolved in 20 ml of phosphoric acid, 4.0 ml of the chloride standard solution (1000 p.p.m. Cl) was added, and the mixture was steam-distilled at 150°C. The recoveries of chloride ranged from 22% to 65.5%, because of adsorption of the chloride by the gelatinous silica deposits.

In order to increase the recoveries of chloride, a volatilization process was added to the steam-distillation process. In this procedure, silicic acid deposits were observed for volatilization temperatures of 200°C and the recoveries of 4 ml of 1000 p.p.m. chloride solution were low (55.5%). The deposits could be dissolved above 230°C, and recovery of chloride then improved to 95.5%, but if the deposits remained on the glass wall of the flask, recoveries decreased to 72.5%. In order to reduce the quantity of water, 0.4 ml of a 10,000 p.p.m. chloride solution was used, but this proved ineffective. At 300°C, volatilization of phosphoric acid increased markedly.

Effect of dehydrating conditions on recovery of chloride. When a dehydration process was added to the volatilization process, in order to reduce the water content in the phosphoric acid solutions, the recoveries were very much improved;

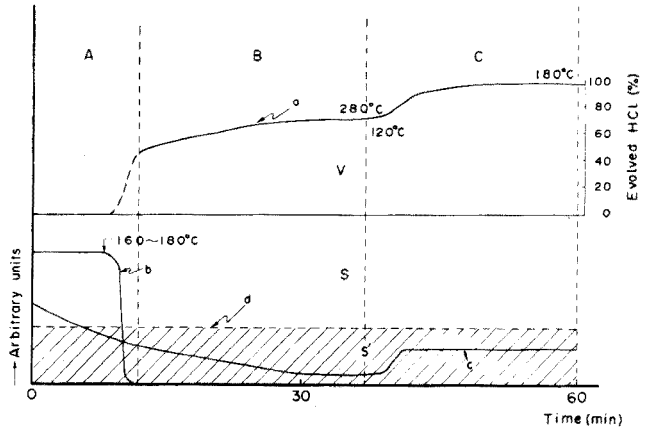

Fig. 2. Schematic diagram of a model derived from the experiments. (A) Sample dissolution; (B) volatilization of HCl; (C) steam distillation. (a) HCl vapor evolved; (b) sample; (c) water to be excluded; (d) critical level of water to be excluded. (V) Vapor; (S) solution; (S') no silicic acid deposits.

no silicic acid deposits were then observed. When the volatilization (dehydration) temperature was 280°C and the distillation temperature was 150–180°C, recoveries of chloride (0.4 ml of 10,000 p.p.m. solution) were 95.5 ± 0.2%. When the distillation step was omitted, the recovery decreased to 69.0%.

Analysis of real samples. The proposed procedure was used to determine chloride in a real sample, yttrium chlorosilicate ($Y_3Si_2O_8Cl$), which has a nominal chloride content of 7.30%. The analytical values were obtained by correcting the chloride concentrations found, with a recovery factor of 0.955. The result obtained was 6.99% with an average error of ±0.15% (6 results). The exact accuracy and precision with respect to real samples could not be estimated, because the available samples were too limited in quantity and type. Nevertheless, the actual type of compound present could easily be elucidated.

Discussion

Figure 2 shows the qualitative relationship between the various steps of the procedure. When phosphoric acid is heated, it dehydrates to a polyphosphoric acid, which dissolves the silicate sample; the exact composition of the polyphosphoric acid is not clear. If the steam distillation is done below 120°C, the water formed decomposes the polyphosphoric acid to phosphoric acid, and silicic acid is deposited.

The authors wish to thank Mr. T. Kano, Mr. S. Yamada and Mrs. M. Mitsui for their interest in this problem and for supplying the yttrium chlorosilicate samples studied, Miss M. Abe for her experimental assistance, and Dr. Iida for valuable discussion.

REFERENCES

1 G. L. Bruton, *Anal. Chem.*, 43 (1971) 579.
2 K. Oshima and N. Shibata, *Jap. Anal.*, 23 (1974) 392.
3 P. J. Duff and J. L. Stuart, *Anal. Chim. Acta*, 57 (1971) 233.
4 J. C. Van Loon, *Analyst (London)*, 93 (1968) 788.
5 H. Yamada, T. Kano and M. Tanabe, *Japanese Patent Application No. 9519, 10333*, 1973.
6 C. Ayasse and H. A. Eick, *Proceedings of the Tenth Rare Earth Research Conference*, United States Atomic Energy Commission Technical Information Center, Oak Ridge, Tennessee, 1973, p. 510.
7 B. H. Priscott, *Analyst (London)*, 92 (1967) 61.
8 I. M. Kolthoff, P. J. Elving and E. B. Sandell, *Treatise on Analytical Chemistry, Part II, Vol. 7*, Interscience, 1961, p. 360.
9 P. J. Elving, *Anal. Chem.*, 28 (1958) 1179.

Analytica Chimica Acta, 76 (1975) 456–460

SHORT COMMUNICATION

Use of a microsampling cup system with a nitrous oxide–acetylene flame for determining less volatile metals

D. G. MITCHELL, A. F. WARD and M. KAHL

Division of Laboratories and Research, New York State Department of Health, New Scotland Avenue, Albany, New York 12201 (U.S.A.)

(Received 23rd October 1974)

Of the four commonest micro-absorption techniques currently being developed for determining trace metals in biological materials, three (the carbon-rod atomizer, heated graphite atomizer, and tantalum strip) are flameless. These techniques are about 1000-fold more sensitive than a conventional nebulizer–flame system: the detection limit is typically $1\text{–}100 \cdot 10^{-12}$ g for most elements. The Delves sampling-cup microtechnique, on the other hand, is flame-assisted. Because of the low cup temperature during sample volatilization it has hitherto been restricted to volatile metals, giving intermediate sensitivities, typically $1\text{–}100 \cdot 10^{-11}$ g, for metals such as zinc, cadmium and lead.

In general, the flameless procedures should be used only when it is possible to exploit their unique capabilities; excellent sensitivity and small sample-size requirements. Otherwise, they are slow (about 2 min per determination[1]) and interference-prone[2–6] and require extremely precise manipulative skills. The Delves cup system also requires only a small sample-size, but it can be used much more efficiently, since sample preparation can be carried out in the cup and measurement is rapid—about 15 s. In blood lead analysis, for example, the Delves technique used with an automated atomic absorption spectrometer is more efficient than a solvent extraction–atomic absorption technique[7]. The major limitation of the Delves cup technique is that so far it has only been suitable for volatile metals. In this communication, preliminary data on a microsampling cup system suitable for less volatile metals are reported.

Experimental

Atomic absorption spectrometer. The atomic absorption system was built up from a hollow-cathode lamp modulated at 285 Hz, a Varian-Techtron Model AA4 0.5-m monochromator fitted with a Hamamatsu R106 photomultiplier and a Princeton Applied Research Model HR-8 phase-sensitive detector fitted with a type A preamplifier. The signal from the amplifier was displayed on an Omniscribe strip chart recorder.

Atomization system. A ceramic absorption tube (10-cm long × 1.4-cm i.d. × 1.8-cm o.d.) was mounted on stainless steel supports which gripped the tube about

1 cm from each end. The tube was positioned so that it stood 15 mm above a Perkin–Elmer 10-cm triple-slot air–acetylene burner, or 20 mm above a Varian-Techtron 10-cm single-slot air–acetylene or 5.5-cm single-slot nitrous oxide–acetylene burner. With the 5.5-cm burner, the supports and the end of the tube were not directly in the flame.

Sampling cups were introduced into the flame in a loop mounted on a sliding unit, which could be adjusted to alter the position of the cups relative to the absorption tube. Two sample-holding devices were evaluated: (a) a tungsten strip 10-cm long, 0.3-cm wide and 0.006-cm thick, cut from a length of tungsten ribbon, mounted in the injector unit so that a flat surface was perpendicular to both the optical path and the hole in the absorption tube; and (b) various types of microsampling cups (see Table I) used with a triangular cup-holding loop constructed from tungsten ribbon 3 mm × 0.06 mm. An optical pyrometer (Pyrometer Instrument Co., Model 87-C) was used to measure the temperatures of various components in the microsampling cup system.

TABLE I

TYPES OF MICROSAMPLING CUP USED

Material	*Dimensions (mm)*			
	Lip i.d.	*Base i.d.*	*Thickness*	*Hole diameter*
Nickel	10	7	0.02	—
Nickel	10	7	0.02	4
Nichrome	10	7	0.03	—
Ceramic	10	7	1	4
Zirconium	10	7	0.03	4
Molybdenum	10	7	0.02	—
Tantalum	10	7	0.03	—
Platinum–rhodium	10	7	0.03	—

Reagents. Stock solutions (1000 μg ml^{-1}) of chromium, cobalt, copper, iron, manganese, nickel, silver and tin were prepared from analytical-grade salts of these metals. These solutions were diluted as required.

Results

Evaluation of flame and burner. The temperatures of the absorption tube, the sampling cups and the cup-holding loop were measured after reaching equilibrium above each of the three burners. The results (Table II) indicate that the nitrous oxide–acetylene flame produces a significantly higher temperature in each component than an air–acetylene flame (except at the unheated ends of the tube in the nitrous oxide–acetylene flame). This increases the volatilization and atomization rates of the sample and reduces possible interference effects of the matrix.

Evaluation of the tungsten strip. The tungsten strip was evaluated by dispensing 10 μl of a 0.5 μg ml^{-1} manganese solution onto the end of the strip, care being taken to prevent the sample spot from spreading. The strip was carefully dried in the edge of the nitrous oxide–acetylene flame and then positioned in the flame so that

TABLE II

EQUILIBRIUM TEMPERATURES (°C) OF COMPONENTS IN THE MICROSAMPLING CUP SYSTEM

Component		*Air–acetylene flame*		*Nitrous oxide–acetylene flame*
		10-cm single-slot	*10-cm triple-slot*	*5.5-cm single-slot*
Ceramic absorption tube				
Center	No cup	1240	1090	1375
	Metal cup	1180	1060	1350
	Ceramic cup	1150	1050	1240
End	No cup	860	1050	890
	Metal cup	860	1050	890
	Ceramic cup	850	1050	880
Triangular loop (tungsten)				
	No cup	1180	1230	1540
	Metal cup	1100	1070	1500
	Ceramic cup	1080	1110	1290
Cups				
	Nickel or nichrome	1090	1070	Melts
	Ceramic	1080	1100	1270
	Platinum–rhodium	1100	1080	1500

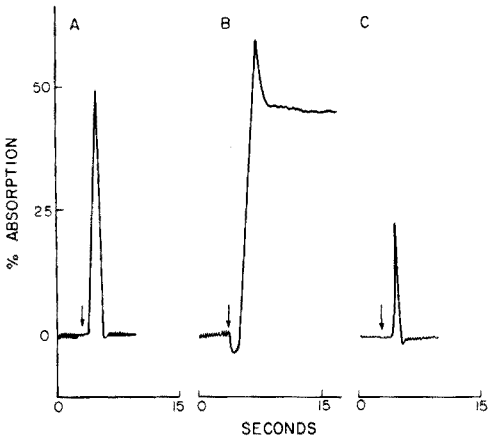

Fig. 1. Absorption signals obtained for manganese at 279.5 nm with: (A) tungsten strip containing 10 μl of solution (0.5 μg ml^{-1}); (B) ceramic cup containing 10 μl of solution (10 μg ml^{-1}); (C) platinum–rhodium cup containing 10 μl of solution (0.5 μg ml^{-1}). Arrows show points where cup was introduced.

the spot was below the hole in the absorption tube. A typical signal is shown in Fig. 1A.

One disadvantage of the tungsten strip is that it becomes brittle after repeated use and oxidizes rapidly, requiring frequent replacement. Perhaps the most serious drawback for routine batch sample handling is that the strip is not a container for the sample, so that the sample cannot be pretreated off-line and sample application requires a skilled operator.

Evaluation of microsampling cups. The different types of cup were evaluated by

dispensing 10 μl of 0.5 μg ml^{-1} manganese solution into each cup, drying for 10 min at 110°C, injecting into the nitrous oxide–acetylene flame and measuring the absorption at 279.5 nm.

The cups made from nickel or nichrome melted in the flame. Ceramic cups gave poor sensitivity and high background absorption (Fig. 1B) and were judged not analytically useful. The apparent absorption signal is probably due both to the physical effect of the cup on the gas flow into the absorption tube and to the "burning" of the cup. These cups became very brittle after this type of heat treatment, and their use was therefore discontinued.

Zirconium, molybdenum and tantalum cups withstood the temperature of the flame. Zirconium and tantalum oxidized rapidly and molybdenum slowly when the hot cup was removed from the flame into the atmosphere. Surrounding the cup with an inert gas shield during its cooling may overcome this problem.

The platinum–rhodium cups gave good sensitivity for manganese and produced no change in flame transmission (Fig. 1C). The cups were virtually unaffected by the flame; and since they are also chemically inert, it is possible to perform digestions with strong acids directly in the cup before analysis.

Detection limit, sensitivity and calibration curve data: platinum–rhodium cups and tungsten strip. Calibration curves were established for aqueous chromium, cobalt, copper, iron, manganese, nickel, silver and tin solutions, with both the tungsten strip and platinum–rhodium cup in a nitrous oxide–acetylene flame. Sensitivities (Table III) were obtained at the optimal distances from the tube for the cup, 3 mm, and the strip, 2 mm. In these positions each was in the "red feather" zone of the flame,

TABLE III

SENSITIVITIES, LINEAR RANGES AND PRECISION OBTAINED WITH TUNGSTEN STRIP AND PLATINUM–RHODIUM CUP

Element	*Atomizer*	*Sensitivity (ng)*	*Linear working range (ng)*	s_r (%)[a]
Chromium	Strip	2.0	10–80	8.7
	Cup	2.9	6–200	2.5
Cobalt	Strip	2.0	10–80	7.7
	Cup	4.3	6–200	7.4
Copper	Strip	1.0	0.9–50	7.5
	Cup	2.3	2–100	4.1
Iron	Strip	5.0	15–250	7.8
	Cup	8.1	10–200	2.2
Manganese	Strip	0.1	0.4–5	7.8
	Cup	0.2	0.2–10	3.9
Nickel	Strip	3.0	15–100	5.8
	Cup	2.6	5–100	7.4
Silver	Strip	0.08	0.06–5	3.7
	Cup	0.1	0.1–5	2.3
Tin	Strip	60	100–2000	4.4
	Cup	170	120–3500	1.8

[a] The relative standard deviation was determined for each metal and atomizer at twenty times the detection limit.

and the sample was in direct contact with the flame gases in this strongly reducing region during volatilization and atomization, which helps to prevent interferences from refractory oxide and compound formation. The absorption tube was about 1 mm above the top of the "red feather" zone.

The working analytical linear ranges are also shown in Table III. The lower limit was set at 5 times the limit of detection, and the upper limit at the point where the calibration curve deviated from linearity by 10%. The detection limit is defined as the least weight of metal that can be determined with a relative standard deviation of 50%.

Discussion

The use of a nitrous oxide–acetylene flame extends the range of application of the microsampling cup technique to at least eight important less volatile metals. This can be attributed to increased cup temperatures, which result in more rapid and complete sample volatilization, and to the strongly reducing nature of the flame.

In this work, the tungsten strip gave slightly better absolute sensitivity than the platinum–rhodium cup and about the same detection limits. The sensitivity of the cup can be improved up to 20-fold in terms of concentration by increasing the sample volume to 200 μl. Increase of the sample volume to 50 μl gave the expected 5-fold increase for copper, manganese and silver. This is not possible with the strip, which has a physical sample-size limit of 10 μl.

An obvious improvement to increase the sensitivity of this technique is a reduction in absorption tube diameter and length, so that the whole tube is directly heated by the flame, producing a more even temperature distribution along its length and preventing condensation of metal at the ends.

The precision obtained for the platinum–rhodium cup was generally better than that obtained for the tungsten strip. The sample tends to spread out irregularly on the surface of the strip, but in the cup it is confined to a fixed area, the base.

A 5-cm absorption tube is currently being evaluated together with some other instrumental improvements such as computerized signal integration. This will be reported in a later communication.

REFERENCES

1 I. W. F. Davidson and W. L. Secrest, *Anal. Chem.*, 44 (1972) 1808.
2 J. P. Matousek and B. J. Stevens, *Clin. Chem.*, 17 (1971) 363.
3 M. Glenn, J. Savory, L. Hart, T. Glenn and J. Winefordner, *Anal. Chim. Acta*, 57 (1971) 263.
4 P. A. Segar and J. G. Gonzalez, *Anal. Chim. Acta*, 58 (1972) 7.
5 F. J. Fernandez and D. C. Manning, *At. Absorption Newslett.*, 10 (1971) 65.
6 C. W. Fuller, *Anal. Chim. Acta*, 62 (1972) 442.
7 D. G. Mitchell, K. M. Aldous and F. J. Ryan, paper presented at the International Symposium on Environmental Health Aspects of Lead, Amsterdam, October, 1972.

Analytica Chimica Acta, 76 (1975) 461–463

SHORT COMMUNICATION

Precise and rapid determination of trace amounts of uranium in inorganic samples by neutron activation and TBP extraction

E. STEINNES

Institutt for Atomenergi, Isotope Laboratories, Kjeller (Norway)

(Received 1st November 1974)

Neutron activation analysis is one of the very few analytical techniques that can be used for reliable determination of uranium at the p.p.10^9 concentration level. A very sensitive version is the one based on measurement of 23.5-min ^{239}U originating from the (n, γ) reaction in ^{238}U, provided that a selective and rapid separation procedure giving high chemical yield is available. Such a procedure might be based on extraction with tri-n-butyl phosphate (TBP) from nitric acid media, which has been extensively used in nuclear fuel reprocessing work. It was recently shown[1] that uranium could be determined in fresh water by a single extraction into TBP from (1 + 1) nitric acid. When the need arose for uranium determination in high-purity yttrium oxide, it was decided to study the applicability of the TBP–HNO_3 system on a wider range of samples.

Distribution coefficients for more than 70 elements in the TBP–HNO_3 system have been given[2]. According to these data extraction from 5 *M* nitric acid into 25% TBP seemed to be the optimal choice. In 100% TBP, it would be necessary to go down to 1–2 *M* nitric acid in order to remove efficiently a number of elements including yttrium and the heavy rare earths, and at those low concentrations the uranium yield would probably be unsatisfactory. In the case of 25% TBP, only Au, Th and Np would be extracted along with uranium from a 5 *M* nitric acid solution to any significant degree. This would allow the determination of thorium *via* 22.4-min ^{233}Th simultaneously with uranium.

Experimental

Samples of about 250 mg were weighed into small polyethylene ampoules and irradiated for 15 min along with standard solutions (U, 0.1 p.p.m.; Th, 5 p.p.m.) in the pneumatic tube system of the JEEP II reactor (Kjeller, Norway) at a thermal neutron flux of $1.7 \cdot 10^{13}$ n cm^{-2} s^{-1} and $R_{Cd}^{Au} = 2.8$. The irradiated sample was dissolved in 10 ml of 5 *M* nitric acid containing carriers (U, 0.5 mg; Th, 10 mg). The solution was extracted with 20 ml of 25% TBP (v/v) in toluene. The organic phase was washed twice with 10 ml of 5 *M* nitric acid. The shaking time was 1 min, and the total time necessary for the separation procedure about 10 min.

The TBP phase was transferred to a 100-ml polyethylene screwcap bottle

and subjected to γ-spectrometry with a 35-cm^3 Ge(Li) detector connected to a 1700-channel pulse-height analyzer based on a small digital computer. The counting time was 10 min, and the 74-keV and 88-keV γ-ray peaks were used for the determination of uranium and thorium, respectively. Peak areas were calculated by the method of Sterlinski[3].

Chemical yield was determined by re-activation. The organic phase was diluted to 25 ml with toluene and 0.500 ml was sealed in a polyethylene ampoule and irradiated for 10 s. Subsequently γ-spectrometry as described above was applied without opening the ampoule.

Results and discussion

Results for uranium by the present method in four samples of high-purity yttrium oxide, a sample of calcium carbonate and a sample of lead acetate are given in Table I. In two of the Y_2O_3 samples, thorium was determined simultaneously. No γ-activities interfering appreciably with the Ge(Li) γ-spectrometry measurements were observed in any of these samples.

TABLE I

DETERMINATION OF URANIUM AND THORIUM IN SOME INORGANIC COMPOUNDS

Sample	*p.p.m. U*		*p.p.m. Th*	
	Single values	*Mean values*	*Single values*	*Mean values*
High-purity Y_2O_3 I	0.0053	0.0057	—	
	0.0049			
	0.0070			
High-purity Y_2O_3 II	0.0167	0.0169	—	
	0.0164			
	0.0176			
High-purity Y_2O_3 III	0.0022	0.0018	0.084	0.074
	0.0014		0.064	
High-purity Y_2O_3 IV	0.0106	0.0099	0.105	0.100
	0.0091		0.095	
$CaCO_3$, p.a.	0.0010	0.0011	—	
	0.0010			
	0.0014			
$PbAc_2$, p.a.	0.0005	0.0004	—	
	0.0004			
	0.0003			

The chemical yield was 86–96% for uranium and 31–39% for thorium. A high uranium yield was accompanied by a relatively high thorium yield and *vice versa*, indicating a fairly strong dependence on the nitric acid concentration, which may not have been exactly the same in all the experiments. The observed yields are in accordance with the literature K_d values[2] (about 50 for U and 2 for Th in 25% TBP–5 *M* HNO_3).

Given the thermal neutron activation cross-section (7.4 b *versus* 2.7 b for the (n, γ) reaction in ^{232}Th and ^{238}U, respectively), the sensitivity for the two elements by the present method should be about the same, when the chemical yields are taken into account. Because of the high resonance activation integral of ^{238}U, however, the effective cross-section is about 9 b for both reactions in a neutron flux with $R_{Cd}^{Au}=2.8$. Furthermore, only 2.7% of the ^{233}Th nuclei decay by emission of 88-keV γ-rays, while the corresponding figure for the 74-keV γ-ray of ^{239}U is 51%. This would yield about 50 times higher sensitivity for uranium, which is in agreement with the detection limits observed, about 0.02 ng U and 1 ng Th, or about 0.0001 p.p.m. U and 0.005 p.p.m. Th in a 200-mg sample.

The present method should be attractive for the determination of uranium in most inorganic samples that can be readily dissolved in strong nitric acid. Thorium can be determined along with uranium without appreciable extra work, but the sensitivity does not make the method similarly attractive for this element.

For substances that are readily soluble in strong nitric acid, and the major elements of which do not become excessively radioactive on a 15-min irradiation, enhancement of the sensitivity may be possible by increasing the sample size.

REFERENCES

1 E. Steinnes, *Radiochem. Radioanal. Lett.*, 16 (1973) 25.
2 T. Ishimori and E. Nakamura (Eds.), *Data of Inorganic Solvent Extraction (1)*, Report JAERI 1047, 1963.
3 S. Sterlinski, *Anal. Chem.*, 40 (1968) 1995.

Analytica Chimica Acta, 76 (1975) 464–466

SHORT COMMUNICATION

Purification of chromeazurol S by paper chromatography

V. MALANÍK and M. MALÁT

Department of Analytical Chemistry, Charles University, 128 40 Prague 2, Albertov 2030 (Czechoslovakia)

(Received 23rd October 1974)

During a study[1] of the spectrophotometric determination of uranium(VI) with chromeazurol S (ref. 2) and cetylpyridinium bromide, it was found that the coloration of the complex formed was affected by the purity of the chromeazurol S used. For this reason, the quality of some commercial chromeazurol S preparations was examined, and a method of obtaining a very pure substance by preparative paper chromatography was developed. Langmyhr and Klausen[3] dealt with the problem of chromeazurol S purity, isolating the pure substance from solution as the free acid.

Experimental

Reagents. Chromeazurol S preparations from Merck AG (Darmstadt, G.F.R.), B.D.H. (Poole, England), and Geigy (Basel, Switzerland) were employed; the last substance had already been partially purified by the firm[2].

The eluent consisted of a 7:1:3 mixture of *n*-butanol, glacial acetic acid, and water.

Apparatus. The u.v. and visible spectra were measured on a Pye-Unicam, SP800 recording spectrophotometer; the infrared spectra were obtained on a Carl Zeiss UR-20 spectrophotometer.

The purification of chromeazurol S

During paper chromatography of the chromeazurol S substances with the above eluent, it was verified that the substances were not homogeneous. For example, the Merck preparation contained at least eight substances; two of these predominated (Fig. 1, column a), one of which was probably pure chromeazurol S.

Preparative scale chromatography was then examined. On Whatman no. 3 chromatographic paper, an aqueous 10% chromeazurol S solution (Merck) was placed in bands; after drying, the paper was placed in a chromatographic chamber for elution. The first spot, proceeding almost with the solvent front, had an R_F value of 0.92 (CAS-I); the other spot had an R_F value of 0.51 (CAS-II). After drying of the papers, spots I and II were cut out and extracted with pure methanol. The extracts were filtered through S4 glass frits and evaporated to dryness *in vacuo*. The residue from spot I was dissolved in a little warm water and precipitated with concentrated hydrochloric acid; the precipitate was filtered through a S3 glass frit and dried *in vacuo* over KOH and P_2O_5 (chromeazurol S-I). The

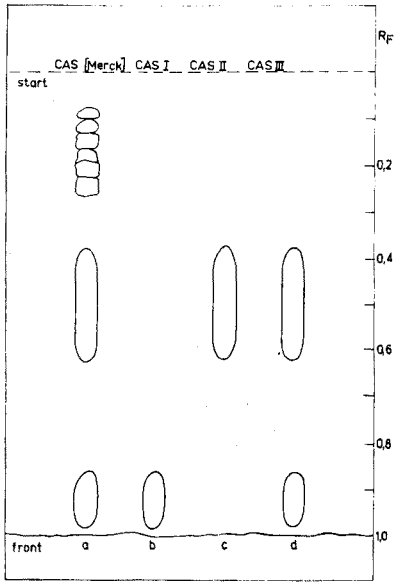

Fig. 1. Chromatograms of the chromeazurol S (CAS) substances: Merck, I, II, III. Whatman no. 3 paper with *n*-butanol–glacial acetic acid–water (7:1:3) eluent. 0.3 mg of each substance was applied.

substance obtained from spot II was converted to the acidic form by passage through a column of Wofatit KPS-200) in the acidic form; the eluate was evaporated to dryness and again dried *in vacuo* over P_2O_5 (chromeazurol S-II).

A purified substance was also prepared from the Merck product by the procedure given by Langmyhr and Klausen[3], (chromeazurol S-III).

Results and discussion

The purities of the above chromeazurol S-I, -II, and -III were checked by paper chromatography and by u.v., visible, and i.r. spectrophotometry. The results obtained indicated (Fig. 1,b,c,d) that CAS-I and CAS-II were homogeneous, while CAS-III remained, even after purification, a mixture of CAS-I and CAS-II. These results were verified by elemental analyses of the three substances; the results together with the theoretical composition of CAS (ref. 3), are given in Table I. CAS-I does not contain sulphur, CAS-II approaches most closely the theoretical composition of chromeazurol S, and CAS-III was evidently not purified perfectly by the procedure described.

TABLE I

ELEMENTAL ANALYSES (%)

Element	*CAS-I*	*CAS-II*	*CAS-III*	*CAS (ref. 3)*
C	56.39	47.90	52.12	48.00
H	3.77	3.66	3.74	3.50
Cl	14.76	12.09	14.35	12.32
S	0.00	5.51	2.79	5.57
O	25.08	30.84	27.00	30.61

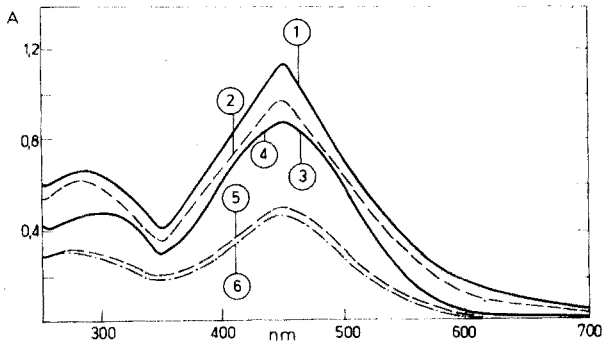

Fig. 2. Absorption spectra. (1)—CAS-I, (2)—CAS-II, (3)—CAS-III, (4)—CAS (Geigy), (5)—CAS (B.D.H.), (6)—CAS (Merck); $c_{CAS} = 6 \cdot 10^{-5}$ *M*, pH 4.7 (acetate buffer).

The absorption spectra in the u.v. and visible regions (Fig. 2) confirmed the results obtained: the pure substances exhibited higher absorbance than the commercial preparations at 445 nm, *i.e.* at the absorption maximum at the given pH. The i.r. spectra confirmed the compositions of substances I and II; the spectra differed significantly only within the range 1000–1400 cm^{-1}. With CAS-II, three intense absorption bands were found in this region, corresponding to the anti-symmetrical (1340 cm^{-1}) and symmetrical (1040 cm^{-1}) valence vibrations of the SO_2 molecule, the third band (1190 cm^{-1}) characterizing a protonized sulpho- group[4,5]. With substance CAS-I, only a medium strong absorption band at 1045 cm^{-1} was registered.

In an attempt to simplify the preparation of pure chromeazurol S, its separation on a cellulose column was tested. The column (30 cm long, 2.5-cm diameter) was obtained by sedimentation of powdered cellulose (Standard Grade, Whatman) in *n*-butanol saturated with water; 1.25 g of CAS (Merck) dissolved in 50 ml of redistilled water was adsorbed on the column and then extracted with n-butanol. The solution obtained contained mostly CAS-I. Further elution with a mixture of *n*-butanol, acetic acid and water (7:1:3) gave a solution containing CAS-II. However, the separation was imperfect: paper chromatography showed that both the CAS-I and CAS-II fractions contained the other components.

It can be concluded that substance CAS-II (m.w. 582.5) corresponds theoretically to chromeazurol S, while CAS-I (m.w. 504.1) is 2″,6″-dichloro-3,3′-dimethyl-4-hydroxyfuchson-5,5′-dicarboxylic acid. For the spectrophotometric determination of uranium(VI) (ref. 1), CAS-I is even more sensitive ($\varepsilon = 95{,}000$) than CAS-II ($\varepsilon = 86{,}700$).

The authors are grateful to Dr. J. Horáček, Institute of Organic Chemistry and Biochemistry, for the elemental analyses.

REFERENCES

1 V. Malaník and M. Malát, *Collect. Czech. Chem. Commun.*, in press.
2 M. Malát, *Anal. Chim. Acta*, 25 (1961) 289.
3 F. J. Langmyhr and K. S. Klausen, *Anal. Chim. Acta*, 29 (1963) 149.
4 N. B. Colthup, L. H. Daly and S. E. Wiberley, *Introduction to Infrared and Raman Spectroscopy*, Academic Press, New York, 1964.
5 K. Nakanishi, *Infrared Absorption Spectroscopy* (Russian translation), Izd. Mir, Moscow, 1964.

Analytica Chimica Acta, 76 (1975) 467–470

SHORT COMMUNICATION

Solid-state luminescence determination of traces of beryllium with dinaphthoylmethane

D. E. RYAN, M. GRANDA and M. JANMOHAMMED

Trace Analysis Research Centre, Chemistry Department, Dalhousie University, Halifax, Nova Scotia, B3H 4J1 (Canada)

(Received 5th September 1974)

Instrumentation is now available for reliable measurement of properties of the solid state and, by using coprecipitation techniques to introduce microgram amounts of activators into milligram amounts of phosphors, bismuth and lead can be determined at the ng ml^{-1} level from the resulting solid state luminescence[1–3].

An evaluation of the use of a carrier precipitate of organic reagent with which the collected trace metal ion reacts to form a luminescent product, and subsequent measurement of the solid state fluorescence, was recently reported[4]; a suitable reagent should be non-fluorescent, insoluble, and selective. The present paper describes the application of such a reagent—dinaphthoylmethane(1,3-di-(2-naphthyl)-1,3-propanedione)—to the determination of traces of beryllium. Beryllium(II) is coprecipitated by dinaphthoylmethane and determined with excellent precision by measuring the *in situ* fluorescence of the precipitate.

The principle of preconcentration of a trace metal ion by using a carrier precipitate of organic reagent with which it reacts, and subsequent direct measurement of some property of the separated solid, appears to have widespread application.

Experimental

Apparatus. Fluorimetric measurements were made on a Farrand Vis-UV Chromatogram Analyzer. The instrument was standardized with a mixture of zinc sulfide phosphorescent (Fisher) and zinc sulfide luminous (BDH).

A blackened aluminum plate (1 mm thick), with drilled holes 5 mm in diameter, was used as the sample cell. The holes were packed with the ground precipitate which was held in place by a thin glass plate on one side and masking tape on the other.

Reagents. A stock solution containing 410 μg Be ml^{-1} was prepared from beryllium nitrate (Fisher) and standardized by the phosphate method[5]. Solutions of desired concentration were prepared by dilution.

A 0.04 *M* solution of dinaphthoylmethane (Kodak) in dimethylsulfoxide (Fisher) was prepared.

The pH 7.2 buffer was obtained by dissolving a mixture of 1.53 g of borax (AnalaR), 11.4 g of boric acid (Fisher) and 2.69 g of sodium chloride (AnalaR) in water and diluting to 1 l.

Procedure. To 100 ml of approximately neutral solution containing 1.5–15 μg of beryllium, add 10 ml of buffer. Add 3.0 ml of dinaphthoylmethane solution, dropwise, with stirring. Allow the precipitate to stand for 30 min, and filter through a medium-porosity filter crucible. Wash with distilled water and dry at 100°C for 2 h. Grind and mix in an agate mortar. Pack the cell and measure the luminescence, using the following settings on the Farrand for highest sensitivity: λ_{ex}—380 nm, λ_{em}—570 nm, emission filter 8, aperture 0.25 and PM RCA 1P21 with slit removed.

Results and discussion

The fluorescence intensity is a linear function of the beryllium concentration over the range 0–20 μg Be/100 ml, as long as there is no saturation of the precipitate. For the range 1.5–20 μg of beryllium, 40 mg of dinaphthoylmethane sufficed; the same results were obtained for 10 μg of beryllium collected from 100- or 500-ml volumes of solution (*i.e.* 20 p.p.b.). With 20 mg of precipitate, good results were obtained in the range 0.5–10 μg of beryllium.

The practical detection limit was 0.3 μg of beryllium in 40 mg of precipitate. The relative standard deviation of seven determinations of 1.5 μg of beryllium was 7%; for 10 μg it was 3.5%.

Factors affecting fluorescence. The emission spectra of dinaphthoylmethane and coprecipitated beryllium complex are shown in Fig. 1. Measurements at the wavelength maximum resulted in a large background because of the closeness of reagent and chelate maxima, and limited the amount of beryllium detectable. However, by making measurements at 570 nm, the reagent background was completely eliminated and very good signals were still obtained for the beryllium standards.

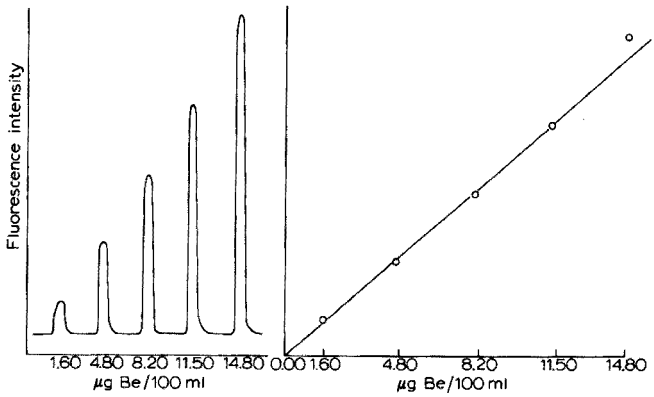

Fig. 1. Emission spectra: A, coprecipitated Be chelate (λ_{ex} = 360 nm); B, dinaphthoylmethane (λ_{ex} = 380 nm).

No apparent reaction occurred below pH 6 and fluorescence was maximal at pH 7.2. The precipitation was therefore done maintaining this pH with a borate buffer.

There was a small initial decrease in luminescence of the coprecipitated beryllium complex with time but constant luminescence was obtained by filtration after 30 min.

Beryllium (10 μg; 100 ng/ml) was successfully determined in the presence of 1000 μg of Ca(II) or Mg(II), 100 μg of Cd(II) or Hg(II), and 100 μg of Cu(II), Ni(II), Zn(II) or Co(II) (if 0.05 g of potassium cyanide was present). Iron(III), Cr(III) and Mn(II) quenched the fluorescence and must be absent. Aluminum(III) gave an enhanced fluorescence but an equivalent amount (10 μg) could be tolerated if 100 μg of EDTA was present. Large amounts of common anions (Cl^-, NO_3^-, BO_2^-, ClO_4^-) did not interfere and 5000 μg of PO_4^{3-} and 100 μg of F^- could be tolerated.

Dibenzoylmethane, which differs from dinaphthoylmethane only in the replacement of two naphthyl groups by two phenyl ones, was also investigated for the determination of beryllium by the same procedure. As expected, however, the higher solubility and smaller π system makes dibenzoylmethane less satisfactory as the coprecipitant; the amount of precipitant obtained is dependent on solution volume and there is lower fluorescence sensitivity.

Application. As a test of the procedure in an organic matrix, known amounts of beryllium (0–20 μg) were added to leaf samples and were then analyzed. To avoid the possible inconveniences of high-temperature dry ashing[6,7], a wet ashing procedure was used.

Dry ground leaf samples (0.5 g) were heated with 10 ml of (1 + 1) nitric acid on a hot plate, evaporated to dryness and baked for 5 min. After cooling, 2 ml of concentrated nitric acid were added, and the solution was evaporated and baked once again. This process was repeated several times and the final organic residue was destroyed with 1 ml of 60% perchloric acid and 2 ml of concentrated nitric acid. The resulting solution was diluted to 100 ml in a volumetric flask and an aliquot was taken for analysis; each sample was neutralized with 50% sodium hydroxide before the usual procedure was applied. A linear calibration curve was obtained.

Conclusion

Trace amounts of beryllium(II) can be pre-concentrated with dinaphthoylmethane and determined directly by measurement of the resulting fluorescence from the solid state. The reagent is insoluble, non-luminescent at the wavelength of measurement and has some selectivity. It should find application to a number of areas (*e.g.* air pollution analysis) for the determination of beryllium.

This work was supported by a grant from the National Research Council of Canada.

REFERENCES

1 D. E. Ryan, R. J. Prime, J. Holzbecher and R. E. Young, *Anal. Lett.*, 6 (1973) 721.
2 D. E. Ryan, H. Rollier and J. Holzbecher, *Can. J. Chem.*, 52 (1974) 1942.
3 D. E. Ryan, J. Holzbecher and H. Rollier, *Anal. Chim. Acta*, 52 (1974) 1942.
4 H. Rollier and D. E. Ryan, *Anal. Chim. Acta*, 74 (1974) 23.
5 N. H. Furman (Ed.), *Standard Methods of Chemical Analysis, Vol. I*, Van Nostrand, Princeton, N.J., 6th edn., 1962.
6 T. Y. Toribara and R. E. Sherman, *Anal. Chem.*, 25 (1953) 159.
7 T. T. Gorsuch, *The Destruction of Organic Matter*, Pergamon, Oxford, 1970.

Analytica Chimica Acta, 76 (1975) 471-476

SHORT COMMUNICATION

Spectrophotometric determination of the stability constant and acid dissociation constant of the vanadium(V)–cyclohexanediaminetetraacetate complex

JUN-ICHI ITOH, TAKAO YOTSUYANAGI and KAZUO AOMURA
Laboratory of Analytical Chemistry, Faculty of Engineering, Hokkaido University, Sapporo (Japan)
(Received 4th October 1974)

Cyclohexanediaminetetraacetic acid (CDTA) has been used as an excellent masking agent for many metal ions. Especially in the spectrophotometric determination of vanadium(V) with xylenol orange[1] or 4-(2-pyridylazo)-resorcinol (PAR)[2,3], CDTA prevents the interference of many metal ions. Ethylenediaminetetraacetic acid (EDTA) does not show such a selective masking behaviour as CDTA, and prevents the color reaction of vanadium(V). Qualitatively, therefore, CDTA shows a special action towards vanadium(V) ion in that the stability order of the CDTA- and EDTA-complexes of vanadium(V) is the reverse of that found for many metal ions. Although some data have been reported for the stability constant of the vanadium(V)–EDTA complex[4,5], no data for the CDTA complex are available.

In this study, the reaction of vanadium(V) ion with CDTA was investigated spectrophotometrically in order to obtain the stability constant, which is essential to understand the special action of CDTA towards vanadium(V) ion in the highly selective and sensitive color reaction with PAR and xylenol orange.

EXPERIMENTAL

CDTA solution. A 0.05 *M* solution was prepared by dissolving 17.32 g of CDTA (Dojindo Co., Kumamoto) and 4 g of sodium hydroxide in water and diluting to 1 l. The solution was standardized by complexiметric titration with a standard lead solution in the usual way.

Vanadium(V) solution. A 0.01 *M* solution was standardized by titration with a standard EDTA solution.

All chemicals used were of analytical-reagent grade.

The pH was adjusted with dilute hydrochloric acid or potassium hydroxide solution. The ionic strength was adjusted to 0.1 with potassium chloride.

Absorbance was measured on a Hitachi-124 model Double-beam Recording Spectrophotometer equipped with 1-cm quartz cells. A Toa Dempa HM-5A Type pH meter was used.

Determination of stability constant and acid dissociation constant. Methods based on the relationship $A = f(pH)$ were employed, on account of the high stability

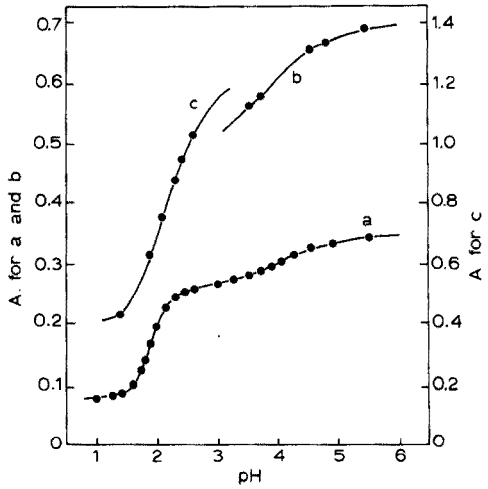

Fig. 1. Absorbance–pH curves for vanadium(V) and CDTA solutions. (a) $C_{VO_2}=2.00\cdot10^{-4}$, $C_{H_4Y}=4.00\cdot10^{-3}$, (b) $C_{VO_2}=4.00\cdot10^{-4}$, $C_{H_4Y}=9.50\cdot10^{-3}$, (c) $C_{VO_2}=C_{H_4Y}=1.00\cdot10^{-3}$.

of the complexes studied. Absorbance (A) and pH were measured for solutions containing a large excess of ligand (at pH 3–7) and for equimolar solutions of metal ion and ligand (at pH 1–3) at 293 K (20°C). Under these experimental conditions (see Fig. 1), hydrolysis of vanadium(V) ion, VO_2^+, was negligible.

RESULTS AND DISCUSSION

It seems very likely that a mononuclear 1 : 1 complex, $VO_2H_{4-m-n}Y^{(m+n-1)-}$, is formed in acidic solution, and the general equation for the complexation is given by:

$$VO_2^+ + H_{4-m}Y^{m-} \rightleftharpoons VO_2H_{4-m-n}Y^{(m+n-1)-} + nH^+ \quad (1)$$

with the stability constant defined as

$$K_c = \frac{[VO_2H_{4-m-n}Y^{(m+n-1)-}]\cdot[H^+]^n}{[VO_2^+]\cdot[H_{4-m}Y^{m-}]} \quad (2)$$

It is evident from the values of the acid dissociation constants of CDTA ($pk_1=2.43$, $pk_2=3.52$, $pk_3=6.12$ and $pk_4=11.70$)[6] that H_4Y and H_3Y^- are the predominant species in the pH range 1–2.6 for the complex formation. Because of the nature of an equilibrium study, the apparent reacting species can be arbitrarily chosen. In this case, data were analyzed by using H_4Y ($m=0$ in eqns. (1) and (2)) as reactant, on the assumption of formation of a single complex in the pH range 1–2.6.

Thus, the absorbance at a wavelength of 310 nm is given by

$$A = \varepsilon_1\cdot[VO_2^+] + \varepsilon_2\cdot[VO_2H_{4-n}Y^{(n-1)-}] \quad (3)$$

where ε_1 ($4.10\cdot10^2$) and ε_2 ($1.30\cdot10^3$) are the molar absorptivities of the vanadyl ion and the complex respectively. For material balance,

$$[VO_2^+] = C_{VO_2} - [VO_2H_{4-n}Y^{(n-1)-}] \quad (4)$$

$$[H_4Y] = C_Y - [VO_2H_{4-n}Y^{(n-1)-}]\cdot\alpha_{H_4Y} \quad (5)$$

where C_{VO_2} and C_Y are the total concentrations of VO_2^+ and CDTA, respectively, and α_{H_4Y} is the mole fraction of H_4Y present as free ligand,

$$\alpha_{H_4Y} = \frac{H_4Y}{\sum_0^4 H_nY} = \left\{1 + \frac{k_1}{[H^+]} + \frac{k_1k_2}{[H^+]^2} + \frac{k_1k_2k_3}{[H^+]^3} + \frac{k_1k_2k_3k_4}{[H^+]^4}\right\}^{-1} \quad (6)$$

Thus, the equilibrium constant for eqn. (1), K_c, is given by

$$K_c = \left\{\frac{A-\varepsilon_1 \cdot C_{VO_2}}{\varepsilon_2 \cdot C_{VO_2} - A}\right\} \cdot \frac{[H^+]^n}{\left(C_Y - \frac{A-\varepsilon_1 C_{VO_2}}{\varepsilon_2 - \varepsilon_1}\right) \cdot \alpha_{H_4Y}} \quad (7)$$

In the presence of a large excess of ligand, $C_Y \gg C_{VO_2}$, the free concentration of H_4Y can be approximated by $C_Y \cdot \alpha_{H_4Y}$ and eqn. (7) becomes:

$$\frac{C_{VO_2}}{A} = \frac{1}{\varepsilon_2} + \frac{1}{\varepsilon_2 \cdot K_c \cdot C_Y} \cdot \frac{(A-\varepsilon_1 \cdot C_{VO_2})[H^+]^n}{A \cdot \alpha_{H_4Y}} \quad (8)$$

The number of protons, n, was examined by applying eqn. (8); the straight-line plots of C_{VO_2}/A against $((A-\varepsilon_1 \cdot C_{VO_2}) \cdot [H^+]^n/A \cdot \alpha_{H_4Y})$ with $n=3$ confirmed the formation of a single complex with the formula VO_2HY^{2-} (Fig. 2). The value of ε_2 was determined from the intercept of the plots.

The stability constant of VO_2HY^{2-} was calculated from the data in Fig. 1 with eqns. (9) and (10), for ligand excess and for equimolar solutions, respectively (Table I).

$$K_{VO_2HY} = \frac{[VO_2HY^{2-}]}{[VO_2^+] \cdot [HY^{3-}]} = \frac{(A-\varepsilon_1 \cdot C_{VO_2})}{(\varepsilon_2 C_{VO_2} - A)} \cdot \frac{1}{C_Y \cdot \alpha_{HY}} \quad (9)$$

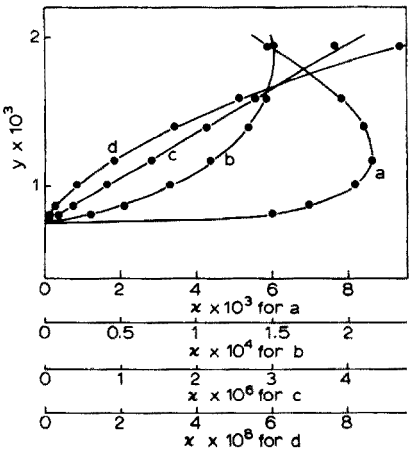

Fig. 2. Analysis of absorbance–pH curve (Fig. 1, curve a) according to eqn. (8). $y = C_{VO_2}/A$, $x = (A-\varepsilon_1 \cdot C_{VO_2}) \cdot [H^+]^n/A \cdot \alpha_{H_4Y}$. (a) $n=1$; (b) $n=2$; (c) $n=3$; (d) $n=4$.

TABLE I

CALCULATION OF STABILITY CONSTANT OF VO_2HY^{2+} FROM EQUATIONS (9) AND (10)

$C_{VO_2}=2\cdot10^{-4}$, $C_{H_4Y}=4\cdot10^{-4}$			$C_{VO_2}=1\cdot10^{-3}$, $C_{H_4Y}=1\cdot10^{-3}$		
pH	*A*	*log* K_{VO_2HY}[a]	*pH*	*A*	*log* K_{VO_2HY}[a]
1.60	0.103	8.88	1.90	0.625	9.12
1.73	0.126	8.90	2.10	0.758	8.99
1.80	0.142	8.89	2.30	0.875	8.98
1.89	0.168	8.91	2.40	0.944	8.78
2.00	0.197	8.89	2.60	1.030	8.78
2.15	0.228	8.89			
2.30	0.245	8.88			

[a] $\log K_{VO_2HY}=8.91$ (average value of 12 experiments).

$$K_{VO_2HY}=\frac{(A-\varepsilon_1\cdot C_{VO_2})}{(\varepsilon_2\cdot C_{VO_2}-A)}\cdot\frac{\varepsilon_2-\varepsilon_1}{\alpha_{HY}} \tag{10}$$

where $\alpha_{HY}=[HY^{3-}]/\Sigma_0^4[H_nY]=\alpha_{H_4Y}\cdot k_1\cdot k_2\cdot k_3/[H^+]^3$. As shown in Table I, fairly constant values of K_{VO_2HY} were obtained, which again proved the formation of the species VO_2HY^{2-} in the pH range studied (1–2.6).

Above pH 3, a second increase in absorbance was observed; this was attributed to acid dissociation of the complex VO_2HY^{2-}, and the constant was calculated in the usual manner (Table II).

$$VO_2HY^{2-}\rightleftharpoons H^+ + VO_2Y^{3-} \tag{11}$$

$$K^H_{VO_2HY}=\frac{[H^+]\cdot[VO_2Y^{3-}]}{[VO_2HY^{2-}]}=\left\{\frac{A-\varepsilon_2\cdot C_{VO_2}}{\varepsilon_3\cdot C_{VO_2}-A}\right\}\cdot[H^+] \tag{12}$$

TABLE II

CALCULATION OF ACID DISSOCIATION CONSTANT OF VO_2HY^{2+} FROM EQUATION (12)

$C_{VO_2}=2\cdot10^{-4}$, $C_{H_4Y}=4\cdot10^{-3}$			$C_{VO_2}=4\cdot10^{-4}$, $C_{H_4Y}=9.5\cdot10^{-3}$		
pH	*A*	$pK^H_{VO_2HY}$[a]	*pH*	*A*	$pK^H_{VO_2HY}$[a]
3.52	0.282	4.01	3.50	0.562	4.03
3.73	0.289	3.96	3.70	0.582	3.99
3.90	0.298	3.99	4.50	0.657	3.95
4.05	0.307	4.02	4.75	0.665	4.06
4.25	0.315	3.98	5.40	0.688	3.96
4.55	0.325	4.02			
4.95	0.338	4.04			

[a] $pK^H_{VO_2HY}=4.00$ (average value of 12 experiments).

where $\varepsilon_3 (1.74 \cdot 10^3)$ is the molar absorptivity of VO_2Y^{3-} at 310 nm. Thus, the stability constant and the acid dissociation constant of VO_2HY^{2-} complex were determined as $\log K_{VO_2HY} = 8.91$ and $\log K^H_{VO_2HY} = -4.00$, respectively. By combining these constants obtained above, the stability constant of VO_2Y^{3-} complex can be calculated

$$K_{VO_2Y} = \frac{[VO_2Y^{3-}]}{[VO_2^+] \cdot [Y^{4-}]} = \frac{K_{VO_2HY} \cdot K^H_{VO_2HY}}{k_4} = 10^{16.61} \tag{13}$$

The values of stability constants of metal–CDTA complexes are plotted against those of metal–EDTA complexes in Fig. 3. The vanadyl ion is shown at two different points A and B in Fig. 3, because two different values have been reported for the stability constant of the VO_2–EDTA complex: $K_{VO_2EDTA} = [VO_2EDTA^{3-}]/[VO_2^+] \cdot [EDTA^{4-}] = 10^{18.05}$ and $10^{15.55}$ by Ringbom *et al.*[4] and Przyborowski *et al.*[5], respectively. The location of points below and above the dashed line, indicates the relationship of $\log K_{M-EDTA} < \log K_{M-CDTA}$ and $\log K_{M-EDTA} > \log K_{M-CDTA}$, respectively. By comparing the results in Fig. 3 with the particular action of CDTA towards vanadium(V) in the color reactions with PAR[2,3] and xylenol orange[1], it may be easily concluded that only the location of point (A) for the VO_2^+ ion in Fig. 3 is reasonable, where $\log K_{VO_2Y}$ (16.61) is smaller than $\log K_{VO_2-EDTA}$ (18.05).

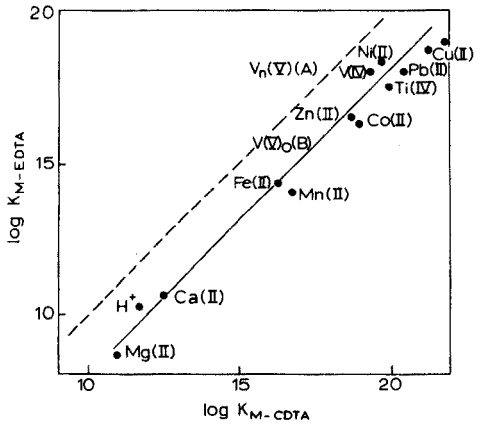

Fig. 3. Linear free energy relationship between the stability of CDTA complexes and EDTA complexes. The dashed line indicates $\log K_{M-CDTA} = \log K_{M-EDTA}$, K is defined as $K = [MY^{(4-n)-}]/[M^{n+}] \cdot [Y^{4-}]$.

For all metal ions except the vanadyl ion at point (A), the points are located well below the dashed line and show a good linear free energy relationship between the stabilities of the EDTA and CDTA complexes. According to chemical bond model studies, the exceptionally low stability of the VO_2^+–CDTA complex compared with that of the VO_2^+–EDTA complex can be largely attributed to steric hindrance between two free $-CH_2COO^-$ groups and the hydrogen atoms on the 3- and 6-carbon atoms in the cyclohexane structure.

REFERENCES

1 O. Budevsky and R. Pribil, *Talanta*, 11 (1964) 1313.
2 O. Budevsky and L. Dzhonova, *Talanta*, 12 (1965) 291.
3 T. Yotsuyanagi, J. Itoh and K. Aomura, *Talanta*, 16 (1969) 1611.
4 A. Ringbom, S. Siitonen and B. Skrifvars, *Acta Chem. Scand.*, 11 (1957) 551.
5 L. Przyborowski, G. Schwarzenbach and Th. Zimmermann, *Helv. Chim. Acta*, 48 (1965) 1556.
6 G. Schwarzenbach and H. Ackermann, *Helv. Chim. Acta*, 32 (1949) 1682.

Analytica Chimica Acta, 76 (1975) 477–482

SHORT COMMUNICATION

Microdetermination of lead as its carminic acid complex by reflectance spectroscopy

R. REISFELD, S. LEVI, E. GREENBERG and W. J. LEVENE*

Department of Inorganic and Analytical Chemistry, The Hebrew University, Jerusalem (Israel)

(Received 16th October 1974)

Recently, a method for the determination of mercury in the range 5–100 p.p.m. was described[1]. Traces of lead are toxic[2], and therefore it appeared of interest to extend the techniques described to the determination of lead. The spot test proposed here does not suffer from interference by mercury. It is carried out on filter-paper strips and is based on the measurement at 600 nm of the diffuse reflectance of the blue complex (I) formed by lead (II) with carminic acid, which was investigated by Jain[3]. The color of this complex is stronger in alkaline conditions, but becomes unstable if the pH is too high. It was therefore necessary to find compromise conditions providing a high sensitivity to the spot test without fading of the color.

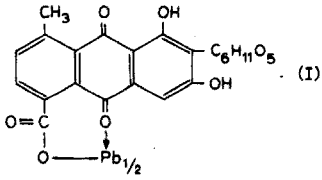

(I)

Experimental

The experimental method and procedure have already been described in detail[1] Measurements of the diffuse reflectance at the center of 6-mm diameter test spots on filter paper were made with the Fast Scanning Spectrocolorimeter type SCF-1 (Israel Electro-Optical Industry, Ltd., Rehovoth) fitted with its diffuse reflectance attachment. The carminic acid, lead acetate and other reagents used were all of reagent grade. The filter paper was Whatman 120.

Reagents. Lead acetate solutions containing 200 p.p.m. of lead (II) (for the lower concentration range) and 2000 p.p.m. (for the higher concentration range) were prepared. All solutions were prepared in triple-distilled water.

Carminic acid solution. Carminic acid (0.5 g; BDH, purified) was dissolved in 100 ml of water, refluxed for 1 h; the solution was cooled to room temperature and filtered. Working solutions were prepared by dilution.

Procedure. The test spots were formed on filter paper strips (22 × 4.5 cm) notched to register with pins on the syringe holder and on the reflectometer[1].

* Present address: Electro-Optical Industry, Ltd., Rehovoth, Israel.

Two lines of 9 test spots each, 1.5 cm apart, were accommodated on each filter paper strip. Before the test spots were placed, a 9-μl drop of 0.005 *M* sodium hydroxide solution was delivered on each of the 18 sites where the test spots were to be formed, by means of a syringe (Brunswick B-501-TB with the needle tip filed off) in its holder. After the paper had dried (10 min at about 50°C) an 11-μl drop of 0.125% (w/v) carminic acid solution was applied to each alkali spot, from a second microsyringe in the same holder so that the drop fell exactly in the center of the spot. Then the paper was dried for another 10 min. (Time can be saved by preparing in advance a day's supply of impregnated filter papers; these should be stored in the dark and used within 24 h; the calibration curve should always be prepared daily from the same stock of papers.) Finally, 9-μl drops of the lead (II) solutions were added centrally from another microsyringe. All the test solutions were at pH 6–7. The paper was again dried for 10 min as above, and the reflectance was measured spot by spot.

Except at the highest concentrations, no rapidly formed precipitates occurred; consequently, the spots formed were very uniform and homogeneous in color density, and it was necessary to measure only 2 spots of each concentration to eliminate random errors. These spots were placed on different parts of the filter paper strip. The test spots were stable. Individual specimens stored in the dark for up to one month retained their spectral reflectance characteristics quantitatively.

Results

Figure 1 shows the reflectance spectra displayed on the oscilloscope of the instrument, which plots percentage reflectance against wavelength. The figure is a multiple-exposure photograph of the oscilloscope, showing the spectra of 5 specimens. The upper curve is the reflectance of the reagent alone; reflectance rises fairly sharply above 530 nm, corresponding to the red color of the carminic acid. The other curves relate to increasing concentrations of lead (II). It is clear that 600 nm is the wavelength at which lead (II) has the greatest effect on the reflectance.

The Kubelka–Munk* function of the reflectance R

$$\frac{K}{S} = \frac{(1-R_\infty)^2}{2R_\infty}$$

at this wavelength was plotted against concentration of lead (II) (Fig. 2). The relationship was linear only for the region 50–120 p.p.m., below which the high absorption of carminic acid interfered too much. This interference had the useful side-effect that, for concentrations below 90 p.p.m., there was a linear relationship between the reflectance R itself and the concentration (Fig. 3). Thus, for concentrations up to about 120 p.p.m., a simple 2-point calibration curve is sufficient for the determination of lead (II) to an accuracy of about 3 p.p.m.

For determinations at concentrations higher than 200 p.p.m., it was necessary to reduce the sensitivity of the technique, and this could of course be done by dilution, although it was easier to reduce the sensitivity by carrying out the test with a neutral solution, omitting the application of sodium hydroxide to the test paper; in

* The function plotted is not strictly the Kubelka–Munk function, since the specimens were not of infinite thickness.

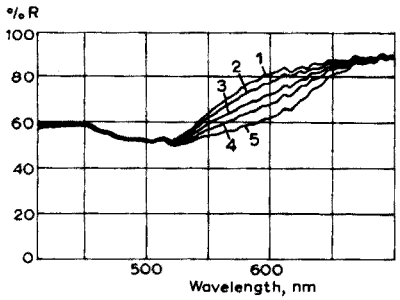

Fig. 1. Reflectance spectra for the lead—carminic acid complex at different concentrations of lead (II) under alkaline conditions: 1, 0 p.p.m.; 2, 20 p.p.m.; 3, 40 p.p.m.; 4, 60 p.p.m.; 5, 100 p.p.m.

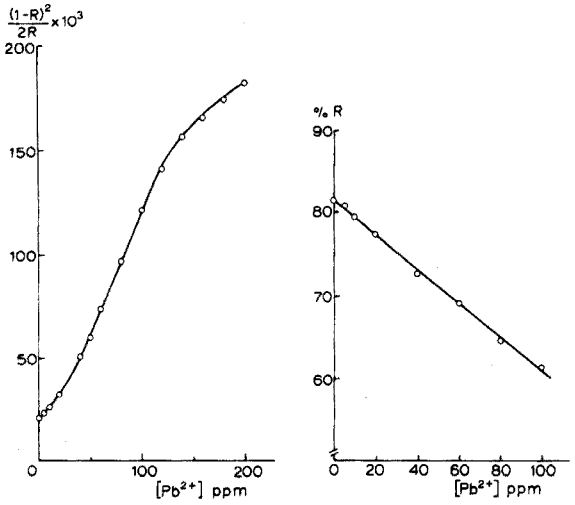

Fig. 2. $(1-R)^2/2R$ *versus* concentration up to 200 p.p.m. at 600 nm under alkaline conditions. Each point is the mean of 4 measurements on separate strips of paper. Reproducibility was better than 2.5 p.p.m.

Fig. 3. *R versus* concentration up to 100 p.p.m. at 600 nm under alkaline conditions. Each point is the mean of 3 measurements on separate strips of paper, the standard deviation being 1.7 p.p.m.

this case, a 0.5% (w/v) carminic acid solution should be used. Figure 4 shows the Kubelka–Munk curve for spot tests carried out in this way with lead (II) solutions up to 1800 p.p.m.; these measurements were also made at 600 nm wavelength, although the shape of the spectral reflectance curve is slightly different.

It should be noted that Fischer and Vratny[4] and Froydma *et al.*[5] obtained similar relationships between the Kubelka–Munk function and the concentration in thin-layer chromatography. Kealy[6] achieved similar results in quantitative reflectometry performed on commercial test-strip papers for nickel.

Effect of interfering substances

In order to test the interference of foreign cations, tests were performed on

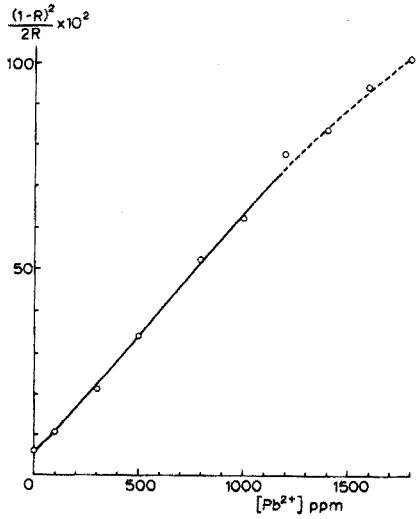

Fig. 4. $(1-R)^2/2R$ *versus* concentration up to 1800 p.p.m. at 600 nm under neutral conditions.

TABLE I

REFLECTANCE MEASUREMENTS WITH DIVERSE IONS PRESENT[a]

Foreign ion	*Reflectance (%) (average of 2 tests)*					
	Reagent alone	*50 p.p.m. Pb^{2+}*	*10 p.p.m. foreign ion*	*50 p.p.m. Pb^{2+} + 10 p.p.m. foreign ion*	*Effect of interfering ion*	*Effect of interfering ion at 0 p.p.m. Pb^{2+}*
	(i)	*(ii)*	*(iii)*	*(iv)*	*(ii)–(iv)*	*(i)–(iii)*
Ag^+	83.3	70.3	83.8	70.5	−0.2	−0.5
Hg^{2+}	83.3	70.3	83.5	69.8	0.5	−0.2
Cu^{2+}	83.5	69.5	71.8	68.0	1.5	11.7
Cd^{2+}	83.3	70.3	83.2	69.9	0.4	0.1
Sn^{2+}	83.9	70.0	81.0	69.5	0.5	2.9
Ni^{2+}	83.9	70.0	79.5	66.4	3.6	4.4
Fe^{2+}	82.7	70.0	59.4	58.3	11.7	23.3
Fe^{3+}	82.7	70.0	70.0	68.8	1.2	12.7
Ba^{2+}	82.0	70.0	81.5	69.7	0.3	0.5
Sr^{2+}	83.5	69.5	84.0	70.0	−0.5	−0.5
Ca^{2+}	83.5	69.5	82.1	68.5	1.0	1.4
Mg^{2+}	82.0	70.0	81.0	69.8	0.2	1.0
Na^+	84.8	70.2	84.5	69.3	0.9	0.3
K^+	82.9	70.0	83.5	70.0	1.0	−0.6

[a] These tests were carried out on different filter paper strips which were individually calibrated.

solutions containing 50 p.p.m. lead and 10 p.p.m. of an interfering ion. The following ions caused no change in the reflectance spectrum: Ag^+, Hg^{2+}, Cd^{2+}, Ba^{2+}, Sn^{2+}, Ca^{2+}, Mg^{2+}, Na^+ and K^+. A representative result for Mg^{2+}, Cd^{2+} and Hg^{2+} is shown in Fig. 5. A summary of the results is presented in Table I.

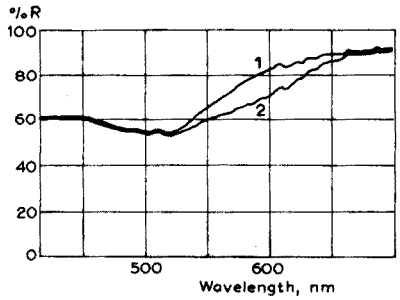

Fig. 5. Reflectance spectra with non-interfering ions (10 p.p.m. each). 1, Spectra for reagent alone and with addition of Hg^{2+}, Cd^{2+}, Mg^{2+}. 2, Spectra for reagent with 50 p.p.m. Pb^{2+}, and with addition of Hg^{2+}, Cd^{2+}, Mg^{2+}.

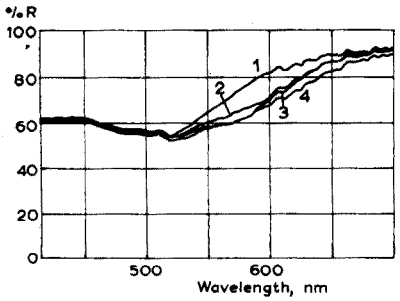

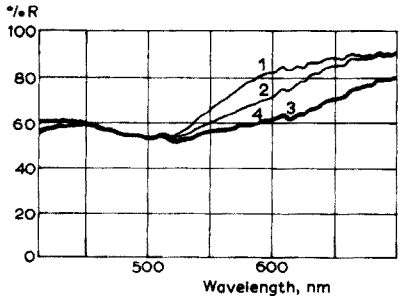

Fig. 6. Reflectance spectra at 600 nm. 1, Reagent. 2, Reagent + 10 p.p.m. Cu^{2+}. 3, Reagent + 50 p.p.m. Pb^{2+}. 4. Reagent + 50 p.p.m. Pb^{2+} + 10 p.p.m. Cu^{2+}.

Fig. 7. Reflectance spectra at 600 nm. 1, Reagent. 2, Reagent + 10 p.p.m. Fe^{2+}. 3,4, Reagent + 50 p.p.m. Pb^{2+}, and reagent + 50 p.p.m. Pb^{2+} + 10 p.p.m. Fe^{2+}.

Only copper(II) and iron(II) interfered at the pH studied. As their complexes have similar reflectance curves, these ions should be tested for before the reflectance analysis. Figure 6 shows the spectra of the reagent with lead and with copper, and Fig. 7 the spectra with iron(II). With iron(II) the spectra of the reagent and the lead complex coincide at 700 nm while the reflectance is strongly reduced even in the presence of only 10 p.p.m. iron(II).

Conclusions

Lead can be determined by a reflectometric method with a lower limit of detection of 5 p.p.m. Fourteen interfering ions were tested; only copper(II) and iron(II) interfered. The test may be useful in environmental analysis.

This work was supported by the Israel National Council of Research and Development.

REFERENCES

1 R. Reisfeld, E. Greenberg and W. J. Levene. *Anal. Chim. Acta*, 74 (1975) 253.

2 A. Tucker, *The Toxic Metals*, Ballantine Books, New York, 1972.
3 T. C. Jain, *J. Indian Chem. Soc.*, 37 (1960) 727.
4 R. B. Fischer and F. Vratny, *Anal. Chim. Acta*, 13 (1955) 593.
5 M. M. Froydma, R. W. Frei and D. J. Williams, *J. Chromatogr.*, 13 (1964) 61.
6 D. Kealey, *Talanta*, 19 (1972) 1563.

Analytica Chimica Acta, 76 (1975) 483–486

SHORT COMMUNICATION

Some observations on the coulometric determination of sulphur dioxide

A. D. CAMPBELL, (the late) D. P. HUBBARD and N. H. TIOH
Department of Chemistry, University of Otago, Box 56, Dunedin (New Zealand)
(Received 30th December 1974)

During recent years the coulometric method has been extensively used for the determination of sulphur compounds, *e.g.* sulphur in hydrocarbons[1–3], and sulphur dioxide both in the atmosphere[4,5] and gas mixtures[6]. The advantages of the technique include selectivity, rapidity, wide range of analytical utility and, perhaps most important, the ease of automation. However, the above-mentioned methods all involve relatively expensive equipment; the work described here was concerned with the possibility of measuring sulphur dioxide in the atmosphere precisely and cheaply with a portable instrument. As a preliminary step, the coulometric titration of sulphur dioxide with electrogenerated iodine[1–3] was assessed in terms of accuracy, precision and interferences.

Experimental

Apparatus. A constant-current coulometer (Metrohm Model E211 A) was used in conjunction with a titration vessel (Metrohm 875-20) equipped with 5 standard ground glass joint inlets. Iodine was electrogenerated at a platinum foil anode separated from a platinum foil auxiliary electrode by a dialysis membrane (Metrohm EA 247). The end-point was detected by a pair of identical platinum electrodes in a variation of the "dead-stop" end-point method described by Hawkins[7]; this indicating unit was arranged so that the 0.3-V full-scale meter (Uchida Yoko Co. Ltd., Japan) acted as a high-resistance voltmeter in parallel with the cell. The voltage across the cell decreased to a relatively low value at the end-point when free iodine was available to depolarize the cathode. The constant current was measured by a milliammeter (Uchida Yoko Co. Ltd., Japan) because the current settings on the coulometer were not accurate.

Electrolyte solution was stored in a reservoir with an inlet into the titration vessel. Solutions containing sulphur dioxide were introduced through one of the other ground-glass joint inlets. Solutions were stirred magnetically.

Electrolyte. Prepare a solution containing 0.2 *M* potassium iodide, 0.055% (w/v) sodium azide and 0.68% (v/v) acetic acid with deoxygenated distilled water.

Standard sulphur dioxide solution. Bubble sulphur dioxide through deoxygenated distilled water and standardize when required by adding acidified iodine solution and back-titrating with sodium thiosulphate solution.

Standard sodium sulphite solution. Dissolve a known amount of anhydrous sodium sulphite in 5% (v/v) glycerol solution.

Standard iodine and thiosulphate solutions were prepared by suitable dilution of "Volucon" standard concentrates (May and Baker, England). Analytical reagent-grade chemicals were used wherever possible.

Procedure. Transfer 30 cm^3 of electrolyte solution to the titration vessel and generate iodine electrolytically at a constant current of 2.97 mA until the needle of the indicating meter registers half full-scale deflection. Introduce a known volume of sulphur dioxide solution into the cell and regenerate iodine to its previous level, recording the electrolysis time. Calculate the concentration of sulphur dioxide in the added solution from:

$$[SO_2] = \frac{I \cdot t \cdot 10^3 \cdot 64.064}{y \cdot 2 \cdot 96487} \text{ p.p.m.}$$

where I is the constant current (mA), t is the time of electrolysis (s), and y is the volume of SO_2 solution added (cm^3).

Results and discussion

Sulphur dioxide reacts with the coulometrically generated iodine (which forms triiodide) in the normal manner, being oxidized to sulphur trioxide. In a comparison of end-points for the coulometric determination of arsenite with iodine, Tackett[8] reported that students generally found the amperometric ("dead-stop") method to be more precise than either colorimetric or potentiometric methods. Moreover, the "dead-stop" method is widely accepted for Karl Fischer titrations, and was therefore chosen here.

The electrolyte selected for study was recommended by Cedergren[3] as a suitable absorption medium for sulphur dioxide after combustion of hydrocarbons. The high concentration of iodide is present to favour the formation of the less volatile triiodide. It has been shown[1] that the presence of sodium azide eliminates the interference of nitrogen and chlorine compounds.

Loss of SO_2 from solution. It is well known that loss of SO_2 from solution occurs on standing[9]. Table I shows the coulometric determination of the standard sulphur dioxide solution immediately after preparation and at 24-h intervals for 3 days; the results are compared with those of the iodine–thiosulphate back titration[10] and the hydrogen peroxide methods[11]. The peroxide method appears to

TABLE I

THE DETERMINATION OF SULPHUR DIOXIDE IN A STANDARD SOLUTION

Day	*SO_2 ($\cdot 10^{-4}$ mol dm^{-3})*		
	Coulometry[a]	*$I_2/S_2O_3^{2-}$*[b]	*H_2O_2*[c]
0	6.54	6.57	6.36
1	4.85		
2	3.23	3.26	6.26
3	2.42		

[a] Mean of 6 or 7 readings.
[b] Iodine added and excess titrated with sodium thiosulphate solution.
[c] Oxidation to sulphur acid and titration with sodium hydroxide solution.

give low results but the 30 min which elapsed between application of the first two methods and the peroxide method could account for the difference. Certainly there is excellent agreement between the coulometric and the back-titration methods which were carried out simultaneously. The results indicate that very little of the sulphur dioxide is lost by volatilization and that most is lost via oxidation to sulphur trioxide. Great care should be exercised whenever solutions containing sulphur dioxide cannot be analysed immediately.

Precision of the method. Syty[12] has suggested that the stability of sulphite solutions may be increased by the addition of glycerol. Consequently, the precision of the method was evaluated by determination of the SO_2 content of a series of freshly prepared sodium sulphite solutions in 5% glycerol (Table II); it should be noted that the glycerol produced a blank value which had to be subtracted from the actual times recorded. In the case of solutions 4 and 5, it was necessary to add only 2 cm^3 of standard solution to the coulometric cell instead of

TABLE II

REPRODUCIBILITY OF THE COULOMETRIC METHOD FOR SULPHITE SOLUTIONS IN 5% GLYCEROL

Solution	*Equivalent SO_2 content (p.p.m.)*	
	Actual	*Found*[a]
1	3.783	3.783±0.016
2	11.83	11.76±0.04
3	19.93	19.73±0.18
4	52.74	52.44±0.21
5	81.39	81.12±0.19

[a] Mean of at least 4 values.

TABLE III

INTERFERENCE STUDY

Interferent (mg)	*Sulphur dioxide found*[a] *(mg)*	
	Alone	*With interferent*
SO_3[b] 2.45	0.171	0.172
NO_2[b] 12.6	0.171	0.171
HCl[b] 7.29	0.157	0.157
H_2S[c] 3.85	0.157	0.157
CO_2[c] 1.69	0.131	0.131
HCHO 18.9	0.112	0.112
Cl_2[c] 1.09	0.112	0.088
CO[c] 0.03	0.125	0.125
CH_4[c] 0.02	0.125	0.124

[a] Added as 10 cm^3 of standard sulphur dioxide solution to the electrolyte solution.
[b] Added as corresponding acid.
[c] Added as saturated solution.

5 cm^3 as for solutions 1–3, otherwise inaccuracies resulted, *i.e.* the accuracy of the determination decreases with increasing sulphur dioxide content probably because of oxidation losses, although in these cases an insufficient excess of iodine may have been present. It is suggested that the sulphur dioxide content of the solution should not exceed *ca.* 4–5 mg dm^{-3} for optimal accuracy. Sodium thiosulphate solution also provides a suitable standard—the mean value of ten successive coulometric determinations was 0.0500 ± 0.0004 mol dm^{-3}.

Interferences. Some species likely to be present in the atmosphere were added to the electrolyte; the results are summarized in Table III. The only interference was from chlorine but this is unlikely to be present in the atmosphere[13]. It should be remembered that sulphides will interfere although the sulphide content of the atmosphere is usually very low compared with that of sulphur dioxide.

These results show that the electrogeneration of iodine and coulometric determination of sulphur dioxide is an accurate and precise method with few interferences. It should be possible to design a very simple coulometric portable meter for determining sulphur dioxide in the atmosphere.

REFERENCES

1 F. C. A. Killer and K. E. Underhill, *Analyst (London)*, 95 (1970) 505.
2 J. P. Dixon, *Analyst (London)*, 97 (1972) 612.
3 A. Cedergren, *Talanta*, 20 (1973) 621.
4 W. L. Bamesberger and D. F. Adams, *Tappi*, 52 (1969) 1302.
5 D. F. Miller, W. E. Wilson Jr. and R. G. Kling, *J. Air Pollut. Contr. Ass.*, 21 (1971) 414.
6 S. I. Krichmar, V. E. Stepanenko and T. M. Galan, *Zh. Anal. Khim.*, 26 (1971) 1340.
7 A. E. Hawkins, *Analyst (London)*, 89 (1964) 432.
8 S. L. Tackett, *J. Chem. Educ.*, 49 (1972) 52.
9 P. L. Bailey and E. Bishop, *Analyst (London)*, 97 (1972) 311.
10 A. I. Vogel, *A Textbook of Quantitative Inorganic Analysis*, Longmans, London, 3rd edn., 1961.
11 M. B. Jacobs, *The Chemical Analysis of Air Pollutants*, Wiley Interscience, New York, 1960.
12 A. Syty, *Anal. Chem.*, 45 (1973) 1746.
13 P. K. Mueller in E. S. Starkman (Ed.), *Combustion-generated Pollution*, Plenum Press, New York, 1971.

Analytica Chimica Acta, 76 (1975) 487–490

SHORT COMMUNICATION

A new application of Landolt-type reactions. The determination of molybdenum, copper and vanadium

HERBERT WEISZ and SIEGBERT PANTEL

Lehrstuhl für Analytische Chemie, Chemisches Laboratorium der Universität Freiburg, Freiburg i.Br. (B.R.D.)

(Received 18th December 1974)

The application of Landolt-type reactions[1–3] offers good possibilities for carrying out kinetic determinations of catalysts; such procedures can be regarded as "fixed concentration methods". In Landolt-type reactions, a slow reaction (1) is connected with a fast one (2) by the reaction product of the first reaction:

$$A + B \rightarrow C \ldots \text{slow} \quad (1)$$

$$C + D \rightarrow E \text{ or } A \ldots \text{fast} \quad (2)$$

It follows that product C will appear visibly only after all substance D ("Landolt reagent") has been consumed. If the first slow reaction can be accelerated by a catalyst, then the time which elapses between the start of the reaction and the first appearance of the free product C, the so-called induction period, is a measure of the concentration of the catalyst. This chronometric method has been successfully applied for the determination of quite a number of catalytic substances[1,4–9]. In this laboratory Landolt-type reactions have been used for the determination of various catalytically active ions with a kinetic difference method[10].

In the present communication, a new variation of the application of Landolt-type reactions is described. Instead of adding the necessary reactants (A, B and D) of the reaction simultaneously to the system together with the catalyst to be determined, here only two of them, namely A and the Landolt reagent D, are added to the catalyst, and a solution of the oxidant B is added from a motor-driven burette at constant speed. This speed of addition must be so high that even at the highest measured catalyst concentration not all of it is consumed; that means the oxidant B piles up. Consequently, the lower the catalyst concentration, the higher will be the volume of oxidant B added until the free final product C of the reaction appears in the system.

This procedure could be regarded as a dynamized Landolt reaction. The two reactions proceed, by definition, one after the other, whereas in the method of competitive reactions recently reported by Klockow and Graf[11], the two reactions proceed simultaneously. The determinations of molybdenum, copper and vanadium by dynamized Landolt reactions are described below. In all three cases, one of the reactants is iodide, the Landolt reagent is either thiosulphate or ascorbic acid,

and the oxidizing reagent is hydrogen peroxide, peroxydisulphate or bromate; the end-point, *i.e.* the appearance of the first free iodine, is indicated biamperometrically.

Experimental and results

The essential measuring device (Fig. 1) consists of a voltage source U, a double platinum electrode Pt and an operational amplifier OA connected to a mV-meter M with the zero point in the middle of the scale.

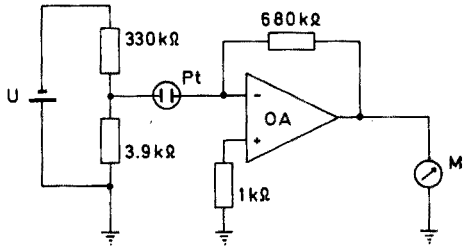

Fig. 1. Measuring circuit. U = Mallory RM 42 R (1.35 V); Pt = double platinum electrode Pt 120 (Schott u. Gen., Mainz, B.R.D.); OA = Philbrick-Nexus Q 200 operational amplifier; M = mV-meter, measuring range 500–0–500 mV.

Determination of molybdenum by the Mo(VI)-catalyzed oxidation of iodide with hydrogen peroxide; thiosulphate as Landolt reagent[1]. Into a 50-ml beaker, add 10 ml of 2 *M* acetate buffer pH 3.5, 1 ml of 0.05 *M* potassium iodide solution, 0.5 ml of 0.02 *N* sodium thiosulphate solution, and a suitable volume of the neutralized molybdenum sample solution or, for preparing a calibration graph, 1–10 ml of a molybdenum solution containing 10 μg Mo(VI) ml^{-1} as sodium molybdate. Make up to 27 ml with twice-distilled water. Stir the solution well and thermostat at 25.0 ± 0.2°C. Start the reaction by addition of hydrogen peroxide (10 mg H_2O_2 ml^{-1}) from a motor-driven syringe burette (after Tölg; Becher oHG, Mainz; B.R.D.), at a speed of 0.13 ml min^{-1}.

Figure 2 shows the calibration graph; some results are given in Table I.

TABLE I

DETERMINATION OF MOLYBDENUM

(Results given as μg Mo/27 ml)

Given	10.6	20.4	30.0	42.0	52.0	60.8	69.0	80.0	89.2	100.0
Found	10.5	20.5	29.5	41.5	51.0	62.5	72.0	76.0	92.0	102.5
Error	−0.1	+0.1	−0.5	−0.5	−1.0	+1.7	+3.0	−4.0	+2.8	+2.5

Determination of copper by the Cu(II)-catalyzed oxidation of iodide with peroxydisulphate; ascorbic acid as Landolt reagent[5]. Into a 50-ml beaker, add 10 ml of 0.4 *M* acetate buffer pH 3.6, 2 ml of 0.05 *M* potassium iodide solution, 0.5 ml of 0.005 *M* solution of ascorbic acid, and a suitable volume of the neutralized copper sample solution or, for preparing a calibration graph, 1–10 ml of a copper solution

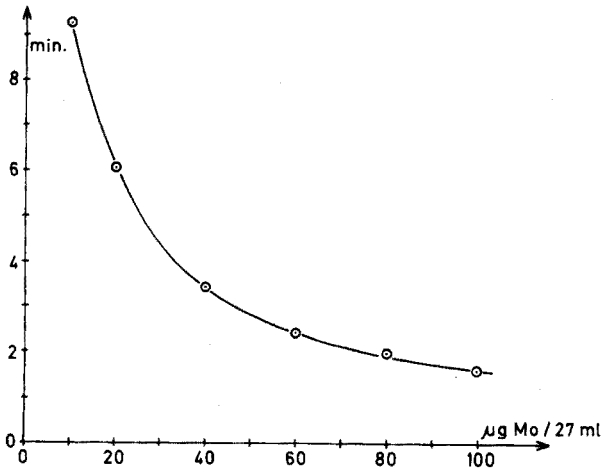

Fig. 2. Calibration graph for the determination of molybdenum.

containing 5 µg Cu(II) ml^{-1} as copper acetate. Make up to 27 ml with twice-distilled water. Stir the solution well and thermostat at 25.0±0.2°C. Start the reaction by addition of potassium peroxydisulphate (40 mg $S_2O_8^{2-}$ ml^{-1}) from the burette at a speed of 0.26 ml min^{-1}.

The calibration graph looks similar to that shown in Fig. 2; some results are given in Table II.

Determination of vanadium by the V(V)-catalyzed oxidation of iodide with bromate; ascorbic acid as Landolt reagent[8]. Into a 50-ml beaker, add 10 ml of a 0.2 *M* citrate–hydrochloric acid buffer pH 2.5, 2 ml of 0.05 *M* potassium iodide solution, 0.5 ml of 0.005 *M* ascorbic acid, and a suitable volume of the neutralized vanadium sample solution or, for preparing a calibration graph, 0.5–10 ml of a vanadium

TABLE II

DETERMINATION OF COPPER

(Results given as µg Cu/27 ml)

Given	6.0	8.2	15.3	20.0	25.0	31.0	38.3	39.8	42.6	49.5
Found	5.8	9.2	16.0	19.5	24.0	34.0	37.5	42.0	40.0	50.0
Error	−0.2	+1.0	+0.7	−0.5	−1.0	+3.0	−0.8	+2.2	−2.6	+0.5

TABLE III

DETERMINATION OF VANADIUM

(Results given as µg V/27 ml)

Given	0.66	1.00	1.62	2.00	2.94	4.00	5.00	5.52	8.00	9.04
Found	0.59	0.95	1.60	1.95	3.05	4.15	4.90	6.00	8.25	9.28
Error	−0.07	−0.05	−0.02	−0.05	+0.11	+0.15	−0.10	+0.48	+0.25	+0.24

solution containing 1 μg V(V) ml^{-1} as sodium metavanadate tetrahydrate. Make up to 27 ml with twice-distilled water. Stir well and thermostat at 25.0 ± 0.2°C. Start the reaction by addition of a 0.3 *M* solution of potassium bromate from the burette at a speed of 0.13 ml min^{-1}.

The calibration graph looks similar to that shown in Fig. 2; some results are given in Table III.

REFERENCES

1 G. Svehla and L. Erdey, *Microchem. J.*, 7 (1963) 206, 221.
2 J. Bognár, *Mikrochim. Acta*, (1968) 455.
3 G. Svehla, *Analyst (London)*, 94 (1969) 513.
4 H. Thompson and G. Svehla, *Microchem. J.*, 13 (1968) 576; *Z. Anal. Chem.*, 247 (1969) 244.
5 A. Páll, G. Svehla and L. Erdey, *Talanta*, 17 (1970) 211.
6 J. Bognár and Sz. Sárosi, *Anal. Chim. Acta*, 29 (1963) 406.
7 J. Bognár and O. Jellinek, *Nehezip. Musz. Egyet. Miskolc. Idegennyelvu Kozlem.*, 24 (1964) 111; *Chem. Abstr.*, 65 (1966) 12848 h.
8 J. Bognár and O. Jellinek, *Nehezip. Musz. Egyet. Miskolc. Idegennyelvu Kozlem*, 25 (1965) 127; *Chem. Abstr.*, 65 (1966) 12849 a; *Mikrochim. Acta*, (1969) 318.
9 J. Bognár, *Mikrochim. Acta*, (1968) 473.
10 H. Weisz and K. Rothmaier, *Anal. Chim. Acta*, 68 (1974) 93.
11 D. Klockow and G. F. Graf, *Symposion Spurenanalyse, Erlangen–Nürnberg (B.R.D.)*, April 1973, preprints p. 54; G. F. Graf, Diploma Thesis, Universität Freiburg (B.R.D.), 1973.

Analytica Chimica Acta, 76 (1975) 491–493

SHORT COMMUNICATION

The standardization of hydroquinone solutions

J. BAREK, A. BERKA
Department of Analytical Chemistry, Charles University, Prague 2, Alberto 2030 (Czechoslovakia)
P. HOFMAN
Research Institute of Water Economy, Prague 6 (Czechoslovakia)
(Received 1st December 1974)

Hydroquinone has about the same reducing strength as iron(II) sulphate, but its acidified solutions are much more stable[1]. However, standardization of solutions of this reagent against a primary standard presents certain problems Potentiometric titration of dichromate[2] is not suitable, since the potential stabilizes too slowly and the break at the equivalence point is small[3]. Better results are obtained by a method[4] based on potentiometric titration of the phosphate complex of manganese(III), formed by oxidation of manganese(II) with dichromate in 12 *M* phosphoric acid; this allows 0.1–0.001 *N* solutions of hydroquinone to be standardized, but it has the disadvantage that the end-point cannot be determined visually. Therefore, a new method based on titration of the pyrophosphate complex of manganese(III) has been developed. The pyrophosphate complex of manganese(III) is prepared by oxidation of manganese(II) with a known amount of dichromate in a sodium pyrophosphate medium[5], so that potassium dichromate serves as a primary standard. The end-point can be determined potentiometrically, or visually with diphenylamine as indicator. The entire procedure can be described by the following equations:

$$6[Mn(H_2P_2O_7)_2]^{2-} + Cr_2O_7^{2-} + 6H_4P_2O_7 + 2H^+ \rightarrow \rightarrow 6[Mn(H_2P_2O_7)_3]^{3-} + 2Cr^{3+} + 7H_2O \quad (1)$$

$$C_6H_4(OH)_2 + 2[Mn(H_2P_2O_7)_3]^{3-} + 2H^+ \rightarrow C_6H_4O_2 + + 2[Mn(H_2P_2O_7)_2]^{2-} + 2H_4P_2O_7 \quad (2)$$

The acidity limits for the titration of the pyrophosphate complex of manganese(III) with 0.1 *N* hydroquinone were first determined. To 10.00 ml of 0.1 *N* potassium dichromate were added 40 ml of a freshly prepared solution of 4.5 g of sodium pyrophosphate in a mixture of 25 ml of 1, 2, 3 or 4 *M* sulphuric acid, 10 ml of 0.5 *M* manganese(II) sulphate and 5 ml of distilled water; after 5 min, this solution of the pyrophosphate complex of manganese(III) was potentiometrically titrated with 0.1 *N* hydroquinone. Under these conditions, the titrated solution contained 0.5–2 *M* sulphuric acid, 0.2 *M* pyrophosphate

and 0.1 *M* manganese(II). The titration could be carried out over the whole acidity range studied. The inflexion potential was in the vicinity of 575 mV (*vs.* SCE), the potential break at the equivalence point amounting to about 150 mV per 0.02 ml of 0.1 *N* hydroquinone. The platinum electrode potential stabilized instantaneously in 0.5 *M* sulphuric acid, but stabilization became slower with increasing acidity.

In 0.5 *M* sulphuric acid, the titration was satisfactory at pyrophosphate concentrations in the range 0.1–0.3 *M*, and at manganese(II) concentrations in the range 0.05–0.25 *M*. At lower concentrations of pyrophosphate and manganese(II), 5 min was insufficient for quantitative reduction of dichromate, and longer periods had to be allowed before the titration. The magnitude of the potential break at the equivalence point was practically independent of the concentrations of manganese(II) and pyrophosphate.

From the point of view of potential stabilization, the best medium was 0.5 *M* in sulphuric acid, 0.2 *M* in sodium pyrophosphate and 0.2 *M* in manganese(II) sulphate. In this medium it was even possible to determine the titre of 0.01 *N* hydroquinone, when 0.01 *N* potassium dichromate was used. The potential break was then about 100 mV per 0.02 ml of 0.01 *N* hydroquinone, and the potential stabilized almost instantaneously. It was impossible to determine the titre of 0.001 *N* hydroquinone in this manner, because of the small equivalence potential break and slow potential stabilization.

Experimental

Hydroquinone, 0.1 and 0.01 N solutions. Prepare solutions in 1% sulphuric acid. All chemicals used were of p.a. purity.

Apparatus. A TTT 1 millivoltmeter (Radiometer, Copenhagen) was used with platinum indicator and saturated calomel reference electrodes. Solutions were stirred magnetically.

Recommended procedure. To 10.00 ml of 0.1 or 0.01 *N* potassium dichromate, add a freshly prepared solution of 4.5 g of sodium pyrophosphate decahydrate in a mixture of 25 ml of 1 *M* sulphuric acid and 20 ml of 0.5 *M* manganese(II) sulphate solution; after 5 min, titrate the pyrophosphate complex of manganese(III) with 0.1 or 0.01 *N* hydroquinone solution. In the titration with 0.1 *N* hydroquinone, diphenylamine can be used as an indicator.

Results and discussion

The standard deviation calculated from 10 determinations was $1.03 \cdot 10^{-2}$ ml for 0.01 *N* hydroquinone and $1.63 \cdot 10^{-2}$ ml for 0.01 *N* hydroquinone, when potentiometric indication was used. The standard deviation of the visual titration with 0.1 *N* hydroquinone was $1.77 \cdot 10^{-2}$ ml.

When the present method is compared with that described earlier[4], which was based on titration of the phosphate complex of manganese(III), the advantage of using potassium dichromate as a primary standard is preserved. An additional advantage is the possibility of using visual diphenylamine end-points. A disadvantage of the proposed method is that 0.001 *N* hydroquinone solutions cannot be standardized.

REFERENCES

1 A. Berka, J. Vulterin and J. Zýka, *Newer Redox Titrants*, Pergamon, Oxford, 1965.
2 I. M. Kolthoff, *Rec. Trav. Chim. Pays-Bas*, 45 (1926) 745.
3 U. A. T. Brinkman and H. A. M. Snelders, *Talanta*, 11 (1964) 47.
4 A. Berka, *Mikrochim. Acta*, (1970) 430.
5 P. Hofmann and P. Štern, *Anal. Chim. Acta*, 45 (1969) 149.

ANALYTICA CHIMICA ACTA, VOL. 76 (1975)

AUTHOR INDEX

ANALYTICA CHIMICA ACTA, VOL. 76 (1975)

SUBJECT INDEX

Wilson and Wilson's

Comprehensive Analytical Chemistry

edited by **G. SVEHLA**, Reader in Analytical Chemistry,
The Queen's University of Belfast.

**Volume IV INSTRUMENTATION FOR SPECTROSCOPY
ANALYTICAL ATOMIC ABSORPTION AND FLUORESCENCE SPECTROSCOPY
DIFFUSE REFLECTANCE SPECTROSCOPY**

1975. 392 pages
US $51.95/Dfl. 125.00 (Subscription price: US $44.25/Dfl. 106.00)
ISBN 0-444-41163-1

Volume IV in the series "Comprehensive Analytical Chemistry" features spectroscopy as its theme.
The book is divided into three main sections. The first part deals with instrumentation and aims at assisting the spectroscopist in the selection of the correct instruments and experimental conditions for measurement. The second section — Analytical Atomic Absorption and Fluorescence Spectroscopy, as well as the last part — Diffuse Reflectance Spectroscopy, cover modern techniques widely used in analytical laboratories. Extensive lists of references are provided as a guide for the search of further information.

From Reviews of Earlier Volumes:

"I warn every practising analytical chemist and every chemical librarian that he had better become resigned to purchasing each volume as it appears."
— Science

"There is no doubt whatsoever that an authoritative book of this nature will find its way on to the bookshelves of all institutions dealing with either the practise or teaching of analytical chemistry and will retain its status as a unique 'vade mecum' for many years to come."
— Nature

Elsevier
P.O. Box 211
Amsterdam, The Netherlands

1595 E

(Continued from page 4 of cover)

CONTENTS

(Continued on inside page of cover)